PALEOBIOLOGY AND INTERRELATIONSHIPS OF PERMIAN–TRIASSIC ACTINOPTERYGIANS

Dissertation

zur

Erlangung der naturwissenschaftlichen Doktorwürde
(Dr. sc. nat.)

vorgelegt der

Mathematisch-naturwissenschaftlichen Fakultät

der

Universität Zürich

von

Thodoris Argyriou

aus

Griechenland

Promotionskommission

Prof. Dr. Marcelo R. Sánchez-Villagra (Vorsitz und Leitung der Dissertation)

PD Dr. Torsten Scheyer

Prof. Dr. Marcus Clauss

Prof. Dr. Olga Otero

Zürich, 2018

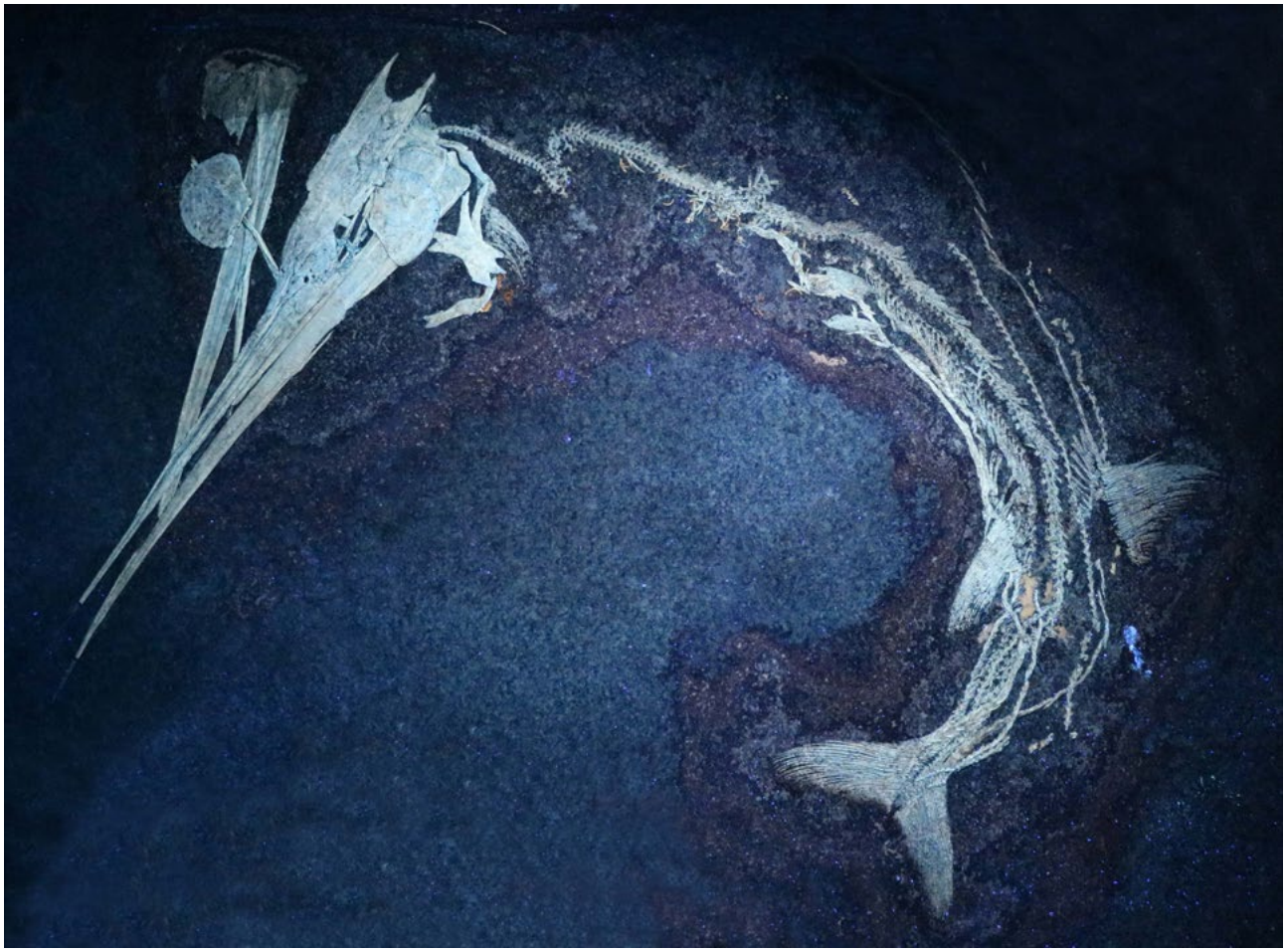

“There’s no easy way out, there’s no shortcut home...”

Robert Tepper, 1985

Actinopterygians (ray-finned fishes) were not as severely affected by the 'End Permian Mass Extinction' event as were many groups of marine organisms, and diversified subsequently during the Triassic, establishing themselves as the most successful and species-rich clade of vertebrate animals. Despite a growing number of taxonomic works for Permian–Triassic forms, their paleobiology and interrelationships remain poorly understood. This Ph.D. thesis is aimed at documenting and analyzing novel anatomical information from exceptionally preserved actinopterygians from this time interval, in order to paint a more vivid picture of the biology of these long extinct animals, while tying them to a broader evolutionary context. Many of the contained works focus on the latest Permian–Middle Jurassic †saurichthyiforms. Their salient representative, †*Saurichthys*, is a particularly important component of many early Mesozoic assemblages across the globe, and its rich fossil record helps establish it as an important model for comparison between fossil and recent ray-fins.

Exceptionally preserved fossils from the Middle Triassic of Switzerland preserve casts of the gastrointestinal tract (GIT) of †*Saurichthys*, fossilized in situ. These faithfully depict the surrounding soft tissues, allowing for a deep-time perspective into the evolution of the GIT of fishes. The GIT of †*Saurichthys* shows differences from that of extant actinopterygians. The most conspicuous one lies in the well-developed spiral intestine, the high turn count of which resembles that of some modern sharks. Anatomical comparisons and a phylogenetically informed statistical analysis of the distribution of spiral valve turn counts across fishes were performed. The high number of turns in the gut of †*Saurichthys* and some recent chondrichthyans reflect both energetically demanding lifestyles and the evolutionary histories of these groups.

Middle Triassic deposits from Switzerland have produced almost complete ontogenetic series of two viviparous species of †*Saurichthys*, ranging from embryos to juveniles and adults. The study of these fossils adds to our understanding of the reproductive biology and early life history of those fishes. Topological criteria are established to distinguish embryos from cannibalized prey. Small juveniles exhibit well-formed crania and dentitions, suggesting they were born capable of exogenous feeding. However, a series of osteological criteria, such as the delayed ossifications of the parietals, the presence of open sensory grooves on the dermatocranium , and the delayed formation of the mid-lateral scale row, allow for distinguishing juveniles from adults. Viviparity and internal fertilization appear as specializations of Middle Triassic †*Saurichthys*.

Despite previous works, the phylogenetic position of †saurichthyiforms remained contested, and needed to be revisited in light of new data. An μCT investigation of some of the earliest representatives of the clade, preserved in three dimensions, resulted in the discovery of several anatomical features. These were either undetected or misidentified by previous workers. Key amongst them is the presence of nasobasal canals in the rostrum, a fused dermohyal on the hyomandibula, and the reconsideration of the homology of the opercular series of †saurichthyiforms. New anatomical information was incorporated in a large-scale morphological phylogeny of Osteichthyes. The recovered phylogenetic hypothesis does not support the historical affiliation of †saurichthyiforms with chondrosteans, but recovers them, along with †*Birgeria*,

as the immediate sister group to crown actinopterygians. Yet the recovered topology is weakly supported, highlighting the need for similar studies to those conducted here in other extinct taxa.

The early Permian actinopterygian †*Brachydegma caelatum* has had a central role in recent discussions on actinopterygian systematics, being often considered as an early neopterygian. However, previous phylogenies relied on interpretations of its external anatomy. The last chapter explores, for the first time, the endoskeletal anatomy of this key taxon, as revealed by μCT. †*Brachydegma* exhibits a mosaic of endoskeletal characters, such as the presence of only four gill arches, or the presence of a double jaw-joint that involves a true symplectic. These are nowadays encountered in distantly related actinopterygian lineages. New data from this and other actinopterygians suggest that the symplectic is not a neopterygian neomorph, and its involvement in the jaw joint is primitive for crown actinopterygians, or osteichthyans. The new phylogenetical hypothesis provided herein suggests that †*Brachydegma* is an early member of the actinopterygian crown group, the membership of which is now slightly expanded.

Actinopterygii (Strahlenflosser) wurden weniger schwer als viele andere Gruppen von marinen Organismen vom Massenaussterben an der Perm-Trias Grenze betroffen und konnten sich anschliessend in der Trias diversifizieren, was sie als erfolgreichste und artenreichste Gruppe innerhalb der Vertebraten etablierte. Abgesehen von der wachsenden Anzahl taxonomischer Arbeiten über die Perm und Trias Formen, bleiben ihre Paläobiologie und ihre Verwandtschaftsverhältnisse nur wenig verstanden. Diese Dissertation hat sich zum Ziel gesetzt neuartige anatomische Informationen von aussergewöhnlich gut erhaltenen Actinopterygiern aus dieser Zeit zu dokumentieren und zu analysieren, um ein lebhafteres Bild der Biologie dieser lang ausgestorbenen Lebewesen zu erschaffen. Die Ergebnisse werden in einem übergreifenden evolutionsbiologischen Kontext diskutiert. Viele der enthaltenen Arbeiten fokussieren sich auf die späten permischen und mitteljurassischen †Saurichthyiformen. Ihr bedeutendster Vertreter, †*Saurichthys,* war ein besonders essentieller Bestandteil vieler Faunengemeinschaften im frühen Mesozoikums weltweit. Der reiche Fossilbericht dieses Taxons hilft bei seiner Etablierung als wichtiger Modellorganismus für Vergleiche zwischen fossilen und rezenten Strahlenflossern.

Ausserordentlich gut erhaltene Fossilien aus der Mittleren Trias der Schweiz enthalten Abdrücke des Gastrointestinaltraktes (GIT) von †*Saurichthys* in situ. Diese stellen wirklichkeitsgetreu die umliegenden Weichgewebe dar, was eine Beobachtung der Evolution des GIT von Fischen auf einer geologischen Zeitebene ermöglicht. Der GIT von †*Saurichthys* zeigt Unterschiede zu rezenten Actinopterygiern. Der auffälligste Unterschied liegt im gut entwickelten Spiraldarm, der eine hohe Wicklungsrate aufzeigt, wie man sie bei modernen Haien finden kann. Anatomische Vergleiche und eine auf Phylogenie basierende statistische Analyse der Verteilung der Wicklungsanzahlen des Spiraldarms innerhalb der Fische wurde durchgeführt. Die hohe Anzahl der Wicklungen im Darm von †*Saurichthys* und einigen rezenten Knorpelfischen spiegeln sowohl den energieaufwendigen Lebensstil als auch die Evolutionsgeschichte dieser Gruppen wider.

Die Ablagerungen aus der Mittleren Trias der Schweiz haben fast vollständige ontogenetische Serien von zwei viviparen †*Saurichthys* Arten produziert, die von Embryonen über Juvenile bis zu Adulten reichen. Die Forschung an diesen Fossilien trägt zu unserem Verständnis der Reproduktionsbiologie und der frühen Lebensentwicklung dieser Fische bei. Topologische Kriterien wurden etabliert um Embryonen von kannibalisierter Beute zu unterscheiden. Kleine Juvenile zeigen gut ausgebildete Schädel und Gebisse und weisen somit auf eine exogene Ernährung direkt nach der Geburt hin. Es gibt eine Reihe von osteologischen Merkmalen, die eine Unterscheidung von Juvenilen und Adulten möglich macht, wie die späte Ossizifierung der Parietalen, das Vorhandensein von offenen Sinnesgruben auf dem Dermatocranium und die verspätete Bildung der mittel-lateralen Schuppenreihe. Viviparie und interne Befruchtung treten als Spezialisierungen der mittel-triassischen †*Saurichthys* auf.

Die phylogenetische Position der †Saurichthyiformen blieb trotz vorheriger Arbeiten strittig und musste angesichts neuer Daten überarbeitet werden. Die μCT Untersuchungen einiger der frühesten Repräsentanten dieser Linie, mit drei dimensionaler Erhaltung, führten zur Identifizierung einiger anatomischen Merkmale, welche bisher entweder unentdeckt waren oder falsch interpretiert

wurden. Zentral unter ihnen ist die Anwesenheit von nasobasalen Kanälen im Rostrum, ein verschmolzenes Dermohyale auf der Hyomandibel und die Neubetrachtung der Homologie der operkularen Serie der †Saurichthyiformen. Diese neue anatomischen Informationen wurden in eine grossangelegte Phylogenie von Osteichthys inkorporiert. Die erhaltene phylogenetische Hypothese unterstützt die historische Zuordnung von †Saurichthyiformen zu Chondrostei, sondern plaziert diese zusammen mit †*Birgeria* als direkte Schwestergruppe zu den Kronen-Actinopterygiern. Jedoch wird die hier erhaltene Topologie nur schwach unterstützt, was wiederum die Notwendigkeit für ähnliche Studien an weiteren ausgestorbenen Taxa aufzeigt.

Der früh-permische Actinopterygier †*Brachydegma caelatum* hatte eine zentrale Rolle in jüngsten Diskussionen über die Systematik der Actinopterigier, in denen er zumeist als früher Neopterygier platziert wurde. Frühere Phylogenien basierten jedoch auf der Interpretation von äusseren anatomischen Merkmalen. Das letzte Kapitel untersucht, zum ersten Mal mithilfe eines µCT-Scanners, die Anatomie des Endoskeletts für dieses Schlüsseltaxon. †*Brachydegma* zeigt ein Mosaik von endoskelettartigen Charaktern, wie die Anwesenheit von nur vier Kiemenbögen oder die Anwesenheit eines doppelten Kiefergelenks das ein Symplektikum beinhaltet. Diese werden heute in entfernt-verwandten Linien der Actinopterygier gefunden. Neue Daten von diesem und anderen Actinopterygiern deutet darauf hin, dass das Symplektikum kein neopterygischer Neomorphismus ist und, dass seine Beteiligung am Kiefergelenk primitiv für die Kronen-Actinopterygier oder Osteichthyes ist. Die hier präsentierte neue phylogenetische Hypothese schlägt vor, dass †*Brachydegma* ein frühes Mitglied der actinopterygischen Kronengruppe ist, deren Mitgliederbereich nun leicht vergrössert ist.

Contribution of each collaborator

Chapter 1

M.R.S.-V., E.E.M. and T.A. conceived the study. T.A. carried out the descriptive and comparative work, created all figures and led the writing of the manuscript. M.C. led the statistical analyses and participated in the interpretation of the results and the writing of the discussion and methods parts. H.F. coordinated the preparation of all specimens studied and provided input in various stages of the manuscript. M.R.S.-V. and E.E.M. supervised the project and provided input in various stages of the manuscript, including the result interpretation. M.R.S.-V. provided funding for the completion of this project.

Chapter 2

E.E.M. conceived the project, led the gathering of data, performed the analyses and led the writing of the manuscript. T.A. participated in the gathering of data, provided anatomical descriptions and figures of cranial anatomy, and contributed to the interpretation of results and writing of the manuscript. R.S. and H.F. coordinated the preparation of studied specimens and provided input in various stages of the manuscript. M.R.S.-V. provided funding for part of this work.

Chapter 3

T.A. and C.R. designed the study. T.A. analyzed the μCT data, produced the digital models, performed the analyses, created the figures and led the writing of this manuscript. S.G. scanned NHMD_157546_A, contributed to the creation of figures and produced the earlier, published, version of the phylogenetic matrix, which was modified by T.A. and S.G. I.K. provided the scan of MNHN F 1980-5. M.F. and M.R.S.-V. supervised this work. M.R.S.-V. provided funding for part of this work. All authors were involved in the discussion and interpretation of the results and contributed to the writing of the manuscript.

Chapter 4

T.A. and M.F. designed the study and performed the scans of MCZ_VPF_6503, MCZ_VPF_6504, and UMMZ_64250. T.A. analyzed the μCT data, produced the digital models, performed the analyses, created the figures and led the writing of this manuscript. S.G. scanned NHMD_73588_A, and NHMD_74424_A, and produced the earlier, published, version of the phylogenetic matrix, which was modified by T.A. M.F. supervised this work. All authors were involved in the discussion and interpretation of the results and contributed to the writing of the manuscript.

INTRODUCTION

Actinopterygii and their modern diversity

Over 50% of living vertebrate species are actinopterygian (ray-finned) fishes (Nelson *et al.* 2016). Modern ray-fins exhibit a wide spectrum of ecological and behavioral adaptations, which are in turn manifested in an impressive diversity of body shapes and anatomical specializations (Helfman *et al.* 2009; Nelson *et al.* 2016). As dictated by the current phylogenetic consensus (Near *et al.* 2012; Broughton *et al.* 2013; Nelson *et al.* 2016); see fig. 1), the highly derived Teleostei encompass more than 99% of the almost 32,000 living ray-fin species. The latter include familiar forms such as carps, herrings and tunas, but also the most peculiar ones, such as the flatfishes, remoras, or anglerfishes. Teleosts can be nowadays found in almost every aquatic niche on the planet, ranging from abyssal depths to lightless caves, or hypersaline volcanic lakes, and also constitute one of the most important protein sources for humans (Helfman *et al.* 2009). A meager 49 actinopterygian species belong to the three surviving non-teleostean lineages, which are almost exclusively freshwater in their habitat occupation and generally restricted in geographic range. These include: the basally deriving bichirs and reedfish (Polypteriformes: 14 spp. in Africa); sturgeons and paddlefishes (Acipenseriformes: 27 spp. in the Northern Hemisphere); and the holosteans, represented by gars (Lepisosteiformes: seven spp. in eastern North America and the Caribbean) and the bowfin (Amiiformes: one sp. in eastern North America) (Nelson *et al.* 2016). Due to plesiomorphies retained in their anatomy (e.g., spiracle, ganoid scales, spiral valve), these relics of ancient radiations have inspired Darwin's concept of "living fossils" (Darwin 1859), and have been treated as such by later authors (e.g., (Eldredge & Stanley 1984). It is well-established that holosteans are the sister-group of teleosts, and together they form the Neopterygii (e.g., (Patterson 1973; Grande 2010; Near *et al.* 2012; Broughton *et al.* 2013).

Brief introduction to the early evolutionary history of Actinopterygii: From humble beginnings in the Devonian to the Triassic revolution.

The major split in the osteichthyan tree of life, which gave rise to the actinopterygian and the sarcopterygian lineages, is thought to have happened in the late Silurian (Ludlow, ~ 419 Ma), close to the time of origin of bony fishes themselves (Zhu *et al.* 2009; Lu *et al.* 2016). The timing of this split event is dictated by the recovery of the first crown osteichthyans, and likely basal sarcopterygians, †*Psarolepis* and †*Guiyu* (Zhu *et al.* 1999; Zhu *et al.* 2009). However, the first actinopterygian fossils are dated to the Early (†*Meemania*, (Lu *et al.* 2016) or Middle Devonian (†*Cheirolepis*, (Pearson & Westoll 1979; Arratia & Cloutier 1996), postdating the timing of the split event by several million years. Devonian actinopterygians can be distinguished from their sarcopterygian cousins on the basis of hard-tissue specializations, such as: the absence of a jugal sensory canal; presence of a median aortic canal in neurocranium; absence of

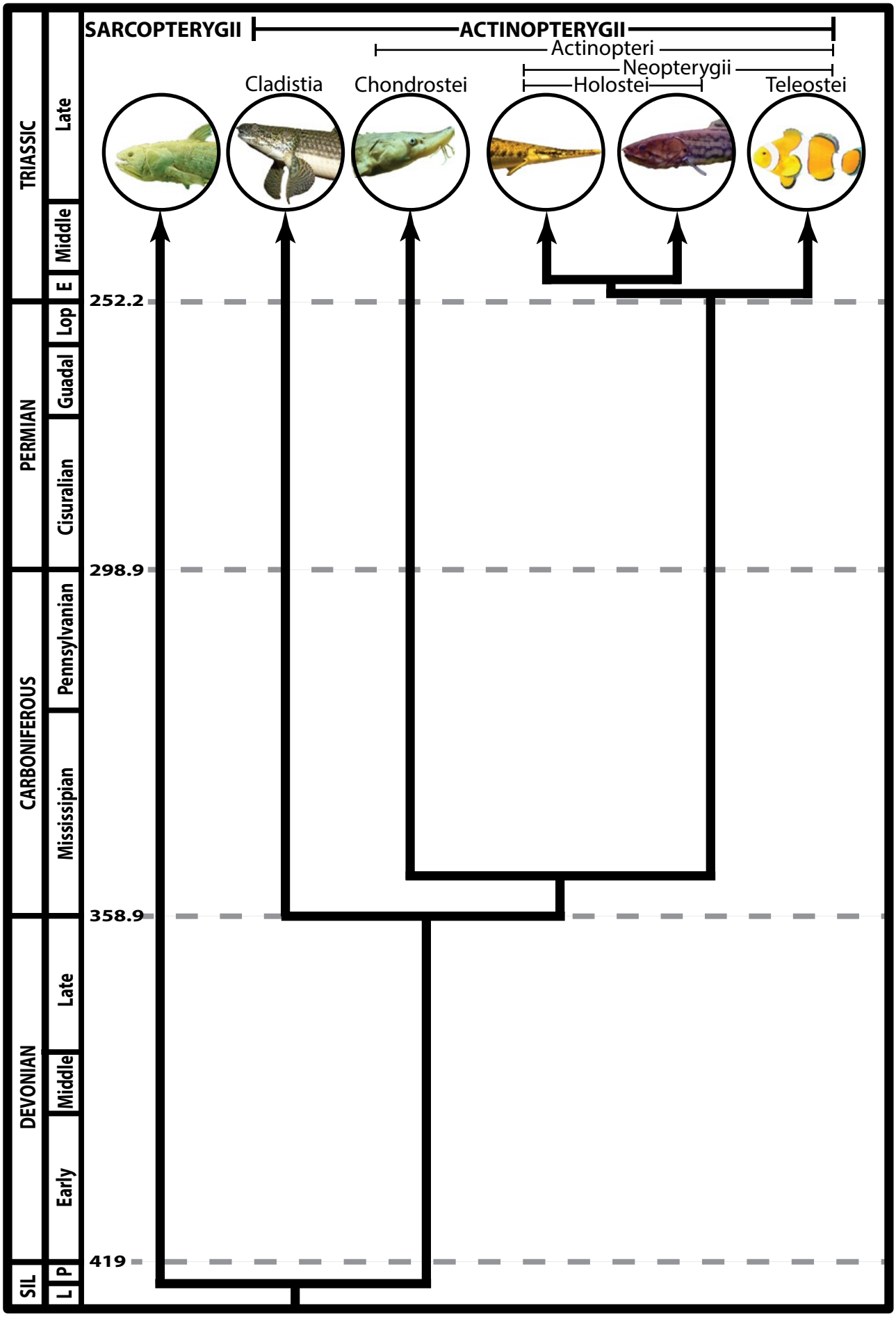
SARCOPTERYGII
ACTINOPTERYGII
Actinopteri
Neopterygii
Holostei
Cladistia
Chondrostei
Teleostei
TRIASSIC
PERMIAN
CARBONIFEROUS
DEVONIAN
SIL
Late
Middle
E
Lop
Guadal
Cisuralian
Pennsylvanian
Mississipian
Late
Middle
Early
L
P
252.2
298.9
358.9
419

Figure 1. Time-calibrated phylogenetic framework of modern actinopterygian lineages and sarcopterygian outgroup. Phylogenetic hypothesis from (Near *et al.* 2012), crown age estimates from (Giles *et al.* 2017). Copyright: *Latimeria* picture by A. Fernandez (in wikemedia commons); *Polypterus* picture by Stan Shebs (in wikimedia commons); remaining pictures are in public domain (in wikimedia commons).

basal plates in median fins; narrow interorbital septum; acrodin caps; ganoin cover of scales and dermal bones (Friedman 2015). Fossil evidence suggests that during the Devonian, actinopterygians remained numerically and morphologically modest, living in the "shadow" of other vertebrates (Sallan & Coates 2010; Friedman & Sallan 2012).

Ray-fins seem to have not been severely affected by the Hangenberg Event, at the end of the Devonian, which is now recognized as a global extinction pulse caused by abiotic factors (Sallan & Coates 2010; Friedman & Sallan 2012; Sallan 2014). The Hangenberg Event is linked with the complete removal or decline of numerous gnathostome groups, including most lobe-fins and †'acanthodians', as well as the emblematic †'placoderms' (Sallan & Coates 2010; Friedman & Sallan 2012; Sallan 2014), and seems to have freed much ecological space for actinopterygian recovery and diversification in the Mississippian. It is in the Lower Carboniferous that ray-fins began to experiment with new body plans (Friedman & Sallan 2012). Examples can be seen in the deep-bodied †platysomoids (Moy-Thomas & Dyne 1938) and †eurynotids (Bradley-Dyne 1939; Sallan & Coates 2013), or the tadpole-shaped †tarrasiids (Moy-Thomas 1934; Lund & Melton 1982). This Early Carboniferous radiation must have also contained some of the earliest members of the actinopterygian crown-group, though only few Paleozoic taxa have been variably allied with it, to date (Patterson 1982; Gardiner & Schaeffer 1989; Coates 1999; Gardiner *et al.* 2005; Hurley *et al.* 2007; Near *et al.* 2012; Broughton *et al.* 2013; Xu *et al.* 2014; Giles *et al.* 2017) see also Chapters 3–4). The presence of representatives of modern clades in the Paleozoic and earliest Mesozoic fossil record is often masked by the primitive/generalized external anatomy of most Paleozoic actinopterygians (conventionally termed "palaeoniscoids", after the archetypal generalized Permian genus †*Palaeoniscum*).

The late Paleozoic actinopterygian record is not as well-known, due to the rarity or restricted nature of such fossiliferous horizons, and their underrepresentation in the scientific literature (Friedman & Sallan 2012; Romano *et al.* 2016) but see e.g., (Aldinger 1937; Dunkle 1939; Schaumberg 1977; Schaeffer & Dalquest 1978; Štamberg 2006). The end-Permian represents the most severe of the "Big Five" Phanerozoic mass extinctions (Raup & Sepkoski 1984), eradicating ~95% of all species on Earth (Benton & Twitchett 2003). Actinopterygians appear less severely affected by this biotic crisis than other organisms, diversifying

during the Early–Middle Triassic, and filling many higher ecological niches that were previously occupied by other animals such as chondrichthyans (Friedman & Sallan 2012; Romano *et al.* 2016). Many fossil groups appear to cross the extinction boundary, with †*Bobasatrania*, †*Pteronisculus*, †*Birgeria* and †*Saurichthys* being some striking examples (Romano *et al.* 2016). The early Mesozoic record of ray-fins is remarkably rich (summarized in (Tintori *et al.* 2014; Romano *et al.* 2016), with remarkably rich faunas known from the Early (e.g., (Stensiö 1921; 1925; 1932; Nielsen 1936; Nielsen 1942; 1949; Lehman 1952; Beltan 1968; Schaeffer & Mangus 1976) and Middle Triassic (Rieppel 1985; Bürgin 1992; Hu *et al.* 2011; Tintori *et al.* 2014). The first unambiguous members of cladistians (polypteriforms and fossil allies; (Giles *et al.* 2017) and neopterygians (Stensiö 1932; Olsen 1984; Arratia 2013) appear in Triassic deposits, but putative relatives of the two might have also been present in the Carboniferous–Permian (Gill 1923; Hurley *et al.* 2007) Chapters 3–4). The ancestry of chondrosteans (acipenseriforms and fossil allies) remains poorly understood (see Chapters 3–4), as the first unambiguous members of the lineage appear in the Early Jurassic (Hilton & Forey 2009). The Middle Triassic actinopterygian radiation, also known as the 'actinopterygian revolution', is accompanied by great increases in taxonomic diversity, evolution of novel body plans and also new feeding and reproductive strategies (Romano *et al.* 2016). Since then, actinopterygian faunas are dominated by neopterygians (Romano *et al.* 2016), which became established as the most speciose and ecologically diverse group of marine vertebrates. Still, the scarcity of Permian fossils and of adequately preserved/described Triassic ones results in a virtual phylogenetic discontinuity between better known Devonian–Carboniferous forms and modern lineages. This knowledge gap hampers our understanding of the interrelationships of early actinopterygians. In turn, the absence of a stable phylogenetic framework does not allow us to fully assess the impact of the end-Permian extinction on life and the timing of origin of the attributes/novelties that influenced the Early–Middle Triassic neopterygian revolution, the largest among vertebrate animals.

Personal motivation

My main motivation for pursuing this thesis stems from the genuine enthusiasm that I have, since my early undergraduate years, for fossil and extant ray-finned fishes and their impressive, but underappreciated, diversity. Early on, I was drawn by their markedly complex anatomy, and the challenge associated with understanding it and unlocking the clues it bears about the eventful and long evolutionary history of the clade, and of vertebrate life as a whole on our blue planet. Apart from the personal aspect, bony fishes can be a particularly useful tool for answering numerous geological and paleobiological questions. As a geologist, and before undertaking this Ph.D. project, the main focus of my research lied mostly on the geological aspect of paleoichthyology. This approach treated fish fossils as a means to understand

depositional environments, changing climatic conditions, and tectonic and hydrological rearrangements at a more or less regional scale. However, it soon became apparent to me that my research asked few questions about the animals themselves, and, thus, provided little to our understanding of the evolution of those organisms. I slowly became interested in how broken remains of fishes could have looked in life, how they could have behaved, and how they were related to each other and to the modern diversity of fishes that surrounds us. This Ph.D. project, kindly offered, supervised and co-developed by my supervisor M. Sánchez-Villagra, gave me a great opportunity to develop a biological and evolutionary background and approach on paleoichthyology. This, in turn, gave me the means to begin treating fossils like living animals, and seek answers for questions pertaining to the greater scheme of things, which is none other than evolution and the tree of life.

Nature of the actinopterygian fossil record and the importance of studying sites of exceptional preservation

Due to their abundance in aquatic fossil assemblages, which can derive from a wide spectrum of paleolatitudes and paleoenvironments, actinopterygians exhibit a particularly rich fossil record, unparalleled by that of other vertebrates. As with most other animals, the largest portion of the anatomy of ray-fins is composed of soft tissues. The paleontological record of soft tissue structures is quite limited, due to the frequent decay of such tissues during fossilization. It is often the case that hypotheses on the evolution of soft tissue anatomical systems rely largely on the study of phylogenetic brackets composed of extant forms (e.g., (Nieuwenhuys 1982; Kotrschal *et al.* 1998; Wilson & Castro 2011), with little or no information coming from fossils. Though extremely rare, exceptionally preserved fossils that exhibit aspects of soft tissue anatomy can lead to leaps in our understanding of the first appearance and evolutionary morphology of specialized organs, and modes of life and behavior. There are numerous examples of the impact of fossilized soft tissues on our understanding of evolution. Some recent ones from the study of fish-like organisms pertain to: modes of axial elongation (Maxwell *et al.* 2013); the evolution of viviparity and internal fertilization (Long *et al.* 2008; Long *et al.* 2014); cardiac evolution and circulation (Maldanis *et al.* 2016), lung homology and evolution across vertebrates (Cupello *et al.* 2017; Lambertz 2017); and the evolutionary morphology of the gastrointestinal tract and the spiral valve (Argyriou *et al.* 2016).

Similarly to soft tissues, fragile skeletal remains of early ontogenetic stages of vertebrates are rarely preserved in the fossil record, with complete ontogenetic trajectories being particularly uncommon, though highly informative for determining character polarity and homology of different structures (e.g., (Cloutier 2010; Sánchez-Villagra 2012). Sites of exceptional preservation, such as the Triassic deposits of Monte San Giorgio, Switzerland, can yield almost complete ontogenetic series. Aside from their potential evolutionary

(phylogenetic) significance, such fossils can provide insights into the reproductive paleobiology and early life history of extinct clades, which can be used to paint a more complete and vivid picture of animal communities in ecosystems from bygone eras.

As a rule, most ray-fin fossils are found in highly stratified deposits, and their rather fragile skeletal elements–when preserved in articulation–are crushed/flattened by the weight of the overlying layers. Therefore, most structures relating to their internal skeletal anatomy are not preserved, or are not observable due to obstruction by the large dermal plates of their dermal skeleton. The overwhelming majority of anatomical descriptions of actinopterygian fossils concentrate on superficial anatomical aspects, while accounts of endoskeletal features are known for only a handful of taxa from the Paleozoic (Watson 1928; Bradley-Dyne 1939; Rayner 1952; Poplin 1974; Schaeffer & Dalquest 1978; Gardiner 1984; Poplin & Véran 1996; Coates 1998; Coates 1999; Hamel & Poplin 2008; Giles *et al.* 2015a; Giles *et al.* 2015b; Pradel *et al.* 2016) and the Triassic (Stensiö 1921; 1925; 1932; Nielsen 1942; 1949; Beltan 1968; Patterson 1975; Olsen 1984; Wu *et al.* 2013; Giles *et al.* 2017). The more complete anatomical information coming from exceptionally preserved, in three dimensions, taxa is indispensable for reconstructing the phylogenetic framework of early actinopterygians (Gardiner & Schaeffer 1989; Coates 1999; Cloutier & Arratia 2004; Gardiner *et al.* 2005; Hurley *et al.* 2007; Mickle *et al.* 2009; Xu & Gao 2011; Wu *et al.* 2013; Xu *et al.* 2014; Giles *et al.* 2015b; Giles *et al.* 2017).

A brief survey through the previously cited, descriptive works, reveals that much of the relevant research on such fossils has been conducted decades ago, with the use of analogue and often destructive techniques that yield results of limited accuracy. Only a tiny fraction of the fossil ray-fin diversity has been investigated. All the above result in a lack of anatomical information, which has had a profoundly negative impact on our understanding of branching patterns and timing, and interrelationships of early ray-fins, as well as their paleobiology (presence or relative development of sensory organs, muscle insertion patterns, putative feeding specializations, etc.). Furthermore, the lack of a stable phylogenetic framework for early actinopterygians, the majority of which do not have closely related relatives surviving to date, does not allow for an accurate assessment of the impact of major events in the history of life, such as the end-Permian mass extinction. Few fossil sites can yield three-dimensionally preserved crania, often enclosed in nodules. Examples of such exquisite preservation can be found in the rich, Early Triassic Lagerstätte deposits of East Greenland (Stensiö 1932; Nielsen 1936; Nielsen 1942; 1949), Spitsbergen (Stensiö 1921; 1925) and Madagascar (Lehman 1952; Beltan 1968). Three-dimensionally preserved fossils can nowadays be imaged with non-invasive computed microtomography methods (μCT) for the production of high-quality digital anatomical models. These models better convey morphological information and are easier to store,

preserve, reproduce and share than their analogue counterparts (e.g., wax models). Moreover, once made available, they can also be then used for conducting downstream analyses (geometric morphometrics, finite element analyses, etc.). The potency of modern imaging methods suggests that they should be used both for extracting information from undescribed fossil taxa, but also for revisiting older anatomical interpretations.

Aims, scope and implications of the present thesis

The present cumulative thesis contains four chapters that are meant for publication, or are already published. They are centered on exploring the paleobiological and phylogenetic potential of exceptionally preserved actinopterygian fossils from the Permian and the Triassic, and attempt to address some of the problems outlined above.

Chapter 1 is led by me, but also includes valuable additions from my coauthors (Argyriou *et al.* 2016). It is focused on the unusual preservation of soft tissue casts of the gastrointestinal tract (GIT) of †*Saurichthys* from Monte San Giorgio, Switzerland. These casts depict faithfully the GIT of the genus, revealing the presence of an anterior, stomach-like compartment, a rather short anterior intestinal portion, a markedly-developed spiral intestine, and a short rectum. It is the first time such information is provided in such detail for a fossil taxon, while previous works were based on more partial specimens, were conducted many decades ago, and have been largely neglected by later authors (e.g., (Neumayer 1919). The GIT anatomy is rigorously compared to that of other extant, but also fossil, actinopterygians, and other piscine vertebrates. Exceptional preservation of the spiral intestine casts opens a rare window into studying the deep-time evolution of this intestinal structure in vertebrates and exploring, for the first time within a broader vertebrate framework, the biological factors that might affect its morphology. We show that the number of spirals in the intestine of vertebrates, including fossil forms like †*Saurichthys*, is influenced by both body size and phylogeny. In addition to the above, we highlight that the high spiral valve turn counts of †*Saurichthys* could be indicative of the energetically demanding lifestyle of a live-bearing predatory actinopterygian.

Chapter 2 is a collaboration led by my colleague Dr. Erin Maxwell, who initiated this work during her postdoc years at the Paleontological Institute and Museum (Maxwell *et al.* 2018). Part of the information and text of the manuscript is based on the work I did, and data I collected, during my PhD. This chapter is aimed at illuminating the ontogenetic changes in anatomy of †*Saurichthys*, as well as the early life history and reproductive biology of those fishes. Again, the deposits of Monte San Giorgio have produced almost complete ontogenetic series for certain species of †*Saurichthys*, represented by few, but exquisitely preserved specimens. These range from tiny embryos in the abdominal cavities of their mothers, to free-

living neonates and juveniles. This chapter builds upon previous research on life history and reproductive biology of the genus (Bürgin 1990; Rieppel 1992; Renesto & Stockar 2009), but is the first one to collectively study all different ontogenetic stages in a fossil actinopterygian. Among the major contributions of this study, are the criteria we provided for distinguishing embryos from cannibalized prey in the abdominal cavity of a female, which can be tested in other fossil species. Moreover, we established ontogenetic markers, based on osteological differences between juveniles and adults. These are expected to be of particular importance to researchers working on the taxonomy of †saurichthyids and other ray-fins, as they provide a basis for distinguishing between juveniles and small sized species in the fossil record. Finally, our observations shed light on the early onset of rostral and tooth formation in †saurichthyids, which are linked to the relative precociality of neonates.

The remaining two chapters (3,4) of this thesis deal with the anatomy and interrelationships of Permian–Triassic actinopterygians. These chapters were led and written by me, but I benefited by extensive discussions and also comments/additions from my coauthors. For conducting this work I was greatly aided by an SNF-funded mobility year at the Friedman lab, at the University of Michigan. The goal of these chapters is to help improve our understanding of the non-teleostean actinopterygian tree of life, while testing several specific hypotheses on their anatomy, paleobiology and phylogenetic relationships. To do so I provided new character information from exceptionally preserved actinopterygian skulls, with the use of potent µCT-aided imaging methods. Chapter 3 examines the endoskeletal anatomy and interrelationships of †*Saurichthys*. During the writing of the first chapter of this thesis, it became apparent to me that morphological characters determining the phylogenetic position of †saurichthyids, and often supporting their association with modern sturgeons and paddlefishes, relied largely on anatomical descriptions of their endoskeletal anatomy that were conducted almost a century ago. The classical anatomical models produced by Stensiö (Stensiö 1925) were produced by analogue, destructive techniques, were somewhat idealized and remained largely unchallenged up until now. My µCT-aided work on a three-dimensionally preserved cranium of †*Saurichthys* from the Early Triassic of East Greenland, and a partially preserved rostrum from the Early Triassic of Nepal, shed light on numerous previously unknown endoskeletal features, and also revealed limitations existing in historical and widely accepted anatomical works. The newly revealed characters were used to update a recently published phylogenetic matrix of Osteichthyes (Giles *et al.* 2017). The phylogenetic analysis did not provide support for the historically proposed affinities between †*Saurichthys* and chondrosteans, but suggests a sister group relationship between †saurichthyids + †birgeriids and crown actinopterygians.

In chapter 4, I employed μCT to study the two known skulls of the Early Permian actinopterygian †*Brachydegma caelatum*. Past interpretations of its external anatomy have assigned this genus a central role in the discussion on early actinopterygian systematics and evolution, establishing it as a model for early neopterygian anatomy (Hurley *et al.* 2007). More specifically, †*Brachydegma* was affiliated with the halecomorph clade, which is nowadays represented by the bowfin (*Amia calva*), though these interpretations were not unanimously accepted. In contrast to †*Saurichthys*, the endocranial anatomy of this genus had been completely unknown, and anatomical information from it could have a more profound effect on tree shape. Moreover, such information would help bridge a major gap in knowledge of endocranial anatomy of late Paleozoic actinopterygians. My work produced the first anatomical models of braincase, branchial and pectoral anatomy for this animal. Newly discovered features were included in a large-scale phylogenetic analysis. The latter does not support a close affinity of †*Brachydegma* with the neopterygian clade, but is suggestive of a more stemward phylogenetic position for the taxon; that of an early, generalized member of the crown. In addition, my work uncovered key anatomical features relating to the jaws and suspensorium of †*Brachydegma*, which were previously thought to be derived, but are now shown to be primitive for crown actinopterygians, or even osteichthyans. Information from this chapter is pivotal for understanding early crown actinopterygian anatomy, and is expected to aid substantially in the recognition of such forms in the Paleozoic fossil record.

Literature cited

Aldinger, H. 1937. Permische Ganoidfische aus Östgrönland. *Meddelelser om Grønland*, **102**(3): 1-392 + 344 tabs.

Argyriou, T., Clauss, M., Maxwell, E.E., Furrer, H. & Sánchez-Villagra, M.R. 2016. Exceptional preservation reveals gastrointestinal anatomy and evolution in early actinopterygian fishes. *Scientific Reports*, **6**: 18758.

Arratia, G. 2013. Morphology, taxonomy, and phylogeny of Triassic pholidophorid fishes (Actinopterygii, Teleostei). *Journal of Vertebrate Paleontology*, **33**(sup1): 1-138.

Arratia, G. & Cloutier, R. 1996. Reassessment of the morphology of *Cheirolepis canadensis* (Actinopterygii). Pp. 165-197 in H.-P. Schultze (ed) *Devonian Fishes and Plants of Miguasha, Quebec, Canada.* Verlag Dr. Friedrich Pfeil, München.

Beltan, L. 1968. La faune ichthyologique de l'Eotrias du N.W. Madagascar: le neurocrâne. *Cahiers de paléontology*: 7-135+131-135+I-Lpl.

Benton, M.J. & Twitchett, R.J. 2003. How to kill (almost) all life: the end-Permian extinction event. *Trends in Ecology & Evolution*, **18**(7): 358-365.

Bradley-Dyne, M. 1939. The skull of *Amphicentrum granulosum*. *Journal of Zoology*, **109**(2): 195-210.

Broughton, R.E., Betancur-R, R., Li, C., Arratia, G. & Ortí, G. 2013. Multi-locus phylogenetic analysis reveals the pattern and tempo of bony fish evolution. *PLoS Currents*, **5**: ecurrents.tol.2ca8041495ffafd8041490c8092756e75247483e.

Bürgin, T. 1990. Reproduction in Middle Triassic actinopterygians; complex fin structures and evidence

of viviparity in fossil fishes. *Zoological Journal of the Linnean Society*, **100**(4): 379-391.

Bürgin, T. 1992. Basal ray-finned fishes (Osteichthyes; Actinopterygii) from the Middle Triassix of Monte San Giorgio (Canton Tessin, Switzerland). *Schweizerische Paläontologische Abhandlungen*, **114**: 1-164.

Cloutier, R. 2010. The fossil record of fish ontogenies: Insights into developmental patterns and processes. *Seminars in Cell & Developmental Biology*, **21**(4): 400-413.

Cloutier, R. & Arratia, G. 2004. Early diversification of actinopterygians. Pp. 217-270 in G. Arratia, M.V.H. Wilson and R. Cloutier (eds) *Recent advances in the origin and early radiation of vertebrates*. Dr. Friedrich Pfeil, München, Germany.

Coates, M.I. 1998. Actinopterygians from the Namurian of Bearsden, Scotland, with comments on early actinopterygian neurocrania. *Zoological Journal of the Linnean Society*, **122**(1-2): 27-59.

Coates, M.I. 1999. Endocranial preservation of a Carboniferous actinopterygian from Lancashire, UK, and the interrelationships of primitive actinopterygians. *Philosophical Transactions of the Royal Society B: Biological Sciences*, **354**(1382): 435-462.

Cupello, C., Meunier, F.J., Herbin, M., Janvier, P., Clément, G. & Brito, P.M. 2017. The homology and function of the lung plates in extant and fossil coelacanths. *Scientific Reports*, **7**(1): 9244.

Darwin, C. 1859. *The origin of species by means of natural selection*. John Murray, London, 502 pp.

Dunkle, D.H. 1939. A new paleoniscid fish from the Texas Permian. *American Journal of Science*, **237**: 262-274.

Eldredge, N. & Stanley, S.M. 1984. *Living fossils*. Springer, New York, Berlin, Heidelberg, Tokyo, 291 pp.

Friedman, M. 2015. The early evolution of ray-finned fishes. *Palaeontology*, **58**(2): 213-228.

Friedman, M. & Sallan, L.C. 2012. Five hundred million years of extinction and recovery: a phanerozoic survey of large-scale diversity patterns in fishes. *Palaeontology*, **55**(4): 707-742.

Gardiner, B., Schaeffer, B. & Masserie, J. 2005. A review of the lower actinopterygian phylogeny. *Zoological Journal of the Linnean Society*, **144**: 511 - 525.

Gardiner, B.G. 1984. The relationships of the palaeoniscid fishes, a review based on new specimens of *Mimia* and *Moythomasia* from the Upper Devonian of Western Australia. *Bulletin of the British Museum (Natural History), Geology series*, **37**(4): 173-428.

Gardiner, B.G. & Schaeffer, B. 1989. Interrelationships of lower actinopterygian fishes. *Zoological Journal of the Linnean Society*, **97**(2): 135-187.

Giles, S., Coates, M.I., Garwood, R.J., Brazeau, M.D., Atwood, R., Johanson, Z. & Friedman, M. 2015a. Endoskeletal structure in *Cheirolepis* (Osteichthyes, Actinopterygii), An early ray-finned fish. *Palaeontology*, **58**(5): 849-870.

Giles, S., Darras, L., Clément, G., Blieck, A. & Friedman, M. 2015b. An exceptionally preserved Late Devonian actinopterygian provides a new model for primitive cranial anatomy in ray-finned fishes. *Proceedings of the Royal Society of London B: Biological Sciences*, **282**(1816).

Giles, S., Xu, G.-H., Near, T.J. & Friedman, M. 2017. Early members of 'living fossil' lineage imply later origin of modern ray-finned fishes. *Nature*, **549**(7671): 265-268.

Gill, E.L. 1923. The Permian Fishes of the Genus Acentrophorus*. *Proceedings of the Zoological Society of London*, **93**(1): 19-40.

Grande, L. 2010. An empirical synthetic pattern study of gars (Lepisosteiformes) and closely related species, based mostly on skeletal anatomy: the resurrection of Holostei. *American Society of Ichthyologists and Herpetologists Special Publication 6 Copeia Suppl*, **10**(2A): 871.

Hamel, M.-H. & Poplin, C. 2008. The braincase anatomy of *Lawrenciella schaefferi*, actinopterygian from the Upper Carboniferous of Kansas (USA). *Journal of Vertebrate Paleontology*, **28**(4): 989-1006.

Helfman, G.S., Collette, B., Facey, D.E. & Bowen, B.W. 2009. *The diversity of fishes*. Wiley-Blackwell, 720 pp.

Hilton, E.J. & Forey, P.L. 2009. Redescription of †*Chondrosteus acipenseroides* Egerton, 1858 (Acipenseriformes, †Chondrosteidae) from the Lower Lias of Lyme Regis (Dorset, England), with comments on the early evolution of sturgeons and paddlefishes. *Journal of Systematic Palaeontology*, **7**(04): 427-453.

Hu, S.-x., Zhang, Q.-y., Chen, Z.-Q., Zhou, C.-y., Lü, T., Xie, T., Wen, W., Huang, J.-y. & Benton, M.J. 2011. The Luoping biota: exceptional preservation, and new evidence on the Triassic recovery from end-Permian mass extinction. *Proceedings of the Royal Society B: Biological Sciences*, **278**(1716): 2274-2282.

Hurley, I.A., Mueller, R.L., Dunn, K.A., Schmidt, E.J., Friedman, M., Ho, R.K., Prince, V.E., Yang, Z., Thomas, M.G. & Coates, M.I. 2007. A new time-scale for ray-finned fish evolution. *Proceedings of the Royal Society of London B: Biological Sciences*, **274**(1609): 489-498.

Kotrschal, K., Van Staaden, M.J. & Huber, R. 1998. Fish Brains: Evolution and Environmental Relationships. *Reviews in Fish Biology and Fisheries*, **8**(4): 373-408.

Lambertz, M. 2017. The vestigial lung of the coelacanth and its implications for understanding pulmonary diversity among vertebrates: new perspectives and open questions. *Royal Society Open Science*, **4**(11).

Lehman, J.P. 1952. Etude complémentaire des poissons de l'Eotrias de Madagascar. *Kungliga Svenska Vetenskapsakademiens Handlingar*, **2**(6): 1-201+201-248pl.

Long, J.A., Mark-Kurik, E., Johanson, Z., Lee, M.S.Y., Young, G.C., Min, Z., Ahlberg, P.E., Newman, M., Jones, R., Blaauwen, J.d., Choo, B. & Trinajstic, K. 2014. Copulation in antiarch placoderms and the origin of gnathostome internal fertilization. *Nature*, **517**: 196.

Long, J.A., Trinajstic, K., Young, G.C. & Senden, T. 2008. Live birth in the Devonian period. *Nature*, **453**(7195): 650-652.

Lu, J., Giles, S., Friedman, M., den Blaauwen, Jan L. & Zhu, M. 2016. The Oldest Actinopterygian Highlights the Cryptic Early History of the Hyperdiverse Ray-Finned Fishes. *Current Biology*, **26**(12): 1602-1608.

Lund, R. & Melton, W.G. 1982. A new actinopterygian fish from the Mississippian Bear Gulch Limestone of Montana. *Palaeontology*, **25**(3): 485-498.

Maldanis, L., Carvalho, M., Almeida, M.R., Freitas, F.I., de Andrade, J.A.F.G., Nunes, R.S., Rochitte, C.E., Poppi, R.J., Freitas, R.O., Rodrigues, F., Siljeström, S., Lima, F.A., Galante, D., Carvalho, I.S., Perez, C.A., de Carvalho, M.R., Bettini, J., Fernandez, V. & Xavier-Neto, J. 2016. Heart fossilization is possible and informs the evolution of cardiac outflow tract in vertebrates. *eLife*, **5**: e14698.

Maxwell, E.E., Argyriou, T., Stockar, R. & Furrer, H. 2018. Re-evaluation of the ontogeny and reproductive biology of the Triassic fish *Saurichthys* (Actinopterygii, Saurichthyidae). *Palaeontology*.

Maxwell, E.E., Furrer, H. & Sanchez-Villagra, M.R. 2013. Exceptional fossil preservation demonstrates a new mode of axial skeleton elongation in early ray-finned fishes. *Nature Communications*, **4**: 2570.

Mickle, K.E., Lund, R. & Grogan, E.D. 2009. Three new palaeoniscoid fishes from the Bear Gulch Limestone (Serpukhovian, Mississippian) of Montana (USA) and the relationships of lower actinopterygians. *Geodiversitas*, **31**(3): 623-668.

Moy-Thomas, J.A. 1934. The Structure and Affinities of Tarrasius probhmaticus Traquair. *Proceedings of the Zoological Society of London*, **104**(2): 367-376.

Moy-Thomas, J.A. & Dyne, M.B. 1938. XVII.—The Actinopterygian Fishes from the Lower Carboniferous of Glencartholm, Eskdale, Dumfriesshire. *Transactions of the Royal Society of Edinburgh*, **59**(2): 437-480.

Near, T.J., Eytan, R.I., Dornburg, A., Kuhn, K.L., Moore, J.A., Davis, M.P., Wainwright, P.C., Friedman, M. & Smith, W.L. 2012. Resolution of ray-finned fish phylogeny and timing of diversification. *Proceedings of the National Academy of Sciences*, **109**(34): 13698-13703.

Nelson, J.S., Grande, T.C. & Wilson, M.V.H. 2016. *Fishes of the world*. John Wiley & Sons, Inc., Hoboken, New Jersey, USA, i-xli + 707 pp.

Neumayer, L. 1919. Vergleichend anatomische Untersuchungen über den Darmkanal fossiler Fische. *Abhandlungen der Bayerischen academie der wissenschaften*, **29**(2): 1-28.

Nielsen, E. 1936. *Some few preliminary remarks on Triassic fishes from East Greenland*. C. A. Reitzels Forlag, Copenhagen, 55 pp.

Nielsen, E. 1942. *Studies on the Triassic fishes from East Greenland I. Glaucolepis and Boreosomus*. C.A. Reitzels, Copenhagen, 394 + 330 pl. pp.

Nielsen, E. 1949. *Studies on Triassic fishes II. Australosomus and Birgeria*. Universitetets zoologiske museum og universitetes mineralogisk-geologiske museum, Copenhagen, 309 + 320pl. pp.

Nieuwenhuys, R. 1982. An Overview of the Organization of the Brain of Actinopterygian Fishes. *American Zoologist*, **22**(2): 287-310.

Olsen, P.E. 1984. The skull and pectoral girdle of the parasemionotid fish *Watsonulus eugnathoides* from the Early Triassic Sakamena Group of Madagascar, with comments on the relationships of the holostean fishes. *Journal of Vertebrate Paleontology*, **4**(3): 481-499.

Patterson, C. 1973. Interrelationships of holosteans. Pp. 233-305 in P.H. Greenwood, R.S. Miles and C. Patterson (eds) *Interrelationships of fishes*. Academic Press, London.

Patterson, C. 1975. The braincase of Pholidophorid and Leptolepid fishes, with a review of the Actinopterygian braincase. *Philosophical Transactions of the Royal Society of London. B, Biological Sciences*, **269**(899): 275-579.

Patterson, C. 1982. Morphology and Interrelationships of Primitive Actinopterygian Fishes. *American Zoologist*, **22**(2): 241-259.

Pearson, D.M. & Westoll, T.S. 1979. The Devonian actinopterygian *Cheirolepis* Agassiz. *Earth and Environmental Science Transactions of the Royal Society of Edinburgh*, **70**(13-14): 337-399.

Poplin, C. 1974. Étude de quelques paléoniscidés pennsylvaniens du Kansas. *Cahiers de paléontology*: 1-148+I-XL pl.

Poplin, M. & Véran, M. 1996. A revision of the actinopterygian fish *Coccocephalus wildi* from the Upper Carboniferous of Lancashire. *Special Papers in Palaeontology*, **52**: 7-30.

Pradel, A., Maisey, J.G., Mapes, R.H. & Kruta, I. 2016. First evidence of an intercalar bone in the braincase of "palaeonisciform" actinopterygians, with a virtual reconstruction of a new braincase of *Lawrenciella* Poplin, 1984 from the Carboniferous of Oklahoma. *Geodiversitas*, **38**(4): 489-504.

Raup, D.M. & Sepkoski, J.J. 1984. Periodicity of extinctions in the geologic past. *Proceedings of the National Academy of Sciences of the United States of America*, **81**(3): 801-805.

Rayner, D.H. 1952. III.—On the Cranial Structure of an Early Palæoniscid, *Kentuckia*, gen. nov. *Transactions of the Royal Society of Edinburgh*, **62**(1): 53-83.

Renesto, S. & Stockar, R. 2009. Exceptional preservation of embryos in the actinopterygian *Saurichthys* from the Middle Triassic of Monte San Giorgio, Switzerland. *Swiss Journal of Geosciences*, **102**(2): 323-330.

Rieppel, O. 1985. Die Triasfauna der Tessiner Kalkalpen XXV: die Gattung *Saurichthys* (Pisces, Actinopterygii) aus der mittleren Trias des Monte San Giorgio, Kanton Tessin. *Schweizerische Paläontologische Abhandlungen*, **108**: 1 - 103.

Rieppel, O. 1992. A new species of the genus Saurichthys (Pisces: Actinopterygii) from the Middle Triassic of Monte San Giorgio (Switzerland), with comments on the phylogenetic interrelationships of the genus. *Palaeontographica Abt A*, **221**(1-3): 63 - 94.

Romano, C., Koot, M.B., Kogan, I., Brayard, A., Minikh, A.V., Brinkmann, W., Bucher, H. & Kriwet, J. 2016. Permian–Triassic Osteichthyes (bony fishes): diversity dynamics and body size evolution. *Biological Reviews*, **91**(1): 106-147.

Sallan, L.C. 2014. Major issues in the origins of ray-finned fish (Actinopterygii) biodiversity. *Biological Reviews*, **89**(4): 950-971.

Sallan, L.C. & Coates, M.I. 2010. End-Devonian extinction and a bottleneck in the early evolution of modern jawed vertebrates. *Proceedings of the National Academy of Sciences*, **107**(22): 10131-10135.

Sallan, L.C. & Coates, M.I. 2013. Styracopterid (Actinopterygii) ontogeny and the multiple origins of post-Hangenberg deep-bodied fishes. *Zoological Journal of the Linnean Society*, **169**(1): 156-199.

Sánchez-Villagra, M.R. 2012. *Embryos in deep time : the rock record of biological development*. University of California Press, Berkeley, Los Angeles, London, 256 pp.

Schaeffer, B. & Dalquest, W.W. 1978. A palaeonisciform braincase from the Permian of Texas, with comments on cranial fissures and the posterior myodome. *American Museum Novitates*, **2658**: 1-15.

Schaeffer, B. & Mangus, M. 1976. An Early Triassic fish assemblage from British Columbia. *Bulletin of the American Museum of Natural History*, **156**(5): 515-564.

Schaumberg, E. 1977. Der Richelsdorfer Kupferschiefer und seine Fossilien, III. Die tierischen Fossilien des Kupferschiefers 2. Vertebraten. *der Aufschluss*, **28**: 297-352.

Štamberg, S. 2006. Carboniferous-Permian actinopterygian fishes of the continental basins of the Bohemian Massif, Czech Republic: an overview. *Geological Society, London, Special Publications*, **265**(1): 217-230.

Stensiö, E.A. 1921. *Triassic fishes from Spitzbergen (Part 1)*. Adolf Holzhausen, Vienna, 307+335 plates pp.

Stensiö, E.A. 1925. *Triassic fishes from Spitzbergen*. Almqvist & Wiksells Boktryckeri-A.-B., Stockholm.

Stensiö, E.A. 1932. *Triassic fishes from East Greenland*. Bianco Lunos Bogtrykkeri A/S, Copenhagen, 305 + XXXIX pl. pp.

Tintori, A., Hitij, T., Jiang, D., Lombardo, C. & Sun, Z. 2014. Triassic actinopterygian fishes: the recovery after the end-Permian crisis. *Integrative Zoology*, **9**(4): 394-411.

Watson, D.M.S. 1928. On some Points in the Structure of Palæoniscid and allied Fish. *Proceedings of the Zoological Society of London*, **98**(1): 49-70.

Wilson, J. & Castro, L. 2011. Morphological diversity of the gastrointestinal tract in fishes. Pp. 1-55 in M. Grosell, A. Farrell and C. Brauner (eds) *The multifunctional gut of fish*. Academic Press, U.S.A.

Wu, F., Chang, M.-m., Sun, Y. & Xu, G. 2013. A new saurichthyiform (Actinopterygii) with a crushing feeding mechanism from the Middle Triassic of Guizhou (China). *PLoS ONE*, **8**(12): e81010.

Xu, G.-H. & Gao, K.-Q. 2011. A new scanilepiform from the Lower Triassic of northern Gansu Province, China, and phylogenetic relationships of non-teleostean Actinopterygii. *Zoological Journal of the Linnean Society*, **161**(3): 595-612.

Xu, G.-H., Gao, K.-Q. & Finarelli, J.A. 2014. A revision of the Middle Triassic scanilepiform fish *Fukangichthys longidorsalis* from Xinjiang, China, with comments on the phylogeny of the Actinopteri. *Journal of Vertebrate Paleontology*, **34**(4): 747-759.

Zhu, M., Yu, X. & Janvier, P. 1999. A primitive fossil fish sheds light on the origin of bony fishes. *Nature*, **397**: 607.

Zhu, M., Zhao, W., Jia, L., Lu, J., Qiao, T. & Qu, Q. 2009. The oldest articulated osteichthyan reveals mosaic gnathostome characters. *Nature*, **458**(7237): 469-474.

Chapter I

www.nature.com/scientificreports

SCIENTIFIC REPORTS

OPEN

Exceptional preservation reveals gastrointestinal anatomy and evolution in early actinopterygian fishes

Received: 30 September 2015
Accepted: 25 November 2015
Published: 06 January 2016

Thodoris Argyriou[1], Marcus Clauss[2], Erin E. Maxwell[3], Heinz Furrer[1] & Marcelo R. Sánchez-Villagra[1]

Current knowledge about the evolutionary morphology of the vertebrate gastrointestinal tract (GIT) is hindered by the low preservation potential of soft tissues in fossils. Exceptionally preserved cololites of individual †*Saurichthys* from the Middle Triassic of Switzerland provide unique insights into the evolutionary morphology of the GIT. The GIT of †*Saurichthys* differed from that of other early actinopterygians, and was convergent to that of some living sharks and rays, in exhibiting up to 30 turns of the spiral valve. Dissections and literature review demonstrate the phylogenetic diversity of GIT features and signs of biological factors that influence its morphology. A phylogenetically informed analysis of a dataset containing 134 taxa suggests that body size and phylogeny are important factors affecting the spiral valve turn counts. The high number of turns in the spiral valve of †*Saurichthys* and some recent sharks and rays reflect both energetically demanding lifestyles and the evolutionary histories of the groups.

The anatomy of the vertebrate gastrointestinal tract (GIT) reflects many aspects of organismal biology, including diet and feeding habits and hence trophic position, nutrient uptake capabilities, osmoregulation and metabolism[1,2]. Although a broad evolutionary perspective on the digestive system has been achieved by studying the distribution of the GIT morphologies in extant vertebrates[1–3], much information is missing due to the vast proportion of vertebrate animals that are now extinct. This is especially true for actinopterygians (ray-finned fishes), the most speciose group of vertebrates[4,5]. Whereas GIT diversity of derived actinopterygians (teleosts) is well documented, this is not the case for the non-teleostean actinopterygians, which are represented in the modern fauna by a few depauperate lineages: bichirs and reedfish (two genera and 16 species), sturgeons and paddlefishes (five genera and 27 species), gars (two genera and seven species) and the bowfin (one species)[4]. These taxa exhibit plesiomorphic GIT morphologies, including the presence of a spiral valve in the posterior part of the intestine (also known as the spiral or valvular intestine) that are reminiscent of those seen in living chondrichthyans and differ from those of teleosts[2,3,6].

The spiral valve is formed by the intestinal mucosa and submucosa and resembles a spiral staircase extending along part of the length of the posterior mid-gut[3,6]. This structure differentiates in ontogeny as an invagination of the intestinal epithelium. The resulting crest, due to significant posteroanterior growth, twists around the median axis of the intestine forming successive spirals[3,6,7]. In several taxa, the initial crest wraps around the median axis of the intestine forming the "scroll valve"[3,6,7]. A spiral or scroll valve in the posterior part of the intestine is a plesiomorphic feature shared amongst chondrichthyans (including most "†acanthodians"), non-teleostean actinopterygians, non-tetrapod sarcopterygians (including extant lungfishes that possess a spiral valve and extant coelacanths that possess a scroll valve) and likely "†placoderms"[8]. The presence of a scroll valve has also been suggested for some early Paleozoic jawless vertebrates[9,10] whereas modern lampreys, but not hagfishes, also exhibit a reduced spiral valve[3,6]. The spiral valve is clearly a character that appeared very early in the evolution of vertebrates.

[1]Paleontological Institute and Museum, University of Zurich, 8006 Zurich, Switzerland. [2]Clinic for Zoo Animals, Exotic Pets and Wildlife, Vetsuisse Faculty, University of Zurich, 8057 Zurich, Switzerland. [3]Stuttgart State Museum of Natural History, 70191 Stuttgart, Germany. Correspondence and requests for materials should be addressed to T.A. (email: argthod@gmail.com)

Most paleontological perspectives on the vertebrate GIT are based on indirect evidence from fossilized faeces (coprolites)[11] because the corresponding soft tissues are highly susceptible to decay and early loss during fossilization[12]. Stomach contents can provide some insights into GIT morphology but have been historically used for tracing feeding habits and trophic positions of extinct organisms[13]. In rare cases, internal casts of the GIT, deriving from fossilized chyme and/or faecal matter and termed "cololites"[14], are preserved in the fossil record[11]. Cololite studies are scarce, mostly because GIT casts associated with taxonomically recognizable individuals are rarely preserved[8,15] (see also Supplementary Table 1 for additional references). Cololites can reflect the gross morphology of the GIT and can provide insights into the biology and phylogeny of the studied organisms.

†Saurichthyids, known from latest Permian to Early Jurassic deposits worldwide, were highly specialized, predatory, non-neopterygian actinopterygians that shared an elongate body, an elongated preorbital region and posteriorly situated median fins[16–18]. Recent phylogenetic analyses consistently place †*Saurichthys*, the most salient genus of this "family", as closely related to or part of the chondrostean clade and, often, close to the Triassic fish †*Birgeria*[19–22] (but see ref. 19: Fig. 9A for an alternate placement of †*Saurichthys*).

As for most fossil organisms, little is known about the soft tissue anatomy of †*Saurichthys*[16,23]. Here, we provide the first detailed description of cololites from Middle Triassic species of †*Saurichthys* that constitute a rare and key source of data for studying the evolution of the GIT in early actinopterygians and fishes in general. The striking dissimilarity of the GIT morphology of †*Saurichthys*, and markedly that of its spiral intestine, to that of extant actinopterygians raises some paleobiological questions. We review the distribution of different morphologies of the GIT across extant and extinct fishes (including elasmobranchs, sarcopterygians and actinopterygians) in order to trace factors including body size, diet, lifestyle and phylogeny that may correlate with different GIT morphologies.

Results

***†Saurichthys costasquamosus*.** Specimen MCSN 5696 (Fig. 1a,b) is an almost complete individual, only missing the anterior half of its rostrum. Total Length (TL) is slightly over 30 cm and thus smaller than the maximum known size for this species (up to 83 cm)[23]. Fossilized gut contents span almost the entire Abdominal Cavity Length (ACL). A complete individual of an early actinopterygian (cf. †*Luganoia*) is preserved as undigested prey in the abdominal cavity just posterior to the head. The prey occupies almost 40% of the ACL (25 vertebral segments[16]), was swallowed head first, and is arranged in an almost straight, uncoiled manner, reflecting the anatomy of the containing GIT chamber. The contained prey, due to its size, bulges out to the venter of the abdominal cavity of the predator. The distensibility of this GIT segment suggests that it is a true straight stomach rather than a pseudogaster (stomach-like thickening of the midgut seen in some agastric species)[2,6,13].

Posterior to the head of the prey fish, the GIT chamber tapers and leads to an amorphous digestal cloud that corresponds topologically to the pyloric caeca. However, this structure does not exhibit any morphological (e.g., vermiform) patterns expected of pyloric caeca. We attribute its formation to tearing of the anterior intestine. Posterior to the digestal cloud, the substantial part of the three-dimensional cololite is observed. It measures 36.7 mm in length (23.3% of the ACL), 3.2 mm in height and spans 15 vertebral segments (30 neural arch-like elements[16]). The surface of the cololite was secondarily smoothened but several visible constrictions indicate the presence of a spiral valve that formed more than 17 turns. No gut infilling was preserved in the area between the end of the cololite and the anal opening. At least part of this empty area was presumably occupied by the rectum.

***†Saurichthys macrocephalus*.** The body of PIMUZ T 3916 is coiled in an S-shape and its head is detached[23] (Fig. 1c). The TL is approximately 24 cm and, thus, smaller than the maximum TL for this species (66 cm, PIMUZ T 5631). Much of the GIT is well-preserved as a flattened white ribbon within the abdominal cavity[23] (Fig. 1c, S1). Visible divisions of the GIT include the putative stomach, a short anterior intestine and part of the spiral intestine (Fig. 1d). The posterior end is obstructed by the pelvic bones, the ventrolateral scale row, and by a small cloud of faecal matter that likely escaped from the intestine after the latter was ruptured.

We refer to the straight and somewhat thickened part of the GIT, connecting the oesophagus to the anterior intestine, as the "stomach". The absence of any sign of a pyloric valve, separating the "stomach" from the intestine, allows us to only tentatively identify a division between the two (Fig. 1c,d, S1). The preserved part of the "stomach" measures 15.3 mm, it spans ~16 neural arch-like elements (~eight vertebral segments[16]) and is straight, without an externally differentiated cardiac and pyloric part. The preserved segment seems to correspond to less than half of the organ's length. The height of the organ is approximately 2.8 mm for most of its length but gradually tapers near the presumed transition to the anterior intestine.

The region we identify as the anterior intestine maintains a constant height, between 1.3 and 1.6 mm, along its length (Fig. 1c,d). The observed coil must have formed post mortem, due to elastic recoil of the GIT after the detachment of the head. The spiral intestine exhibits a larger diameter than the anterior intestine, with its depth reaching 1.9 mm. Approximately 17 constrictions on the preserved part of the spiral intestine correspond to spiral valve turns. The caudal part of the cololite is partially obscured by a digestal cloud and skeletal elements. The total turn count is estimated to have been comparable to that of †*S. paucitrichus* (see below).

***†Saurichthys paucitrichus*.** The specimen (PIMUZ T 59) has an estimated TL of 21.5 cm and ACL of 7.5 cm and exhibits a well-preserved, three-dimensional cololite of the post-gastric portion of the GIT (Fig. 2a–c). This corresponds to part of the anterior intestine, which is uncoiled, the complete spiral intestine and likely the cranial tip of the rectum. The cololite's longitudinal axis is straight and runs parallel to the notochord, along the ventral part of the abdominal cavity. The anterior part of the cololite corresponds to part of the non-spiral anterior intestine and measures 3.9 mm in length (19% of the ACL), 0.6 mm in height and spans approximately three vertebral segments (six neural arch-like elements[16]).

The largest portion of the cololite is 29 mm in length (38.7% of the ACL), corresponds to the spiral intestine, forms 30 turns and spans approximately 27 to 28 neural arch-like elements (14 vertebral segments[16]). When viewed

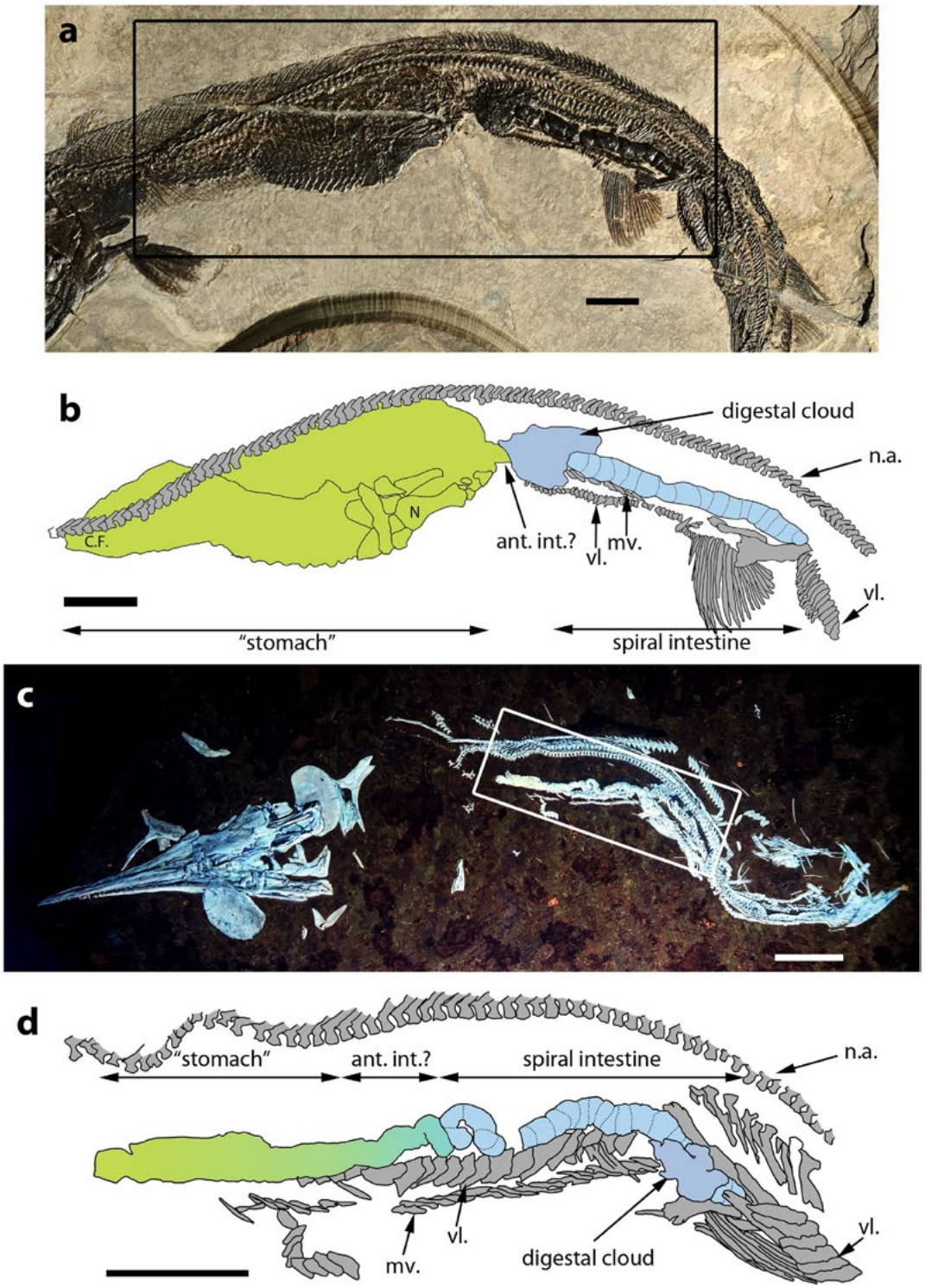

Figure 1. †*Saurichthys* specimens with preserved GIT casts. (**a**) †*Saurichthys costasquamosus* (MCSN 5696) with undigested actinopterygian prey (cf. †*Luganoia*) followed by a three dimensional spiral cololite. The area of interest is delineated by a box; (**b**) Interpretative drawing of the area of interest of the previous specimen. Scales of the midlateral row were omitted; (**c**) †*Saurichthys macrocephalus* (PIMUZ T 3916), photographed under UV light, with a two dimensional cololite present, extending from the stomach to the spiral intestine. The area of interest is delineated by a box; (**d**) interpretative drawing of the area of interest around the cololite. Abbreviations are as follows: ant.int.: anterior intestine; C.F.: caudal fin of the contained prey; mv.: medioventral scale row; N.: neurocranium of the contained prey; n.a.: neural arch-like elements; vl: ventrolateral scale row. All scale bars equal 1 cm.

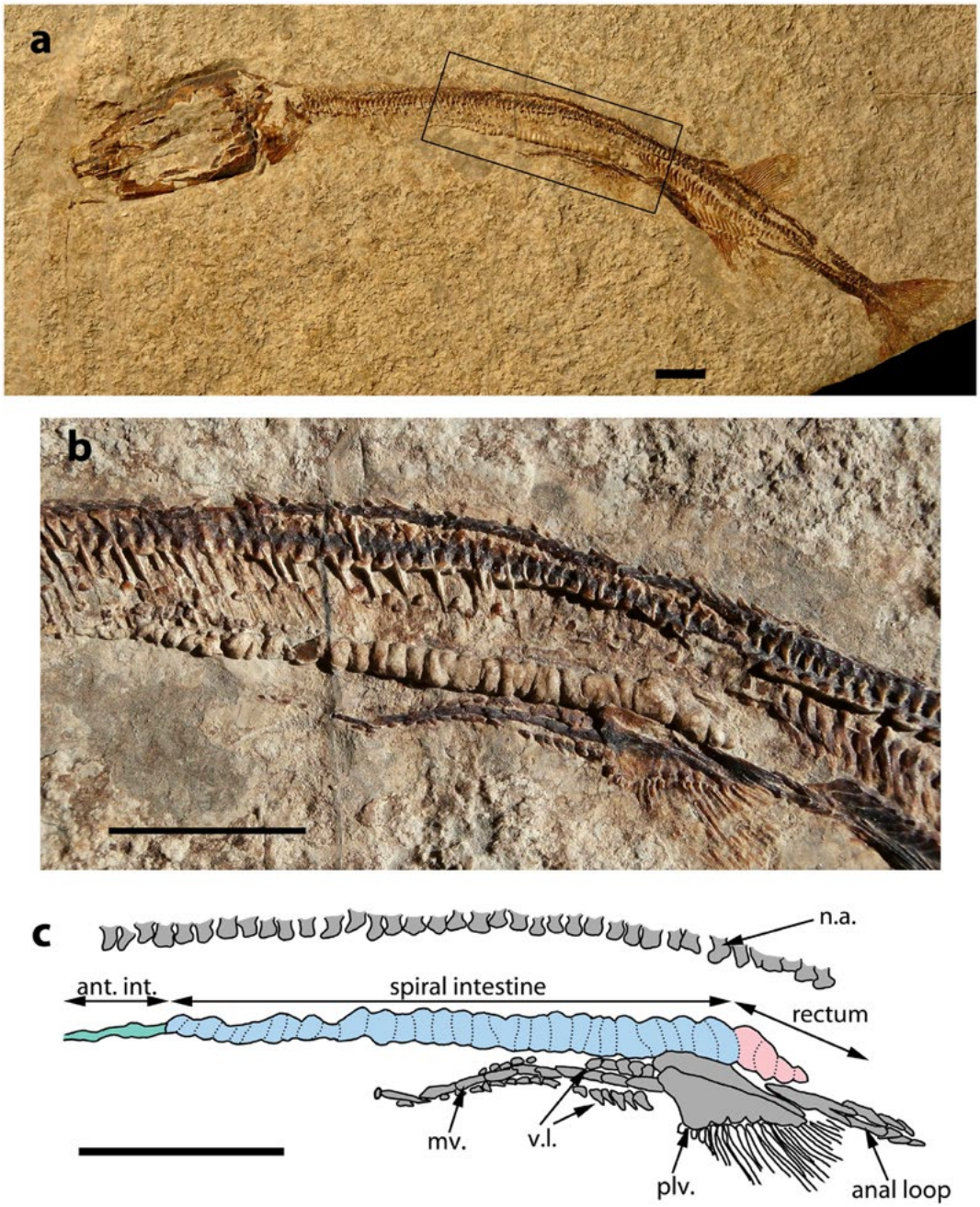

Figure 2. †*Saurichthys paucitrichus* with preserved GIT cast. (**a**) †*Saurichthys paucitrichus* (PIMUZ T 59) with a three dimensional intestinal cololite preserved *in situ*, the area of interest is delineated by a box; (**b**) Detail of the area of interest containing the spiral cololite in the previous specimen; (**c**) Interpretative drawing of the spiral cololite of the previous specimen. Abbreviations are as follows: ant.int.: anterior intestine; mv.: medioventral scale row; n.a.: neural arch-like elements; plv.: pelvic bone; vl: ventrolateral scale row. All scale bars equal 1 cm.

from anterior, the spiral part of the cololite exhibits a counter-clockwise spiral coiling pattern. The valvate portion gradually increases in height to 2 mm. The posterior-most part of the cololite tapers off before reaching the cloaca, which is delineated by the scales of the mid-ventral scale row that form a loop around the cloaca (anal loop). The individual turns are tightly packed and maintain a relatively constant width of 0.8–1 mm. The cranial portion of the spiral cololite indicates that the fecal ribbon wrapped around a median axis (typhlosole in life) without forming overlapping cones. This suggests that the radius of the mucosal folds was not larger than that of the intestinal casing and is similar to Parker's "type B"[24].

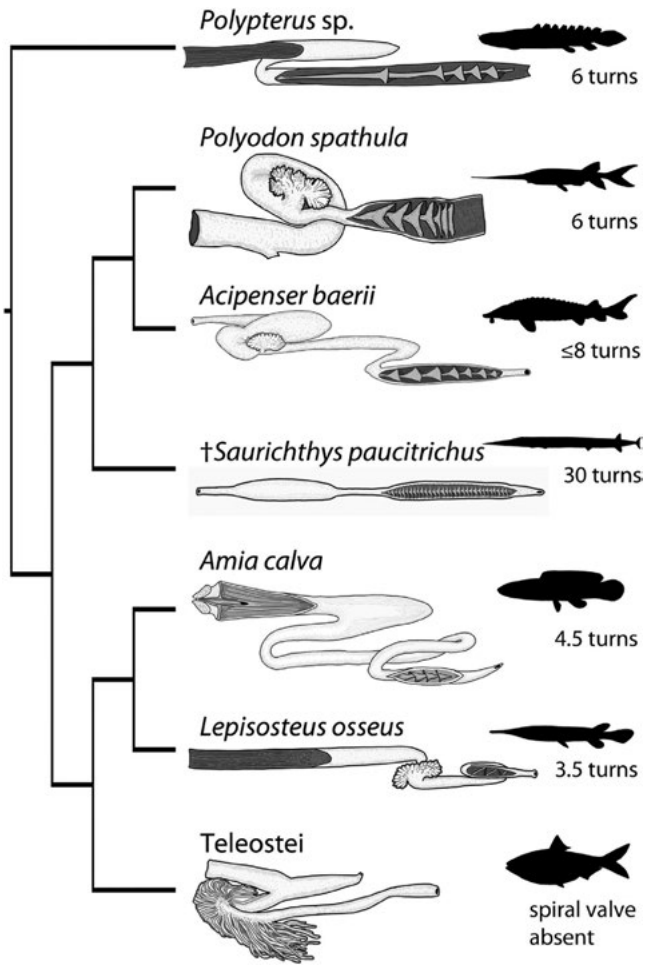

Figure 3. Phylogenetic framework of GIT morphology and spiral valve turn counts of actinopterygians, including †*Saurichthys paucitrichus*. Phylogenetic hypothesis based on refs 5,20. Interpretative drawings of GITs of *Polypterus*, *Polyodon spathula*, *Lepisosteus osseus* and the teleost *Alosa* redrawn and modified from ref 27. The interpretative drawing of the *Amia calva* GIT is redrawn and modified from ref 7. The drawings of the *Acipenser baerii* and †*S. paucitrichus* GITs are based on our observations. All drawings depict the GIT in ventral view with foregut to the left and hindgut to the right.

A thickening and deformation of the cololite is visible at the level of the 30th turn of the spiral valve. The last 4 mm of the cololite, including three to four additional turns, were likely preserved inside the rectum. The rectum measures 7.5 mm or 10% of the ACL.

Comparisons with other taxa. One striking difference between GIT anatomy in †*Saurichthys* and extant non-teleostean actinopterygians is the linear arrangement of the GIT in the former. All known non-teleostean actinopterygians show either an S-shaped arrangement (*Polypterus*, *Acipenser*, *Polyodon*) or a more complex arrangement consisting of two intestinal loops (*Lepisosteus*, *Amia*) (Fig. 3, S4,5).

The stomach of basal actinopterygians shows an array of forms. In extant lepisosteiforms[25] and in †*Saurichthys* the stomach is straight, tube-shaped, and the cardiac and pyloric regions cannot be macroscopically differentiated. However, in extant lepisosteiforms the stomach is easily distinguishable from the intestine in having a larger diameter and clearly tapering caudal end[25]. In †*Saurichthys macrocephalus* (Fig. 1c) there is no clear constriction between the stomach and the intestine that could correspond to a pyloric valve. Therefore, the lack of a stomach cannot be ruled out. This agastric condition occurs in some extant teleosts but is unknown in extant non-teleostean actinopterygians[2,6,13]. Stomachs of other extant non-teleostean actinopterygians exhibit macroscopically recognizable cardiac and pyloric portions. In *Polypterus* the stomach is Y-shaped (cecal [sic] type[26]) forming posterior caecum-like structures that increase the storage capabilities of the organ[27] (Fig. 3.). In acipenseriforms (S4,5) and *Amia* the stomach is U-shaped[25,28–30] (Fig. 3).

In †*Saurichthys,* the anterior intestine appears to be short and straight (Figs 1c,d and 2b,c). Short anterior intestines are also seen in *Polypterus* and *Polyodon* (S5), but they form a curvature before connecting to the spiral intestine[27,30]. In acipenserids the anterior intestine is slightly longer and is arranged in an S-shaped manner[29,31](S4). The gars and the bowfin have longer anterior intestines that are more coiled than in more basal taxa, forming two loops[25,28].

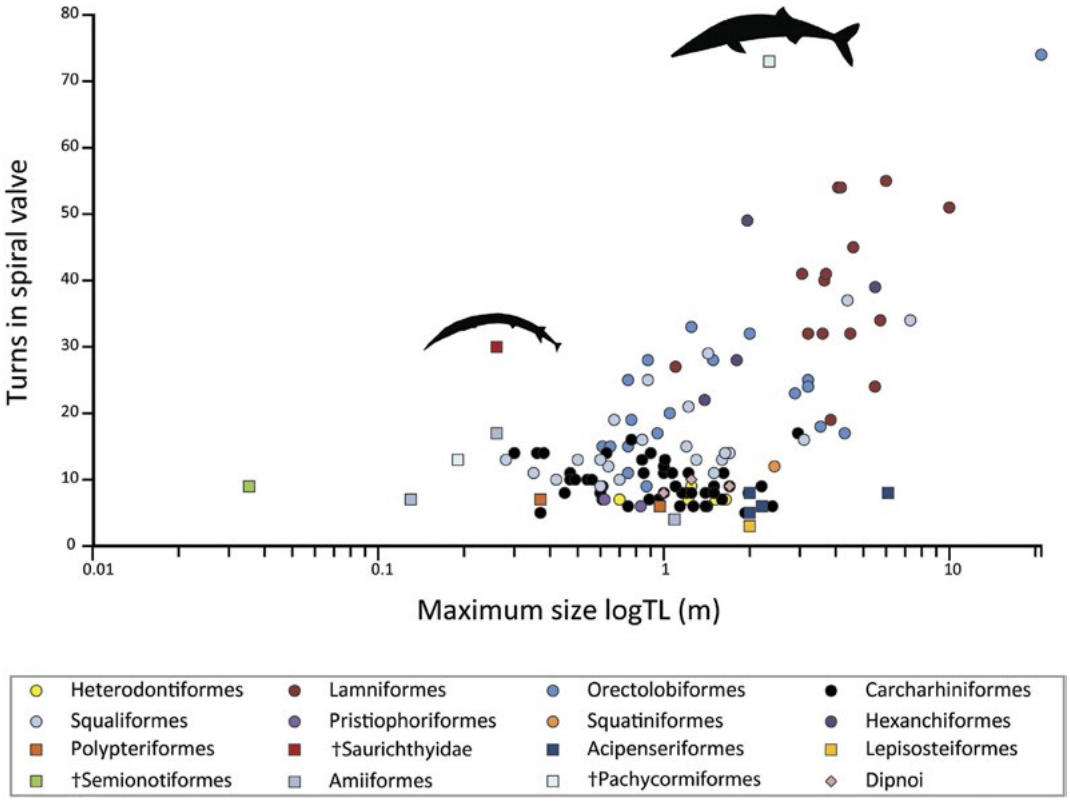

Figure 4. Relationship between maximum body size (logTL) and maximum spiral valve turn counts. Data and references in ST1. Different fish groups ("orders") are color coded. Elasmobranchs: The general trend of turn increase with body size is evident. However, the constancy or decreased variability of turn counts within groups is also marked. †*Saurichthys paucitrichus* (PIMUZ T 59, thinner black outline) and †*Asthenocormus titanius* (thicker black outline) plot as outliers, exhibiting a much higher turn count than all extant osteichthyans and elasmobranchs of similar size. It should be noted that extant osteichthyans tend to exhibit fewer turns than most elasmobranchs despite achieving moderate body sizes.

Dataset	Statistics	λ (95% CI)	a (95% CI)	t	p	b (95% CI)	t	p	AIC
Including osteichthyans	OLS	(0)	12.4 (10.3;14.4)	47.161	<0.001	0.35 (0.24;0.47)	6.108	<0.001	34.408
(n = 134)	PGLS[1]	1.000 (0.963;NA)	10.9 (8.0;13.9)	5.809	<0.001	0.11 (0.01;0.21)	2.094	0.038	−44.016
Elasmobranchs only	OLS	(0)	12.5 (10.4;14.6)	50.558	<0.001	0.47 (0.35;0.58)	7.939	<0.001	−7.430
(n = 117)	PGLS[2]	0.982 (0.933;NA)	13.8 (11.5;16.2)	14.327	<0.001	0.19 (0.11;0.27)	4.630	<0.001	−153.952

Table 1. Statistical analysis of the relationship between TL and spiral valve turn count of fishes. Statistical analyses of the relationship between the maximum length of species (x) and the maximum number of turns in their spiral valve (y) according to $y = a\,x^b$ (for analysis by linear regression, values were log-transformed), using Ordinary Least Squares (OLS) or Phylogenetic Generalized Least Squares (PGLS). Data from Supplementary Table 1. NA not applicable. [1]with branch lengths set to 1.0. [2]including branch lengths.

†*Saurichthys* deviates from the common conicospiral condition (mucosa forming a median typhlosole and overlapping cones) seen in living non-teleostean actinopterygians, approaching the ring-type condition seen in some extant elasmobranchs[2,6] and some fossil †pachycormids[15,26,32]. The most striking aspect is the number of turns of the spiral valve (up to 30). Extant non-teleostean actinopterygians exhibit between 3.5 to 8 turns[25,27–31,33] (Fig. 3; Supplementary Table 1). Several Mesozoic actinopterygians exhibited a low spiral valve turn count, comparable to that of extant species[15], but the †pachychormid †*Asthenocormus titanius* is a notable exception, with a turn count >70[15]. Some 17 turns were also described for intestines of †*Amblysemius pachyurus*[15]. The rectum was short in †*Saurichthys*, comparable to extant non-teleostean actinopterygians.

A statistical evaluation of the association of maximum body length and maximum turns of the spiral valve (Supplementary Table 1) indicates a significant increase in the number of turns with increasing body size (Fig. 4), both in Ordinary Least Squares (OLS, without accounting for the phylogenetic structure of the dataset) and in Phylogenetic Generalized Least Squares (PGLS, i.e. with accounting for the phylogenetic structure of the dataset), in the complete dataset and the dataset of sharks only (Table 1). In both datasets, the phylogenetic signal λ is not different from 1, and the PGLS model has a lower AIC than the OLS model, indicating that there is phylogenetic structure in the dataset. Visually, this structure corresponds to the statistical result that, when accounting for

phylogeny, the increase in the number of turns with body size is much less steep, and because the number of turns is taxon-specific, the confidence interval of the intercept increases (Table 1).

Discussion

†*Saurichthys* possessed a short GIT that spanned the length of the abdominal cavity and consisted of a straight stomach or, less likely, a pseudogaster, a short anterior intestine and a markedly developed spiral intestine, all arranged in a linear manner. The presence of a straight stomach is a rare condition found in some carnivorous actinopterygian fish clades (convergently evolved in lepisosteiforms and esociforms) and is considered a precursor of stomach loss[2]. Stomach loss occurred independently in lampreys, chimaeras and several teleost groups including cypriniforms, beloniforms, labrids, and tetraodontiforms, among others[2,6].

†*Saurichthys* swallowed their prey whole and unchewed[23] (Fig. 1a,b; S1). In addition, the intestinal contents in †*Saurichthys* are homogeneous and do not exhibit macroscopically recognizable bony elements. These facts suggest a reliance on chemical digestion that probably involved a true stomach, rendering an agastric condition in †*Saurichthys* unlikely. The apparent absence of any trace of pyloric caeca can be attributed to either incomplete preservation or to an actual absence of pyloric caeca in †*Saurichthys*. The second possibility is more likely because extant agastric actinopterygians as well as actinopterygians with straight stomachs do not possess pyloric caeca[34]. Gars deviate from this pattern and exhibit well-developed caeca[25] (TA pers. obs. on *Lepisosteus osseus*), as do most carnivorous actinopterygians[34].

A spirally coiled portion indicating the presence of a spiral valve with a very high turn count is a remarkable feature of †*Saurichthys* cololites. The main function of the spiral valve is to increase the length of the intestinal lumen, and therefore maximize the effective surface for absorption and enzymatic digestion while maintaining a relatively short intestinal casing[2,6]. The spiral valve can increase the intestinal surface threefold (ring-type valves without a median typhlosole) to sixfold (strongly conicospiral valves)[7]. Fishes with a spiral valve have shorter overall intestinal lengths than other species[35], conserving space in the abdominal cavity for other purposes (such as developing embryos)[36]. These two features characterize †*Saurichthys*. In contrast, teleosts, which do not possess a spiral intestine, increase intestinal surface area by increasing total length of the intestine, which subsequently forms loops and becomes tightly packed within the abdominal cavity[2,6], or through the development and multiplication of pyloric caeca[34].

In teleosts, an increase in intestinal length is associated with a transition from carnivorous to omnivorous or more herbivorous diets[35,37,38]. Indeed, diet has been historically considered as the prevailing factor influencing the number of spiral valve turns[36,39–41]. For instance, the "voracious" and often pelagic predators (such as most lamniforms and hexanchiformes) and the planktivorous chondrichthyans (such as *Rhinchodon typus*, *Cetorhinus maximus, Megachasma pelagios* and the mobulid rays) exhibit ring-type valves with very high turn counts[39] (Supplementary Table 1). In contrast, the only extant non-teleostean actinopterygian with a planktivorous diet, the Mississippi paddlefish (*Polyodon spathula*), does not exhibit a similar increase in spiral valve turns, but the last three turns become closely stacked to resemble the ring-type condition (Fig. 3). However, the functional significance of this close stacking of the spiral valve turns is still unclear.

Being large is common to pelagic top predators and planktivores. Given the overarching relevance of body size for dimensions in anatomical structures and biology[42,43], we examined its relation to spiral valve turns for the first time. Our analysis suggests that even though there is distinct phylogenetic inertia with respect to number of turns across a range of body sizes, larger animals have a higher number of turns when corrected for relatedness. Limited evidence suggests that the number of turns in the spiral valve is ontogenetically stable, suggesting little influence of growth on this characteristic[44] (TA pers. obs. on juveniles of *Acipenser gueldenstaedtii*).

Among fishes with similar diets, metabolism and activity levels have also been suggested to correlate with intestinal length. For example, active pelagic carnivores (e.g., tunas) tend to have longer intestines than ambush predators (e.g., pikes)[40,45]. An analogous condition might apply to recent elasmobranchs. For example, the pelagic and active lamniforms exhibit high spiral valve turn counts in comparison with more benthic taxa like some orectolobiforms or some carcharhiniforms[39] (Supplementary Table 1). However, a reliable classification for activity level or metabolic rate is not yet available and will be required to test this hypothesis. Phylogeny also plays an important role in understanding the variation in spiral valve counts in fishes, with closely related species and genera tending to exhibit similar turn counts[39,46]. This applies generally to extant taxa despite fluctuations in size and different trophic niches, rendering functional interpretations questionable if not controlled for relatedness.

The high number of spiral valve turns in both †*Saurichthys paucitrichus* and †*Asthenocormus titanius* places these species as outliers to the common pattern of extant fishes (Fig. 4). The biology of †*Saurichthys* provides clues for the potential role of a well-developed spiral valve. First, †*Saurichthys* might have been particularly active, or had an unusually high metabolism[40]. However, †*Saurichthys* has been described as an ambush predator, likely incapable of rapid sustained swimming[16,23,47,48], which is incongruent with an energetically demanding lifestyle[49]. Viviparity[23,50] and potential maternal provisioning could only partially explain such an increase in energetic demand. Alternatively, given the relationship between spiral valve turns and body size, this position indicates, if maturity is assumed (Supplementary Note 1), a secondary dwarfed form that retained a characteristic typical of a larger ancestor. For instance, the closely related and sympatric †*S. costasquamosus* attained a total length of ~85 cm (PIMUZ T 1275)[23], and the Early Triassic †*S. dayi* exceeded 1.5 m in length[51]. Furthermore, the potential close phylogenetic proximity of †*Saurichthys* to the larger and more pelagic †*Birgeria*[19–22] might also explain the high number of spiral valve turns in †*S. paucitrichus*. We therefore hypothesize that the presence of such well-developed spiral intestines is a plesiomorphic condition for †Saurichthyidae, retained in smaller species. The multi-valvate condition seen in †*Asthenocormus* invites a similar interpretation based on its sister taxon relationship with the emblematic giant †*Leedsichthys*[32]. The turn counts in the spiral valves of †saurichthyids and †pachycormids reveal that increased turn multiplication occurred, independently, at least twice in the evolutionary history of actinopterygians; once

in the chondrostean clade and once on the teleost stem. Also, the independent occurrences of high turn counts in large chondrichthyans and actinopterygians constitute examples of broad evolutionary convergence and underline the potential functional relevance of this trait and its relationship to body size.

In conclusion, we emphasize the importance of investigating gastrointestinal contents in fossils, because they often reflect the morphology of the surrounding soft tissue and therefore provide information on palaeobiology and phylogeny that would otherwise remain elusive.

Methods

Locality information and specimens. The fossils treated here come from the Middle Triassic UNESCO World Heritage Site of Monte San Giorgio, Switzerland (Besano and Meride formations[52]). The Lagerstätte deposits exposed at the site are known for the exceptional preservation of delicate structures including embryos[23,50] and soft tissues[16,23]. Several †*Saurichthys* specimens exhibit traces of fossilized digesta within their body cavities, but very few provide a clear and more complete picture of the GIT. This work focuses on three specimens: one †*Saurichthys paucitrichus* (PIMUZ T 59) from the Besano Formation (earliest Ladinian), one †*S. macrocephalus* (PIMUZ T 3916) and one †*S. costasquamosus* (MCSN 5696) from the overlying (early Ladinian) Meride Formation[23,47]. Additional information was extracted from other, less well-preserved specimens including: †*S. macrocephalus* (PIMUZ T 4106, S2); †*S. breviabdominalis* (PIMUZ T 890, S3); †*S. curionii* (PIMUZ T 5679, PIMUZ T 5684, PIMUZ T 5827) and †*Saurichthys* sp. (PIMUZ T 1768a,b).

We compared the morphology of the GIT of †*Saurichthys* to that of living bracketing or closely related actinopterygian taxa (Fig. 3). We dissected wet specimens including: *Polypterus* sp. (Z-M-UZH 140016, alcohol preserved, Zoological Museum, University of Zurich); *Acipenser baerii* and *A. gueldenstaedtii* (fresh juvenile and adult specimens donated by Frutigen AG and discarded after the dissection); *Polyodon spathula* (VIMS 12227, alcohol preserved, Virginia Institute of Marine Science); *Lepisosteus osseus* (VIMS 17602, alcohol preserved). Our observations were supplemented with data from the literature.

Photography. Specimens were photographed under "normal" light. We experimented with an Ultraviolet (UV) hand lamp (230V, 50Hz, 40VA) in order to enhance the contrast and the visibility of the studied structures[53] but, this produced adequate results only in the case of †*S. macrocephalus* (PIMUZ T 3916) from the Meride Fm., which is heavily phosphatized.

Literature data. We collated literature data on recent and fossil fishes in order to explore the relationship of the number of turns in the spiral valve to body size (134 taxa, Supplementary Table 1). When the TL of fossil taxa was not readily available, we measured it from published figures. We tested the relationship between log-transformed maximum body length and log-transformed maximum number of turns of the spiral valve according to $log\ (number\ of\ turns) = a + b\ log\ (maximum\ Total\ Length)$, using Ordinary Least Squares (OLS) and Phylogenetic Generalized Least Squares (PGLS) in the whole dataset and in a taxonomic subset. For the PGLS analysis, we used a tree constructed based on a recent phylogeny of elasmobranchs[54], to which several extant and extinct osteichthyan taxa, including †*Saurichthys paucitrichus*, were added (see Supplementary Note 2 for additional methods and references) while chimaeriforms and batoids were excluded (data on spiral valve morphology not readily available in the literature and/or body size not effectively explained by TL). Branch lengths of this modified tree were set to 1, because the resulting tree was not based on our own calculations of branch lengths after consistent use of the same characters. In contrast, the analysis for sharks alone included the original information on branch lengths[54].

PGLS was used with Pagel's λ[55], estimated by maximum likelihood. λ can vary between 0 (no phylogenetic signal) and 1 (the observed pattern is predicted by the phylogeny; similarity among species scales in proportion to branch length)[55]. OLS and PGLS models were compared for goodness-of-fit using Akaike's Information Criterion (AIC), with better-supported models having a lower AIC[56]. Statistical tests were performed in R 2.15.0[57] using the packages caper[58], and nlme[59]. We display results of both OLS and PGLS analyses, because a comparison of the respective results facilitates interpretation[60], e.g. such as realizing whether accounting for phylogeny leads to a steeper or shallower relationship than expected from the raw data.

References

1. Stevens, C. E. & Hume, I. D. *Comparative physiology of the vertebrate digestive system*. (Cambridge University Press, 2004).
2. Wilson, J. & Castro, L. In *The multifunctional gut of fish* Vol. 30 (eds Grosell, M., Farrell, A. & Brauner, C.) Ch. 1, 1–55 (Academic Press, 2011).
3. Jacobshagen, E. In *Handbuch der vergleichenden Anatomie der Wirbeltiere* Vol. 3 (eds Bolk, L., Göppert, E., Kallius, E. & Lubosch, W.) Ch. IV, 563–724 (Urban and Schwartzenberg, 1937).
4. Nelson, J. S. *Fishes of the world*. Fourth Edition, (John Wiley & Sons, 2006).
5. Near, T. J. *et al.* Resolution of ray-finned fish phylogeny and timing of diversification. *Proc. Natl. Acad. Sci. USA* **109,** 13698–13703 (2012).
6. Harder, W. *Anatomy of fishes*. 1–612 (E. Schweizerbart'sche Verlagsbuchhandlung, 1975).
7. Bertin, L. In *Traité de zoologie. Anatomie, systématique, biologie* Vol. 13 (ed Grassé, P. P.) 1248–1302 (Masson et Cie éditeurs, 1958).
8. McAllister, J. A. Phylogenetic distribution and morphological reassesment of the intestines of fossil and modern fishes. *Zool. Jb. Anat.* **115,** 281–294 (1987).
9. Gilmore, B. Scroll coprolites from the Silurian of Ireland and the feeding of early vertebrates. *Palaeontology* **35,** 319–333 (1992).
10. Aldridge, R. J., Gabbott, S. E., Siveter, L. J. & Theron, J. N. Bromalites from the Soom Shale Lagerstätte (Upper Ordovician) of South Africa: Palaeoecological and palaeobiological implications. *Palaeontology* **49,** 857–871 (2006).
11. Hunt, A. P., Lucas, S. G., Milàn, J. & Spielmann, J. A. In *Vertebrate coprolites* Vol. 57 (eds Hunt, A. P., Milàn, J., Lucas, S. G. & Spielmann, J. A.) 1–24 (New Mexico Museum of Natural History & Science, 2012).
12. Sansom, R. S., Gabbott, S. E. & Purnell, M. A. Atlas of vertebrate decay: A visual and taphonomic guide to fossil interpretation. *Palaeontology* **56,** 457–474 (2013).
13. Viohl, G. In *Evolutionary paleobiology of behavior and coevolution* (ed Boucot, A. J.) 287–303 (Elsevier, 1990).
14. Agassiz, L. *Recherches sur les poissons fossiles*. Vol. 3 (Imprimerie de Petitpierre, 1833–1843).

15. Neumayer, L. Vergleichend anatomische untersuchungen über den darmkanal fossiler fische. *Abh. Bayer. Akad. Wiss.* **29,** 1–28 (1919).
16. Maxwell, E. E., Furrer, H. & Sanchez-Villagra, M. R. Exceptional fossil preservation demonstrates a new mode of axial skeleton elongation in early ray-finned fishes. *Nat. Commun.* **4,** 2570 (2013).
17. Maxwell, E. E., Romano, C., Wu, F. & Furrer, H. Two new species of *Saurichthys* (Actinopterygii: Saurichthyidae) from the Middle Triassic of Monte San Giorgio, Switzerland, with implications for character evolution in the genus. *Zool. J. Linn. Soc.* **173,** 887–912 (2015).
18. Romano, C., Kogan, I., Jenks, J., Jerjen, I. & Brinkmann, W. *Saurichthys* and other fossil fishes from the late Smithian (Early Triassic) of Bear Lake County (Idaho, USA), with a discussion of saurichthyid palaeogeography and evolution. *Bull. Geosci.* **87,** 543–570 (2012).
19. Coates, M. I. Endocranial preservation of a Carboniferous actinopterygian from Lancashire, UK, and the interrelationships of primitive actinopterygians. *Philos. Trans. R. Soc. London Biol.* **354,** 435–462 (1999).
20. Gardiner, B., Schaeffer, B. & Masserie, J. A review of the lower actinopterygian phylogeny. *Zool. J. Linn. Soc.* **144,** 511–525 (2005).
21. Wu, F., Chang, M.-m., Sun, Y. & Xu, G. A new saurichthyiform (Actinopterygii) with a crushing feeding mechanism from the Middle Triassic of Guizhou (China). *PloS one* **8,** e81010 (2013).
22. Xu, G.-H., Gao, K.-Q. & Finarelli, J. A. A revision of the Middle Triassic scanilepiform fish *Fukangichthys longidorsalis* from Xinjiang, China, with comments on the phylogeny of the Actinopteri. *J. Vertebr. Paleontol.* **34,** 747–759 (2014).
23. Rieppel, O. Die Triasfauna der Tessiner Kalkalpen xxv: Die Gattung *Saurichthys* (Pisces, Actinopterygii) aus der mittleren Trias des Monte San Giorgio, Kanton Tessin. *Schweiz. Palaeontol. Abh.* **108,** 1–103 (1985).
24. Parker, T. J. V. On the intestinal spiral valve in the genus *Raia*. *Zool. Soc. Lond. Trans.* **11,** 49–61 (1880).
25. Macallum, A. B. Alimentary canal and pancreas of *Acipenser*, *Amia*, and *Lepidosteus*. *J. Anat. Physiol* **20,** 604–636 (1886).
26. Arratia, G. & Schultze, H.-P. In *Mesozoic fishes* Vol. 5 (eds Arratia, G., Schultze, H.-P. & Wilson, M.) 87–120 (Dr. Friedrich Pfeil, 2013).
27. Gegenbaur, C. *Vergleichende Anatomie der Wirbelthiere mit Berücksichtigung der Wirbellosen*. Vol. 2 696 (Verlag von Wilhelm Engelmann, 1901).
28. Hilton, W. A. On the intestine of *Amia calva*. *Am. Nat.* **34,** 717–735 (1900).
29. Buddington, R. K. & Christofferson, J. P. Digestive and feeding characteristics of the chondrosteans. *Environ. Biol. Fish.* **14,** 31–41 (1985).
30. Weisel, G. F. Anatomy and histology of the digestive system of the paddlefish (*Polyodon spathula*). *J. Morphol.* **140,** 243–255 (1973).
31. Weisel, G. F. Histology of the feeding and digestive organs of the shovelnose sturgeon, *Scaphirhynchus platorynchus*. *Copeia* **1979,** 518–525 (1979).
32. Liston, J. In *Mesozoic fishes 4. Homology and phylogeny* (eds Arratia, G., Schultze, H.-P. & Wilson, M. V. H.) 181–197 (Verlag Dr. Friedrich Pfeil, 2008).
33. Purser, G. L. IV.—*Calamoichthys calabaricus* J. A. Smith. Part i. The alimentary and respiratory systems—concluded. *Earth Environ. Sci. Trans. R. Soc. Edinb.* **56,** 89–101 (1929).
34. Buddington, R. K. & Diamond, J. M. Pyloric ceca of fish: A "new" absorptive organ. *Am. J. Physiol. Gastrointest. Liver Physiol.* **252,** G65–G76 (1987).
35. Karachle, P. K. & Stergiou, K. I. Gut length for several marine fish: Relationships with body length and trophic implications. *Mar. Biodivers. Rec.* **3,** e106 (2010).
36. Wetherbee, B. M., Cortés, E. & Bizzarro, J. J. In T*he* biology *of* shar*ks and their relatives* (eds Carrier, J. C., Musick, J. A. & Heithaus, M. R.) 239–264 (CRC Press, 2012).
37. Wagner, C. E., McIntyre, P. B., Buels, K. S., Gilbert, D. M. & Michel, E. Diet predicts intestine length in lake Tanganyika's cichlid fishes. *Funct. Ecol.* **23,** 1122–1131 (2009).
38. Kramer, D. & Bryant, M. Intestine length in the fishes of a tropical stream: 2. Relationships to diet—the long and short of a convoluted issue. *Environ. Biol. Fish.* **42,** 129–141 (1995).
39. Qingwen, M. & Yuanding, Z. A study of the spiral valves of chinese cartilaginous fishes. *Acta Zool. Sin.* **31,** 277–284 (1985).
40. Buddington, R. K., Krogdahl, A. & Bakke-McKellep, A. M. The intestines of carnivorous fish: Structure and functions and the relations with diet. *Acta Physiol. Scand.* **161,** *Suppl.* 368, 67–80 (1997).
41. Holmgren, S. & Nilsson, S. In *Sharks, skates, and rays: The biology of elasmobranch fishes* (ed Hamlett, W. C.) 144–173 (The John Hopkins University press, 1999).
42. Calder, W. *Size, function and life history* (Havard University Press, 1996).
43. Peters, R. H. *The ecological implications of body size*. Vol. 2 (Cambridge University Press, 1986).
44. Neumayer, L. Die Entwicklung des Darms von *Acipenser*. *Acta Zool.* **11,** 39–150 (1930).
45. Suyehiro, Y. A study on the digestive system and feeding habits of fish. *Jpn. J. Zool.* **IX,** 1–303 (1942).
46. White, E. G. Interrelatonships of elasmobranchs with a key to the Order Galea. *Bull. Am. Mus. Nat. Hist.* **74,** 25–138+151 tables (1937).
47. Rieppel, O. A new species of the genus *Saurichthys* (Pisces: Actinopterygii) from the Middle Triassic of Monte San Giorgio (Switzerland), with comments on the phylogenetic interrelationships of the genus. *Palaeontogr. Abt. A* **221,** 63–94 (1992).
48. Wu, F., Sun, Y., Xu, G., Hao, W. & Jiang, D. New saurichthyid actinopterygian fishes from the Anisian (Middle Triassic) of southwestern China. *Acta Palaeontol. Pol.* **56,** 581–614 (2011).
49. Fu, S.-J. *et al.* The behavioural, digestive and metabolic characteristics of fishes with different foraging strategies. *J. Exp. Biol.* **212,** 2296–2302 (2009).
50. Renesto, S. & Stockar, R. Exceptional preservation of embryos in the actinopterygian *Saurichthys* from the Middle Triassic of Monte San Giorgio, Switzerland. *Swiss J. Geosci.* **102,** 323–330 (2009).
51. Mutter, R. J., Cartanyà, J. & Basaraba, S. A. In *Mesozoic fishes* Vol. 4 (eds Arratia, G., Schultze, H.-P. & Wilson, M.) 103–127 (Verlag Dr. Friedrich Pfeil, 2008).
52. Furrer, H. Der Monte San Giorgio im Südtessin-vom Berg der Saurier zur fossil-Lagerstätte internationaler Bedeutung. *Njbl. natf. Ges. Zürich* **206**, 1–64 (Koprint, 2003).
53. Tischlinger, H. & Arratia, G. In *Mesozoic fishes* Vol. 5 (eds Arratia, G., Schultze, H.-P. & Wilson, M. V. H.) 549–560 (Verlag Dr. Friedrich Pfeil, 2013).
54. Naylor, G. J. *et al.* In *The biology of sharks and their relatives* (eds Carrier, J. C., Musick, J. A. & Heithaus, M. R.) 31–56 (CRC Press, 2012).
55. Pagel, M. Inferring the historical patterns of biological evolution. *Nature* **401,** 877–884 (1999).
56. Burnham, K. P. & Anderson, D. R. *Model selection and multimodel inference: A practical information-theoretic approach*. (Springer Science & Business Media, 2002).
57. R Core Team (2013). R: A language and environment for statistical computing. R Foundation for Statistical Computing, Vienna, Austria. URL http://www.R-project.org/.
58. Orme, D., Freckleton, R., Thomas, G., Petzoldt, T., Fritz, S., Isaac, N. & Pearse, W. (2012). Caper: comparative analyses of phylogenetics and evolution in R. Version 0.5. URL http://caper.r-forge.r-project.org/.
59. Pinheiro, J., Bates, D., DebRoy, S., Sarkar, D. & R Core Team (2011). Nlme: linear and nonlinear mixed effects models. R package version 3. URL http://cran.r-project.org/package=nlme.
60. Clauss, M., Dittmann, M. T., Müller, D. W. H., Zerbe, P. & Codron, D. Low scaling of a life history variable: Analysing eutherian gestation periods with and without phylogeny-informed statistics. *Mamm. Biol.* **79,** 9–16 (2014).

Acknowledgements

All the fossils were found during systematic excavations directed by B. Peyer, E. Kuhn-Schnyder and H. Furrer (Paleontological Institute and Museum, University of Zurich, PIMUZ). The careful preparation was done by A. Fassnacht (Winterthur), H. Lanz (PIMUZ), U. Oberli (St. Gallen), and C. Obrist (Rickenbach). The Museo Cantonale di Storia Naturale in Lugano funded the excavation of H. Furrer and the preparation of specimens. T. Bürgin (St. Gallen) determinated specimen MCSN 5696. We also thank E. Hilton (Virginia Institute for Marine Science), B. Oberholzer (Zoological Museum, University of Zurich) and P. Sindilariu (Tropenhaus Frutigen AG) for providing wet specimens for comparison. We extend our gratitude to T. Simoes-Rodriguez for helping with UV photography. Funding for this project was provided by Swiss National Science Foundation (SNF) Sinergia grant CRSII3-136293.

Author Contributions

The project was conceived by M.R.S.-V., E.E.M. and T.A. T.A. carried out the descriptive and comparative work, created all figures and led the writing of the manuscript. M.C. led the statistical analyses and participated in the interpretation of the results and the writing of the discussion and methods parts. H.F. coordinated the preparation of all specimens studied and provided input in various stages of the manuscript. M.R.S.-V. and E.E.M. supervised the project and provided input in various stages of the manuscript, including the result interpretation. M.R.S.-V. provided funding for the completion of this project. All authors have read and approved the final manuscript.

Additional Information

Supplementary information accompanies this paper at http://www.nature.com/srep

Competing financial interests: The authors declare no competing financial interests.

How to cite this article: Argyriou, T. *et al.* Exceptional preservation reveals gastrointestinal anatomy and evolution in early actinopterygian fishes. *Sci. Rep.* **6**, 18758; doi: 10.1038/srep18758 (2016).

Supplementary information

Exceptional preservation reveals gastrointestinal anatomy and evolution in early actinopterygian fishes

Thodoris Argyriou, Marcus Clauss, Erin E. Maxwell, Heinz Furrer, and Marcelo R. Sánchez-Villagra

Supplementary Figure S1│ †*Saurichthys macrocephalus* (PIMUZ T 3916) detail of the preserved cololite, photographed under UV light. Scale bar equals 1 cm.

Supplementary Figure S2 | †*S. macrocephalus* (PIMUZ T 4106) with preserved straight stomach outline (stomach length is indicated by a double, black arrow) and a smaller *Saurichthys* specimen as undigested prey (N indicates the neurocranium of the prey). Scale bar equals 1 cm.

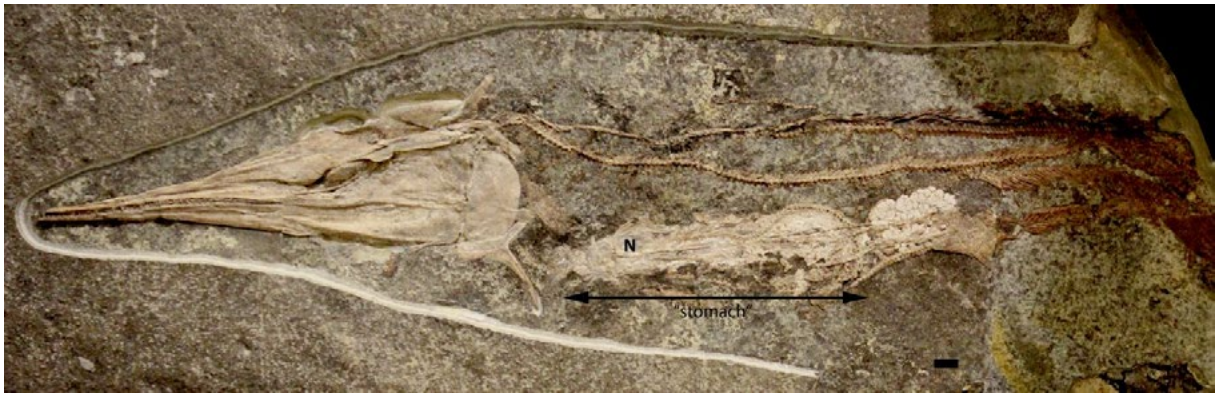

Supplementary Figure S3 | †*S. breviabdominalis* (PIMUZ T 890) exhibiting an incomplete spiral cololite. Scale bar equals 1 cm.

Supplementary Figure S4 | *Acipenser baerii* dissected GIT in ventrolateral view (top) and dissected spiral intestine (bottom), for comparison. Scale bars equal 1 cm.

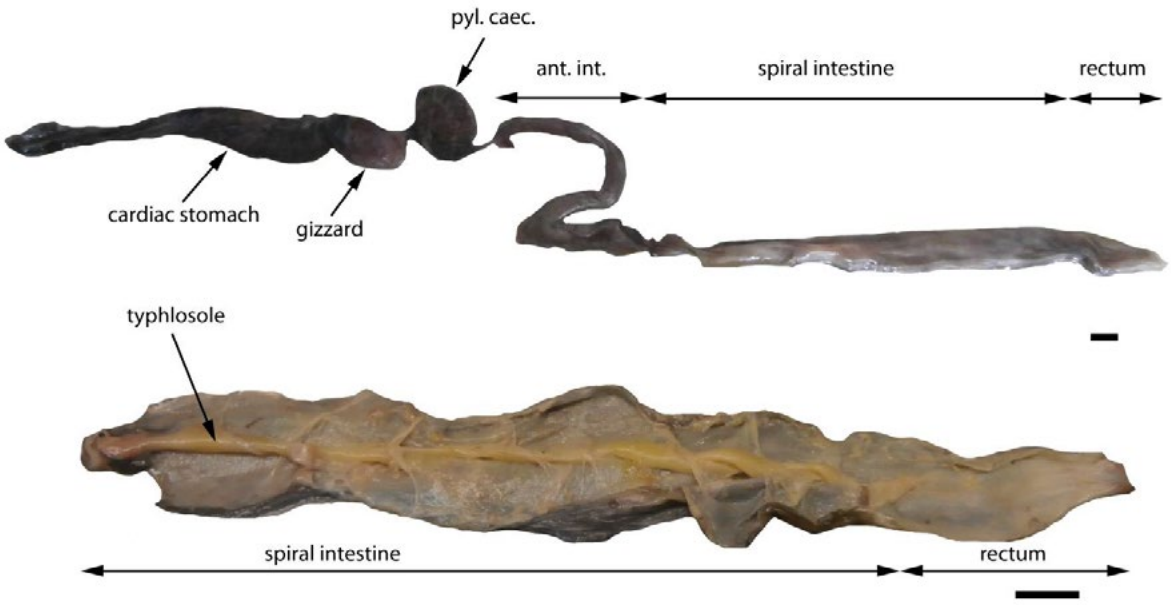

Supplementary Figure S5 | *Polyodon spathula* (VIMS 12227) dissected GIT in lateral (top left) and ventral (bottom left) views and dissected spiral intestine of the same specimen (right), for comparison. Scale bars equal 1 cm.

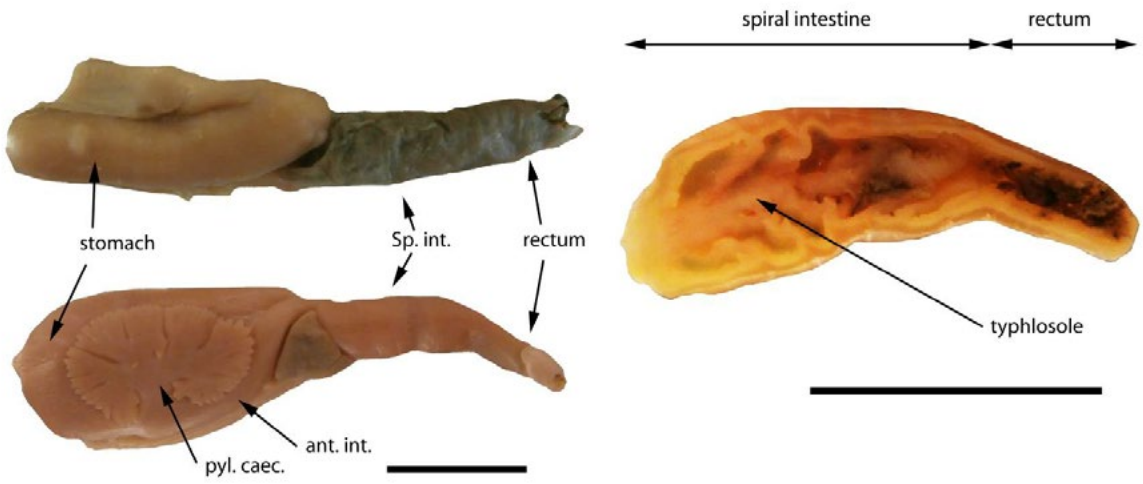

Supplementary Note 1, on the maturity of PIMUZ T 59

We consider the examined specimen of †*S. paucitrichus* (PIMUZ T 59) to be a mature individual. The developed gonopodium, the ossifications ventral to the notochord in the abdominal region and the ossified proximal and distal radials of the unpaired fins are all in support of this view (EEM and TA pers. obs.). The validity of †*S. paucitrichus* as a species as well as the attribution of various specimens to this taxon should be revisited[1].

Supplementary Note 2, on the tree used in the PGLS analysis.

We used Mesquite[2] to construct a composite tree based on an existing molecular tree of living elasmobranchs[3]. We manually added the extant actinopterygians sensu Near et al.[4] and the sarcopterygians following the consensus presented by Nelson[5]. The placement of fossil taxa is as follows: †*Saurichthys* sensu Gardiner et al.[6]; †*Liodesmus* and †*Amblysemius*, both grouped under the "superfamily" †Caturoidea, were placed as sister taxa on the *Amia* clade, following Grande and Bemis[7]; †*Macrosemius* (†Macrosemiidae) and †*Pericentrophorus* (†Semionotidae) were placed as sister taxa on the *Lepisosteus* clade following López-Arbarello[8]; †*Eurycormus* and †*Asthenocormus* were placed on the teleost stem sensu Arratia[9].

"Order"	Species	Maximum TL (m)	Maximum turn count	References
Heterodontiformes	*Heterodontus mexicanus*	0.7	7	10,11
Heterodontiformes	*Heterodontus portujacksoni*	1.65	7	10,11
Heterodontiformes	*Heterodontus zebra*	1.25	9	10,11
Heterodontiformes	*Heterodontus galeatus*	1.52	7	10,11
Heterodontiformes	*Heterodontus francisci*	1.22	7	10,11
Lamniformes	*Odontaspis ferox*	4.5	32	10,11
Lamniformes	*Odontaspis noronhai*	3.6	32	10,11
Lamniformes	*Carcharias taurus*	3.2	32	10,11
Lamniformes	*Mitsukurina owstoni*	3.84	19	10,11
Lamniformes	*Pseudocarcharias kamoharai*	1.1	27	10,11
Lamniformes	*Megachasma pelagios*	5.49	24	10,11
Lamniformes	*Alopias pelagicus*	3.65	40	10,11
Lamniformes	*Alopias superciliosus*	4.61	45	10,11
Lamniformes	*Alopias vulpinus*	5.73	34	10,11
Lamniformes	*Cetorhinus maximus*	10	51	10,11
Lamniformes	*Carcharodon carcharias*	6	55	10,11
Lamniformes	*Isurus oxyrinchus*	4.08	54	10,11
Lamniformes	*Isurus paucus*	4.17	54	10,11
Lamniformes	*Lamna ditropis*	3.05	41	10,11
Lamniformes	*Lamna nasus*	3.7	41	10,11
Orectolobiformes	*Parascyllium colare*	0.87	9	10,11
Orectolobiformes	*Brachaelurus waddi*	1.22	11	10,11
Orectolobiformes	*Brachaelurus cocloughi*	0.75	11	10,11
Orectolobiformes	*Eucrossorhinus dasypogon*	1.25	33	10,11
Orectolobiformes	*Orectolobus maculatus*	3.2	25	10,11
Orectolobiformes	*Orectolobus ornatus*	2.88	23	10-12
Orectolobiformes	*Orectolobus parvimaculatus*	0.88	28	10,11,13
Orectolobiformes	*Orectolobus halei*	2	32	10-12
Orectolobiformes	*Orectolobus floridus*	0.75	25	10,11,13
Orectolobiformes	*Orectolobus hutchinsi*	1.49	28	10,11,14
Orectolobiformes	*Chiloscyllium griseum*	0.77	19	10,11
Orectolobiformes	*Chiloscyllium hasseltii*	0.61	15	10,11
Orectolobiformes	*Chiloscyllium indicum*	0.65	15	10,11
Orectolobiformes	*Chiloscyllium plagiosum*	0.95	17	10,11
Orectolobiformes	*Chiloscyllium punctatum*	1.05	20	10,11
Orectolobiformes	*Stegostoma fasciatum*	3.54	18	10,11
Orectolobiformes	*Ginglimostoma cirratum*	4.3	17	10,11
Orectolobiformes	*Nebrius ferrugineous*	3.2	24	10,11
Orectolobiformes	*Pseudoginglymostoma brevicaudatum*	0.75	15	10,11
Orectolobiformes	*Rhincodon typus*	21	74	10,11
Carcharhiniformes	*Apristurus profundorum*	0.54	10	10,15
Carcharhiniformes	*Apristurus ampliceps*	0.85	11	10
Carcharhiniformes	*Scyliorhinus canicula*	1	11	10,16

Carcharhiniformes	*Scyliorhinus capensis*	1.22	11	[10,16]
Carcharhiniformes	*Scyliorhinus retifer*	0.47	11	[10,16]
Carcharhiniformes	*Scyliorhinus stellaris*	1.62	11	[10,16]
Carcharhiniformes	*Cephaloscyllium ventriosum*	1	12	[10,16]
Carcharhiniformes	*Poroderma africanum*	1.01	13	[10,16]
Carcharhiniformes	*Poroderma pantherinum*	0.84	13	[10,16]
Carcharhiniformes	*Asymbolus analis*	0.61	9	[10,16]
Carcharhiniformes	*Galeus arae*	0.36	14	[10,16]
Carcharhiniformes	*Galeus sauteri*	0.38	14	[10,16]
Carcharhiniformes	*Galeus polli*	0.3	14	[10,16]
Carcharhiniformes	*Galeus melastomus*	0.9	14	[10,16]
Carcharhiniformes	*Galeus murinus*	0.63	14	[10,16]
Carcharhiniformes	*Halaelurus lineatus*	0.56	10	[10,16]
Carcharhiniformes	*Halaelurus natalensis*	0.47	10	[10,16]
Carcharhiniformes	*Halaelurus buergeri*	0.49	10	[10,16]
Carcharhiniformes	*Haploblepharus edwardsii*	0.6	8	[10,16]
Carcharhiniformes	*Holohalaelurus regani*	0.61	7	[10,16]
Carcharhiniformes	*Parmaturus xaniurus*	0.45	8	[10,16]
Carcharhiniformes	*Eridacnis*	2	8	[10,16]
Carcharhiniformes	*Gollum attenuatus*	1.07	11	[10,16]
Carcharhiniformes	*Pseudotriakis microdon*	2.95	17	[10,16]
Carcharhiniformes	*Leptocharias smithii*	0.77	16	[10,16]
Carcharhiniformes	*Furgaleus macki*	1.6	7	[10,16]
Carcharhiniformes	*Galeorhinus galeus*	1.93	5	[10,16]
Carcharhiniformes	*Hemitriakis japanica*	1.2	8	[10,16]
Carcharhiniformes	*Hemitriakis leucoperiptera*	0.96	7	[10,16]
Carcharhiniformes	*Hypogaleus hyugaensis*	1.27	6	[10,16]
Carcharhiniformes	*Iago omanensis*	0.37	5	[10,16]
Carcharhiniformes	*Iago garricki*	0.75	6	[10,16]
Carcharhiniformes	*Mustelus asterias*	1.4	8	[10,16]
Carcharhiniformes	*Mustelus californicus*	1.16	8	[10,16]
Carcharhiniformes	*Mustelus canis*	1.5	9	[10,16]
Carcharhiniformes	*Mustelus henlei*	1	8	[10,16]
Carcharhiniformes	*Mustelus lenticulatus*	1.25	8	[10,16]
Carcharhiniformes	*Mustelus lunulatus*	1.7	9	[10,16]
Carcharhiniformes	*Mustelus manazo*	2.2	9	[10,16]
Carcharhiniformes	*Mustelus norrisi*	1.1	9	[10,16]
Carcharhiniformes	*Scylliogaleus quecketti*	0.89	7	[10,16]
Carcharhiniformes	*Triakis megalopterus*	1.42	6	[10,16]
Carcharhiniformes	*Triakis scyllium*	1.5	8	[10,16]
Carcharhiniformes	*Triakis semifasciata*	1.98	8	[10,16]
Carcharhiniformes	*Hemipristis elongatus*	2.4	6	[10,16]
Carcharhiniformes	*Hemigaleus microstoma*	1.14	6	[10,16]
Carcharhiniformes	*Paragaleus pectoralis*	1.4	6	[10,16]
Squaliformes	*Echinorhinus brucus*	3.1	16	[10,17]
Squaliformes	*Squalus acanthias*	1.6	13	[10,17]

Squaliformes	*Squalus suckleyi*	1.3	13	10,18
Squaliformes	*Squalus brevirostris*	0.6	9	10,19
Squaliformes	*Centrophorus granulosus*	1.7	14	10,17
Squaliformes	*Centrophorus lusitanicus*	1.6	13	10,17
Squaliformes	*Centrophorus squamosus*	1.64	14	10,17
Squaliformes	*Deania profundorum*	0.88	25	10,20
Squaliformes	*Centroscyllium fabricii*	0.7	10	10,17
Squaliformes	*Etmopterus gracilispinis*	0.35	11	10,21
Squaliformes	*Etmopterus bigelowi*	0.67	19	10,22
Squaliformes	*Etmopterus pussilus*	0.5	13	10,22
Squaliformes	*Etmopterus unicolor*	0.64	12	10,23
Squaliformes	*Etmopterus granulosus*	0.6	13	10,23
Squaliformes	*Centroscymnus coelolepis*	1.22	21	10,17
Squaliformes	*Centroscymnus owstoni*	1.2	15	10,17
Squaliformes	*Somniosus microcephalus*	7.3	34	10,17
Squaliformes	*Somniosus rostratus*	1.43	29	10,24
Squaliformes	*Somniosus pacificus*	4.4	37	10,24
Squaliformes	*Zameus squamulosus*	0.84	16	10,17
Squaliformes	*Oxynotus*	1.5	11	10,17
Squaliformes	*Isistius brasiliensis*	0.42	10	10
Squaliformes	*Squaliolus laticaudus*	0.28	13	10,17
Pristiophoriformes	*Pristiophorus nancyae*	0.62	7	10,25
Pristiophoriformes	*Pristiophorus lanae*	0.83	6	10,26
Squatiniformes	*Squatina*	2.44	12	10,17
Hexanchiformes	*Chlamydoselachus anguineus*	1.96	49	10,17
Hexanchiformes	*Heptranchias perlo*	1.39	22	10,17
Hexanchiformes	*Heptranchias griseus*	5.5	39	10,17
Hexanchiformes	*Heptranchias nakamurai*	1.8	28	10,17
Ceratodontiformes	*Neoceratodus forsteri*	1.7	9	10,27
Ceratodontiformes	*Protopterus annectens*	1	6	10,28
Polypteriformes	*Polypterus*	0.97	6	10,28
Polypteriformes	*Erpetoichthys calabaricus*	0.37	7	10,29
Acipenseriformes	*Polyodon spathula*	2.21	6	10,30, pers. obs.
Acipenseriformes	*Acipenser baerii*	2	8	10,31, pers. obs.
Acipenseriformes	*Acipenser transmontanus*	6.1	8	10,31, pers. obs.
Acipenseriformes	*Scaphirhynchus*	2	5	10,32
incerta	†*Saurichthys paucitrichus*	0.26	30	pers. obs.
Lepisosteiformes	*Lepisosteus osseus*	2	2	10,33, pers. obs.
†Semionotiformes	†*Pericentrophorus minimus*	0.04	8	34,35
†Semionotiformes	†*Macrosemius rostratus*	0.26	4	36,37
Amiiformes	*Amia calva*	1.09	4	10,38
Amiiformes	†*Amblysemius pachyurus*	0.26	17	37,39
Amiiformes	†*Liodesmus gracilis*	0.13	7	37,39
†Pachycormiformes	†*Asthenocormus titanius*	2.34	73	37,40
incerta	†*Eurycormus speciosus*	0.19	13	37,41

Supplementary Table 1 | Spiral valve turn count and maximum TLs of extant elasmobranch, sarcopterygian and actinopterygian taxa, and †*Saurichthys paucitrichus*, included in the regression analyses.

References

1 Maddison, W. P., & Maddison D. R (2008). Mesquite: A modular system for evolutionary analysis Version. 2.5. URL http://mesquiteproject.org/.

2 Naylor, G. J. *et al.* in *The biology of sharks and their relatives* (eds Carrier, J. C., Musick, J. A. & Heithaus, M. R.) 31-56 (CRC Press, 2012).

3 Near, T. J. *et al.* Resolution of ray-finned fish phylogeny and timing of diversification. *Proc. Natl. Acad. Sci. U.S.A.* **109**, 13698-13703 (2012).

4 Nelson, J. S. *Fishes of the world*. Fourth edn, (John Wiley & Sons, 2006).

5 Gardiner, B., Schaeffer, B. & Masserie, J. A review of the lower actinopterygian phylogeny. *Zool. J. Linn. Soc.* **144**, 511 - 525 (2005).

6 Grande, L. & Bemis, W. E. A comprehensive phylogenetic study of amiid fishes (Amiidae) based on comparative skeletal anatomy. An empirical search for interconnected patterns of natural history. *J. Vertebr. Paleontol. Mem.* **18**, 1-696 (1998).

7 López-Arbarello, A. Phylogenetic interrelationships of ginglymodian fishes (Actinopterygii: Neopterygii). *PLoS ONE* **7**, e39370 (2012).

8 Arratia, G. New teleostean fishes from the Jurassic of Southern Germany and the systematic problems concerning the 'pholidophoriforms'. *Paläontol. Z.* **74**, 113-143 (2000).

9 Maxwell, E. E., Romano, C., Wu, F. & Furrer, H. Two new species of *Saurichthys* (Actinopterygii: Saurichthyidae) from the Middle Triassic of Monte San Giorgio, Switzerland, with implications for character evolution in the genus. *Zool. J. Linn. Soc.* **173**, 887-912 (2015).

10 Froese, R. & Pauly, D. (2015). *Fishbase*. URL www.fishbase.org (accessed 5th of November 2015).

11 Compagno, L. J. V. *Sharks of the world. An annotated and illustrated catalogue of shark species known to date. Volume 2. Bullhead, mackerel and carpet sharks (Heterodontiformes, Lamniformes and Orectolobiformes). No. 1*. Vol. 2 (FAO, 2001).

12 Huveneers, C. Redescription of two species of wobbegongs (Chondrichthyes : Orectolobidae) with elevation of "*Orectolobus halei*" Whitley 1940 to species level. *Zootaxa*, 29-57 (2006).

13 Last, P. R. & Chidlow, J. A. Two new wobbegong sharks, *Orectolobus floridus* sp. nov. and *O. parvimaculatus* sp. nov. (Orectolobiformes: Orectolobidae), from southwestern Australia. *Zootaxa*, 49-67 (2008).

14 Last, P. R., Chidlow, J. A. & Compagno, L. J. V. A new wobbegong shark, *Orectolobus hutchinsi* n. sp. (Orectolobiformes: Orectolobidae) from southwestern Australia. *Zootaxa*, 35-48 (2006).

15 Rodríguez-Cabello, C., Pérez, M. & Bañon, R. Occurrence of *Apristurus* species in the Galicia bank seamount (NE Atlantic). *J. Appl. Ichthyol.* **30**, 906-915 (2014).

16 Compagno, L. J. V. *Sharks of the order Charcharhiniformes*. (Princeton University Press, 1988).

17 Ebert, D. A. & Stehmann, M. F. W. *Sharks, batoids and chimaeras of the north Atlantic*. Vol. 7 523 (Food and Agriculture Organization of the United Nations, 2013).

18 Ebert, D. A. *et al.* Resurrection and redescription of *Squalus suckleyi* (Girard, 1854) from the north Pacific, with comments on the *Squalus acanthias* subgroup (Squaliformes: Squalidae). *Zootaxa*, 22-40 (2010).

19 Qingwen, M. & Yuanding, Z. A study of the spiral valves of chinese cartilaginous fishes. *Acta Zool. Sin.* **31**, 277-284 (1985).
20 Coelho, R. & Erzini, K. On the occurrence of the arrowhead dogfish, *Deania profundorum* (Chondrichthyes: Squalidae) off southern Portugal, with a missing gill slit. *Cybium* **30**, 93-96 (2006).
21 Compagno, L. J. V., Ebert, D. A. & Smale, M. J. *Guide to the sharks and rays of southern Africa*. (Struik, 1989).
22 Shirai, S. & Tachikawa, H. Taxonomic resolution of the *Etmopterus pusillus* species group (Elasmobranchii, Etmopteridae), with description of E. bigelowi, n. sp. *Copeia* **1993**, 483-495 (1993).
23 Yano, K. First record of the brown lanternshark, *Etmopterus unicolor*, from the waters around New Zealand, and comparison with the southern lanternshark, *E. granulosus*. *Ichthyol. Res.* **44**, 61-72 (1997).
24 Yano, K., Stevens, J. D. & Compagno, L. J. V. A review of the systematics of the sleeper shark genus *Somniosus* with redescriptions of *Somniosus* (*Somniosus*) *antarcticus* and *Somniosus* (*Rhinoscymnus*) *longus* (Squaliformes: Somniosidae). *Ichthyol. Res.* **51**, 360-373 (2004).
25 Ebert, D. A. & Cailliet, G. M. *Pristiophorus nancyae*, a new species of sawshark (Chondrichthyes: Pristiophoridae) from southern Africa. *Bull. Mar. Sci.* **87**, 501-512 (2011).
26 Ebert, D. A. & Wilms, H. A. *Pristiophorus lanae* sp. nov., a new sawshark species from the western north Pacific, with comments on the genus *Pristiophorus* Müller & Henle, 1837 (Chondrichthyes: Pristiophoridae). *2013* **3752**, 15 (2013).
27 Rafn, S. & Wingstrand, K. G. Structure of intestine, pancreas, and spleen of the australian lungfish, *Neoceratodus forsteri* (Krefft). *Zool. Scripta* **10**, 223-239 (1981).
28 Jollie, M. *Chordate morphology*. (Rheinhold publishing corporation, 1968).
29 Purser, G. L. IV.—*Calamoichthys calabaricus* J. A. Smith. Part i. The alimentary and respiratory systems—concluded. *Earth Environ. Sci. Trans. R. Soc. Edinb.* **56**, 89-101 (1929).
30 Weisel, G. F. Anatomy and histology of the digestive system of the paddlefish (polyodon spathula). *J. Morph.* **140**, 243-255 (1973).
31 Buddington, R. K. & Christofferson, J. P. Digestive and feeding characteristics of the chondrosteans. *Environ. Biol. Fish*. **14**, 31-41 (1985).
32 Weisel, G. F. Histology of the feeding and digestive organs of the shovelnose sturgeon, *Scaphirhynchus platorynchus*. *Copeia* **1979**, 518-525 (1979).
33 Macallum, A. B. Alimentary canal and pancreas of *Acipenser*, *Amia*, and *Lepidosteus*. *J. Anat. Physiol.* **20**, 604-636 (1886).
34 Gall, J. C., Grauvogel, L. & Lehman, J. P. Les poissons fossiles de la collection Grauvogel-Gall. *Ann. paléontol. (Vertébrés)* **60**, 129-147+i-x tables (1974).
35 Jörg, E. Fischfunde im oberen Buntsandstein (Untertrias) von Karlsruhe-Durlach. *Zeits. Deuts. Geol. Ges.* **121**, 105-110 (1970).
36 Bartram, A. W. H. The macrosemiidae, a mesozoic family of holostean fishes. *Bull. Br. Mus. (Nat. Hist.), Geol.* **29**, 137-234 (1977).
37 Neumayer, L. Vergleichend anatomische untersuchungen über den darmkanal fossiler fische. *Abh. Bayer. Akad. Wiss.* **29**, 1-28 (1919).
38 Hilton, W. A. On the intestine of *Amia calva*. *Am. Nat.* **34**, 717-735 (1900).
39 Lambers, P. H. The halecomorph fishes *Caturus* and *Amblysemius* in the lithographic limestone of Solnhofen (Tithonian), Bavaria. *Geobios* **27, Supplement 1**, 91-99 (1994).
40 Liston, J. in *Mesozoic fishes 4. Homology and phylogeny* (eds Arratia, G., Schultze, H.-P. & Wilson, M. V. H.) 181-197 (Verlag Dr. Friedrich Pfeil, 2008).
41 Arratia, G. & Schultze, H.-P. *Eurycormus* - *Eurypoma*, two Jurassic actinopterygian genera with mixed identity. *Foss. Rec.* **10**, 17-37 (2007).

CHAPTER II

Palaeontology The Palaeontological Association www.palass.org

[Palaeontology, 2018, pp. 1–16]

RE-EVALUATION OF THE ONTOGENY AND REPRODUCTIVE BIOLOGY OF THE TRIASSIC FISH *SAURICHTHYS* (ACTINOPTERYGII, SAURICHTHYIDAE)

by ERIN E. MAXWELL[1], THODORIS ARGYRIOU[2], RUDOLF STOCKAR[3] *and* HEINZ FURRER[2]

[1]Staatliches Museum für Naturkunde Stuttgart, Rosenstein 1, 70191, Stuttgart, Germany; erin.maxwell@smns-bw.de
[2]Paläontologisches Institut und Museum Universität Zürich, Karl-Schmid Strasse 4, 8006, Zurich, Switzerland; thodoris.argyriou@pim.uzh.ch, heinz.furrer-paleo@bluewin.ch
[3]Museo Cantonale di Storia Naturale, Viale Carlo Cattaneo 4, 6900, Lugano, Switzerland; rudolf.stockar@ti.ch

Typescript received 7 September 2017; accepted in revised form 5 January 2018

Abstract: Viviparity has evolved independently at least 12 times in ray-finned fishes. However, the fossil record of actinopterygian viviparity is poor, with only two documented occurrences. Both of these are from the non-teleost actinopterygian *Saurichthys*, and include *S. curionii* and *S. macrocephalus* from the Middle Triassic Meride Limestone (Monte San Giorgio, Switzerland). Here, we present new data on the reproductive biology of these species, giving unprecedented insights into their life-history. Based on positional and preservational criteria, six specimens were identified as unambiguously gravid. Embryos were positioned dorsal to the gastrointestinal tract, parallel to the axial skeleton and to each other, in the posterior two-thirds of the abdominal region. A minimum of 16 embryos are preserved in the most fecund females and, based on the largest preserved embryos and smallest preserved neonates, birth must have occurred at 7–12% of maternal fork length. Embryonic crania and teeth are relatively well-ossified, however ossification of the parietal region is delayed. In the postcranium, the median scale rows and lepidotrichia are ossified, but not the lateral scale rows. Ossified squamation and gradual allometric growth suggests that neonates did not undergo metamorphosis and were relatively precocial. When considered in a phylogenetic context, neither live birth nor internal fertilization appears to represent the primitive state for saurichthyid fishes.

Key words: Actinopterygii, *Saurichthys*, Triassic, Monte San Giorgio, viviparity, allometry.

COMPLETE ontogenetic trajectories of extinct vertebrates are only preserved under exceptional circumstances, yet have the ability to dramatically change our view of the evolution of life history traits and the palaeobiology of fossil organisms (Sánchez-Villagra 2012). Fossil ontogenies are known for all major vertebrate groups. Among actinopterygian fishes, species with preserved ontogenetic series are known from the Carboniferous to the Pliocene, but this still only encompasses a tiny fraction of the known diversity of fossil actinopterygians (Cloutier 2010). An understanding of the morphological changes undergone during ontogeny can be helpful for accurate taxonomy, but also has the potential to improve our understanding of macroevolutionary processes, such as the generation of morphological novelties, biogeography and extinction.

Fish ontogeny typically consists of four phases: embryo, larva, juvenile and adult (Kendall *et al.* 1984), with the larval phase being absent in direct developing taxa (Balon 1999). The transition from the embryonic to the larval phase occurs with the beginning of exogenous feeding, and is thus unrelated to hatching (Balon 1999); the larval phase ends with metamorphosis which, vaguely defined, relates to settling in taxa with pelagic larvae, and may also encompass the loss of larval characters (Kendall *et al.* 1984; Balon 1999). The juvenile phase ends with sexual maturity. All phases are represented in the fossil record (Cloutier 2010).

Viviparity, defined as hatching of the embryos inside the female reproductive tract (Wourms & Lombardi 1992), has evolved independently at least 12 times in actinopterygian fishes, with 11 of those 12 origins occurring in the Teleostei. Unlike in squamates, where viviparity has evolved multiple times at the generic or lower taxonomic levels, viviparity in fishes tends to characterize higher taxonomic levels (family or sub-family) (Blackburn 2005), and has been correlated with increased diversification rates in some

doi: 10.1111/pala.12355

clades (Helmstetter *et al.* 2016). Unlike in viviparous placoderms, chondrichthyans, and to a lesser extent some coelacanths, which give birth to large, fully developed young (Blackburn 1999; Long *et al.* 2008; Wen *et al.* 2013), viviparity in extant actinopterygians encompasses the entire altricial–precocial spectrum, with birth occurring anywhere from embryonic stages (*sensu* Balon 1999) to sexually mature offspring (Wourms & Lombardi 1992). Positive selection for viviparity in fishes has been correlated with a range of factors, summarized by Wourms & Lombardi (1992). These include reduction in competition for demersal nesting habitats and territories, facilitated exploitation of pelagic niches, and small body size. In addition, occupation of habitats enriched in hydrogen sulphide also appears to favour viviparity, presumably to maintain homeostasis during development (Riesch *et al.* 2015).

Among non-teleost actinopterygians, only a single occurrence of viviparity has been reported, in the Triassic fish *Saurichthys* (reviewed by Blackburn 2005). Saurichthyidae is a speciose, long-lived clade, with a stratigraphic range extending from the late Permian to the Middle Jurassic (Romano *et al.* 2012; Maxwell 2016). Viviparity has been reported in only two species, *S. curionii* and *S. macrocephalus*, both from the Middle Triassic (Ladinian) Meride Limestone, from Monte San Giorgio, Switzerland (Rieppel 1985; Bürgin 1990; Renesto & Stockar 2009). In addition to preserving some of the earliest ontogenetic stages, limited growth series are available, and preliminary observations have been published (Bürgin 1990; Rieppel 1992). Ongoing work on this locality has led to a wealth of newly-prepared finds, including new embryonic material. Here, we present new data on the reproduction and growth of *S. macrocephalus* and *S. curionii*, giving unprecedented insights into the life-history of these 240 million year old fishes.

MATERIAL

Most described specimens were collected from the Cassina beds of the Meride Limestone (Monte San Giorgio, Switzerland) in systematic bed-by-bed excavations by teams from the University of Zurich, directed in 1933 by Bernhard Peyer, and between 1971–1975 by Emil Kuhn-Schnyder (Kuhn-Schnyder 1974), but most specimens have only recently been prepared as part of a large SNF-funded project on the palaeobiology of *Saurichthys*. The material is deposited in the collection of the Paläontologisches Institut und Museum Universität Zürich (PIMUZ). Additional juvenile specimens come from a new excavation started in 2006 by the Museo Cantonale di Storia Naturale (Lugano, MCSN) in the Cassina beds at the type locality (Stockar 2010).

The Cassina beds of the Meride Limestone are late early to early late Ladinian in age (Stockar *et al.* 2012). It is considered to represent a restricted basin, with low-oxygen benthic conditions and relatively rapid sedimentation, facilitating exceptional preservation of vertebrate fossils (Stockar 2010; Beardmore & Furrer 2016). This includes phosphatized muscle tissues, embryonic remains, and details of gastrointestinal anatomy in *Saurichthys* (Renesto & Stockar 2009; Maxwell *et al.* 2013; Argyriou *et al.* 2016*a*). Two species of *Saurichthys* have been described from these beds, *S. curionii* and *S. macrocephalus* (Rieppel 1985). These two taxa are differentiated by several characteristics. These include subopercle shape (see Argyriou *et al.* (2016*b*) for discussion of homologies), development of the dentition, and skull fineness (Rieppel 1985), in addition to the degree of interorbital constriction (Maxwell *et al.* 2015). In earlier analyses, these two taxa formed a species pair sister to the other saurichthyids from Monte San Giorgio (Rieppel 1992). Subsequent analyses place them as outgroups to the Late Triassic-Jurassic *Saurorhynchus* species group (Maxwell *et al.* 2015).

METHOD

Homologies of the opercular series

The dorsalmost bone in the opercular series of *Saurichthys* has historically been interpreted as an expanded opercle. However, reanalysis of the homologies of this element suggests that it is in fact an expanded subopercle based on its articulation with the ventral rather than dorsal hyomandibula (Argyriou *et al.* 2016*b*). The terminology used in the current contribution reflects this new interpretation.

Embryos versus gastric contents

Distinguishing embryos from neonatal prey items is problematic in fossil taxa (Sánchez-Villagra 2012). It is especially problematic in saurichthyids, since unambiguous cannibalism of congeners has been thoroughly documented in these piscivorous fishes (Rieppel 1985; Furrer 2015; Renesto & Stockar 2015; Argyriou *et al.* 2016*a*; Kogan & Romano 2016). We apply a combination of criteria to distinguish between embryos and gastric contents in *S. curionii* and *S. macrocephalus*:

1. *Gastric contents*. Small specimens mixed in with the stomach contents (Fig. 1A, B), or in the branchial region (Fig. 1C) are considered to have been ingested as prey items.
2. *Three-dimensional phosphatization of postcranial soft tissues* (Renesto & Stockar 2009). If three-dimensional

FIG. 1. Small saurichthyids as gastric contents. A–B, PIMUZ T 5690, a female *Saurichthys curionii* with small saurichthyids preserved in a ball medial to phosphatic chyme. C, UVA photo of PIMUZ T 2639, a small female *S. macrocephalus* with smaller saurichthyids chaotically oriented within the abdominal region. *Abbreviations*: 1, anterior tip of the most anterior skull; liv, liver; sop, subopercle. Scale bars: in cm (A); in mm (B); represents 10 mm (C). Colour online.

phosphatized postcranial soft tissues are present (Figs 2–4), we consider the small individuals inside the abdominal cavity of a larger individual to represent embryos. This type of preservation is not seen in small specimens which are unambiguously gastrointestinal contents. This pertains to the special type of preservation seen in the Cassina beds, and thus is likely to be of limited use in differentiating embryonic from gastric material in other lithological units. However, it is our primary criterion for distinguishing gastric contents from embryos, even within the abdominal cavity of a single large individual.

3. *Position*. In the rare cases where the stomach, with clearly defined contents, is well preserved, small individuals located dorsal to the stomach, ventral to the vertebral column, and clearly distinct from the gastric contents are considered to be embryos. This criterion is only applied to the embryos of PIMUZ T 4106 (Fig. 3), the majority (but not all: Fig. 4C) of which lack phosphatized postcranial structures.

Ambiguity. The nature of the small individuals within the abdominal cavity of *Saurichthys* is unambiguous for the majority of specimens. However, the nature of many specimens is unclear. Understanding the relationship between female size and embryo size, as well as aspects of embryonic morphology may help clarify these ambiguous specimens.

Assigning juveniles to species

Juveniles of *Saurichthys curionii* and *S. macrocephalus* were assigned to species based on several criteria, including the relative length and gracility of the jaws, degree of interorbital constriction, and shape of the subopercle (Fig. 5A, C). Dentition provides another useful character for distinguishing between the two species. *S. curionii* individuals exhibit few, fine, and coarsely arranged laniaries on their jaws, with the space between them being lined with smaller teeth (Rieppel 1985, 1992). *S. macrocephalus* juveniles exhibit heavier dentitions, characterized by more numerous, larger and more closely spaced laniaries (Rieppel 1985). Although smaller teeth between the laniaries are known in larger *S. macrocephalus* specimens (Rieppel 1985), they are barely observable in small juveniles. PIMUZ T 4451 (Fig. 5C) was assigned to *S. curionii* rather than *S. macrocephalus* by Rieppel (1992); however this specimen appears to be more consistent with *S. macrocephalus* based on subopercle shape and jaw morphology.

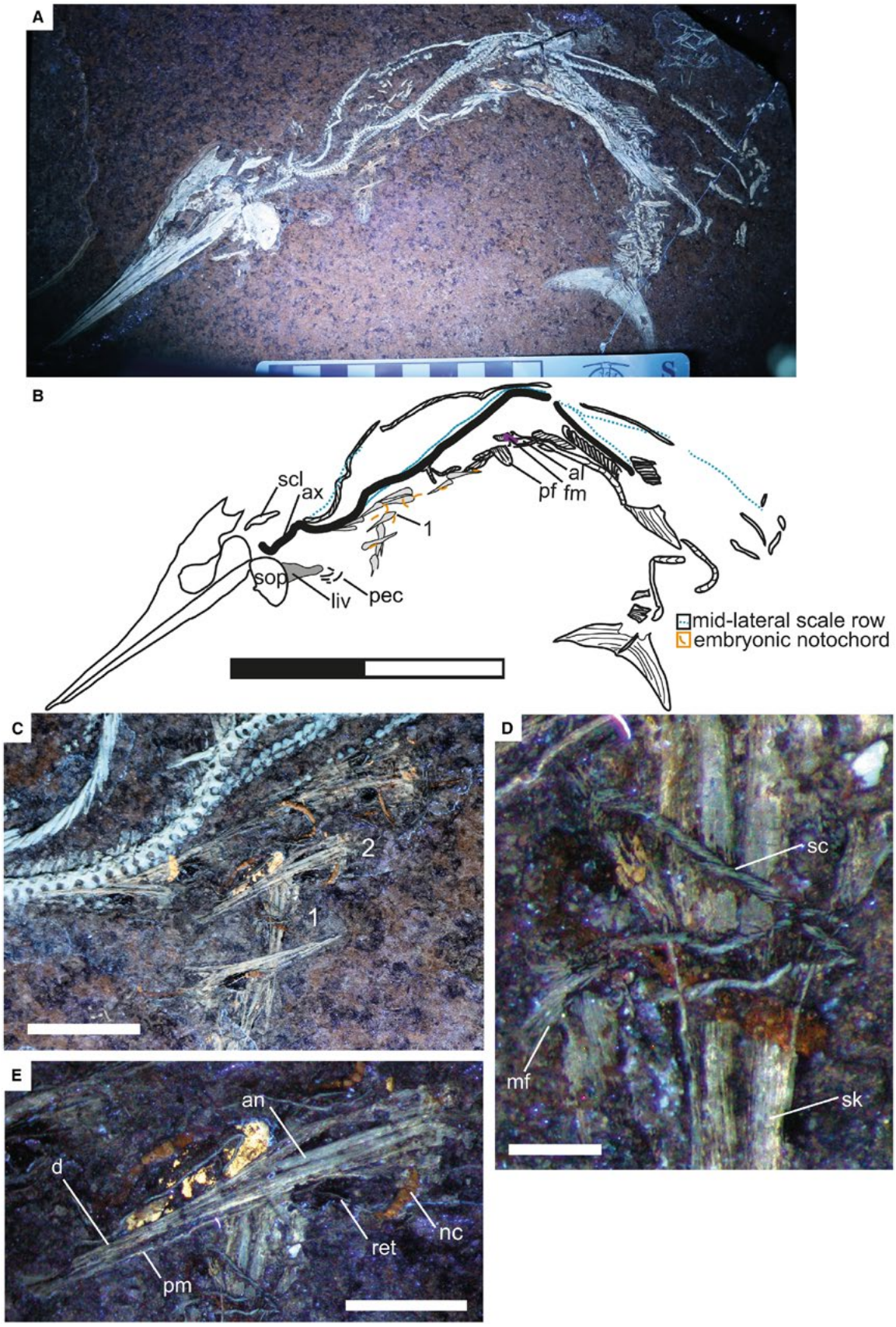
A
B
scl
ax
pf
al
fm
1
sop
liv
pec
mid-lateral scale row
embryonic notochord
C
2
1
D
sc
mf
sk
E
an
d
ret
nc
pm

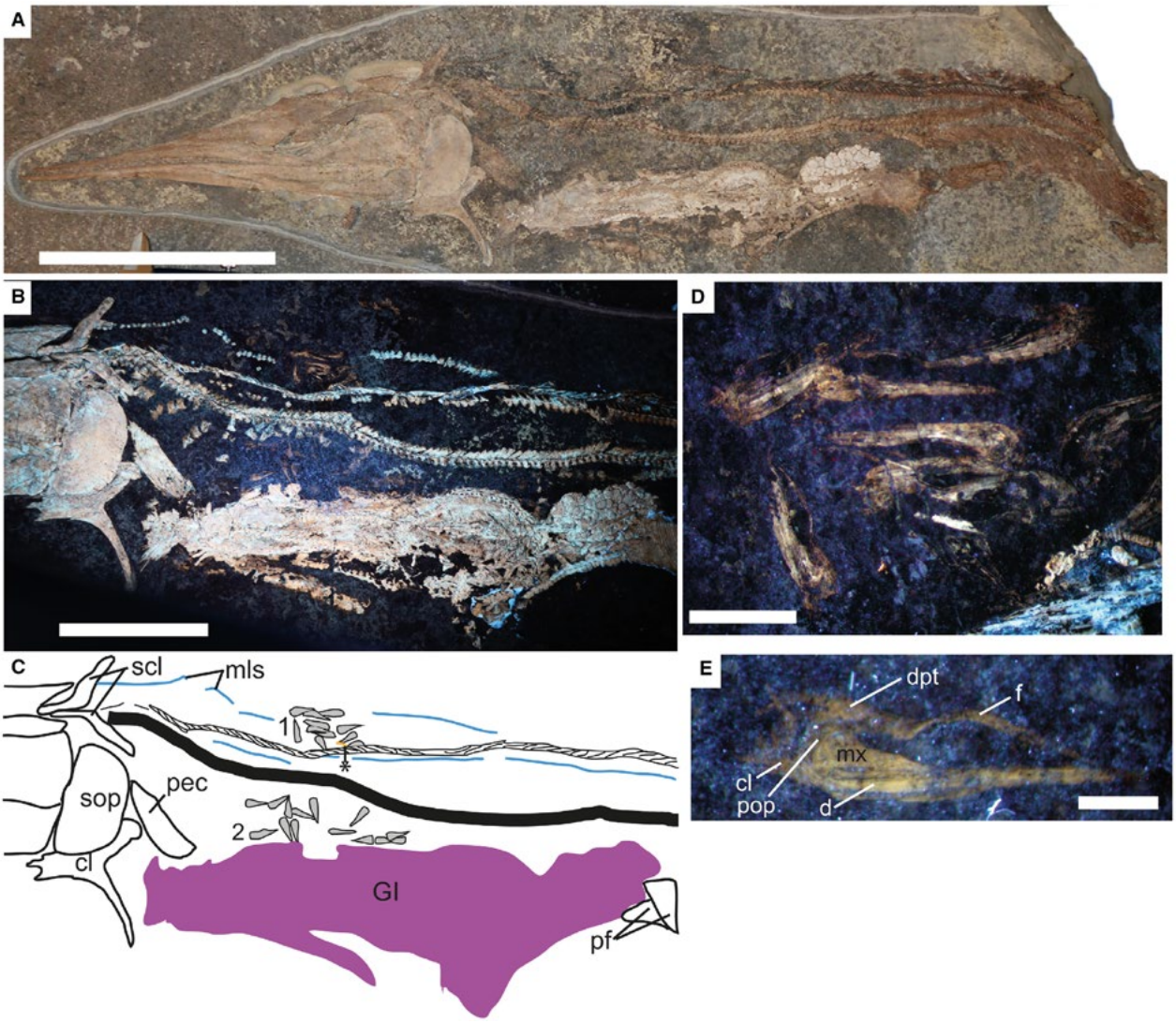

FIG. 3. PIMUZ T 4106, female *Saurichthys macrocephalus* containing gastric contents and embryos inside the abdominal cavity. A, overview. B, abdominal region photographed under handheld UVA light. C, interpretive drawing, asterisk indicates the phosphatized embryonic postcranium, grey triangles represent embryonic skulls. D, magnified view of a cluster of embryonic skulls (indicated by the number 1 on the interpretive drawing). E, photo of the embryonic skull figured by Bürgin (1990) (indicated by the number 2 on the interpretive drawing). *Abbreviations*: cl, cleithrum; d, dentary; dpt, dermopterotic; f, frontal; GI, contents of the gastrointestinal tract; mls, midlateral scale row; mx, maxilla; pec, pectoral fins; pf, pelvic fins; pop, preopercle; scl, supracleithrum; sop, subopercle. Scale bars represent: 100 mm (A); 50 mm (B); 5 mm (D); 2 mm (E). Colour online.

Allometry

Several authors have commented on allometry in *S. curionii* and *S. macrocephalus* (Bürgin 1990; Rieppel 1992). However, these studies both relied on changing ratio values between small and large individuals, and did not examine growth curves *per se*. Here, we present explicit growth data for four measurement pairs: antorbital

FIG. 2. PIMUZ T 5764, female *Saurichthys curionii* containing embryos inside the abdominal cavity; photographed under handheld UVA light. A, overview. B, interpretive drawing; grey triangles represent embryonic skulls. C, magnified view of the main group of embryos (indicated by the number 1 on B). D, magnified view showing ossified squamation and lepidotrichia, location indicated by the number 1 on C. E, magnified view of a single skull, location indicated by the number 2 on C. *Abbreviations*: al, anal loop; an, angular; ax, axial skeleton; d, dentary; fm, phosphatic fecal matter; liv, liver; mf, median fin lepidotrichia; nc, notochord; pec, pectoral fin lepidotrichia; pf, pelvic fins; pm, rostropremaxilla; ret, retinal pigment; sc, median scale row; scl, supracleithrum; sk, embryonic skull; sop, subopercle. Scale bars: in cm (A); represent: 100 mm (B); 10 mm (C); 1 mm (D); 4 mm (E). Colour online.

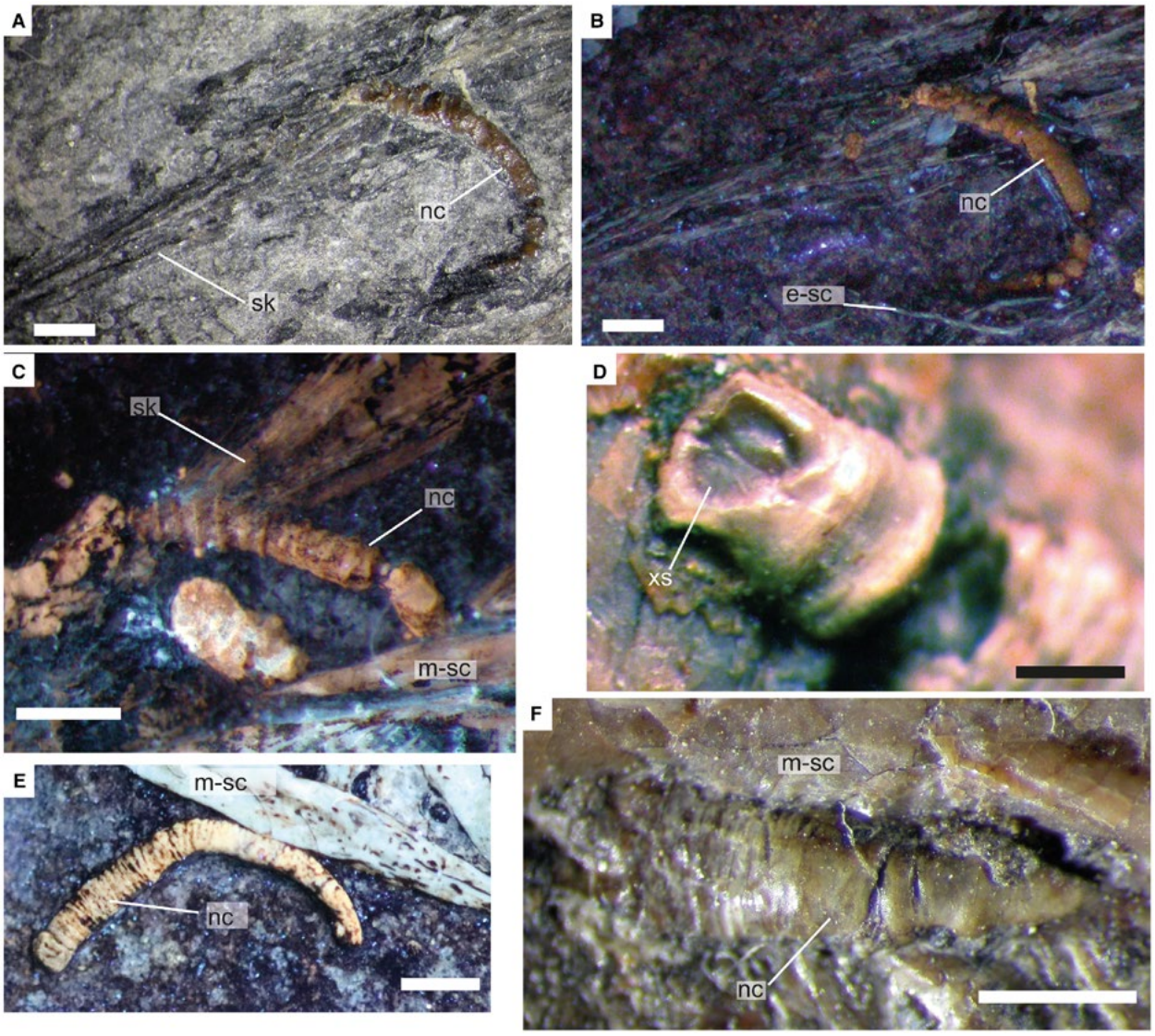

FIG. 4. Phosphatized embryonic postcranial structures, interpreted as the notochord, showing different types of preservation. A–B, PIMUZ T 5864: A, relationship between the phosphatic structure and the embryonic skulls in terms of colour, texture and three-dimensionality; B, same specimen, photographed under UVA light. C, PIMUZ T 4106 (*Saurichthys macrocephalus*), sole embryo showing phosphatization of postcranial soft tissues, photographed under UVA light. D, cross-section (PIMUZ T 5638); note the two-layered structure. E, PIMUZ T 4156, photographed under UVA light. F, PIMUZ T 5638 (different embryo from the one figured in D), note the segmentation and fibrous texture of the outer layer. *Abbreviations*: e-sc, embryonic scale row; m-sc, maternal scale; nc; embryonic notochord; sk, embryonic skull; xs, cross-section of the notochord. Scale bars represent: 1 mm (A–C, E, F); 0.5 mm (D). Colour online.

length (measured from the anterior edge of the orbit to the tip of the rostrum): mandibular length; subopercle length: height, anterior insertion of the dorsal fin to length of the vertebral column, and cranial length (measured from the tip of rostrum to the jaw joint) to length of the vertebral column (Maxwell *et al.* 2018, appendix S1). These pairs were explicitly selected to test: (1) the reported isometric growth of the antorbital rostrum relative to the skull (Rieppel 1992); (2) ontogenetic changes in subopercle shape (Rieppel 1992); and (3) differential growth within the axial skeleton and between the axial skeleton and the skull. Specimens were assigned *a priori* to species based on the criteria listed above. All measurement data were log transformed prior to analysis and fit to a linear curve using RMA regression ($y = mx + b$, where m is the slope). If the 95% confidence interval for the slope ($m \pm 1.96 \times \mathrm{SE}$) differs from 1, this means that the structures grow allometrically. Analyses were performed in PAST (Hammer *et al.* 2001).

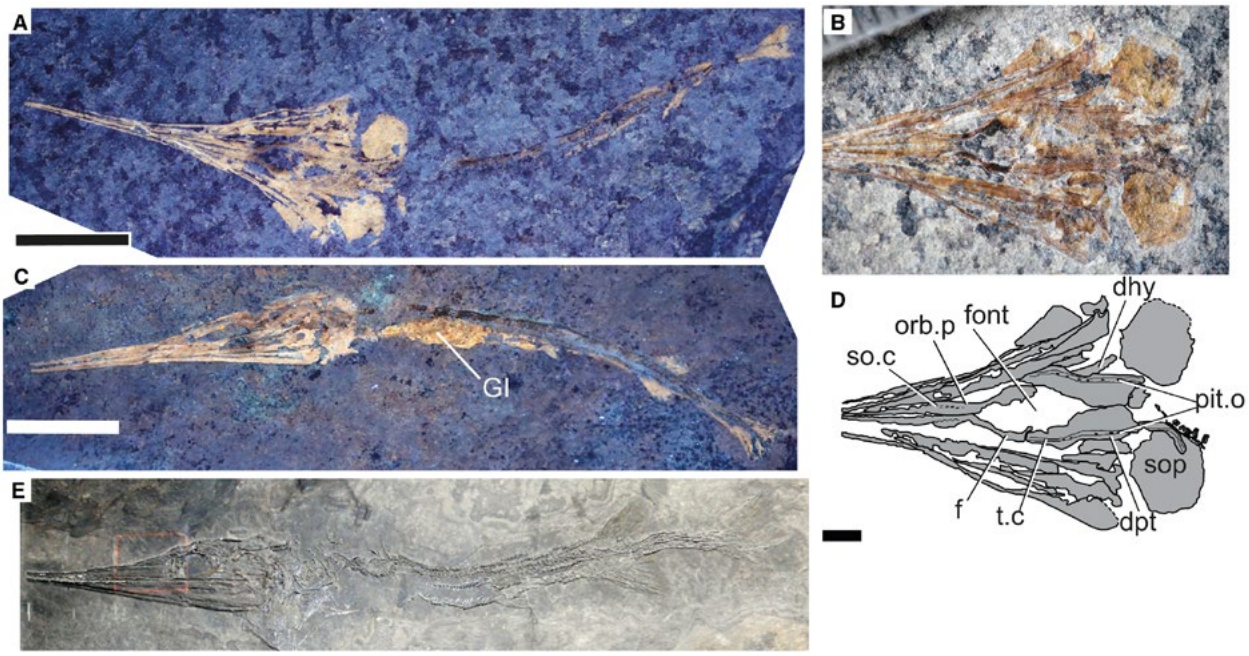

FIG. 5. A–B, D, juvenile *Saurichthys curionii* (PIMUZ T 5752, mirrored, fork length = 69 mm); B, detail of dermal skull roof; D, interpretative drawing. C, juvenile *S. macrocephalus* with phosphatic stomach contents (PIMUZ T 4451; fork length = 68 mm); note the shorter and more robust rostrum and larger teeth relative to A. E, adult *S. macrocephalus* (PIMUZ T 3805, mirrored, fork length = 216 mm) to the same scale to illustrate the degree of negative cranial allometry. *Abbreviations*: dhy, dermohyal; dpt, dermopterotic; f, frontal; font, fontanelle; GI, gastrointestinal contents, orb.p, mineralized supraorbital pad of the frontal; pit.o, pit organs; so.c, supraorbital sensory canal; sop, subopercle; t.c, temporal sensory canal. A, D photographed under UVA light. Scale bar represents 10 mm. Colour online.

RESULTS

Males and females of *Saurichthys curionii* and *S. macrocephalus* can be distinguished based on the presence of a mineralized copulatory organ consisting of modified mid-ventral scales posterior to the anal loop in males (Rieppel 1985; Bürgin 1990). Of the adults in which the anal loop was well preserved, 10/15 (*S. curionii*) and 5/7 (*S. macrocephalus*) were female (67% and 71%, respectively). All of the largest specimens were female, indicating reverse sexual size dimorphism in these species. In both taxa the largest males are of similar size to mid-sized mature females (*S. curionii*: 350–370 mm fork length; 479 mm, *S. macrocephalus*).

In total, 18 specimens were identified as containing small specimens inside the abdominal cavity of larger females, including the two specimens previously described as gravid (PIMUZ T 3917, PIMUZ T 4106: Bürgin 1990; Rieppel 1992). Of these, embryos were unambiguously present in six specimens, five of which are referable to *S. curionii* (PIMUZ T 5660, PIMUZ T 5764, PIMUZ T 4156, PIMUZ T 5673, PIMUZ T 5638) and one (PIMUZ T 4106; Fig. 3) to *S. macrocephalus*. Gravid females of *S. curionii* ranged in size from 34.7 cm fork length (PIMUZ T 5830) to over 63.1 cm in length (PIMUZ T 5638, rostrum broken anteriorly; the largest *S. curionii* specimen available). The gravid specimen of *S. macrocephalus* measured 43.9 cm as preserved, with fork length estimated at 65.3 cm.

As noted in the Method, above, distinguishing between embryos and gastric contents was challenging, even within a single female. For the following description, we rely heavily on PIMUZ T 5764, one of the best-preserved specimens containing embryos.

Litter size and position

At least 12 embryos are preserved in the abdominal cavity of PIMUZ T 5764 (estimated fork length = 373 mm; Fig. 2). The most anterior part of the most anterior embryo is 29 mm from the jaw joint of the female (29% of the length of the abdominal region). Embryos are situated posterior to the black mass often preserved medial to the pectoral fins in Monte San Giorgio saurichthyids and possibly representing the liver. Some poorly ossified remains lying ventral and anterior to this embryo are interpreted as damaged pectoral lepidotrichia. The main clump of embryos is 35 mm long, such that most of the embryos occupy the middle third of the abdominal region of the female. They lie close to the female's vertebral column, with the exception of four embryos that have been displaced ventrally from the main clump, and two lying posterior to the main clump that are also

in a more ventral position. All embryos in the clump appear to be facing anteriorly. One of the ventrally displaced skulls is facing posteriorly, as is one of the posteroventral skulls. As these two skulls appear to have been displaced, their original orientation is uncertain. Many of the embryos, especially those in the main clump, are coated with a black film.

PIMUZ T 5638 (estimated fork length = 675 mm), the largest female, contains an indeterminate number of embryos, the minimum count of which is 16 and the total count of which was probably much higher. Only four of the embryos are *in situ* in the posterior abdominal region, the rest have been scattered. The tip of the rostrum of the most anterior confirmed embryo, determined based on postcranial phosphatization, is located at 35% of the length of the abdominal region. A similar-sized skull anterior to the confirmed embryo is more heavily ossified, is oriented posteriorly, and lacks postcranial phosphatization. Its embryonic nature is questionable.

PIMUZ T 4156, a mid-sized female (fork length = 452 mm), also has a large number of embryos inside the abdominal cavity. Although an exact count is again difficult, 16 embryos appear to be present. Only the phosphatized postcranial elements are preserved (Fig. 4E). The delicate embryonic bones either were not well preserved or were removed during preparation; ossification was definitely at an advanced stage based on embryonic bone fragments adhering to a single postcranium. The most anterior embryonic postcranium is positioned at 44% of the female abdominal length. The majority of the embryos are in a large clump located at 61–73% of abdominal length. The most posterior embryos appear to have been displaced and are scattered outside the body cavity.

The single confirmed gravid specimen of *S. macrocephalus* was reported to have 16 embryos in the abdominal cavity (Bürgin 1990). The female, PIMUZ T 4106 (Fig. 3), lacks the caudal region but fork length is estimated at 653 mm. Reexamination under UVA light suggests that a minimum of 24 embryos were present. The most anterior embryo is 62 mm from the jaw joint, at 30% of the female abdominal length. Embryos are also absent in the posterior third of the abdominal region. The 'stomach' (Argyriou *et al.* 2016*a*) extends further anteriorly and ventral to the preserved embryos. Only one embryo preserves three dimensional phosphatized postcranial remains (Fig. 4C). All embryos are chaotically oriented dorsal to the well-defined gastric contents. Ten of these are situated in a clump near the right-hand midlateral scale row, which has been displaced dorsally. A further 14 are situated ventral to the vertebral column.

Embryonic morphology

The embryonic skulls in PIMUZ T 5764 are the most heavily ossified parts of the skeleton, and are between 11 and 15 mm in length, less than 16% of the skull length of the female (broken anteriorly, but with a preserved length of 94 mm). Embryonic skulls preserved in PIMUZ T 5638 are of a similar size (11–15 mm, less than 9% of the preserved female skull length). Although this variation in embryonic skull length within a litter is substantial, it may partially reflect preservation or preparation damage to the extremely delicate anterior rostrum. The embryonic bones have a smooth to slightly fibrous texture; ganoine ornamentation was not observed. Teeth are visible under UVA light. Retinal pigmentation is preserved in many of the embryos (e.g. Fig. 2E). In addition to the skulls, the embryos have preserved postcrania. These consist of a three-dimensional phosphatized component ('somites' of Renesto & Stockar 2009), as well as ossified fin rays and median scales (Fig. 2D). In the best-preserved embryos, the phosphatized component begins posterior to the skull and curls anteriorly (Fig. 4A, B). It measures ~0.3–0.5 mm wide at its midpoint, and up to 5 mm long. Whereas preserved width of this structure is remarkably consistent between embryos, preserved length is highly variable. Examination at higher magnifications reveals the reason for this: phosphatization decreases posteriorly, and so the structures often appear to taper or even become disjointed. Ossified postcranial elements (median scale rows, lepidotrichia) are situated posterior to the end of the phosphatized structure indicating that it does not represent the entire postcranium. The phosphatized structure shows ring-like segmentation, often somewhat uneven both in length between adjacent segments and width within a segment. Based on PIMUZ T 5638, the phosphatized structure is formed from two components: a thin outer layer with a fibrous texture, and a solid inner core (Fig. 4D, F). These are differentiated based on colour as well as texture, with the outer layer being lighter in colour than the inner layer. We interpret these phosphatized structures as the notochord (see discussion for details of interpretation). Due to their microscopic size, few morphological details can be added regarding the ossified portion of the postcranium. The median scales are extensively overlapping and bifurcate anteriorly. Lepidotrichia appear to be unsegmented.

PIMUZ T 5673 includes multiple small skulls associated with the abdominal cavity of a larger individual of *S. curionii*. However, of these only one is associated with a small amount of postcranial phosphatization in the anterior notochord. This skull, 16.5 mm in length, is associated with ossified neural arches, but more significantly, a well-preserved subopercle. This subopercle shows a prominent angle along the anterior edge similar to that noted in adult *S. curionii* (Wilson *et al.* 2013), and justifies the referral of PIMUZ T 4451 (which has a straight anterior edge of the subopercle: Rieppel 1992) to *S. macrocephalus*.

In *S. macrocephalus* (PIMUZ T 4106), the embryos are not as well preserved as in PIMUZ T 5764. In particular, the anterior rostrum is rarely preserved (Fig. 3D, E). Given variation in the quality of preservation between the embryos, we attribute the short length of the antorbital rostrum in most specimens to preservational factors relating to weak ossification of the rostrum (and loss during preparation) rather than allometric growth. The longest preserved embryonic skull has a length of 8.9 mm, only 5.5% the length of the female skull and smaller than the embryonic skulls of PIMUZ T 5764. The antorbital length is approximately 5.0 mm. All skulls are relatively well ossified, with robust dentition. A single embryo preserves ossified scales and lepidotrichia.

Juvenile morphology

We also examined juvenile specimens of *Saurichthys curionii* and *S. macrocephalus* in order to document qualitative post-natal changes in shape and ossification. In juvenile specimens PIMUZ T 5752 (*S. curionii*; fork length = 69 mm) and PIMUZ T 4451 (*S. macrocephalus*; fork length = 68 mm) there is incomplete contact between the right and left frontals along the midline. The first contact between the frontals occurs between the orbits and is already present in all adequately preserved specimens. However, the anteromedial and posteromedial edges of the frontals do not meet on the midline until later in postnatal ontogeny (Fig. 5B, D). In addition, the parietals ossify relatively late in ontogeny, after birth, and the area between the posteromedial frontals and anteromedial dermopterotics is open as a fontanelle in neonatal specimens in both *S. curionii* and *S. macrocephalus*.

During actinopterygian development, the lateral line system of the skull is initially open in grooves, which are progressively enclosed in bony canals. These canals are at first situated on top of the developing dermal plates of the skull, but are gradually invested into the latter, and in most cases end up bulging out from their internal surface (Jollie 1984 and references therein). The early stage of this process can be seen in a small *S. curionii* specimen (PIMUZ T 5752; Fig 5B, D), which exhibits partially enclosed and superficially situated temporal sensory canals/grooves running along the length of the dermopterotics. At least five and six oval openings are seen along the course of the temporal canal on the left and right dermopterotic respectively. These openings probably correspond to pit organs, which are completely covered by bone in adult specimens (see material figured in Rieppel 1985). The supraorbital cranial sensory canal appears to close earlier in ontogeny. Also, in small specimens, well-mineralized pads form the dorsal margin of the orbit (see Fig. 5). The remaining portions of the cranial sensory canals cannot be described in any of the juveniles. Finally, juvenile dermatocranial bone ornamentation is characterized by a coarser honeycomb-like pattern, with higher relief than in adults.

In terms of postcranial morphology, lepidotrichia in embryos and neonates are unsegmented, as previously noted (Rieppel 1992). Counts are very difficult to establish as both hemitrichia are compressed and appear on the same plane (Rieppel 1992). However, the shape of the unpaired fins does vary between adult and juvenile specimens, with juveniles having lower, more elongate fins (Rieppel 1992). Since the number of neural arches is theoretically fixed prior to the onset of ossification, these appear much more closely packed in juveniles than in adult individuals, and neural spines are greatly reduced or entirely absent. The mid-dorsal scale row is consistently present and well-developed. The mid-ventral scale row is somewhat more difficult to observe, but is probably also present. It is likely that other scale rows are absent in small specimens. At minimum, the lateral scale rows begin to ossify between 68 and 87 mm fork length in *S. macrocephalus* (PIMUZ T 4451; PIMUZ T 5768) and sometime after 69 mm fork length in *S. curionii* (PIMUZ T 5752; Fig. 5A).

Allometry

Subopercle growth in height is isometric relative to length in *S. curionii* ($N = 19$; $y = 1.03x + 0.10$; SE (m) = ± 0.08; $r^2 = 0.90$) and shows weak positive allometry in *S. macrocephalus* ($N = 12$; $y = 1.13x + 0.05$; SE (m) = ± 0.06; $r^2 = 0.97$). The observed overlap in subopercle dimensions at the lower end of the adult body size range was surprising, as subopercle ratios have been successfully used to separate the two taxa (Wilson *et al.* 2013). We attribute the difference to a larger sample size of *S. macrocephalus* in our study ($N = 11$ vs $N = 3$). Of the linear measurements examined over the course of this study, the relationship between subopercle height and length of the antorbital rostrum are the two that most clearly separate *S. curionii* from *S. macrocephalus.*

Antorbital length increases isometrically relative to jaw length. Moreover, the *S. curionii* and *S. macrocephalus* data are largely non-overlapping. *S. curionii*: ($N = 14$) $y = 1.02x - 0.19$, SE (m) = ± 0.02; $r^2 = 0.99$; *S. macrocephalus* ($N = 13$): $y = 1.04x - 0.27$; SE (m) = ± 0.02, $r^2 = 0.99$.

In *S. curionii*, the position of the dorsal fin does not shift relative to the vertebral column with increasing body size ($N = 18$; $y = 1.02x - 0.20$; SE (m) = ± 0.02, $r^2 = 0.99$). Males are not differentiated from females. In *S. macrocephalus*, the same pattern is observed, although an outlier (PIMUZ T 3805) is responsible for a decrease in slope relative to *S. curionii* ($N = 8$, $y = 0.94x - 0.07$; SE (m) = ± 0.04; $r^2 = 0.99$).

The length of the skull, from the tip of the rostrum to the jaw joint, grows with negative allometry relative to the vertebral column in *S. curionii* and *S. macrocephalus* (*S. curionii*: $N = 12$, $y = 0.79x + 0.21$; SE (m) = ±0.03, $r^2 = 0.98$. *S. macrocephalus*: $N = 9$, $y = 0.72x + 0.27$, SE (m) = ±0.04, $r^2 = 0.98$). The length of the skull, from the tip of the rostrum to the jaw joint, relative to the vertebral column is statistically indistinguishable from isometry (slope = 1.01) in the *S. curionii* adult sample (static allometry), although it should be noted that the fit of the curve is not statistically well-supported ($r^2 = 0.68$). Although at very large body size the growth of the skull appears to decrease relative to the vertebral column in *S. macrocephalus*, the influence of outlier PIMUZ T 5631 in driving this pattern cannot be entirely discounted.

DISCUSSION

Reproductive anatomy

The anatomy of the female reproductive tract of extant non-teleostean actinopterygians is of the generalized vertebrate type, comprising two ovaries disconnected from their respective oviducts, and broadly resembling those of chondrichthyans and piscine sarcopterygians (Jollie 1973; Wourms & Lombardi 1992). In viviparous members of the latter two groups, the posterior part of the oviduct(s) in the posterior part of the abdominal cavity and close to the genital opening is modified into an enlarged uterine structure, where developing embryos are accommodated (Wourms *et al.* 1991; Wourms & Lombardi 1992). Teleosts, by contrast, seem to lack oviducts, and in viviparous forms, embryos are either retained in the ovary(ies) or are released inside the abdominal cavity (Wourms *et al.* 1988; Wourms & Lombardi 1992). The presence of clusters of confirmed embryos in the anterior and middle parts of the abdominal cavity of *Saurichthys*, dorsal to the stomach, suggests that these were accommodated in their respective oviduct for at least part of their embryonic development. In PIMUZ T 4156 and PIMUZ T 4106, there are two clumps of embryos, one on each side of the mid-dorsal scale row (Fig. 3B, C). These clumps probably correspond to functional left and right oviducts, as in other non-teleostean actinopterygians (Jollie 1973).

Staging and precociality

Saurichthys curionii embryos exhibit ossified cranial elements, but also partially ossified squamation, dentition and lepidotrichia (Fig. 2C). The jaws of the largest preserved embryos cluster around 15 mm in length, with the largest probable embryo having a skull 16.5 mm in length (estimated fork lengths 32–36 mm based on the allometric equation presented in the results). The smallest free-living saurichthyids from the Meride Limestone are around 50 mm in length (jaws 18 mm in length: MCSN 8340 (*S. macrocephalus*); jaws 22 mm in length: MCSN 8091 (*S. curionii*)). Skulls falling in the size range of 17–20 mm are observed inside the abdominal cavities of larger females, but while some of these may be late-stage embryos not preserving phosphatized postcrania, others are most likely to be gastric contents (e.g. PIMUZ T 5639: small skulls 20% of female skull length, chaotically arranged throughout the abdominal cavity and penetrating the branchial region). Birth in *S. curionii* apparently occurred at skull lengths of 17–19 mm (estimated body lengths of 37–42 mm), which is approximately 12% of maternal fork length in the smallest females, and only 7% in the largest. Observed litter size in *Saurichthys curionii* is moderate, with a range of 12 to more than 16 embryos (these data; Renesto & Stockar 2009). In *S. macrocephalus*, 24 embryos were noted (PIMUZ T 4106); these were proportionately small relative to the female but only slightly smaller than those of *S. curionii* PIMUZ T 5764 (Bürgin 1990). In our sample, large females are not associated with significantly larger young, suggesting that reverse sexual size dimorphism (i.e. larger females) in *S. curionii* and *S. macrocephalus* results in increased fecundity rather than larger offspring. Among extant viviparous fishes, embryos up to 20% female length and litter sizes surpassing 15 young are not unusual (e.g. *Latimeria*: Wen *et al.* 2013; *Galeocerdo*: Whitney & Crow 2007; some surfperches: LaBrecque *et al.* 2014).

Postnatal growth of the premaxillary rostrum is essentially isometric in *Saurichthys curionii* (Rieppel 1992) and also in *S. macrocephalus*, differing from the reported pattern of prenatal rostral growth (Bürgin 1990). This is largely due to interobserver differences: Bürgin (1990) reported the mandibular length: antorbital length ratio as 1.4 (adult) and 1.85 (embryos) in PIMUZ T 4106, whereas our values suggest a much smaller difference in ratios, at 1.64 (adult) versus 1.78 (embryos). The relationship between subopercular length and height in both species was also particularly surprising, as it implies that fineness is relatively constant, that is, body shape does not undergo any major changes with increasing size; however a slight increase in depth with increasing body size was noted for *S. macrocephalus*. Constant body shape is also supported by the isometric relationship between dorsal fin position and axial length. Unlike growth within the skull, the relationship of the skull to axial length indicates a major allometric change in postnatal proportions. Negative cranial allometry (skull length relative to body length) is common among vertebrates, including early actinopterygian fishes (e.g. Schultze & Bardack 1987), and *S. curionii* and *S. macrocephalus* conform to this pattern

(Fig. 5C, E). Negative cranial allometry seems to be largely driven by growth in juveniles, and does not reflect static allometry (i.e. size variation within the adult sample).

Onset of ossification of the squamation is sometimes used to define the larval–juvenile transition in fishes (Kendall *et al.* 1984; Webb 1999). Proportional scaling of axial fineness, rostral length and posterior position of the median fins between the smallest free-living *S. curionii* specimens and adults suggests the absence of a large postnatal ecological shift with accompanying morphological changes (i.e. metamorphosis: Balon 1999). Moreover, changes in the relative length and profile of the unpaired fins suggest that the juveniles may have employed a more anguilliform swimming style than adults. In extant fishes with a similar body plan to *Saurichthys*, for instance Lepisosteidae and Belonidae, the antorbitally elongated jaws typical of adult fishes are not present in juveniles. In both the latter clades, strong positive allometric growth of the jaws is directly associated with changes in diet, specifically with a shift away from a plankton-dominated diet towards piscivory (Boughton *et al.* 1991; Kammerer *et al.* 2006). The presence of phosphatic gastric contents in a small juvenile of *Saurichthys macrocephalus* (PIMUZ T 4451; Fig. 5C) is consistent with morphological correlates of predatory feeding habits at an early postnatal stage. All of these observations support the assertion that *S. curionii* and *S. macrocephalus* gave birth directly to juveniles, and that these were relatively precocial. However, based on delayed ossification of the lateral scale rows and proportionately small size of the neonates relative to the females, the neonates of *S. curionii* and *S. macrocephalus* cannot be considered as precocial as lamniform sharks or surfperches, for example.

Postnatal ontogeny

Various authors have provided preliminary information on qualitative and quantitative ontogenetic changes in saurichthyids. In *Saurichthys curionii* and *S. macrocephalus*, previously discussed ontogenetic characters include negative cranial allometry, fin shape, and the degree of segmentation and bifurcation of the lepidotrichia (Rieppel 1992). Postnatal changes in subopercle shape in *S. curionii* were not observed; those previously noted (Rieppel 1992) were due to the incorrect attribution of PIMUZ T 4451 to *S. curionii*. Drastic changes in subopercle shape in *S. macrocephalus* were not observed postnatally, but may occur during embryonic stages (Bürgin 1990). In other saurichthyid species, differences in dermal ornamentation of the cranial elements have been noted (Werneburg *et al.* 2014), as well as delayed ossification in the parietal region (Maxwell *et al.* 2016). Similar observations in *S. curionii* suggest that late ossification in this part of the skull may be relatively widespread within Saurichthyidae. In addition, the extremely delayed ossification of the parietals may partially explain their variability in number and arrangement, both within and between species of *Saurichthys* (Beltan 1958; Werneburg *et al.* 2014; Kogan & Romano 2016). The parietals are very consistent in morphology in Acipenseriformes, being either paired or fused (Jollie 1980; Grande & Bemis 1991), and are among the earliest elements to ossify during development (Jollie 1980; Hilton *et al.* 2011).

Ossification of the squamation in most fishes begins with the scales surrounding the lateral line (Tintori & Lombardo 1999; Helfman *et al.* 2009; Grande 2010; Schmid 2012). However, in *Saurichthys curionii* and *S. macrocephalus*, ossification of the lateral line scales has been delayed relative to the median scale rows and appears to occur sometime after birth. Thus, the frequent evolutionary loss of the lateral line scales prior to loss of the median rows in saurichthyids (e.g. in the *Saurorhynchus* species group: Romano *et al.* 2012) is consistent with simple heterochronic processes (*contra* Schmid 2012).

Soft tissue preservation

The structure we consider to be the notochord (Fig. 4) was previously identified as the somites (Renesto & Stockar 2009). Renesto & Stockar (2009) concluded that the phosphatized structures were too large to represent the notochord; however the reasoning behind this conclusion may have been based on comparisons with acipenseriform pre-hatching embryos rather than morphology-derived stages. Reinterpretation was based on several factors. Firstly, the structure does not show the v- or w-segmentation that typifies the somites, but instead is segmented into irregular blocks. Secondly, it has a fibrous sheath and homogenous, round inner cross-section (Fig. 4D). Even in taxa in which the notochord is unconstricted, as in Acipenseriformes (e.g. Hilton *et al.* 2011) and presumably also in saurichthyids, the notochord forms irregular blocks inside the sheath as it decays (Sansom *et al.* 2013). The notochordal sheath and surrounding cartilages are some of the soft tissues most resistant to decay (Sansom *et al.* 2013). Preserved myomeres are not uncommon in adult fishes from the Meride Limestone (Maxwell *et al.* 2013); however these are not expected to have a round cross-section. Some of the fibrous outer texture of the notochord (e.g. Fig. 4F) may result from adhering myomeres, as muscle tissue adjacent to the notochord is often more decay resistant (Sansom *et al.* 2013).

Embryos or gastric contents?

The small individuals within the abdominal cavity of the female PIMUZ T 3917 have been described as representing embryos (Rieppel 1985; Bürgin 1990). However, no phosphatized postcranial remains are preserved, preservation of the female in ventrolateral view prevents a clear interpretation of topological relationships of the small specimens to the vertebral column of the female, and yellowish material, visible under UV light, is found in the same area as the embryos and is interpreted as gastric secretions. At 31.8 cm fork length, PIMUZ T 3917 is slightly smaller than those females identified as gravid based on phosphatized embryonic postcrania, but differs in abdominal length from PIMUZ T 5764 by only 5 mm.

At least seven small skulls are preserved inside the abdominal cavity of the female, of which three are facing posteriorly and four, including the two most anterior specimens, are facing anteriorly. Average skull length of the small individuals is 12 mm (Bürgin 1990), 10% of female cranial length. The anteriormost embryo is positioned at ~34% of the distance between the jaw joint and abdominal-caudal transition of the female, in other words in the posterior two-thirds of the body cavity, and posterior to the liver. Both of the anterior two small specimens show exquisite preservation of the postcranium, which is curled anteriorly and appears to be slightly shorter than the skull (i.e. <50% skull length). In the smallest free-living individuals, the postcranium is always longer than the skull, and this increases from skull = 44% of total length in the smallest isolated saurichthyid from the Meride Limestone down to skull = 31% total length in large adults. The postcrania of the small individuals are consistent with the embryos of PIMUZ T 5764 in degree of ossification and identity of the ossified structures (i.e. lepidotrichia, median scale row). This specimen highlights some of the difficulties in differentiating late-stage embryos from neonates. Size and abdominal position of the small individuals, as well as preservation of exquisitely tiny postcranial structures support an embryonic identity rather than gastric contents. Prey items would be expected to be minimally as large as the smallest free-living individual, to be larger in proportion to the female, and the fragile, weakly ossified portions of the skeleton would be expected to be more jumbled or even dissolved entirely. Prey items may be located in the anteriormost abdominal region, unlike embryos, and may be associated with chyme in cases of phosphatic preservation (e.g. Fig. 1).

Evolution of viviparity in Saurichthyidae

Viviparity is typically associated with decreased fecundity as a tradeoff for increased offspring survival. However, its evolution appears to be favoured by a series of selective factors, which vary in primacy depending on the clade in question. In 12 of the 14 families of viviparous teleosts, viviparity is associated with small body size (<30 cm) (Wourms & Lombardi 1992). Saurichthyids are not, on average, particularly small fishes and thus this explanation is unlikely to explain viviparity in the group. Viviparity is also correlated with exploitation of pelagic habitats in chondrichthyans and comephorids, as it allows for a dissociation between reproduction and the sea floor (Wourms & Lombardi 1992).

Internal fertilization is a key prerequisite of a viviparous reproductive strategy (Wourms & Lombardi 1992). The first report of a copulatory organ for Saurichthyidae was of the modified pelvic fins of *S. calcaratus*, from the Upper Triassic of Austria (Griffith 1977). However, a copulatory organ consisting of modified mid-ventral scales posterior to the anal loop is known in *S. curionii* (Rieppel 1985; Bürgin 1990) and *S. macrocephalus* (PIMUZ T 5634, PIMUZ T 5703) from the Meride Limestone, and *Saurichthys paucitrichus*? (PIMUZ T 5981) from the upper Besano Formation (Rieppel (1992) previously misinterpreted the posterior anal loop scales in *S. paucitrichus* as a copulatory organ). These two types of copulatory organs in *Saurichthys* are very divergent in homology and structure.

Early phylogenetic analyses placed *S. curionii* and *S. macrocephalus* as sister species, forming a monophyletic group with the taxa now included in the *Costasaurichthys* species group (Rieppel 1992). Later analyses have placed them as forming successive sister taxa to the Late Triassic and Early Jurassic *Saurorhynchus* species group, to which *S. calcaratus* belongs (Fig. 6; Maxwell *et al.* 2015). These two topologies have very different implications for the evolution of internal fertilization and viviparity in saurichthyids. In the first scenario, internal fertilization, and probably viviparity, arose once, at the base of the Middle Triassic western Tethyan radiation (or, alternatively, internal fertilization arose at the base of this radiation, and viviparity arose prior to the divergence of *S. curionii* from *S. macrocephalus*). The second scenario is more complex. In this case, internal fertilization arose within Saurichthyidae prior to the divergence of the *Costasaurichthys* and *Saurorhynchus* species groups *sensu* Maxwell *et al.* 2015 (Fig. 6). Then, at the base of the *Saurorhynchus* species group, either internal fertilization and viviparity were secondarily lost and potentially re-evolved in *S. calcaratus*, or gonopodium function was transferred from a copulatory organ derived from the anal loop scales to one derived from the pelvic fins. We hypothesize that internal fertilization is not primitive for Saurichthyidae because the posterior anal loop scales in some basally diverging saurichthyids (e.g. *S. rieppeli* from Monte San Giorgio) are tiny, delicate, situated immediately anterior

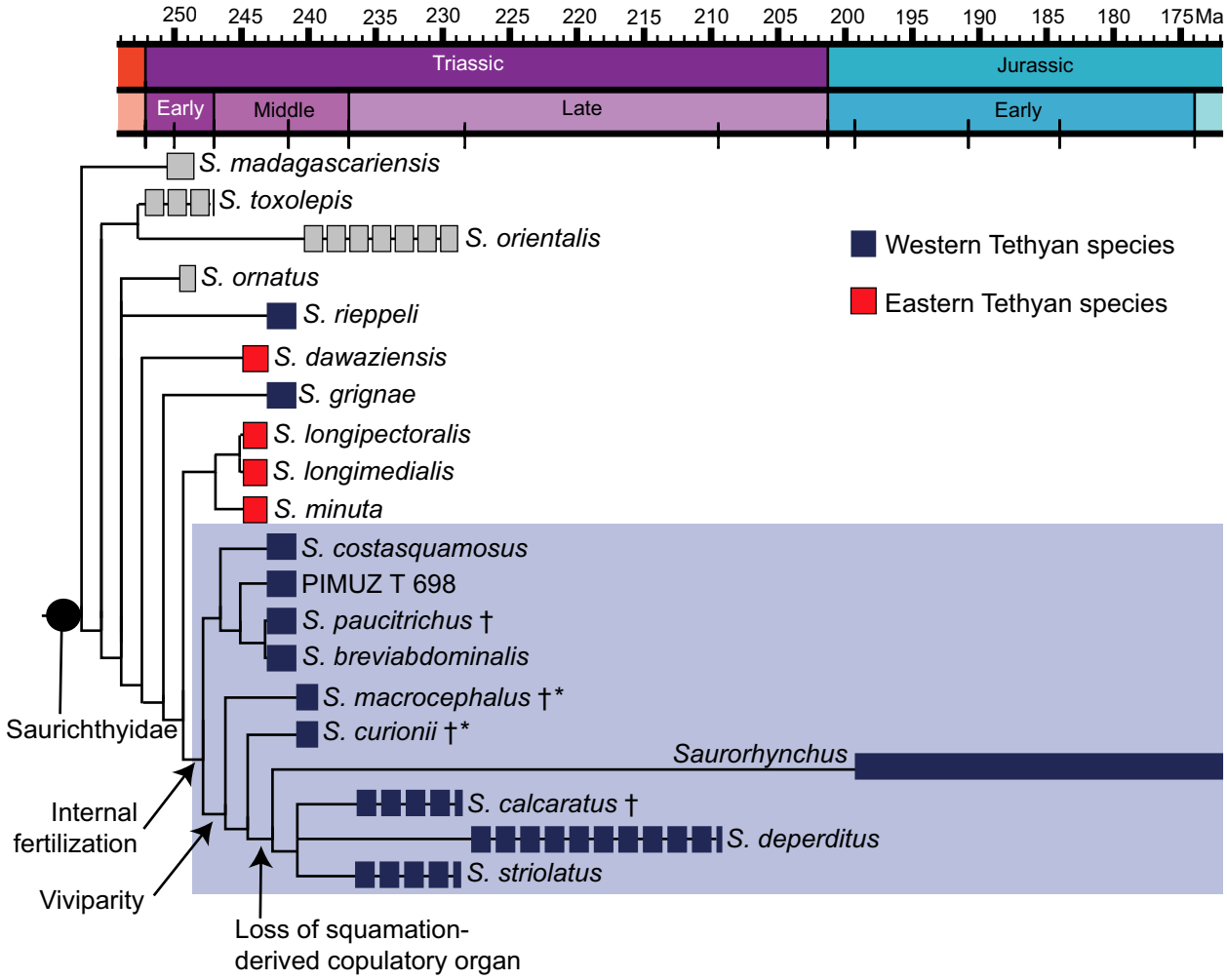

FIG. 6. Occurrence of internal fertilization and viviparity within Saurichthyidae. The shaded clade is the most inclusive group for which evidence of internal fertilization is present. Taxa for which direct evidence of viviparity is available (*Saurichthys curionii* and *S. macrocephalus*) are indicated with asterisks (*); those for which copulatory organs are known are indicated with daggers (†). Time-calibrated phylogenetic hypothesis modified from Maxwell *et al.* (2015). Colour online.

to the anal fin, and thus cannot be modified to form a robust copulatory organ of the type seen in *S. curionii*; in addition the pelvic fins are not positioned near the anal loop (Maxwell *et al.* 2015).

Viviparity has been associated with a higher rate of speciation in some freshwater teleosts (Helmstetter *et al.* 2016). Although the reasons for this are not clear, it may potentially due to increased dispersal abilities relative to demersal spawners (e.g. a single gravid female can colonize a geographically disjunct habitat, founding an allopatric population), reducing competition for territories or nest sites (Wourms & Lombardi 1992), as well as more rapid post-zygotic reproductive isolation (Helmstetter *et al.* 2016). Middle Triassic saurichthyids from the western Tethys, in particular, seem to show both high species diversity in sympatry and species-level divergence between coeval neighbouring basins; for example, Prosanto Formation near Davos (Canton Grisons, Switzerland) or Buchenstein Formation of the Northern Grigna Mountains (Lombardy, Italy) (Bürgin *et al.* 1991; Tintori 2013; Furrer 2015; Maxwell *et al.* 2015). Interestingly, the speciation rate in the *Saurorhynchus* group appears to be dramatically lower than in the Middle Triassic saurichthyids, with few species broadly distributed over multiple basins (e.g. Maxwell & Martindale 2017; Maxwell & Stumpf 2017).

CONCLUSIONS

Saurichthys curionii and *S. macrocephalus* from the Middle Triassic Meride Limestone share similar life history traits, including reverse sexual size dimorphism and a female-

biased sex ratio. The young were born as juveniles, with ossified lepidotrichia and median scales. Two key sequence heterochronies are noted in *S. curionii* and *S. macrocephalus* relative to outgroups, namely the delayed ossification of the midlateral scales relative to the median scales, and delayed ossification of the parietals relative to the rest of the dermatocranium, with both ossifying sometime after birth. In juveniles, growth of the jaws is isometric, but strong negative allometry characterizes the growth of the skull relative to the postcranium, providing a means of potentially distinguishing between juveniles of large species and adults of small species. Viviparity and internal fertilization may not be widespread in Saurichthyidae, and may have contributed to high species diversity in the Middle Triassic of the Western Tethys.

In conclusion, understanding life-history traits in the oldest documented case of actinopterygian viviparity will provide additional data towards uncovering the biological and ecological underpinnings driving the repeated evolution of this life-history strategy. We also provide criteria regarding the relative size and position of embryos in *Saurichthys curionii* and *S. macrocephalus* that can be utilized as a basis for identifying embryos in other saurichthyids, and possibly fossil actinopterygians more generally.

Acknowledgements. HF thanks H. Lanz (PIMUZ), U. Oberli (St Gallen) and C. Obrist (Rickenbach) for their excellent preparation of the PIMUZ specimens. Max Kuhn (Uster) provided financial support for the preparation of some specimens. RS thanks Fabio Magnani (MCSN) for the excellent preparation of juvenile specimens from the MCSN excavation at Cassina and for helpful discussions. Two anonymous reviewers and L. Cavin provided comments which improved the manuscript. Financial support to the MCSN was granted by the Cantone Ticino and the Swiss Federal Office for the Environment. T. Argyriou was supported by SNF doctoral mobility grant P1ZHP3_168253. This project was funded through the Swiss National Science Foundation (SNF) Sinergia grant CRSII3-136293 to M. Sánchez-Villagra, H. Furrer, and W. Salzburger, SNF 144462.

DATA ARCHIVING STATEMENT

Data for this study (including specimens and measurements used in regression analyses) are available in the Dryad Digital Repository: https://doi.org/10.5061/dryad.vc8h5

Editor. Lionel Cavin

REFERENCES

ARGYRIOU, T., CLAUSS, M., MAXWELL, E. E., FURRER, H. and SÁNCHEZ-VILLAGRA, M. R. 2016*a*. Exceptional preservation reveals gastrointestinal anatomy and evolution in early actinopterygian fishes. *Scientific Reports*, **6**, 18758.

—— FRIEDMAN, M., ROMANO, C., KOGAN, I. and SÁNCHEZ-VILLAGRA, M. R. 2016*b*. Endocranial anatomy and interrelationships of the Permo-Triassic early actinopterygian *Saurichthys* with high-resolution computer-assisted microtomography (MCT). 89. *In* FARKE, A., MACKENZIE, A. and MILLER-CAMP, J. (eds). *Society of Vertebrate Paleontology 76th Annual Meeting, Salt Lake City, Meeting Program & Abstracts*.

BALON, E. K. 1999. Alternative ways to become a juvenile or a definitive phenotype (and on some persisting linguistic offenses). *Environmental Biology of Fishes*, **56**, 17–38.

BEARDMORE, S. R. and FURRER, H. 2016. Taphonomic analysis of *Saurichthys* from two stratigraphic horizons in the Middle Triassic of Monte San Giorgio, Switzerland. *Swiss Journal of Geosciences*, **109**, 1–16.

BELTAN, L. 1958. Remarques concernant la variabilité du nombre des pariétaux chez le genre *Saurichthys*. *Comptes rendus des Séances de l'Académie des Sciences*, **247**, 1634–1636.

BLACKBURN, D. G. 1999. Viviparity and oviparity: evolution and reproductive stages. 994–1003. *In* KNOBIL, E. and NEILL, J. D. (eds). *Encyclopedia of reproduction*. Academic Press.

—— 2005. Evolutionary origins of viviparity in fishes. 287–301. *In* GRIER, H. J. and URIBE, M. C. (eds). *Viviparous fishes*. New Life Publications, Homestead, FL.

BOUGHTON, D. A., COLLETTE, B. B. and MCCUNE, A. R. 1991. Heterochrony in jaw morphology of needlefishes (Teleostei: Belonidae). *Systematic Zoology*, **40**, 329–354.

BÜRGIN, T. 1990. Reproduction in Middle Triassic actinopterygians; complex fin structures and evidence of viviparity in fossil fishes. *Zoological Journal of the Linnean Society*, **100**, 379–391.

—— EICHENBERGER, U., FURRER, H. and TSCHANZ, K. 1991. Die Prosanto-Formation - eine fischreiche Fossil-Lagerstätte in der Mitteltrias der Silvretta-Decke (Kanton Graubünden, Schweiz). *Eclogae Geologicae Helvetiae*, **84**, 921–990.

CLOUTIER, R. 2010. The fossil record of fish ontogenies: insights into developmental patterns and processes. *Seminars in Cell & Developmental Biology*, **21**, 400–413.

FURRER, H. 2015. *Saurichthys – Versteinerte Jäger der Triasmeere*. Paläontologisches Institut und Museum der Universität Zürich, 16 pp.

GRANDE, L. 2010. An empirical synthetic pattern study of gars (Lepisosteiformes) and closely related species, based mostly on skeletal anatomy. The resurrection of Holostei. American Society of Ichthyologists and Herpetologists Special Publication 6. *Copeia*, **10** (Suppl.), 871.

—— and BEMIS, W. E. 1991. Osteology and phylogenetic relationships of fossil and recent paddlefishes (Polyodontidae) with comments on the interrelationships of Acipenseriformes. *Journal of Vertebrate Paleontology Memoir*, **11**, 1–121.

GRIFFITH, J. 1977. The Upper Triassic fishes from Polzberg bei Lunz, Austria. *Zoological Journal of the Linnean Society*, **60**, 1–93.

HAMMER, Ø., HARPER, D. A. T. and RYAN, P. D. 2001. PAST: paleontological statistics software package for education and data analysis. *Palaeontologia Electronica*, **4**, 9.

HELFMAN, G. S., COLLETTE, B. B., FACEY, D. E. and BOWEN, B. W. 2009. *The diversity of fishes: biology, evolution, and ecology*. Wiley-Blackwell.

HELMSTETTER, A. J., PAPADOPULOS, A. S. T., IGEA, J., VAN DOOREN, T. J. M., LEROI, A. M. and SAVOLAINEN, V. 2016. Viviparity stimulates diversification in an order of fish. *Nature Communications*, **7**, 11271.

HILTON, E. J., GRANDE, L. and BEMIS, W. E. 2011. Skeletal anatomy of the shortnose sturgeon *Acipenser brevirostrum* Lesueur, 1818, and the systematics of sturgeons (Acipenseriformes, Acipenseridae). *Fieldiana Life & Earth Sciences*, **3**, 1–168.

JOLLIE, M. 1973. *Chordate morphology*. Rheinhold, New York, 492 pp.

—— 1980. Development of head and pectoral girdle skeleton and scales in *Acipenser*. *Copeia*, **1980**, 226–249.

—— 1984. Development of the head and pectoral skeleton of *Polypterus* with a note on scales (Pisces: Actinopterygii). *Journal of Zoology*, **204**, 469–507.

KAMMERER, C. F., GRANDE, L. and WESTNEAT, M. W. 2006. Comparative and developmental functional morphology of the jaws of living and fossil gars (Actinopterygii: Lepisosteidae). *Journal of Morphology*, **267**, 1017–1031.

KENDALL, A. W. Jr, AHLSTROM, E. H. and MOSER, H. G. 1984. Early life history stages of fishes and their characters. 11–22. *In* MOSER, H. G., RICHARDS, W. J., COHEN, D. M., FAHAY, M. P., KENDALL, A. W. J. and RICHARDSON, S. L. (eds). *Ontogeny and systematics of fishes*. The American Society of Ichthyologists & Herpetologists, Special Publication, **1**.

KOGAN, I. and ROMANO, C. 2016. Redescription of *Saurichthys madagascariensis* Piveteau, 1945 (Actinopterygii, Early Triassic), with implications for the early saurichthyid morphotype. *Journal of Vertebrate Paleontology*, **36**, e1151886.

KUHN-SCHNYDER, E. 1974. Die Triasfauna der Tessiner Kalkalpen. *Neujahrsblatt der naturforschenden Gesellschaft in Zürich*, **176**, 1–119.

LaBRECQUE, J. R., ALVA-CAMPBELL, Y. R., ARCHAMBEAULT, S. and CROW, K. D. 2014. Multiple paternity is a shared reproductive strategy in the live-bearing surfperches (Embiotocidae) that may be associated with female fitness. *Ecology & Evolution*, **4**, 2316–2329.

LONG, J. A., TRINAJSTIC, K. and YOUNG, G. C. 2008. Live birth in the Devonian period. *Nature*, **453**, 650–653.

MAXWELL, E. E. 2016. First Middle Jurassic record of Saurichthyidae (Actinopterygii). *Paläontologische Zeitschrift*, **90**, 287–291.

—— and MARTINDALE, R. C. 2017. New *Saurorhynchus* (Actinopterygii: Saurichthyidae) material from the Early Jurassic of Alberta, Canada. *Canadian Journal of Earth Sciences*, **54**, 714–719.

—— and STUMPF, S. 2017. Revision of *Saurorhynchus* (Actinopterygii: Saurichthyidae) from the Early Jurassic of England and Germany. *European Journal of Taxonomy*, **321**, 1–29.

—— FURRER, H. and SÁNCHEZ-VILLAGRA, M. 2013. Exceptional fossil preservation demonstrates a new mode of axial skeleton elongation in early ray-finned fishes. *Nature Communications*, **4**, 2570.

—— ROMANO, C., WU, F. and FURRER, H. 2015. Two new species of *Saurichthys* (Actinopterygii: Saurichthyidae) from the Middle Triassic of Monte San Giorgio, Switzerland, with implications for character evolution in the genus. *Zoological Journal of the Linnean Society*, **173**, 887–912.

—— DIEPENDAAL, H., WINKELHORST, H., GORIS, G. and KLEIN, N. 2016. A new species of *Saurichthys* (Actinopterygii: Saurichthyidae) from the Middle Triassic of Winterswijk, The Netherlands. *Neues Jahrbuch für Geologie und Paläontologie Abhandlung*, **280**, 119–134.

—— ARGYRIOU, T., STOCKAR, R. and FURRER, H. 2018. Data from: Re-evaluation of the ontogeny and reproductive biology of the Triassic fish *Saurichthys* (Actinopterygii: Saurichthyidae). *Dryad Digital Repository*. https://doi.org/10.5061/dryad.vc8h5

RENESTO, S. and STOCKAR, R. 2009. Exceptional preservation of embryos in the actinopterygian *Saurichthys* from the Middle Triassic of Monte San Giorgio, Switzerland. *Swiss Journal of Geosciences*, **102**, 323–330.

—— —— 2015. Prey content in a *Saurichthys* reveals the presence of advanced halecomorph fishes in the Middle Triassic of Monte San Giorgio. *Neues Jahrbuch für Geologie und Paläontologie Abhandlung*, **278**, 95–107.

RIEPPEL, O. 1985. Die Triasfauna der Tessiner Kalkalpen XXV. Die Gattung *Saurichthys* (Pisces, Actinopterygii) aus der mittleren Trias des Monte San Giorgio, Kanton Tessin. *Schweizerische Paläontologische Abhandlungen*, **108**, 1–103.

—— 1992. A new species of the genus *Saurichthys* (Pisces: Actinopterygii) from the Middle Triassic of Monte San Giorgio (Switzerland), with comments on the phylogenetic interrelationships of the genus. *Palaeontographica Abteilung A*, **221**, 63–94.

RIESCH, R., TOBLER, M. and PLATH, M. 2015. Hydrogen sulfide-toxic habitats. *In* RIESCH, R., TOBLER, M. and PLATH, M. (eds). *Extremophile fishes: ecology, evolution, and physiology of teleosts in extreme environments*. Springer, 137–159.

ROMANO, C., KOGAN, I., JENKS, J., JERJEN, I. and BRINKMANN, W. 2012. *Saurichthys* and other fossil fishes from the late Smithian (Early Triassic) of Bear Lake County (Idaho, USA), with a discussion of saurichthyid palaeogeography and evolution. *Bulletin of Geosciences*, **87**, 543–570.

SÁNCHEZ-VILLAGRA, M. 2012. *Embryos in deep time: the rock record of biological development*. University of California Press, 256 pp.

SANSOM, R. S., GABBOTT, S. E. and PURNELL, M. A. 2013. Atlas of vertebrate decay: a visual and taphonomic guide to fossil interpretation. *Palaeontology*, **56**, 457–474.

SCHMID, L. 2012. Reconstructing the molecular underpinnings of morphological diversification: a case study of the Triassic fish *Saurichthys*. 133–165. *In* ASHER, R. J. and MÜLLER, J. (eds). *From clone to bone: the synergy of morphological and molecular tools in palaeobiology*. Cambridge University Press.

SCHULTZE, H.-P. and BARDACK, D. 1987. Diversity and size changes in palaeonisciform fishes (Actinopterygii, Pisces) from the Pennsylvanian Mazon Creek fauna, Illinois, U.S.A. *Journal of Vertebrate Paleontology*, **7**, 1–23.

STOCKAR, R. 2010. Facies, depositional environment, and palaeoecology of the Middle Triassic Cassina beds (Meride Limestone, Monte San Giorgio, Switzerland). *Swiss Journal of Geosciences*, **103**, 101–119.

—— BAUMGARTNER, P. O. and CONDON, D. 2012. Integrated Ladinian bio-chronostratigraphy and geochronology of Monte San Giorgio (Southern Alps, Switzerland). *Swiss Journal of Geosciences*, **105**, 85–108.

TINTORI, A. 2013. A new species of *Saurichthys* (Actinopterygii) from the Middle Triassic (early Ladinian) of the northern Grigna Mountain (Lombardy, Italy). *Rivista Italiana di Paleontologia e Stratigrafia*, **119**, 287–302.

—— and LOMBARDO, C. 1999. Late Ladinian fish faunas from Lombardy (North Italy): stratigraphy and paleobiology. 495–504. *In* ARRATIA, G. and SCHULTZE, H.-P. (eds). *Mesozoic fishes 2: systematics and fossil record*. Friedrich Pfeil, Munich.

WEBB, J. F. 1999. Larvae in fish development and evolution. 109–158. *In* HALL, B. K. and WAKE, M. H. (eds). *The origin and evolution of larval forms*. Academic Press.

WEN, W., ZHANG, Q.-Y., HU, S.-X., BENTON, M. J., ZHOU, C.-Y., TAO, X., HUANG, J.-Y. and CHEN, Z.-Q. 2013. Coelacanths from the Middle Triassic Luoping Biota, Yunnan, South China, with the earliest evidence of ovoviviparity. *Acta Palaeontologica Polonica*, **58**, 175–193.

WERNEBURG, R., KOGAN, I. and SELL, J. 2014. *Saurichthys* (Pisces: Actinopterygii) aus dem Buntsandstein (Trias) des Germanischen Beckens. *Semana*, **29**, 3–35.

WHITNEY, N. M. and CROW, G. L. 2007. Reproductive biology of the tiger shark (*Galeocerdo cuvier*) in Hawaii. *Marine Biology*, **151**, 63–70.

WILSON, L. A. B., FURRER, H., STOCKAR, R. and SÁNCHEZ-VILLAGRA, M. R. 2013. A quantitative evaluation of evolutionary patterns in opercle bone shape in *Saurichthys* (Actinopterygii: Saurichthyidae). *Palaeontology*, **56**, 901–915.

WOURMS, J. P. and LOMBARDI, J. 1992. Reflections on the evolution of piscine viviparity. *American Zoologist*, **32**, 276–293.

—— GROVE, B. D. and LOMBARDI, J. 1988. 1. The maternal-embryonic relationship in viviparous fishes. *Fish Physiology*, **11**, 1–134.

—— ATZ, J. W. and STRIBLING, M. D. 1991. Viviparity and the maternal-embryonic relationship in the coelacanth *Latimeria chalumnae*. *Environmental Biology of Fishes*, **32**, 225–248.

CHAPTER III

Internal cranial anatomy of Early Triassic species of †*Saurichthys* (Actinopterygii: †Saurichthyiformes): implications for the phylogenetic placement of †saurichthyiforms

Thodoris Argyriou[1*], Sam Giles[2], Matt Friedman[3], Carlo Romano[1], Ilja Kogan[4], and Marcelo R. Sánchez-Villagra[1]

*Correspondence: thodoris.argyriou@pim.uzh.ch; argthod@gmail.com

Email addresses: Thodoris Argyriou: thodoris.argyriou@pim.uzh.ch; argthod@gmail.com; Sam Giles: samantha.giles@earth.ox.ac.uk; Matt Friedman: mfriedm@umich.edu; Carlo Romano: carlo.romano@pim.uzh.ch; Ilja Kogan: i.kogan@gmx.de; Marcelo R. Sánchez-Villagra: m.sanchez@pim.uzh.ch

Abstract

Background: †Saurichthyiformes was a successful group of latest Permian–Middle Jurassic predatory actinopterygian fishes and constituted important and widely-distributed components of Triassic marine and freshwater faunas. Their systematic affinities have long been debated, with †saurichthyiforms often being aligned with chondrosteans, a group today comprising sturgeons and paddlefishes. However, their character-rich endocranial anatomy has not been investigated in detail since the first half of the 20th century. Since that time, major advances have occurred in terms of our understanding of early actinopterygian anatomy, as well as techniques for extracting morphological data from fossils.

Results: We used µCT to study the internal cranial anatomy of two of the stratigraphically oldest representatives of †*Saurichthys*, from the Early Triassic of East Greenland and Nepal. Our work revealed numerous previously unknown characters (e.g., cryptic oticooccipital fissure; intramural diverticula of braincase; nasobasal canals; lateral cranial canal; fused dermohyal), and permitted the reevalution of features relating to the structure of cranial fossae, basicranial circulation and opercular anatomy of the genus. Critically, we reinterpret the former †saurichthyiform opercle as an expanded subopercle. For comparison, we also produced the first digital models of a braincase and endocast of a sturgeon (*A. brevirostrum*). New information from these taxa was included in a broad phylogenetic analysis of Actinopterygii. †Saurichthyiforms are resolved as close relatives of †*Birgeria*, forming a clade that constitutes the immediate sister group of crown actinopterygians. However, these and other divergences near the actinopterygian crown node are weakly supported.

Conclusions: Our phylogeny disagrees with the historically prevalent hypothesis favoring the chondrostean affinities of †saurichthyiforms. Previously-proposed synapomorphies uniting the two clades, such as the closure of the oticooccipital fissure, the posterior extension of the parasphenoid, and the absence of an opercular process are widespread amongst actinopterygians. Others, like those relating to basicranial circulation, are found to be based on erroneous interpretations. Our work renders the †saurichthyiform character complex adequately understood, and permits detailed comparisons with other early crown actinopterygians. Our phylogenetic scheme highlights outstanding questions concerning the affinity of many crown actinopterygians, such as the Paleozoic–early Mesozoic deep-bodied forms, which are largely caused by lack of endoskeletal data.

Keywords: Actinopterygii, †*Saurichthys*, Chondrostei, *Acipenser*, Triassic, microtomography (μCT), phylogeny, cranial fossae, East Greenland, Nepal.

Background

Actinopterygii (ray-finned fishes), with more than 32,000 living species [1], encompass over half of extant vertebrate species and possess an evolutionary history of at least 415 myr [2, 3]. This extant diversity is unevenly distributed among three major clades: Cladistia (bichirs and the reedfish), Chondrostei (sturgeons and paddlefishes), and Neopterygii, the latter containing the depauperate Holostei (gars and the bowfin) and the very speciose Teleostei [4, 5]. The monophyly of these three modern clades is well-supported, and identification of fossil members within them is fairly uncontroversial [6-9], but see [10]. However, with the exception of some derived fossils that branch close to the crown radiation, for example †*Chondrosteus* in the case of Chondrostei [11], the content of more distant portions of the stems of the three major actinopterygian lineages is highly equivocal. In spite of considerable differences in details, molecular and paleontological timescales place the divergence of these three lineages in the mid-late Paleozoic [4, 5, 12]. Abundant fossil actinopterygians of Paleozoic and early Mesozoic age are known [13-15], but their systematic placement relative to neopterygians, chondrosteans, and cladistians is highly unstable and variable between phylogenetic analyses [12, 16-20]. Although some of this ambiguity doubtlessly reflects genuine character conflict, the limited documentation of anatomy in many fossils of this age presents the chief obstacle.

Set against this backdrop, the latest Permian [21] to Middle Jurassic [22] †saurichthyids represent a case of contested evolutionary history. This group of predatory actinopterygians is characterized by an elongate body, a prominent rostrum, posteriorly situated median fins and an unusual abbreviated-diphycercal tail-fin [23-30]. †*Saurichthys*, the iconic representative of the family, encompasses at least two or more potential subgenera, including †*Sinosaurichthys* [30] and likely †*Saurorhynchus* [27]. The type species, †*Saurichthys apicalis* [31], is known from a fragmentary rostrum. †*Yelangichthys* (†Yelangichthyidae), a durophagous form from the Middle Triassic of China, has been identified as the sister lineage of †saurichthyids [32], and with them forms the †Saurichthyiformes.

†*Saurichthys* is known from thousands of specimens belonging to over 40 nominal species, associated with marine, freshwater and brackish settings and occurring on all continents except

Antarctica and South America [14, 25]. Abundant and well-preserved fossils permit investigation of soft-tissue features, with studies revealing reproductive mode and details of ontogeny [33-35], mode of axial elongation [26, 36], swimming mode and efficiency [37], as well as gastrointestinal anatomy [38]. Although the wealth of potential paleobiological information about †*Saurichthys* is unrivalled among early fossil actinopterygians, some basic anatomical aspects of this genus are known in limited detail relative to other taxa.

Key to understanding the systematic placement of †saurichthyids is the character-rich internal anatomy of the cranium (which can constitute up to 80% of published character matrices), comprising the braincase and associated dermal bones, suspensorium, and hyoid and branchial arches. Stensiö [29], based on direct observations and serial grinding of mechanically prepared, three-dimensionally preserved fossils from the Lower Triassic of Spitsbergen, provided a lengthy, but often idealized, account of the character-rich internal cranial anatomy of †*Saurichthys*. Few additions on the internal cranial anatomy of †*Saurichthys* have been made by subsequent authors [39, 40]. Critically, Stensiö's [29] observations on †*Saurichthys*, and his conclusion of a close relationship with acipenseriforms, set the stage for most later phylogenetic intepretations of non-neopterygian actinopterygians and the widespread association of †*Saurichthys* with Chondrostei [16-19, 24, 27, 32]. Numerous anatomical similarities have been treated as features supporting a chondrostean placement for †saurichthyids, such as: i) ethmoidal elongation; ii) presence of large craniospinal processes; iii) absence of parabasal canals and a circulus cephalicus; iv) presence of a spiracular canal; v) absence of a lateral cranial canal; vi) absence of a basipterygoid process; vii) posteriorly expanded parasphenoid reaching the basioccipital; viii) absence of gulars; ix) reduced squamation. However, many of these features are either more general in their distribution, or are demonstrably homoplastic within non-neopterygian actinopterygians.

Phylogenetic schemes that resolve †*Saurichthys* outside the chondrostean clade, but with uncertain placement within non-neopterygian actinopterygians, have also been proposed [41, 42]. †*Saurichthys* has additionally been interpreted as a stem neopterygian, on the basis of the reduction of the branchiostegal series and the presence of elongate epaxial rays [18]. However, past solutions were often a product of limited taxon sampling [16-18, 24], and/or were based on matrices aimed at resolving relationships within the †saurichthyid clade and lacking broader taxonomic context [24, 26, 27, 32]. In many cases, terminal taxa taken into account were coded as composites [16-19, 41]. These interpretations were also influenced by critical errors in the coding of characters (see

discussion). A more recent analysis, drawing characters from a variety of sources and coding a single, non-composite taxon recovered †*Saurichthys* as the immediate sister taxon to the actinopterygian crown [12], but this study is still hampered by a limited taxonomic sampling of †saurichthyids and lack of data related to their cranial endoskeleton.

Considering the important phylogenetic position †saurichthyids seem to occupy relative to the actinopterygian crown, as well as the unparalleled amount of paleobiological information available for some examples, a critical reinvestigation of their internal cranial anatomy and interrelationships is warranted. In this work, we employ μCT in order to study the structure of the skull in two Early Triassic specimens of †*Saurichthys*, which are amongst the stratigraphically oldest representatives of the clade. The main goals of this work are: 1) to provide an up-to-date account of the internal cranial anatomy of †*Saurichthys*; 2) to test the classical models of internal cranial anatomy, which were produced with the use of destructive techniques [29]; and 3) to reappraise the phylogenetic affinities of †saurichthyids among actinopterygians generally, and to chondrosteans specifically, based on a combination of new information from μCT investigation and an expanded character-by-taxon matrix. In addition, to improve the available comparative material, we provide the first digital models of the braincase and endocast of *Acipenser*. Finally, given the lack of nomenclatural consistency in the literature, and aided by our observations on †*Saurichthys* and *Acipenser*, we provide a review and discussion on the evolution and function of several cranial fossae in the actinopterygian braincase.

Methods

Following [43], fossil taxa are preceded by the dagger symbol (†) throughout the text.

Comparative materials

†Saurichthyiformes: PIMUZ A/I 4648, unnamed †saurichthyid from the Prosanto Formation (Ladinian, Canton Graubünden, Switzerland) exhibiting hyoid, lower jaw and opercular anatomy.

†*Pteronisculus*: NHMD 73588 A, †*Pteronisculus gunnari,* physical holotype and scan of specimen including a complete skull with lower jaw, opercular series and pectoral girdle attached (Griesbachian, East Greenland).

Acipenseriformes: FMNH 113538, *Acipenser brevirostrum*, scan of braincase and parasphenoid; UMMP teaching collection, *Acipenser* sp., disarticulated skeleton; UMMP teaching collection, *Acipenser* sp., skull with suspensorium, lower jaw, hyoid and branchial arches, and pectoral girdle attached; UMMP teaching collection, *Polyodon spathula*, two complete and partially disarticulated dry skeletons; UMMZ 64250, *Acipenser brevirostrum*, scan of stained head.

Holostei: PIMUZ A/I 4171a, skull of *Atractosteus spatula*; UMMP teaching collection, *Amia calva*, skull with suspensorium, lower jaw, hyoid and branchial arches attached.

Anatomical nomenclature

Our discussion of the neurocranium of †*Saurichthys* focuses on four broad regions (occipital, otic, orbitosphenoid and ethmoid), following Gardiner [44]. Anatomical terminology for general cranial anatomy follows Gardiner [44] and Kogan & Romano [25] for the dermal skull specifically. To aid the reader, we have included abbreviations of anatomical structures depicted in the figures throughout the text. The abbreviations are also explained in the figure legends.

Tomographic and digital rendering methods

The scan of the Greenland †*Saurichthys* (NHMD_157546_A) was performed using a using a Nikon XT H 225 ST scanner at the University of Bristol Palaeobiology Research Group, Bristol, U.K. The specimen was scanned in three stacks, which were subsequently stitched together. The same parameters were used for each scan, as follows: 220 kV, 110 uA, no filtering. The scan of †*Saurichthys nepalensis* (MNHN F 1980-5) was performed at the Muséum National d'Histoire Naturelle, Paris, France, with a AST-RX scanner. The scan parameters were as follows: 120kV, 480uA, filterred with 0.5mm of copper. The scan of *Acipenser brevirostrum* (FMNH 113538) was performed in the CTEES facilty of the University of Michigan using a Nikon XT H 225 ST scanner. The scan parameters were as follows: 75 kV, 290 uA, no filtering. The resulting volumes were segmented using Mimics Research v19.0 (biomedical.materialise.com/mimics; Materialise, Leuven, Belgium). The resulting 3D objects were exported as PLY files and processed in Blender (blender.org) for imaging purposes.

Phylogenetic dataset assembly and analyses

For our phylogenetic analyses, we modified and expanded the morphological matrix developed by

Giles et al. [12] using Mesquite Version 3.2 [45]. We removed a total of three characters (pertaining to the presence or absence of lepidotrichia; hypohyal; pelvic fins), due to their uninformative status. We now treat C.256 (presence and arrangement of scutes anterior to the dorsal fin) the as unordered. Twelve new binary and one multistate morphological characters (C.20; C.24; C.44; C.112; C.154; C.170; C.181; C.189; C.204; C.205; C.212-multistate; C.228; C. 268), a third state for C.159 and a fourth state for C.177 were added, resulting to a total of 275 equally weighted characters (see additional file 1, 3). †*Brachydegma caelatum* was also removed from the matrix, since a major reinterpretation of its anatomy is pending following μCT investigation (Argyriou et al. in prep.). We added five new taxa, giving a total of 97 taxa in our dataset. In order to test the monophyly of saurichthyiforms we included: 1) the Early Triassic †*Saurichthys* from Greenland (NHMD_157546_A); 2) the Early Triassic †*Saurichthys ornatus* (coded after [29]); 3) the Middle Triassic saurichthyiform †*Yelangichthys macrocephalus* (coded after [32]); 4) *Polyodon spathula* was included as an additional member of the chondrostean crown (coded after our observations on UMMP dry skeletons); 5) †*Birgeria stensioei* from the Middle Triassic of Monte San Giorgio (coded after [46, 47]). Finally, we extensively rescored *Acipenser brevirostrum*, †*Birgeria groenlandica* and †*Saurichthys madagascariensis*, and changed the scoring in some additional taxa (rescoring details in additional file 1, 3).

The maximum parsimony analyses were performed with 'New Technology Search' algorithms implemented in TNT [48]. The 'placoderm' †*Dicksonosteus arcticus* was set as outgroup, but we placed a constraint on the monophyly of osteichthyans using an artificial tree that exhibited the following outgroup relationship: (†*Dicksonosteus* (†*Entelognathus* ((†*Acanthodes* (†*Ozarcus* †*Cladoidodes*)) Osteichthyes). Following [49], we used a combination of 'Ratchet' and 'Sectorial Search' algorithms. Initial trees were produced with a combination of 'Sectiorial Search', 'Ratchet', 'Drift' and 'Tree Fusing' (1000 trees by RAS with 100 iterations of each mentioned algorithm), while the number of suboptimal trees to be kept was set to 10 and the relative fit difference was set to 0.1. Initial trees were subjected to 2x3 consecutive rounds of analyses. The first round comprised 1000 iterations of 'Sectiorial Search', complemented by one run of 1000 iterations of 'Ratchet' and another run of **'Sectiorial Search'. The second round comprised 1000 iterations of 'Ratchet', followed by 1000 iterations of 'Sectiorial Search', and 1000** iterations of 'Ratchet'. Each run was complemented by 1000 iterations of 'Tree Fusing'. Trees resulting from the two rounds of analyses were combined, and all suboptimal trees were discarded, before the calculation of the strict consensus. From all available trees we visualized the distribution of synapomorphies and we calculated an agreement subtree using the relevant function in TNT. Using all trees produced during the successive rounds of analysis,

including suboptimals, we calculated Bremer values for clades. The matrix was re-analyzed with 'Traditional Search' (1000 iterations) for estimating bootstrap supports. The agreement subtree functions implemented in TNT aided the identification of wildcard taxa [48]. The matrix and trees can be found in Additional file 3.

Results

Systematic Paleontology

ACTINOPTERYGII Cope, 1887 [50] (sensu [51])

†SAURICHTHYIFORMES Aldinger, 1937 [52] (sensu [32])

†SAURICHTHYIDAE Owen, 1860 [53] (sensu [29])

†*SAURICHTHYS* Agassiz, 1834 [31]

†*Saurichthys* sp.

2008 – †*Saurichthys* cf. *ornatus* Mutter et al. [54]

Material

NHMD_157546_A, †*Saurichthys* sp., almost complete skull and lower jaw.

Fossil age and locality information

The Early Triassic (Induan: Griesbachian–early Dienerian; see also [55]) Wordie Creek Formation of East Greenland contains six well-demarcated horizons ('Fish Zones I–V', 'Stegocephalian Zone' [56]) that yielded a plethora of vertebrate fossils, including a sizable fossil fish sample, dominated by actinopterygians [56-61]. The bulk of this material is deposited in the collections of the Natural History Museum of Denmark, and a substantial portion of this collection remains unprepared. †*Saurichthys* remains are comparatively rare in East Greenland (<30 out of over 2,200 identifiable fish fossils collected), and were only recovered from zones II and V, and potentially zone III [54, 56, 57, 60, 62]. The material from horizon II is laterally compressed and was referred to †*Saurichthys*

aff. *S. dayi* on the basis of postcranial anatomy, although it likely corresponds to a new species [62]. 'Fish Zone V' is the youngest of the 'Fish Zones' on East Greenland and is associated with the former '*Proptychites* beds' [56], which likely correspond to the †*Bukkenites rosenkrantzi* zone of late Griesbachian–early Dienerian (~250.4 Ma) age [55]. The latter zone has produced at least two three-dimensionally preserved crania, which were identified as †*Saurichthys* cf. *S. ornatus*, on the basis of external anatomical similarities with younger (Smithian) material from paleogeographically close localities in Spitsbergen [54]. The present work focuses on the better-preserved NHMD_157546_A from the River 7 locality on Kap Stosch, Hold with Hope Peninsula, which was collected during the 1930s. For additional information on local stratigraphy and locality information the reader is referred to [56] and [55].

Anatomical description

General features of the neurocranium

The specialized neurocranial morphology of †*Saurichthys* is dominated by elongate occipital and ethmoidal (rostral) regions, as well as large orbital spaces (Figs. 1–4). In dorsal view the neurocranium is bullet-shaped, attaining its maximum width at the level of the postorbital process. In lateral view, the orbitotemporal and ethmoidal regions are much longer than the occipital and otic regions.

Occipital region

The occipital region (Figs. 1–4, 5A) is delineated by the craniospinal processes posteriorly ('crsp'), and the cryptic oticooccipital fissure anteriorly. Despite being externally covered by perichondral bone, the oticooccipital fissure persists as a weakly mineralized belt, forming a break in the perichondral and endochondral lining of the endocavity (Figs. 4A,B; 6A,B; 7A,B; Additional Fig. 1A: 'otcf'). The oticooccipital fissure begins dorsolaterally, intersects the vagus ('X') foramen and extends ventrally to below the level of the saccular recess of the inner ear. The anterodorsal surface of the occipital region is poorly mineralized, but a posterior dorsal fontanelle was likely absent, as evidenced by the presence of dorsally-directed, mineralized canals, tentatively interpreted as passages for the dorsal rami of the vagus (Figs. 6A,B; 7A,B: 'n'). There are no vestibular fontanelles. The ventral floor of the braincase is weakly mineralized, and the condition of the ventral otic fissure cannot be assessed.

The narrow foramen magnum ('fm') is ovoid in cross-section and is the most dorsal of the two openings on the posterior face of the occipital region. The notochordal canal ('not') lies ventral to the foramen magnum, and is much wider than the latter and approximately circular in cross-section. No thickened notochordal calcification was observed. The two canals communicate posteriorly through the parachordal notch, which terminates slightly posterior to the level of origin of the craniospinal processes. Anterior to this point, the notochordal canal and the foramen magnum are completely enclosed in bone and separated by a continuous horizontal shelf. The notochordal canal extends until almost the anterior margin of the occipital region, but its radius decreases abruptly anterior to the level of origin of the craniospinal processes. Two small canals issue from the notochordal canal and open laterally on each side of the specimen. An aortic canal is absent.

The prominent craniospinal processes originate from the dorsal half of the occipital region, and expand posterolaterally. The posterior face of each craniospinal process bears a deep craniospinal fossa ('crsf'). The two fossae are separated on the midline by a shallow occiptal crest ('occ'), which extends along the dorsal margin of the occipital region and widens anteriorly. The laterodorsal part of the braincase between the craniospinal processes and the otic region bears a paired concavity, which extends anteriorly to the posteromedial surface of the otic region, and is mesial to the otic crest formed by the posterior semicircular canal. We consider this concavity to be an expanded tectosynotic fossa ('tsf', see also discussion). This fossa sits adjacent to an expanded muscle attachment shelf on the hyomandibula. A common canal for both roots of the first spinooccipital nerve (Spinooccipitalis α of [29]) opens laterally below the craniospinal process. A canal that transmitted either another spinooccipital nerve (ventral root of the N. Spinooccipitalis z of [29]), or the occipital artery, opens anterior and slightly ventral to the previous canal ('nocc/aocc').

Remarks The oticooccipital fissure is externally closed in several actinopterygian taxa, including †*Saurichthys*, †*Amphicentrum*, Cladistia, Chondrostei, living Holostei and crown Teleostei [44, 63, 64]. This contrasts with the open oticooccipital fissure of most Paleozoic–early Mesozoic actinopterygians and early neopterygians [39, 40, 44, 58, 59, 63, 65-69]. The discovery of a cryptic oticooccipital fissure allows, for the first time, the mapping of the boundary between the occipital and otic regions in †saurichthyids.

†*Saurichthys* resembles living neopterygians in the sense that the dorsal aorta and lateral dorsal aortae extend ventral to the elongated posterior stalk of the parasphenoid (e.g., [70, 71]). Presumed

similarities in vascularization between †*Saurichthys* and acipenseriforms are often emphasized in character descriptions [16, 29, 32]. However, there are notable differences between the latter two groups. The most conspicuous difference can be found in the course of the lateral dorsal aortae, which bifurcate posterior to the occiput and extend ventral to the parasphenoid in †saurichthyids (Figs. 4, 5, 8). In acipenserifoms they are embedded in a groove on the ventral surface of the first few abdominal vertebrae, extend mostly dorsal to the parasphenoid, are flanked by the deep parasphenoid notch, and bifurcate anterior to the occiput [72, 73] (Additional Fig. 3, 4). In some specimens of *Acipenser*, the dorsal aorta can be embedded in a short aortic canal immediately before it bifurcates to efferent branchial arteries (Additional Fig. 4: 'abreff').

The occipital region of †saurichthyids and most non-neopterygians [6, 29, 44, 58, 59, 63, 65-69, 74, 75] bears laterally-extending craniospinal processes. Based on comparison with acipenseriforms [73, 75, 76], the only living examples exhibiting craniospinal processes, the latter processes form fossae that must have accommodated the first few epaxial muscle segments [44]. An expanded, laterally-facing tectosynotic fossa is present in acipenseriforms (Suppl. Fig. 2), and it hosts the origin of the hyoid and opercular retractors and the branchial levator muscles [73, 76, 77]. We hypothesize a similar arrangement in †*Saurichthys*, based on fossa orientation and the arrangement of the hyomandibula. Due to difficulties in mapping different regions of the neurocranium in adult acipenseriforms, it is unclear whether the tectosynotic fossa crosses to the occipital region as it does in †*Saurichthys*.

†*Kansasiella* and †*Saurichthys* are reconstructed with two spinooccipital foramina [29, 65], whereas only one is present in the lateral occipital region of †*Mimipiscis*, †*Pteronisculus*, †*Australosomus*, †*Kentuckia* and †*Lawrenciella* [44, 58, 59, 67, 78]. Yet, such attributions in fossils should be treated with caution, since these foramina could also have transmitted blood vessels. Acipenseriforms exhibit three spinooccipital nerves [73, 77]; Fig. 9, Suppl. Fig. 2), although a fourth, blind-ending canal is present anterior to the remaining spinooccipital nerves in the endocast of *Acipenser* we examined. *Erpetoichthys*, *Amia* and gars exhibit two spinooccipital nerve foramina, while *Polypterus* shows three [70, 75, 79-81].

Otic and orbitotemporal regions

The otic region (Fig. 3, 4, 5C,D) includes the portion of the braincase enclosing the bony labyrinth, the anterior tip of which terminates slightly beyond the level of the broad postorbital process

('porp'). Ventrally, it extends up to the posteroventral margin of the myodome. The orbitotemporal region extends anteriorly up to the posterior wall of the ethmoidal region. There is no clear boundary between the otic and orbitotemporal regions, so they are considered collectively here. The flat dorsal surface of the otic and orbitotemporal regions is poorly mineralized and not well-resolved in our scan. The anterior fontanelle appears extensive, but is tentatively reconstructed. The posterior tip of the postorbital process is the widest part of the braincase, but the width decreases abruptly at the level of the orbits.

In lateral view, the anterior portion of the tectosynotic fossa (Fig. 3A,B, 4A,B; 5C,D) is bounded medially by the occipital crest and laterally by the process containing the posterior semicircular canal ('otp'). Anterolaterally to the tectosynotic fossa, and roughly constrained by the planes of the three semicircular canals, there is a depressed area, which corresponds to the fossa bridgei ('fb'). The latter exhibits a deep posterior subdivision, which opens posterolaterally, towards the anteromedial surface of the hyomandibula. The anterior and medial walls of the posterior subdivision of the fossa bridgei connect to perichondrally-lined, intramural diverticula in the braincase (Fig. 6D,E, 7D,E: 'id'). The posterior diverticulum extends medially towards the cranial cavity, while the anterior one extends anteriorly, reaching past the level of the crus communis. The posterior opening of the fossa bridgei is succeeded laterally by a posterolaterally-facing, subtriangular, shallow hyomandibular facet. The hyomandibular facet ('hmf') is separated from the broad postorbital process by the ascending process of the parasphenoid ('asp'). The presence of an enclosed spiracular canal could not be verified due to limited contrast in tomograms, and may have been absent. Anterolaterally, the tip of the ascending process of the parasphenoid gives way to a shallow, posteriorly-facing dilatator fossa ('dlf') on the caudal surface of the postorbital process, which is likely to have hosted the hyomandibular protractor muscle. The levator arcus palatini likely originated from the broad fossa of the ventral part of the postorbital process.

A foramen for the vagus nerve, and potentially the posterior cerebral vein [29], opens on the posterolateral surface of the otic region. The jugular vein extended through a depression beginning immediately ventral to the exit of the vagus. The glossopharyngeal nerve ('IX') exited ventral to the jugular depression. The jugular depression continues anteriorly and slightly dorsally to become the jugular canal ('jc'; trigeminofacialis chamber in [29]), which pierces the lateral commissure and opens on the posteroventral part of the orbitotemporal region. The canal for the facial nerve ('VII') opens into the jugular canal through its posteromedial wall. Dorsomedial to the anterior opening of

the jugular canal, there is a large opening for the trigeminal nerve ('V'), and potentially the profundus and the anterior trunks of the facial nerve. Slightly anterodorsal to the latter there is a vertical canal for the mid-cerebral vein. A lateral pillar (alisphenoid pedicel) is absent.

The external (Fig. 8:'ace') and internal carotid arteries ('aci') split from the common carotids ('ccar') upon entering the parasphenoid. Then, they extended anterodorsally along a canal formed between the parasphenoid and the braincase, to merge with the anterior opening of the jugular canal. From that point, each external carotid likely bifurcated to a posterior (hyomandibular, not reconstructed) and an anterior (orbital, 'aorb') branch. The internal carotids continued anteriorly along parabasal canals below the lateral openings of the posterior myodome. At this point the palatine artery ('apal') branched off and continued its anterior course through a parabasal canal, completely enclosed within the parasphenoid. The remaining internal carotid branches enter the ventral part of the orbital region. A foramen for the efferent pseudobranchial artery ('eps') opens on each side, anteroventrally to the anterior margin of the posterior myodome (Additional Fig. 2A). Anterior to the pseudobranchial foramina, each internal carotid bifurcated into the (greater) ophthalmic artery ('oph') and an ascending ('ci') branch. The ophthalmic arteries extended anteriorly and exited the braincase forming troughs immediately ventral to the optic foramen, while the ascending branches enter the brain cavity through the lower margin of the optic foramen.

The median posterior myodome (Figs. 3A, 4A: 'pmy') is well-developed and situated in front of the ascending process of the parasphenoid, anteroventral to the anterior opening of the jugular canal. The anterior wall of the posterior myodome is in communication with the hypophyseal chamber. The course of the pituitary vein could not be observed. It was likely confluent with the hypophyseal chamber or with the paired canal for the abducens nerve ('VI'), which opens on the roof of the myodome. There is no basipterygoid process. The cranial cavity becomes markedly convex above the myodome to accommodate the expanded optic tecta. A foramen for the trochlear nerve ('IV') is located on the dorsal margin of this convexity. A foramen for the anterior cerebral vein ('acv') opens anterior to the trochlear foramen, followed anteroventrally by the foramen for the olfactory nerve ('I'), on each side of the specimen. The anterior face of the orbitotemporal region is dominated by the median foramen for the optic nerve ('II'), which opens onto the posterior margin of the large interorbital fenestra. The optic foramen is flanked on each side by the foramina for the oculomotor nerve ('III'). The canals for the (greater) ophthalmic artery and potentially the exit of the anterior cerebral artery opens ventral to the optic foramen (Figs. 5E,F, 8: 'oph'). The olfactory nerve exited

the cranial cavity above the mid-length of the optic fenestra. Upon exiting the braincase, each tract extended in a shallow groove along the dorsal margin of the interobital fenestra ('iof') to enter the ethmoidal region through a paired, funnel-shaped foramen. The interorbital fenestra is greatly enlarged, reducing the thin interorbital septum to its anterior and anterodorsal parts.

Remarks An expanded anterior fontanelle is present in most post-Devonian non-neopterygian actinopterygians in which the condition can be assessed [58, 59, 65, 67, 79, 82]. A fossa bridgei is present in most Carboniferous or younger actinopterygians, but unlike in †*Saurichthys*, it is posteriorly delimited by an endochondral wall [29, 44, 58, 59, 63, 67, 83]. Based on orientation and proximity to the hyomandibula, we hypothesize that the elimination of the posterior wall of the fossa bridgei of †*Saurichthys* is linked to the attachment of the hyomandibular retractor muscle, and not to the attachment of epaxial musculature, which is the case in many neopterygians [63]. The opening of intramural diverticula in the fossa bridgei is observed in †*Kansasiella* [65], †*Saurichthys* (Figs. 6D,E, 7D,E) and *Acipenser* (Fig. 9G–J, Additional Fig. 3). In the latter two taxa, where the condition can now be assessed, the diverticula are subdivided into two distinct portions on each side and show a similar arrangement. However, the contact between the two portions is contained within the braincase in †*Saurichthys*, but happens in the fossa bridgei in *Acipenser*. In *Polyodon*, but also in †*Pteronisculus* and †*Boreosomus*, the lateral cranial canal opens in the floor of the fossa bridgei at a topologically equivalent position [58, 59, 84]. This topological correspondence could be suggestive of homology between intramural diverticula and parts of the lateral cranial canal.

The position of the hyomandibular facet of †*Saurichthys*, dorsal to the jugular canal, is reminiscent of the condition seen in Devonian actinopterygians [44, 69]. However in the latter, the facet is oriented laterally, rather than posteriorly as in †*Saurichthys*. The posterior orientation of the †saurichthyid dilatator fossa, which in analogy with modern taxa must have carried the hyoid protractor muscle [73, 76, 77], is similar to that of gars, likely reflecting the elongate geometry of their skulls. It differs from that of most neopterygians [63], in both its position (anterior to hyomandibular facet versus anterodorsal in most neopterygians) and orientation (posterior versus lateral in most neopterygians).

The jugular canal of †*Saurichthys* resembles that of †*Kansasiella*, differing from that of †*Mimipiscis*, †*Lawrenciella*, *Acipenser*, and several fossil holosteans in not having the orbital artery entering the jugular canal posteriorly, but rather entering it ventrally along its course [44, 63, 65, 67]. †*Saurichthys* differs from †*Pteronisculus*, †*Kentuckia*, the Greenland †'*Perleidus*' and early teleosts in not exhibiting

separate foramina for the exit of the hyomandibular trunk of the facial nerve above the posterior exit of the jugular canal [58, 63, 78]. The profundus nerves also form separate foramina, dorsal–dorsomedial to the anterior opening of the jugular canal in many fossil actinopterygians [44, 58, 63], but likely share the same exit with other nerves in †*Saurichthys*, †*Australosomus*, polypterids, acipenseriforms [59, 73, 79]. The presence of a median posterior myodome in †*Saurichthys* resembles the condition in †*Lawrenciella*, †*Pteronisculus*, †*Boreosomus*, †*Australosomus*, and neopterygians [44, 58, 59, 63, 67]. †*Yelangichthys*, however, exhibits a paired posterior myodome [32]. In stem osteichthyans, sarcopterygians, †*Mimipiscis*, *Polypterus*, and acipenseriforms the posterior myodome is absent [18, 44, 74, 79, 85, 86]; (Additional Fig. 3).

An endochondral or dermal basipterygoid process is absent in acipenseriforms, †*Saurichthys*, †*Australosomus*, extant polypterids, †*Caturus*, *Amia*, and likely also in †*Birgeria* [6, 7, 29, 59, 74, 79, 83]. A gentle thickening formed by the canal of the pseudobranchial artery was described as an endochondral basipterygoid process in †*Yelangichthys* [32]. However, its small size and shape contrasts sharply with the well-developed and acute endochondral basipterygoid processes of generalized actinopterygians [44, 58, 65], leading us to also consider it absent.

Ethmoidal region

In dorsal view, the ethmoidal region of NHMD_157546_A widens rapidly before tapering again anteriorly, forming the core of the elongate rostrum of †saurichthyids. The posterior face of the ethmoidal region is concave. Near its contact with the postnasal wall, the interorbital septum (‘ios’) exhibits a dorsal and a ventral fenestra, the dorsal (‘damy’) and ventral (‘vamy’) anterior myodomes, which must have accommodated the superior and the inferior oblique muscles of the eyes, respectively. The olfactory nerve tracts enter the ethmoidal region dorsomedially through a funnel-shaped foramen on each side of the interorbital septum. Posteromedially, the two foramina coalesce with the anterodorsal fenestra of the interorbital septum. A pair of canals likely carrying the branches of the profundus nerve and/or the origin of the inferior oblique muscle (‘vamy+prof?’) merges ventrally with the olfactory canals, near their point of entry in the ethmoidal region. No other foramina are present on the posterior wall of the ethmoidal region.

The dorsal face of the ethmoidal region is mostly flat, bearing two shallow, longitudinal depressions on each side (Fig. 3B, 4B), which must have transported the superficial ophthalmic ramus and the

ramus ophthalmicus lateralis of the trigeminal nerve ('Vopts') and the supraorbital sensory canal ('soc'). The two external nares open laterally ('nao'). A groove extends along the lateroventral margin of the ethmoidal region, probably hosting the maxillary trunk of the trigeminal nerve ('Vmx'). The ventral ethmoidal surface bears a median longitudinal ridge to which the parasphenoid attaches. This ridge is flanked by a shallow longitudinal depression on each side. A shallow V-shaped fossa for the articulation of the autopalatine ('auf') is present on both posterolateral margins of the ventral ethmoidal region (Figs. 3C, 4C). The endoskeletal anatomy of the rostrum is not well-resolved in our scan, but we note the presence of wide nasobasal canals (Figs. 6, 7: 'nbc') beginning at the anterior margin of the nasal cavity and extending anteriorly, along the preserved length of the rostrum. The area immediately posterior to the nasal cavities is weakly mineralized, exhibiting asymmetrical, pocket-like spaces.

Remarks See remarks section for †*Saurichthys nepalensis* below.

Brain and inner ear endocasts

The roof of the brain endocast (Figs. 6,7) and the floor of the saccular recess ('sac') of NHMD_157546_A are incompletely mineralized and cannot be reconstructed. The remainder of the endocast shows increased anatomical complexity (non tube-like), reflecting the position and relative development of different sensory centers, unlike in e.g., teleosts where there is almost no correspondence between endocast and brain anatomy [18, 87]. The brain endocast is markedly elongate and narrow in dorsal view, except in the area of the optic tectum ('to'). Anteriorly, it terminates above the mid-length of the interorbital fenestra. The different sensory regions appear serially arranged.

The rhombencephalic region, including the cerebellum, constitutes more than two thirds of the endocast length, reaching anterior to the crus communis ('cc'). A spinooccipital nerve canal ('nocc') and a canal for an additional spinooccipital nerve or the occipital artery stem from posterior to anterior on the base of the rhombencephalon, on each side of the specimen. Anteriorly, the rhombencephalic region gains height and leads to a dorsally bulging globular structure between the posterior semicircular canals. The vagus stems from the base of this globular structure, which we thus interpret as the vagal lobe ('vl') of the rhombencephalon (e.g., [88]). Two mineralized canals ('n?'), one on each side, stem from the dorsal surface of the vagal lobe, and could be associated with

dorsal rami of the IX or X cranial nerves. Their dissociation from the osseus labyrinth endocast (sinus superior) precludes their attribution to endolymphatic ducts. Immediately anterior to the vagal lobe, the lateral cranial ('lcc') canal forms a laterally-bulging, blind-ended diverticulum, terminating medially to the loop of the posterior semicircular canal ('psc'). Anterior to the lateral cranial canal, the brain endocast is markedly constricted by the overarching development of the bony labyrinth, whose crura communes converge medially, above the hindbrain part of the endocast.

The cerebellar auricles ('aur') are poorly developed and expand laterally, in front of the crura communes, being dorsally restricted by the anterior semicircular canals ('asc'). The facial nerve exits below the junction between the anterior and the horizontal semicircular canals, to enter the jugular canal. The stem of the abducens nerve exits from the ventral surface of the endocast, at the level of the anterior tip of the cerebellum, and enters the posterior myodome. The trigeminal nerve exits at the same level, at about mid-height of the brain endocast. A downward-facing canal for the median cerebral vein ('mcv') is situated at the boundary between each cerebellar auricle and the optic tectum.

The optic tectum is well-developed laterally. The trochlear nerve branches off anteriorly from the anterolateral surface of the optic tectum. Ventrally, there is no differentiation between the latter and the diencephalon. The posterior margin of the hypophyseal recess is not mineralized; hence, the extent of the saccus vasculosus cannot be assessed. The dorsum sellae is reduced to a bony bar ('bb'), separating the hypophyseal recess from the overlying mesencephalon. The buccohypophyseal canal ('bhc') extends posteroventrally through the parasphenoid, but the course of the pituitary vein is not observable. The optic nerve exits through an enlarged median optic foramen below the boundary between the optic tectum and the telencephalon ('tel'). The posterior boundary of the telencephalon is marked by a gentle constriction, separating it from the bulge of the tectal and the underlying diencephalic regions. The telencephalon is short. The olfactory bulbs stem from the anteroventral part of the telencephalon. The two tracts of the olfactory nerve originate at the anterior tip of the telencephalon and are well-separated along their length by the interorbital septum, being uninvested for much of the course through the orbit. They diverge laterally upon entering the ethmoidal region, leading to sizable nasal cavities.

The bony labyrinth of NHMD_157546_A is well-ossified, apart from the ventral part of the saccular recess. Medially, in the absence of an ossified boundary, it is continuous with the rest of the

endocranial cavity. The semicircular canals are large and robust, with the posterior and especially the anterior ones being dorsoventrally shallow. This compression is natural and not due to post-mortem distortion. The posterior semicircular canal is the shortest of the three and is somewhat dorsoventrally flattened. A small constriction precedes the sizable posterior ampulla ('pamp'). The anterior canal is the largest of the three; it is flattened dorsoventrally, forming a sharp anterior angle. The region around the anterior ampulla ('aamp') is thicker and is separated by both the dorsal part of the canal and the utricular recess by means of gentle constrictions. The utriculus ('utr') appears as a lateral projection of the endocast and is somewhat flat rather than globular. The ampulla of the horizontal canal ('hamp') extends dorsal to the utriculus. The horizontal canal ('hsc') forms a hemi-elliptical curve. It enters the cranial cavity slightly ventral to the level of the posterior ampulla. The sinus superior is short. The saccular recess is laterally convex, but its full ventral extent is not visible due to the absence of mineralization. The stem of the glossopharyngeal nerve is situated on the boundary between the sacculus and the ampullary space of the posterior semicircular canal.

Remarks The anatomy of non-neopterygian actinopterygian brain endocasts is thought to mirror that of the contained soft tissues [18, 87], due to the presence of only a single layer of meningeal tissue separating the latter from the braincase [89] Descriptions of partial brain and/or inner ear endocasts were provided for †*Saurichthys ornatus*, †*S. elongatus*, †*S. hamiltoni* and †*S. minimahleri* [29, 90]. The digital endocast presented here is the first to depict the brain and inner ear cavities of the same individual in all views, and conveys information missing in previous studies. This is a valuable addition to the small number of fossil actinopterygian endocasts described to date (see supplement to [87] and [3, 69, 82, 91] for more recent entries). Surprisingly, endocast information is still lacking for extant non-teleostean actinopterygians, with the exception of *Acipenser brevirostrum* (Fig. 9) and *Erpetoichthys* (partial endocast in supplement to [12]). .

In most Paleozoic–early Mesozoic species the area of the vagal lobe is confluent with the posterior dorsal fontanelle. Nevertheless, a prominent vagal swelling like that of †*Saurichthys*, is reconstructed for †*Lawrenciella*, †*Kansasiella*, and †*Pteronisculus* [58, 65, 67], and is also present in the endocast of *Acipenser* (Fig. 9). In life, however, this part of the brain of sturgeons is narrow and rod-shaped, and does not fill the vagal space [73]:fig. 270a. A pronounced mismatch between endocast and brain morphology at the level of the vagal lobe has also been demonstrated for the lungfish *Neoceratodus* [92], suggesting that paleoneurological information from this region of the endocast of bony fishes is should be treated with caution.

Primitively for actinopterygians, the lateral cranial canal was a blind-ending pocket extending from the endocavity through the posterior semicircular canal [3, 44, 65, 67, 69], and a similar arrangement is also seen in †*Saurichthys* and likely in extant polypterids [12]. In *Acipenser*, the lateral cranial canal is absent (Fig. 9), but in *Polyodon* it is present and extends laterally through the loop of the posterior semicircular canal, to connect with the fossa bridgei [84]. This is suggestive of increased variation of this feature even amongst closely-related taxa. In fossil holosteans and stem teleosts, the lateral cranial canal wraps around the sinus superior to form an additional connection with the endocavity, through the loop of the anterior semicircular canal [63, 83, 91]. The lateral cranial canal is lost in extant holosteans and crown teleosts [63, 83]. The function of the lateral cranial canal is unknown, but an association with the lateral development of an epimyelencephalic hemopoetic organ has been suggested [85, 93].

In †*Saurichthys*, the cerebellum appears small, due to the extensive development of the optic tecta. An increase in tectal development relative to the cerebellum is also commonly seen in neopterygians, and is particularly pronounced in teleosts [91, 94]. Primitively, in the endocasts of †*Mimipiscis*, †*Raynerius*, †*Pteronisculus*, and to a lesser extent in those of †*Kansasiella* and †*Lawrenciella*, the cerebellar auricles are broader than the optic tecta [58, 65, 69, 87]. In *Acipenser*, the auricular space is also broader than the tectal space (Fig. 9), but the optic tectum remains poorly differentiated, despite a clear separation between the two sensory centers in the actual brain [73]. In *Erpetoichthys*, the auricles are poorly differentiated, but still broader than the optic tecta [12]:ext. fig. 9. A poor differentiation of tectal and auricular spaces is also seen in †*Boreosomus* [58]. In †*Saurichthys*, †*Mimipiscis* [87], and †*Pteronisculus* [58], the middle cerebral vein enters the endocast below the cerebellar auricles. In †*Kansasiella* and †*Lawrenciella*, it reaches the dorsolateral surface of the auricles [65, 67, 82]. The arrangement of this vessel is unknown in other taxa. The stem of the trochlear nerve lies in a dorsolateral position on the optic tectum in †*Saurichthys*, †*Mimipiscis* [87], †*Pteronisculus* [58], and, albeit less-so, in †*Kentuckia* [87]. In †*Kansasiella*, †*Lawrenciella*, and †*Mesopoma*, it extends from the ventrolateral part of the optic tectum [18, 65, 67, 82].

A well-developed hypophyseal chamber with a clearly differentiated and prominent saccus vasculosus and a ventrally-to-anteroventrally directed buccohypophyseal duct characterize all known Paleozoic actinopterygians, as well as †*Pteronisculus* and †*Australosomus* [18, 58, 59, 65, 67, 82, 87]. †*Saurichthys* shares with sturgeons and bichirs a posteroventrally-directed hypophyseal void, differing from that of other non-neopterygian actinopterygians [18, 94]. In neopterygians

the hypophyseal chamber is almost vertical, but the space of the saccus vasculosus is reduced [39, 91]. A rod-like bony bar, which likely corresponds to the dorsum sellae, drives laterally through the endocast, above the saccus vasculosus, is not seen in any actinopterygian other than †*Saurichthys*.

The olfactory bulbs are merged with the telencephalon in the endocast of †*Mimipiscis* [87], *Polypterus* and *Acipenser* [18, 94]; Suppl.Fig.2), but are better marked by a dorsal to lateral constriction in †*Saurichthys*, †*Kansasiella*, †*Lawrenciella*, †*Mesopoma*, and extant neopterygians [18, 65, 67, 82, 94]. Primitively, the olfactory nerves are not carried in a single tract, with paired tracts present in actinopterygian outgroups (e.g., [85] and also in †*Mimipiscis* [87]). This condition re-evolved in acipenseriforms (Fig. 9). †*Saurichthys* also shows distinct olfactory tracts, but these are carried in shallow grooves on the lateral surface of the interorbital septum, as in gars (pers. obs. on PIMUZ A/I 4171a). In most Paleozoic–Triassic actinopterygians and *Amia*, the olfactory tracts are transmitted to the ethmoidal region via a median endochondral tube [39, 58, 59, 65, 67, 70, 82, 87, 91].

The overall morphology of the osseus labyrinth of †*Saurichthys* is broadly similar to that of generalized non-neopterygian actinopterygians [87], with a few notable modifications. The large degree of medial convergence of the crura communes is the most distinct feature of the osseus labyrinth of †*Saurichthys*. A reduced level of crural convergence, but a greater degree of superimposition on the brain cavity occurs in †*Meemania*, †*Mimipiscis* and to a lesser degree in †*Raynerius* [3, 69, 87]. Crural convergence is seen in some neopterygians [91] and polypterids [12], but superimposition is typically absent in other actinopterygians [12, 18, 39, 58, 59, 65, 67, 87, 91];Fig. 9). In sarcopterygians [95], and less so in †*Mimipiscis*, †*Kentuckia* [87], †*Pteronisculus* [58] and fossil neopterygians [91], there is a ventrally-expanded utricular recess. This feature is less-pronounced in †*Saurichthys*, polypterids [12], *Acipenser* (Fig. 9) and in other non-neopterygians [59, 67].

Parasphenoid and associated dermal bones

The parasphenoid of †*Saurichthys* is cross-shaped in ventral view (Fig. 3C,D, 4C,D), bearing a well-developed posterior stalk that underlies the occipital region and projects posterior to the braincase. The posterior margin of the parasphenoid is notched at the midline, presumably for the passage of the aorta, although the exact shape is obscured due to breakage. Ventrally, there is a prominent median keel (‘pspk’) that extends from slightly anterior to the posterior notch, to the level of the ascending processes, where the foramina for the passage of the common carotids (‘ccar’)

into the braincase are located. Anterior to the foramina for the common carotids, the keel of the parasphenoid blends gently into the convex ventral surface of the anterior process of the bone. The ventral keel of the parasphenoid is laterally concave on both sides, marking the external course of the common carotids. The branching of the common carotids from the dorsal aorta must have occurred immediately posterior to the ventral keel. The ascending processes ('asp') of the parasphenoid extend dorsally and posteriorly, passing over the lateral commissure, to terminate anterolateral to the hyomandibular facets, near the dorsal margin of the braincase. The lateral surface of each ascending process bears a spiracular groove ('spig'). The anterior process of the parasphenoid is narrower than the posterior, but is elongate; it can be followed anteriorly all the way below the preserved part of the ethmoidal region, where it overlies the vomers. The bucco-hypophyseal canal ('bhc') opens on the ventral keel of the parasphenoid. A median parasphenoid canal runs through the bucco-hypophyseal canal, reaching the level of the anterior margin of the interorbital fenestra, where it opens ventrally ('apal'). This canal must have accommodated the palatine branch of the internal carotid artery and we consider it to be homologous with the parabasal canals of other actinopterygians. A small patch of tiny teeth occurs on the parasphenoid, slightly anterior to the palatine opening.

The paired vomers are elongate and underlie the parasphenoid. Their posterior tips lie slightly rostral to the anterior margin of the orbit, whereas their anterior tips could not be located due to breakage. Each vomer forms an elongate toothplate that bears numerous tiny teeth. The two vomers seem to form a midline suture, whose posterior end is located at the level of the anterior margin of the anterior narial opening. No teeth are observed along the suture line.

Remarks The well-developed posterior stalk as well as the high ascending processes distinguish the parasphenoid of †*Saurichthys* from the primitive actinopterygian condition, exemplified by the lozenge-shaped parasphenoid of †*Raynerius* and †*Mimipiscis* [44, 69]. Ascending processes are typically more developed in post-Devonian actinopterygians, but in many generalized forms the posterior stem still stops short of the occipital region and rarely underlies the ventral otic fissure [39, 40, 44, 52, 58, 59, 67, 96, 97]. The parasphenoid crosses the ventral otic fissure in several Carboniferous and younger actinopterygians; e.g., in †*Amphicentrum*, †*Eurynotus*, †*Sphaerolepis*, †*Errolichthys*, †*Birgeria*, and early neopterygians like †*Watsonulus*, whereas in polypterids and most neopterygians it reaches the level of, and sutures with, the basioccipital and–when this can be assessed–incorporated vertebrae [7, 9, 40, 59, 63, 64, 79, 98-100]. At least in Early Triassic †saurichthyids [29] and in sturgeons [73-75], the parasphenoid extends well past the occiput,

underlying a variable number of rigidly-connected vertebrae (Suppl. Fig. 2). As with †*Saurichthys*, the posterior stem of the parasphenoid also bears a notch (albeit deeper) in *Polypterus*, *Acipenser*, *Polyodon*, *Lepisosteus*, *Amia,* as well as in fossils such as †*Amphicentrum*, and †*Birgeria* [6, 7, 9, 29, 59, 64, 79].

A closer comparison between the parasphenoid of †*Saurichthys* and that of *Acipenser* reveals conspicuous differences in basicranial circulation that contradict orthodox hypotheses of a close relationship between the two. The parasphenoid of *Acipenser* lacks the enclosed arterial system [73] seen in †*Saurichthys* (Fig.8). In *Acipenser* the two variably present ventral foramina on the posterior process of the parasphenoid serve as the exit of the aortic branch that later gives off the first and second efferent branchial arteries and the common carotids [73](Additional Fig. 4). These foramina have been erroneously homologized with the foramina serving as the entrance for the common carotids in †*Saurichthys* [16]. Like in most sturgeons, the common carotids run and bifurcate below the parasphenoid and enter the neurocranium at different points in *Polyodon* [72]. Furthermore, a buccohypophyseal opening is absent in acipenseriforms, and their anterior parasphenoid process terminates underneath the posterior ethmoidal region, giving way to a pair of edentulous vomers [6, 74]. In some Middle Triassic †saurichthyids from China and Switzerland, as well as in †*Saurorhynchus*, the efferent pseudobranchial artery exits through the foramina located near the base of the ascending processes of the parasphenoid [22, 23, 30]. Foramina or notches for internal carotid branches are present in the parasphenoid of †*Boreosomus* [58], most Mesozoic holosteans and stem teleosts [63].

The paired vomers, and associated toothplates, of NHMD_157546_A, and other †saurichthyids [29, 30] seem to reflect the primitive actinopterygian condition, as seen in anatomically generalized Paleozoic (e.g., †*Mimipiscis* and †*Moythomasia*) [44] and Mesozoic (e.g., †*Pteronisculus* and †*Australosomus*) [58, 59] taxa. This paired vomerine architecture is also encountered in extant holosteans [7, 9]. The presence of a median vomer and associated toothplate in the adult, has evolved independently in several clades, such as Cladistia [79] and †scanilepiforms [12], some stem neopterygians (e.g., †*Luganoia*) [101], and teleosts [102]. A single vomer, with a toothplate that bears larger teeth along its midline, has been observed in the †saurichthyiform †*Yelangichthys* [32]. Given the broader distribution of this feature, we consider this condition as an apomorphy of †*Yelangichthys*. Acipenseriforms posses a series of paired or median, vomer-like elements, which may vary in number and lie immediately anterior to the parasphenoid [6, 74]. The homology of these elements is yet unclear, though the posterior-most ossifications have been considered as vomers [6, 74].

Palatoquadrate and associated dermal ossifications of the cheek

The palate of †*Saurichthys* (Fig. 10A–E) consists of rigidly connected dermal and endochondral ossifications that hosted the enlarged mandibular adductor muscle. The palatoquadrate is endochondrally ossified in at least two, and potentially three, parts. The quadrate ('q') forms the posteroventral margin of the endochondral palate, and the metapterygoid ('mtp') forms the dorsal margin. These two elements were previously described in †*Saurichthys* as being fused into a quadratometapterygoid [29], but no endochondral connection between the two was evident in the scan of NHMD_157546_A. An independent autopalatine ('au') forms the anterior margin of the endochondral palate. The quadrate forms the posterior margin of the adductor mandibulae fenestra ('addf') and bears two convex ventral condyles for articulation with the articular bone of the lower jaw. Medially, it exhibits a dorsoventrally oblique groove, where the ventral limb of the hyomandibula was accommodated. The metapterygoid is neither fenestrated, nor does it show any kind of anterodorsally-expanded articular process. The only direct articulation between each palate and the neurocranium is seen anteriorly, where the independently ossified, triangular, pad-shaped autopalatine inserts to a similarly shaped fossa on the posterolateral floor of the ethmoidal region of the braincase.

Due to thinness, strong fusion among individual elements and breakage, the margins between individual bones of the dermal palate could not be reconstructed. The dermal palate ('dpal') forms a medially convex, cleaver-shaped apparatus. Laterally, it is rigidly connected to the maxilla. The posteroventral margin of the palate forms the anterior and medial surfaces of the large adductor foramen. The medial surface of the dermal palate, which likely corresponds to the area occupied by the entopterygoid [29], bears a prominent median shelf ('pals') along the length of its posterior half, which was likely associated with the palatine levator muscle, or with other ligaments connecting it to the parasphenoid. The anterodorsal margin of the bone is concave, without forming evident articular processes. The lingual surface of the dermal palate, anterior to the adductor fossa, bears sparsely-arranged tiny teeth. Anteriorly, the part corresponding to the dermopalatine [29] forms a ventromedial crest that bears better-defined, tiny teeth and occludes with the dorsomedial surface of the prearticular crest.

The maxilla is cleaver-shaped (Fig. 11), forming an expanded posterior plate to which the arcuate preopercle (posterodorsally) and the quadratojugal (posteroventrally) suture, to form a rigid unit.

As with most other superficial dermal elements, the dermal bones of the cheek are poorly preserved in the specimen. The preoperculum is boomerang-shaped, forming two distinct limbs, a horizontal and a more robust vertical one, separated by a dorsovental constriction of the bone. The course of the preopercular canal could not be clearly traced. The dorsal and posterior surfaces of the bone meet almost at a right angle, forming a rounded posterodorsal corner.

Remarks A single endochondral palatal ossification persists throughout ontogeny in most non-neopterygian actinopterygians, such as †*Cheirolepis*, †*Moythomasia*, the Madagascan †*Pteronisculus*, †*Australosomus*, and seemingly some neopterygians [44, 59, 103, 104]. In other non-teleostean actinopterygians, the adult palatoquadrate consists of distinct bones (or cartilages) arising from different ossification centers and exhibiting several variations [104], none of which includes a separate autopalatine and quadratometapterygoid ossifications as postulated by Stensiö [29] for †*Saurichthys*. The palatoquadrate of NHMD_157546_A likely conformed to the tripartite ossification pattern seen in polypterids, acipenseriforms, †*Birgeria stensioei*, †*Watsonulus*, *Amia*, and many teleosts [46, 47, 58, 74, 98, 104].

A high posterior extension of the palate is the plesiomorphic condition seen in Devonian actinopterygians [44, 103], and retained in most generalized forms of the Paleozoic and the Mesozoic [58, 59], including †*Saurichthys*. In †*Saurichthys*, †*Fukangichthys*, †*Birgeria*, and †*Woodichthys*, the dorsal part of the palatoquadrate forms no evident processes for articulation with the neurocranium [12, 59, 97]. In Devonian actinopterygians the metapterygoid bears a circular opening for articulation with the basipterygoid process of the neurocranium [44, 103], whereas, in stratigraphically younger forms, the metapterygoid forms a notch (e.g., †*Australosomus*, [59]) or two processes (†*Pteronisculus*, *Amia*, [58, 104]) for articulation with the neurocranium and/or the attachment of ligaments connecting to the parasphenoid. As in other non-neopterygian actinopterygians [44, 58, 59, 79], the maxilla of †*Saurichthys* is non-kinetic. The shape of the preopercle of NHMD_157546_A is similar to the preopercle of †*Saurichthys* cf. *elongatus* from the Early Triassic (late Smithian) of Idaho [28] in exhibiting a dorsoventrally-wide horizontal limb. An anterior thickening of the preopercle is absent in †*Saurichthys ornatus*, or in any other species from Spitsbergen [29].

Dermal bones of the skull roof and rostrum

Our observations on NHMD_157546_A (Fig. 11) are in agreement with those of Mutter et al.

[54], although further information on the skull roof is provided here, following our examination of the dorsal counterpart of the fossil. The superficial layers of the dermal bones, which bear ganoin ornamentation and the sensory canals, are missing from NHMD_157546_A, but are preserved in the counterpart. A single pair of elliptically-shaped median extrascapulars (‘exsc’) is present on the posteromedial part of the skull roof, giving way anterolaterally to a pair of elongate dermopterotics (‘dpt’). The latter converge on the midline, but their anterior and posterior ends flare laterally. Part of the endochondral occipital crest (‘occ’) appears between the posterior part of the dermopterotics and the median extrascapulars, due to removal of the superficial layers of the bone during preparation. A field that contained the paired parietal bones (‘pa’) is present between the anterior part of the dermopterotics and the frontals (‘fr’). There is one semicircular parietal on each side of the midline. Each parietal seems to carry two pit lines (‘papl’), one extending posteromedially from the anterolateral part of the bone, and one extending medially from the lateral edge of the bone. The frontals are elongate and roughly triangular and taper rostrally, but their anterior tip is not preserved due to breakage in NHMD_157546_A. The frontals bear a lateral notch posteriorly for accommodating the supraorbital elements.

Anterior and lateral to the orbit, the frontals give way to the so-called nasalo-antorbitals (‘nsao’), which cover the posterolateral part of the rostrum, and encompass both narial openings (‘nao’) and the horizontal and ascending portions of the infraorbital sensory canal (‘ioc’), and its commissure with the supraorbital sensory canal. The ventrolateral margin of the preserved rostrum is occupied by the tooth-bearing rostropremaxilla (‘rpmx’). It is unclear whether the rostropremaxilla is paired or median, due to breakage. We did not find evidence for an ethmoidal sensory canal, but it is unclear if it was destroyed during preparation. The rostropremaxilla is ornamented with subvertical striae, as seen in some parts where the superficial ornamentation is preserved, and is also intimately connected with the maxilla (‘mx’). It comprises a dorsoventrally-oriented lamina and a medially-directed shelf, extending below the ethmoidal region and connecting medially with the vomers. The ventromedial part of the lamina bears two rows of sparsely arranged teeth. There is one marginal row of ventrally-directed tiny conical teeth, and another row of ventromedially-directed tiny teeth, the latter being interrupted at points by large laniaries. The median shelf of the rostropremaxilla forms a rostrocaudally-directed groove for the accommodation of the largest teeth of the dentary. Large teeth also develop on that groove.

Remarks One pair of (median) extrascapulars is present in most Early Triassic †saurichthyids and †*Sinosaurichthys*, but an independent ossification is not apparent in Middle Triassic or younger forms [23, 25, 29, 30, 40]. A second extrascapular pair is present in at least some specimens of †*Saurichthys madagascariensis* [25]. One or two pairs (median and lateral) of extrascapulars, typically carrying the supratemporal sensory commissure, are usually present in non-neopterygian actinopterygians [20, 44, 52, 58, 59, 105]. An increased number of extrascapular elements is seen for example in †*Chondrosteus* (one median, three paired; [11]). Living non-neopterygian actinopterygians display important inter- and intraspecific variations, with three to four paired extrascapular-like elements present on the skull of *Polypterus* [9, 80], one to two paired extrascapulars and a median extrascapular in *Acipenser* [74], and two paired extrascapulars in *Polyodon* [6]. In most actinopterygians, including most †saurichthyiforms, a single pair of parietals meets at the midline [17, 23, 25, 30, 32, 44, 52, 58]. Two pairs of parietals are present in †*Saurichthys ornatus* from Spitsbergen [29], suggesting that a different specific attribution of the Greenland specimen is warranted. An large number of tiny parietals is present in †*Saurichthys piveteaui* [39]. Additional variation in the number and shape of the parietals can also be seen in the sympatric †*Saurichthys* species from the Buntsandstein (Anisian) [90].

Primitively, in Devonian and some Carboniferous actinopterygians, the supratemporal sensory canal is carried by two bones, the supratemporal posteriorly and the intertemporal anteriorly [44, 69, 96, 97, 106, 107]. In younger forms, like †*Saurichthys*, †*Birgeria*, †*Pteronisculus*, †*Australosomus*, †*Fukangichthys*, fossil neopterygians, and all extant actinopterygians, a single bone, the dermopterotic, occupies this position [6, 7, 9, 20, 29, 30, 58, 59, 74, 80, 98, 102]. One pair of frontals is present on the actinopterygian skull roof, bearing the supraorbital sensory canal and enclosing the pineal opening, when present [17, 44, 52, 58, 59, 69].

Uniquely among actinopterygians, †saurichthyiforms possess likely compound nasalo-antorbitals [23, 29, 30, 32], a term established on the fact that these bones carry both nasal openings and the triradiate canal, formed by the horizontal, the ascending and the ethmoidal rami of the infraorbital sensory canal. The traditional terminology is retained herein. In most other non-neopterygian actinopterygians, the anterior nares are situated between the nasal and adjacent bones (either rostral or postrostral, e.g. in †*Mimipiscis*, †*Birgeria*, †*Pteronisculus*), and the posterior nares are located between the nasal and the antorbital (e.g. †*Birgeria*), or between the nasal and the orbital opening (e.g. †*Mimipiscis*, †*Boreosomus*, †*Pteronisculus*) [44, 58, 59]. The triradiate canal is primitively

accommodated in the premaxilla [44], but in many late Paleozoic and younger taxa (e.g., †*Kalops*, †*Birgeria*, †*Teffichthys*, *Amia*) it is accommodated in an independent ossification, the antorbital [7, 59, 108, 109]. A commissure between the infraorbital and supraorbital canals accommodated between the nostrils occurs in some generalized genera like †*Kalops* and †*Boreosomus* [58, 108], in †saurichthyiforms [23, 29]; Fig.11C,D), and stem (e.g., †*Teffichthys* [109]) and crown neopterygians [7, 9]. A commissure between the two sensory canals is absent in †*Birgeria* [59]. In Acipenseriformes, the infraorbital sensory canal does not form an ascending ramus [6, 74]. In *Polypterus*, the connection between the infraorbital and supraorbital canals takes place anterior to the single nasal opening, through a likely compound element formed by the premaxilla and the rostral [80].

The prominent †saurichthyid rostrum is formed mainly by the rostropremaxilla(e), whose ontogenetic origin remains unknown. Due to the acuteness of the snout, it is unclear if these elements are paired [23, 29, 30] or unpaired [25]. The presence of an anterior ramus of the infraorbital sensory canal and teeth in the rostropremaxillae of most †saurichthyids [23, 29, 30], combined with their topology and posterior development, suggests that the premaxilla, and potentially the rostral, plays an integral part in the development of the rostrum. This also seems to also apply to †*Birgeria*, although in the latter taxon the rostropremaxilla additionally borders the anterior narial opening [59]. In primitive actinopterygians, the anterior-most rostral is often expanded ventrally, bears the ethmoidal commissure and teeth, and forms the anterodorsal tip of the oral rim, for instance in †*Moythomasia* [44]. The rostral is flanked by paired premaxillae, bearing the anterior and the ascending rami of the infraorbital sensory canal [44]. Loss, fusion or fragmentation of those elements is common in non-neopterygians (e.g., in †*Wendyichthys*, †*Cyranorhis*, †*Pteronisculus*, †*Australosomus* and in acipenseriforms, the premaxilla is probably absent, [40, 58, 59, 74, 106]), but a detailed discussion is beyond the scope of this work. A pair of postrostral elements, situated between the frontals and the rostropremaxilla(e), is potentially present in Early Triassic †*Saurichthys* species from Spitsbergen [29]. A higher number of postrostrals were tentatively reconstructed for †*S. stensioi* and †*S. piveteaui* from Madagascar [39, 40]. Postrostrals are unknown in most other †saurichthyids [22, 23, 25, 30], although a single pair was tentatively reconstructed for †*Saurorhynchus acutus* [110].

Circumorbital bones and ossifications of the orbit

Most circumorbital bones of NHMD_157546_A have been pushed medially inside the orbits and are still covered by matrix (Fig. 1A, 2A). As a result, they were not previously described [54]. The

dorsal margin of the orbit is formed by one or two supraorbitals (incompletely preserved and broken on both sides of the skull, 'so') and the dermosphenotic ('dsph'). Mutter et al. [54] misidentified the externally exposed postorbital process of the braincase as the dermosphenotic. The dermosphenotic is anteroposteriorly elongate and laterally convex and bears a broad ventral articulation surface for the attachment of the jugal. The jugal ('ju'), being anteriorly concave and posteriorly convex, forms the posterior margin of the orbit. It starts vertically below the dermosphenotic, but forms a gentle anterior curve and tapers towards its articulation with the second infraorbital ('io2'). The latter is talon-shaped and forms the posterior part of the ventral orbital margin. The infraorbital canal passes anteriorly to an elongate first infraorbital (Fig. 11:'io1') wedged between the nasalo-antorbital and the anterior prossess of the maxilla. A single, well-developed, sub-triangular anamestic suborbital ('subo') bone covers the space between the jugal and the expanded posterodorsal process of the maxilla. All the above dermal bones are ornamented with tubercles that are sometimes connected to form short, vermiform ridges.

A thin sclerotic ring (Fig. 1A,B, 2A,B:'sclt') is preserved in situ on both sides of the skull. The number of individual ossifications could not be confidently determined. The diameter of the sclerotic ring is only slightly smaller than that of the enlarged orbital space. The outer dorsal and ventral surfaces of the sclerotic ossicles are ornamented with randomly arranged turbercles, whereas the inner surface is smooth. Traces of the cartilaginous sclera ('scla') are also preserved, contained within the sclerotic rings and curving towards the midline of the skull.

Remarks Amongst †saurichthyids, supraorbitals seem to be restricted to Early Triassic forms [25, 29, 39, 40] (Fig. 1A, 2A), and are unknown from stratigraphically younger species [22, 23, 27, 30]. Supraorbitals are primitively absent in actinopterygians [18, 40, 44, 58, 59, 96], but are also absent in *Polypterus* and *Amia* [7, 80]. One supraorbital is present in †*Discoserra* and *Acipenser*, †*Watsonulus*, and gars, but three or more are seen in forms like †*Kalops*, †scanilepids, stem neopterygians (†'subholosteans') such as †*Luganoia* and †*Peltopleurus*, and some stem teleosts [9, 12, 20, 74, 101, 102, 108, 111, 112]. The dermosphenotic of †*Saurichthys* resembles that of e.g., †*Pteronisculus,* †*Boreosomus* and *Acipenser* [58, 74] in lacking a posterior process. This contrasts with both the primitive actinopterygian condition and that seen in e.g., †*Birgeria groenlandica* and extant forms like *Polyodon*, where the dermosphenotic forms a posterior process [6, 59].

NHMD_157546_A resembles the Early Triassic †saurichthyids from Spitsbergen [29] and Madagascar [39] in exhibiting three infraorbitals. This seems to be the primitive condition in the group. All Devonian and most Carboniferous actinopterygians exhibit two infraorbitals: a jugal (forming the posteroventral margin of the orbit) and a first infraorbital (or lachrymal, forming the anteroventral margin of the orbit) [44, 96, 105]. Additional infraorbitals, often more than one, are seen in many stratigraphically younger forms like †*Boreosomus* [58] and †*Birgeria* [59]. At least two infraorbitals are present in *Acipenser* [74], whereas numerous small, canal-bearing ossicles are seen in *Polyodon* [6]. Only a single infraorbital bone is present in *Polypterus*, with the infraorbital canal largely borne by the maxilla [80]. †Scanilepids have two infraorbitals [19, 20].

The numbers of suborbital bones vary greatly in post-Devonian actinopterygians, with Early Triassic †saurichthyids having one [29] (Fig. 1A, 2A), †*Pteronisculus* having two or more, †*Boreosomus* having five [58], and †*Birgeria* having more than 10 [59]. No suborbitals are known in post-Early Triassic †saurichthyids [22, 23, 27, 30]. Suborbitals are absent in extant Acipenseriformes [6, 74]. A series of small anamestic bones homologous to suborbitals, but referred to as 'spiraculars', separate the cheek from the orbit and the dorsal skull roof in extant polypteriforms [80]; three of these elements are typically present in †scanilepids [12]. In *Amia* the suborbitals are also absent, whereas in Lepisosteiformes they are greatly reduced in size and multiplied to form a mosaic on the lateral surface of the cheek [7, 9]. Numerous suborbitals are present in stem teleosts, but are absent in extant taxa [102].

Lower jaw

The lower jaws are almost straight (Fig. 10H–K, 11). Three dermal bones are seen on the lateral surface of each mandible. The posterolateral corner is occupied by the elongate, triangular surangular ('sang'). The angular ('ang'), on the posteroventral corner of the jaw, is more elongate and reaches the level of the external nares anteriorly. Though damaged during preparation, a faint groove along its ventral margin indicates the course of the mandibular sensory canal ('mdc'). Posteriorly it wraps around the posterior surface of the articular and reaches the posteromedial surface of the lower jaw. The dentary ('d') is the largest and the main dentigerous bone of the lower jaw. It begins posteriorly between the angular and the supraangular, and in †saurichthyids it usually extends to the symphysis. Only its dorsal part is visible in tomograms. The dentary curves medially to form a medial dermal lamina, which supports an elongate dental lamina along its preserved length. The tooth plate

is occupied by patches of tiny teeth, starting from below the otic region of the neurocranium and becoming more numerous and better developed anteriorly. Starting from the level below the nostril and extending to the tip of the preserved part of the jaw, a single file of coarsely-spaced, caniniform teeth interrupt the continuity of smaller tooth patches. Although few caniniform teeth are actually preserved in our specimen, we can deduce that they occur in alternate positions between the two jaws, forming a dental basket. The base of the caniniform teeth is made of crenelated dentine (plicidentine), while the apex is formed by an acrodin cap, equal or slightly shorter than a fifth of the tooth height. The pulp cavity is wide and terminates slightly above the mid-height of the tooth, but does not reach the acrodin cap (Additional Fig. 2B). Caniniform teeth in the upper jaw seem to share the same structure.

The large prearticular ('part') covers most of the dorsomedial aspect of the lower jaw posteriorly, and tapers anteriorly. A dorsolateral projection of the bone articulates between the medial dermal lamina of the dentary and the overlying dental lamina. Miniscule teeth appear at the same level as the teeth of the dentary. More anteriorly, below the mid-length of the orbit, the prearticular forms a dorsomedial crest, which becomes more prominent at the level of appearance of the caniniform teeth of the dentary. This crest is largely edentulous and occluded with the vomers.

The endochondral articular ('art') is triangular in shape and bears a dorsal glenoid fossa with two pits for the articulation of the condyles of the quadrate. Anteroventrally, the articular passes to the very thin and weakly ossified meckelian cartilage ('mk'). It is unclear if the two elements were connected. The meckelian cartilage is ventral to the prearticular and partially covered by the latter bone, taking the form of an internal lining. A series of wide, circular ventral openings is present and can be associated with the innervation from the trigeminal nerve ('Vmand'). A large fenestra for the mandibular adductor muscle is present on the posterodorsal corner of the bone, immediately anterior to the articular, and is bounded by the articular, the dentary and the prearticular bones.

Remarks A surangular in the lower jaw seems primitively present in Devonian actinopterygians [69, 105, 113], and is common in Permian–Triassic taxa such as †*Saurichthys*, †*Pteronisculus*, †*Australosomus*, †*Birgeria*, and †*Fukangichthys*, and early crown neopterygians like †*Watsonulus* and †'pholidophorids' [12, 29, 58, 59, 98, 102]. Loss of the surangular has occurred multiple times in non-neopterygians, like e.g., †*Mimipiscis*, †*Gogosardina*, †*Amphicentrum*, †*Aesopichthys*, the acipenseriforms and *Polypterus* [44, 64, 80, 114, 115]. †*Saurichthys,* like most fossil non-

neopterygian actinopterygians, lacks a coronoid process in the lower jaw for the attachment of the adductor mandibulae [44, 58, 59]. By contrast, cladistians (inclusive of †*Fukangichthys*), †*Birgeria* and neopterygians bear a dermal coronoid process. The components of this structure vary between groups, suggesting multiple independent origins [12, 59, 80, 98]. The lower jaw dentitions of Early Triassic †saurichthyids have neither been described nor adequately illustrated [29], hampering further comparison with the Greenland specimen. Plicidentine has occurred multiple times in modern lineages of hyper-piscivorous actinopterygians, but is also present in †*Cheirolepis*[116]. The expanding list of taxa exhibiting plicidentine, which now includes †*Saurichthys*, suggests that the distribution of this feature is controlled by function, rather than phylogeny.

Operculogular series

The opercular series is largely not preserved in NHMD_157546_A. Only a single branchiostegal ray is preserved in this specimen (Fig. 1C, 2C:'rbr'), underlying the posterior part of the ceratohyal. The branchiostegal is lozenge-shaped, with rounded anterior and posterior ends. Its ventral face is ornamented with well-developed tubercles, but bears an unornamented field along its posteromedial margin. On the opposite (right) side of the branchiostegal, and anterior to it, there is a flat, splint-like dermal element, underlying the anterior part of the right ceratohyal and extending anteriorly slightly past its rostral end. Its ventral face is also ornamented with tubercles. There is no sign of a lateral field for the insertion/overlap of the branchiostegal element, allowing us to identify the splint-like element as a lateral gular ('latg').

Remarks One pair of branchiostegals is known in Early Triassic [25, 29] and Middle Triassic †saurichthyids [23, 25, 29]. A second pair has been identified in the Middle Triassic †*Saurichthys yangjuanensis* [36]. The number of branchiostegal rays varies among Paleozoic actinopterygians, being usually higher than 10 [44]. The single pair of splint-shaped gulars of the Greenland †*Saurichthys* seems to correspond to the primitive condition in the clade. Gulars were previously thought to be absent in †saurichthyids. Given the large sample sizes investigated, they are likely lost in Middle Triassic and younger forms (e.g., [22-24, 27, 30, 36]. Most non-teleostean actinopterygians exhibit gulars, with the primitive pattern corresponding to the presence of one median gular and a pair of lateral gulars, like in †*Cheirolepis*, †*Mimipiscis*, †*Raynerius*, †*Pteronisculus,* †*Birgeria*, †*Watsonulus* and some Triassic '†pholidophorids' [44, 58, 59, 69, 96, 98, 102, 103]. Acipenseriforms, †*Chondrosteus*, ginglymodians and most crown teleosts have no gulars [6, 9-11, 74].

Despite the limitations of the material described here, a comment on the opercular bones of †saurichthyids is warranted. The largest bone of the †saurichthyid opercular series is historically identified and treated as an operculum [22, 23, 25, 27, 29, 30, 117]. Nevertheless, Stensiö also considered the possibility of a more complex evolutionary history for this bone through fusion of separate elements [29]. In most actinopterygians, the opercle forms an anteromedial process and fossa which articulates with the opercular process of the hyomandibula [7, 9, 58, 59, 79]. In primitive forms like †*Cheirolepis*, †*Mimipiscis*, †*Moythomasia* and †*Raynerius*, the opercle articulates directly with the posterior face of the 'knee' of the hyomandibula [44, 68, 69, 103]. In fossil chondrosteans with a reduced opercle, like †*Chondrosteus*, †*Peipiaosteus* and †*Stichopterus*, the latter bone is not in contact with the hyomandibula, but sits on the dorsal side of an enlarged subopercle [11, 118].

Additional †*Saurichthys* material from the Middle Triassic of Switzerland (Fig. 12D,E), as well as a review of figured specimens (e.g. [29]: Pl. 11, 14, 22, 27, 28) reveals that the articulation between the so-called 'operculum' and the hyomandibula occurs much more ventrally than previously thought, at the ventral tip of the latter bone. This mode and topology of articulation implies that the 'opercle' is actually an expanded subopercle ('sop'), and is broadly comparable to that of Chondrostei, where the expanded subopercle articulates with the posteroventral cartilaginous head of the hyomandibula [6, 11, 74]. However, †*Saurichthys* is the only known actinopterygian whose subopercle forms an anteromedial articular process and fossa for articulation with the hyomandibula [23, 29]. In other actinopterygians, the subopercle articulates with the posterior surface of the preopercle and the ventral surface of the opercle, and is ligamentously attached to the ventral limb of the hyomandibula [7, 70, 79].

This inference gains additional support with the identification of an additional opercular element in †*Saurichthys ornatus* and †*S. hamiltoni* from the Early Triassic of Spitsbergen (unlabeled in [29]: Pl. 11, 27, 28) and †*Saurichthys madagascariensis* (termed as antoperculum in [39]: fig. 10; [25]: fig. 6). This small dermal bone wedged between the preopercle, the dermohyal (present although not labelled) and the expanded subopercle is situated at the level of the back of the 'knee' of the hyomandibula, and is topologically equivalent and likely homologous to the opercle. An expansion of the subopercle at the expense of the opercle has occurred several times in Actinopterygii, with early chondrosteans [11, 118], †*Canobius* [119], †*Styracopterus* [120], and †*Teffichthys* [109] being some examples of seemingly independent acquisition of this character.

Hyoid and branchial arches

The slender, boomerang-shaped hyomandibula (Fig. 10A, 12A–C:'hm') has a well-defined horizontal anterodorsal limb and a posteroventral limb. The dorsal surface of the dorsal limb is flat and wide, potentially serving as the insertion point of the retractor muscle. A dermohyal ('dhy') is firmly fused on the dorsolateral to lateral surface of the anterodorsal limb of the hyomandibula. No ornamentation of the dermohyal is apparent in the scan. However, the compactness of the dermohyal ossification contrasts sharply with the cancellous endochondral nature of the main body of the hyomandibula, testifying to its dermal origin. The dermohyal expands dorsally, forming a lateral wall with a T-shaped cross section on the hyomandibula. The dorsal surface of the dermohyal was accommodated between the preopercle and the dermopterotic in life. The posterodorsal tip of the dermohyal stands out from the body of the hyomandibula, forming an angular projection. This projection was previously erroneously identified as an opercular process in †*Saurichthys curionii* [23]. An opercular process is absent from the hyomandibula of NHMD_157546_A. A canal for the hyomandibular trunk of the facial nerve ('VIIhm') starts at the posteromedial part of the dorsal limb and exits laterally at the 'knee' of the bone. Additional ossifications intercalated between the hyomandibula and the ceratohyal (e.g., interhyal, symplectic) were not observed. A single ceratohyal (Fig. 13:'chy') is present on either side of NHMD_157546_A. The ceratohyal is slender, slightly twisted around its long axis and of elongate hourglass shape. The lateral surface of the bone bears a shallow groove for the afferent hyoidean artery. The hypohyals ('hh') are slightly dislocated from their natural position. They are strongly curved medially, and they likely articulated with the first basibranchial element. Their median part is thicker than their posterior part, the latter forming an elliptical head for articulation with the ceratohyal. No basihyal was observed.

The branchial skeleton of †*Saurichthys* is only partially preserved and largely disarticulated (Fig. 13). A rod-like and grooveless endochondral structure on the left side likely corresponds to the first infrapharyngobranial. Posterior to the rod-like bone there are two dorsoventrally short and robust pharyngobranchials ('pbr'). They form a medial shelf for the passage of the efferent branchial arteries. Immediately ventral to the posterior tip of the rod-like bone, there is a dislocated epibranchial ('epi'), which was likely the first of the series. Its dorsal tip bears two surfaces for articulation of the pharyngobranchials, but no uncinate processes. The epibranchial bears a lateral groove for the corresponding efferent artery. The ventral elements of the first two branchial arches are preserved. The ceratobranchials ('cbr') are straight, exhibiting a conspicuous ventral groove

for their corresponding efferent arteries. The hypobranchials ('hbr') are imperforate, straight for the most part and deeply grooved ventrally for the passage of the efferent arteries. The grooves disappear slightly before their anterior articular head. The first hypobranchials are hatchet-shaped, with their anterior tip forming a broad, median expansion for articulation with the corresponding basibranchial element. They lack facets for articulation with the hypohyals. The mesial head of the second hypobranchial is narrower. Nothing remains of the more posterior arches. One basibranchial (out of the expected three [29]) is preserved. It has a subtriangular cross-section, a flat dorsal surface and weak ventral keel. No articulation surfaces for the hypobranchials were identified on the basibranchial.

Remarks †*Saurichthys* shares a similar hyomandibular morphology (boomerang-shaped; single head for articulation with the braincase; lack of opercular process, canal for the facial nerve (VII), fused dermohyal) with Devonian actinopterygians like †*Mimipiscis*, †*Moythomasia*, †*Howqualepis* and †*Raynerius* [44, 69, 96]. In †*Saurichthys*, the dermohyal occupied a more dorsal position, being wedged between the preoperculum and the dermopterotic, rather than between the preoperculum, the dermopterotic (or homologues), and the operculum as in other early actinopterygians. It is possible that this is due to the hypothesized changes to the opercular series outlined above, and/or the elongation of the posterior portion of the †saurichthyid skull. The hyomandibula of chondrosteans lacks both an opercular process, and a dermohyal [6, 11, 74]. *Polypterus*, †*Fukangichthys*, †*Pteronisculus*, †*Boroesomus*, †*Australosomus* and the neopterygians bear a distinct opercular process [7, 9, 12, 58, 59, 79, 98]. The dermohyal is not fused to the hyomandibula in other post-Devonian actinopterygians, including *Polypterus* [18, 47, 58, 59, 66, 79]. It is generally absent in crown neopterygians [7, 98], although it is present in crownward members of the stem lineage like †*Luganoia* and †*Peltopleurus* (Bürgin 1992), and likely also in gars [9]. The presence of a facial nerve canal on the hyomandibula is widespread in Actinopterygii (e.g., [44, 98]), but is absent in polypterids, †*Fukangichthys*, acipenseriforms, †*Cheirolepis*, and †*Boreosomus* [6, 12, 58, 68, 74, 79].

In Devonian actinopterygians and in †*Fukangichthys* and *Polypterus* the ceratohyal consists of a single ossification [12, 44, 79], but in †*Pteronisculus* and neopterygians there is a smaller posterior ceratohyal ossification [7, 9, 58, 98]. A groove for the afferent hyoidean artery is a plesiomorphic osteichthyan feature retained in many fossil actinopterygians like †*Raynerius*, †*Mimipiscis*, †*Moythomasia*, †*Pteronisculus*, †*Australosomus*, †*Fukangichthys* [44, 58, 59, 69]. It is absent in *Polypterus*, *Polyodon* and †*Chondrosteus* [11, 74, 79]. However, a shallow depression is seen in the

posterolateral half of the ceratohyal of *Acipenser* (TA pers. obs on *Acipenser*, UMMP unnumbered teaching collection specimen). †*Watsonulus* [98] also shows a groove, but this feature is absent in living holosteans and teleosts [7, 9].

Current knowledge about the fossil record of actinopterygian gill skeletons is limited, largely because such structures are rarely preserved, and, where present, are difficult to access without recourse to destructive methods (but see [121]). The overall anatomy of the †*Saurichthys* gill skeleton does not appear to differ significantly from that of generalized Permian–Triassic actinopterygians like †*Pteronisculus* [58]. A ventral gill skeleton of a †saurichthyid from Spitsbergen, figured by Stensiö ([29]: Pl. 7), preserves four ceratobranchials. Stensiö's reconstruction ([29], fig. 26), however, depicts five ceratobranchials, but no further evidence was provided. Five ceratobranchials are primitively present in actinopterygians, with the fifth being usually less well-developed [44, 58, 69]. Cladistians have only four gill arches, missing the fifth arch completely [122], which is likely an apomorphic feature of the clade, inclusive of †*Fukangichthys* [12].

The morphology of most branchial elements is slightly modified in †*Saurichthys*, becoming more elongate, straight and more slender, to follow the pattern of cranial elongation seen in the clade. In †*Pteronisculus*, there is an expanded infrapharyngobranchial, suspending the third and fourth branchial arches [58]. In †*Mimipiscis* the hypobranchials are proximally perforated [44], but this feature was not observed in other actinopterygians like †*Raynerius* [69] or †*Saurichthys*. The hypobranchials of †*Saurichthys* form a single, median articulation with the corresponding basibranchial elements and show no ventromedial processes, like those present in the second and third hypobranchials of *Amia* and other neopterygians [7, 71] (TA pers. obs. on *Amia calva*, UMMP unnumbered teaching collection specimen).

The ventral branchial skeleton of †*Saurichthys ornatus* from Spitsbergen exhibits three distinct basibranchial ossifications [29]. Only a single basibranchial is preserved in the Greenland †*Saurichthys*, but is dorsally displaced and is anteroposteriorly short and bears no lateral ossification surfaces for the hypobranchials, differing from the massive, single basibranchial copula of Devonian actinopterygians [44, 69], and *Polypterus* [79]. †Saurichthyids seem to bear three basibranchial ossifications [29] like †*Pteronisculus* [58]. At least two basibranchials are present in '†*Elonichthys*' [123], and two basibranchials were described in †*Funkangichthys* [12]. †*Australosomus* exhibits four basibranchial ossifications, with the posterior-most basibranchial being longitudinally

pierced by a paired canal for the fourth afferent branchial arteries [59]. Living chondrosteans have no ossifications in their ventral gill skeleton. Instead, there is an enlarged, cartilaginous anterior basibranchial that articulates with hypobranchials 1–3, and a posterior cartilaginous basibranchial that articulates with the fourth hypobranchials [6, 74]. However, there is considerable variation within sturgeons, and one or two additional basibranchial cartilages might be present in some individuals [74]. In *Amia,* only the posterior part of the anterior basibranchial ossifies, while the two posterior basibranchials remain cartilaginous [7]. Two basibranchials are present in *Lepisosteus*, with only the anterior part of the second basibranchial known to ossify [9]. The basibranchial series of teleosteans comprise between three and five distinct ossifications [124].

Dermal bones of the pectoral girdle

Only two elements of the pectoral girdle are preserved in the Greenland †*Saurichthys*, both disarticulated from their adjacent bones and dislocated from their life position. Posterodorsally there is an angled, anamestic dermal element (Fig. 1C,E, 2C,E: 'pt-sc'). This bone forms an unornamented anteriorly–anteromedially expanding process and a lateroventrally–ventrally expanding lamina, which bears tubercles. A clavicle ('clav') is preserved ventrally, and has been displaced to punch through the gill skeleton. It is thin, with an elongate triangular shape, pointing anteriorly, and is strongly convex laterally. Its mesial surface is slightly thickened and was likely abutting its antimere in life.

Remarks In Early Triassic †saurichthyids and in †*Yelangichthys* there are two canal-bearing, dermal bones, the posttemporal and the supracleithrum, connecting the cleithrum with the skull [25, 29, 32]. The arched bone in NHMD_157546_A resembles the compound posttemporal-supracleithrum of Middle Triassic †saurichthyids [23, 30], however the latter bone is always canal-bearing. The absence of a canal in NHMD_157546_A could either be a peculiarity of the specimen/species, or could imply that a presupracleithrum is present. The latter ossification is absent or unknown in most †saurichthyids, but has been tentatively reconstructed in the anisian species †*Sinosaurichthys longimedialis* [30]. Well-developed triangular clavicles are typically present in all non-neopterygian actinopterygians (e.g., [6, 44, 58, 59, 74, 80]), and also in some early neopterygians such as †*Watsonulus* [98]. Clavicles become much reduced or lost in holosteans and early teleosteans [7, 9, 102, 125].

Systematic Paleontology

†*Saurichthys nepalensis* Beltan and Janvier 1978 [126]

Material

MNHN F 1980-5, †*Saurichthys nepalensis*, partial skull.

Fossil age and locality information

Fossil fishes from the Lower Triassic of the Himalayas are rare and poorly known [14, 126, 127]. The Early Triassic deposits of the Annapurna, Nepal have only produced a single actinopterygian fossil (MNHN F 1980-5): the holotype of †*Saurichthys nepalensis* [126]. The skull was found as in the Thini Gaon area, but was lying amongst debris and the precise geological horizon remains unknown. The surrounding matrix was tentatively correlated, on the basis of lithological similarities, with lowest Triassic ('lower Scythian'; ~251 Ma) ammonoid-bearing facies that occur in the area [126]. Additional details of Triassic stratigraphy of the Annapurna, including Thini Gaon, are given by Garzanti et al. [128]. The holotype of †*S. nepalensis* corresponds to a fragmented skull, preserving only the anterior orbital region and the posterior rostroethmoidal region. During preparation for the initial description, the skull was immersed in 5% formic acid [126]. Although this procedure damaged the specimen, the almost complete removal of the matrix resulted in excellent contrast using μCT.

Anatomical description

Ethmoidal region

The ethmoidal region of †*Saurichthys nepalensis* (MNHN F 1980-5; Fig. 14) differs in some respects from that of the Greenland †*Saurichthys* (NHMD_157546_A). More specifically, in †*S. nepalensis*, the interorbital septum is not ossified along the course of the olfactory tracts, although this may well be an artefact of preservation or preparation. The interorbital fenestra is much smaller and kidney-shaped, rather than oval. The anteroventral myodome is paired and not median. The remainder of the ethmoidal region is otherwise very similar to that of NHMD_157546_A. In terms of internal anatomy (Fig. 14E–H), the olfactory lobes ('I') diverge laterally towards the external nares, upon entering the ethmoidal region. They give off multiple branches that connect with the nasal cavities and openings

('nao'). At the level of the posterior tip of the nasal cavity, each dorsal-most branch receives a canal of posterodorsal origin, which must have carried the superficial opthalmic nerve ('Vopts'). Two to three thicker branches on each side, including the ones carrying the latter nerve, continue anteriorly past the nasal cavity, to form the nasobasal canals ('nbc'). These canals continue anteriorly along the preserved length of the rostrum. They connect with a lateral groove for the maxillary ramus of the trigeminal nerve ('Vmx') via a canal, slightly anterior to the nasal cavities. At the same point, a canal leading to the floor of the ethmoidal region branches off ('paop'). More anteriorly, the nasobasal canals extend gradually to the laterodorsal surface of the braincase, but appear to be contained within the dermal bones without connecting to the lateral surface of the skull.

Remarks Primitively, in most fossil non-neopterygian actinopterygians, but also in †parasemionotids, and †caturids, there are two paired anterior myodomes (dorsal and ventral) notching the posterior wall of the ethmoidal region [44, 58, 63, 66, 98]. In †*Lawrenciella* and †*Kansasiella*, there is a paired anterodorsal myodome, but the anteroventral myodome is median and situated on the interorbital septum [65, 67], as in †*Saurichthys nepalensis*. The aforementioned conditions are likely dependent on the development of the interorbital septum and the orbit. We consider the anterodorsal and anteroventral myodomes, paired or median, to be homologous across taxa. The fenestrations present on the anterior part of the interorbital septum of the Greenland †*Saurichthys* are therefore deemed homologous to the anterodorsal and anteroventral myodomes of most fossil actinopterygians. †*Yelangichthys* exhibits paired anterodorsal and anteroventral myodomes [32], and this may correspond to the primitive condition for the group. Anterior myodomes are absent in acipenseriforms and lepisosteiforms, potentially due to the reduction in orbit size [63].

To date, the internal anatomy of the anterior ethmoidal region in fossil non-neopterygian actinopterygians is virtually unknown, as this region of the braincase is often not mineralized. The nasobasal canals of †*Saurichthys* correspond topologically to the the fenestrae exonarinae anterior in †*Youngolepis* [129] and the nasobasal canals of other Devonian sarcopterygians, such as †*Eusthenopteron* [85] and †*Gogonasus* [130], and to those tentatively reconstructed in †*Mimipiscis* [44]. In these taxa the nasobasal canals begin their course at the anterior margin of the nasal cavity. Actinopterygian nasobasal canals differ from the rostral tubules of sarcopterygians, as the latter issue posterior to the nasal cavities and form a mesially extending, web-like structure (e.g., [95, 131]). Although soft tissue contents remain unknown, the relationship of the nasobasal canals of †*Saurichthys* with branches of the trigeminal nerve, and their communication with the floor of the

rostrum, are indicative of at least gustatory functions. They must have also contained blood vessels supplying the growing rostrum. These canals are for the first time confidently reconstructed and described in †*Saurichthys*, or any other fossil actinopterygian.

Phylogenetic analysis

The maximum parsimony analysis produced, after the deletion of suboptimal trees, a total of 2430 most parsimonious trees (MPTs) of 1421 steps (C.I: 0.217, R.I: 0.645). In the strict consensus (Fig. 15A), Actinopterygii is monophyletic, but weakly supported (Bremer decay index [BDI]=2), with †*Meemania* and †cheirolepidids being successive sister groups to the remaining members of the group. †*Osorioicthys* and †*Tegeolepis* are resolved as a deeply diverging clade on the actinopterygian stem, followed by a clade formed by the remaining Devonian taxa (BDI=2). All post-Devonian actinopterygians form a clade (BDI=3), supported by 15 synapomorphies. Post-Devonian taxa are divided in two, albeit weakly supported clades. The first clade contains all Paleozoic-early Mesozoic anatomically generalized forms, whose monophyly is supported by characters that cannot be assessed in most taxa. †*Australosomus* is resolved as the sister taxon to the clade that contains †saurichthyiforms + †*Birgeria* and crown actinopterygians. The immediate sister group relationship between †saurichthyiforms + †*Birgeria* and the actinopterygian crown is supported by four common synapomorphies, none of which is unambiguous: i) absence of complete enclosure of spiracle by canal-bearing bones (C.68); ii) palatoquadrate forming separate ossifications (C.102); iii) absence of vestibular fontanelles (C.148); iv) dorsal aorta open in a groove (C.155); v) lateral dorsal aortae bifurcating below parasphenoid (C.159); vi) posterior stem of parasphenoid extending to basioccipital (C.177); vii) presence of an aortic notch in parasphenoid (C.184); viii) absence of a triradiate scapulocoracoid (C.244).

Our analyses recovered †saurichthyiforms (inclusive of †*Yelangichthys*) as a clade (BDI=2), with †*Yelangichthys* being the sistergroup to †saurichthyids, on the basis of: i) both nostrils accommodated within single ossification (C.21); ii) frontals broad posteriorly, but tapering anteriorly (C.31). Amongst †saurichthyids, †*Saurichthys madagascariensis* and NHMD_157546_A form a clade to the exclusion of †*Saurichthys ornatus*. †Saurichthyiforms cluster with †*Birgeria* (BDI=1), sharing the following characters: i) presence of more than two infraorbitals (C.53); ii) head of dermohyal projecting above opercle (C.66); iii) absence of peg-and-socket articulation on scales (C.213); iv) absence of an anterodorsal process on scales (C.215); v) absence of an anocleithrum (C.240). The placement of the

clade containing †saurichthyiforms and †birgeriids as sistergroup to the actinopterygian crown has very low nodal support (BDI=1).

Within the actinopterygian crowngroup, cladistians (†scanilepiforms + polypterids; see [12]) are resolved as sister to chondrosteans. This unusual, and poorly supported (BDI=1) topology is supported by six synapomorphies: i) presence of a posterior junction between supraorbital and infraorbital canals (C.34); ii) presence of a broad interorbital septum (C.130); iii) absence of a posterior myodome (C.139); iv) anterolaterally diverging olfactory lobes (C.186); v) absence of fringing fulcra (C.218); vi) hyomandibula imperforate (C.220). Chondrostei receive high nodal support (BDI≥6), but support for Cladistia is moderate (BDI=3). A number of Paleozoic–early Mesozoic taxa, most of which are deep-bodied, form branches at the base of the neopterygian stem. †*Platysomus* is the deepest-diverging taxon on the neopterygian stem (BDI=1), and is united with the remaining neopterygian total group by: i) premaxilla not contributing to the orbit (C.7); ii) quadrate parietals (C.29); iii) vertical preopercle (C.118); iv) presence of a basipterygoid process (C.142); v) absence of a buccohypophyseal canal (C.179). †*Peltopleurus*, †*Luganoia*, and †*Dipteronotus* form a clade at the neopterygian stem. The neopterygian crown is well supported (BDI≥6), on the basis of: i) maxillary kinesis (C.74); ii) peg-like process on maxilla (C.75); iii) subopercle forming anterodorsal process (C.115); iv) interopercle present (C.121); vi) internal carotids piercing parasphenoid (C.182). The interrelationships of crown neopterygians, however, are not clear due to the uncertain placement of †*Tetragonolepis*, †*Hulettia* and †dapediids relative to teleosts or holosteans.

Discussion

Phylogenetic position of †Saurichthyiformes and implications of new anatomical data.

The new anatomical features of the cranial endoskeleton of †*Saurichthys* described herein allow us to reconsider characters previously used to assess the relationships of the genus with other actinopterygians. †Saurichthyiforms exhibit a combination of primitive (e.g., contact of infraorbital and supraorbital canals between external nares; co-ossified neurocranium; craniospinal processes; dermohyal fused on hyomandibula; absence of an opercular process on hyomandibula) and derived (e.g., external elimination of the oticooccipital fissure; absence of an endoskeletal aortic canal; absence of vestibular fontanelles; absence of endoskeletal basipterygoid process; posterior elongation of parasphenoid; separate ossifications of palatoquadrate) characters, which collectively

indicate a close phylogenetic proximity to the base of the actinopterygian crown. †*Yelangichthys* is confirmed as a †saurichthyiform [32]. The recently proposed immediate sister-group relationship between †*Saurichthys* and crown actinopterygians [12] is favored in our analysis, although nodal support is very low. In contrast to the previous analysis [12], †saurichthyiforms and †*Birgeria* form a clade. Although the two taxa have been previously recovered in a clade [18], most phylogenies resolved †*Birgeria* as the most stemward member of Chondrostei [16, 19, 20, 32]. We note that the †*Birgeria* + †saurichthyiform relationship presented here is weakly supported, and could be challenged in the future. Amongst the key factors uniting the latter two groups are the absence of a peg-and-socket articulation and the absence of an anterodorsal process on scales. The endoskeletal anatomy of †*Birgeria* appears to be dissimilar to that of †*Saurichthys*, for example in the presence of an open oticooccipital fissure; the reduction of craniospinal processes; the absence of a dorsal fontanelle; and the apparent differentiation of braincase ossifications [59, 132].

Contrary to many previous analyses, we did not recover a close relationship between †saurichthyids and Chondrostei [16-19, 24, 29, 32], despite their broad similarity in neurocranial and dermal anatomy. Many of the characters uniting the two groups are now found to be widespread around the base of the actinopterygian crown (see above). In addition, other previously evoked similarities between the two groups can now be dismissed. †Saurichthyids were erroneously thought to share with acipenseriforms a rudimentary posttemporal fossa [16], but this feature is absent in both groups (as well as stem actinopterygians and polypterids). Our reinterpretation of the basicranial circulation pattern in †*Saurichthys* is also of particular importance. The common carotids are now shown to penetrate the parasphenoid posteroventrally to the ascending processes in †saurichthyids, and conceivably in †*Yelangichthys*, forming a complete circulus cephalicus and parabasal canals. These features were previously believed to be absent, as for acipenseriforms [16, 19, 29, 32]. We note the presence of a lateral cranial canal, suborbitals, fused dermohyals, and lateral gulars in Early Triassic †saurichthyids, all of which were previously coded as absent, favoring a chondrostean topology [16, 18, 19]. The presumed increased height and width of the ascending processes of the parasphenoid, and their broad overlap of the lateral commissure in †saurichthyids, †*Birgeria* and chondrosteans, were combined into a single character state in past analyses, setting them apart from the condition seen in taxa like *Amia*, or †*Pteronisculus* [16, 17, 19]. We found evidence to support a single character to capture these complex anatomies lacking, given the fact that acipenseriforms possess thin ascending processes [74, 84], reaching the spiracular opening like in many other stem and crown actinopterygians [7, 58, 59]. The dorsoventral extent of the ascending processes could be

of phylogenetic importance, but it remains difficult to assess in laterally-flattened fossils.

Despite the poorly supported tree topology, we observed some similarities between †saurichthyids and acipenseriforms, which appear as homoplasies in this study. Amongst these is the apparent functional resemblance of the tectosynotic fossa, which in both clades seems to perform the same function (attachment of hyoopercular and branchial musculature). We also noted the presence of intramural diverticula opening to the fossa bridgei in both taxa, though these features must have also been widespread in generalized actinopterygians [65]. These features could influence future phylogenies, when more neurocranial data from fossils become available. The reduction of the opercular bone and the corresponding process on the hyomandibula appear as homoplasies under our phylogenetic scheme. Other features, such as the absence of peg-and-socket articulation and the lack of an anterodorsal process on scales, appear as parallelisms between chondrosteans and †saurichthyids + †*Birgeria*, but these characters are difficult to assess in fossils.

Shape of the actinopterygian tree and directions for future research.

The interrelationships of Devonian actinopterygians remain unchanged from the latest analysis involving an previous version of this matrix [12]. †*Meemania* and †*Cheirolepis* are successively crownward members of the actinopterygian stem, an arrangement also well-established by other works (e.g., [3, 68, 69, 133]). The clustering of post-Devonian actinopterygians, albeit weakly supported, is congruent with Giles et al. [12] and might reflect a bottleneck in actinopterygian evolution related to the Hangenberg Event [134, 135], or simply a need to re-examine the anatomy of these taxa using modern investigative techniques. Our strict consensus exhibits a Carboniferous-Triassic generalized actinopterygian clade, though nodal support is very low.

The divergence age of crown actinopterygians appears congruent with the hypothesis of Giles et al. [12], as it only contains Carboniferous or younger taxa. However, in our phylogenetic hypothesis, the interrelationships of crown actinopterygians are rearranged. We recovered cladistians and chondrosteans as a clade, in spite of morphological [12, 16-20, 41, 44, 133], and strong molecular [4, 5, 136] evidence supporting cladistians as sister group to Actinopteri (the historical group containing chondrosteans and neopterygians to the exclusion of cladistians[41]). We note that our topology is weakly supported. Moreover, cladistians and chondrosteans constitute particularly long phylogenetic branches, lacking early representatives from the Paleozoic, or the Triassic, in the case

of the latter. Neurocranial data from early chondrosteans are almost absent [11, 118], and there is a considerable gap of knowledge related to the basicranial circulation, endocast and posterior neurocranial anatomy of early cladistians [12].

In contrast to Giles et al. [12], †*Platysomus* branches from the neopterygian, rather than the chondrostean stem, with other Paleozoic-Mesozoic deep-bodied taxa also branching deep on the neopterygian stem. †*Amphicentrum* forms a clade with the †styracopterids (see †eurynotiforms [120]), but this clade was previously found to branch outside the actinopterygian crown [12]. A close relationship between †eurynotiforms and other deep-bodied taxa is also implied by previous phylogenies [17, 20, 107, 112], but see [120]. However, these forms show conspicuous phylogenetic fluidity, alternating in positions amongst the actinopterygian, the chondrostean, and the neopterygian stem [12, 17, 20, 107, 112, 133, 137], and their endoskeletal anatomy requires investigation. Previous anatomical information for these forms is largely limited to homoplasic features of their external dermal skeleton [61, 119, 138, 139], with the exception of †*Amphicentrum* [64]. †*Peltopleurus*, †*Dipteronotus* and †*Luganoia* are consistently affiliated with the neopterygian stem [12, 17, 20, 137]. This longstanding hypothesis is also reflected in our trees. Endoskeletal data from stem neopterygians is limited [39, 63], but given their likely systematic position, such knowledge seems pivotal for understanding the early evolution of the neopterygian anatomy. The monophyly of the neopterygian crown and its immediate sister groups [12] remains unchallenged in our phylogenetic scheme, despite a loss of resolution within the crown.

Cranial fossae diagnosis, function and evolution in Actinopterygii

Cranial fossae, located on the occipital and otic regions of actinopterygian braincases, constitute important anatomical landmarks that convey both phylogenetic and functional signals. Despite this, the available terminology is not always established on a solid anatomical basis or homology, leading to the perplexing use of various terms in the literature, which in turn has affected the shape of published trees (see [16-18, 63, 93]). We hereby attempt a re-diagnosis of cranial fossae (Fig. 16), on the basis of their topology, function and their relationships with other cranial landmarks. The scheme presented herein should be treated as a working hypothesis.

Craniospinal fossa This term, coined here, refers to the paired fossae on the posterior surface of the craniospinal processes of most Paleozoic–early Mesozoic actinopterygians. These fossae are

confined within the occipital region and likely served for the origin of the first few epaxial muscle segments, as in acipenseriforms [73, 76]. In fossil forms with reduced or absent craniospinal processes, the trunk musculature must have attached to the otic region [59, 63], as in modern polypterids or neopterygians (e.g., [63, 70, 75, 81]). The craniospinal fossae of †*Saurichthys* and acipenseriforms have been previously homologized with the posttemporal fossae in the otic region of neopterygians [9, 16, 17, 32], solely on the basis of their function. However, the formation of the craniospinal fossa in the occipital region, and the posttemporal fossa in the otic region of actinopterygians, dispels any notion of homology between the two (see also [18]).

Tectosynotic fossa The anterior–anterolateral boundary of the tectosynotic fossa is always formed by the otic process of the posterior semicircular canal. However, given the differences in anatomy and orientation of this fossa among sarcopterygians and actinopterygians, as well as among different groups of actinopterygians, the tectosynotic fossa cannot be considered homologous across taxa. It still constitutes an important anatomical landmark, which can convey functional information. A tectosynotic fossa is present in Devonian sarcopterygians such as †*Eusthenopteron*, †*Youngolepis* and †*Diplocercides* (=†*Nesides*), where it likely accommodated epaxial muscles [85, 93, 129]. In chondrosteans, and likely in †*Saurichthys*, the latter fossa accommodates the poorly-differentiated dorsal hyoid and opercular retractors (the latter modified to attach to the subopercle), and the underlying branchial levators [73, 76, 77]. Due to the poor development of the otic process in *Acipenser*, the tectosynotic fossa contacts an anterolaterally situated fossa, which hosts part of the hyoid retractor muscle (Additional Fig. 3). The first epaxial muscle segments attach in a shallow topological equivalent of the tectosynotic fossa in polypterids and gars [75, 79, 81]. A very shallow, paired tectosynotic fossa in the otic region of *Amia*, mesial to the posterior semicircular canal, hosts epaxial muscle segments early in ontogeny, which later migrate to the posttemporal fossa [93]. A paired depression occupies a similar position in the posterodorsal part of the otic region in †*Lawrenciella*, †*Kansasiella* and †*Australosomus*, but is oriented towards the posterior dorsal fontanelle [59, 65, 67, 82] and it is, thus, unlikely to have served for muscle attachment.

Fossa bridgei Stensiö [29] coined the term fossa bridgei to describe a paired depression seen on the dorsal part of the braincase of living acipenseriforms, constrained by the planes of the three semicircular canals (Additional Fig. 3). He homologized it with the posteriorly opening depression seen in the posterodorsal otic region of †*Saurichthys*, a view which is accepted here (Figs. 3A,B, 4A,B, 5B). Stem osteichthyans and Devonian actinopterygians like †*Mimipiscis*, †*Moythomasia* and

†*Raynerius*, as well as polypterids, lack a fossa bridgei, as the dermal bones of the skull roof are firmly attached to the dorsal chondrocranium [44, 69, 79, 86]. A fossa bridgei is present in Carboniferous and younger actinopterygians [29, 58, 59, 63, 65, 67, 82], but in crown neopterygians it becomes confluent with the posttemporal fossa [63]. The absence of a fossa bridgei appears to be the primitive condition in Actinopterygii, but this fossa was secondarily lost in polypterids.

Posttemporal fossa This fossa in the otic region of neopterygians (e.g., in †*Dorsetichthys* or †caturids) is primitively delimited by the posterior and horizontal semicircular canals medioventrally, and the dermal skull roof laterally, whereas a bony wall separates it anteriorly from the fossa bridgei [63, 83]. The anterior expansion of the posttemporal fossa in other neopterygians (e.g., *Amia*) [63, 70], and likely also in †*Amphicentrum* [64], eliminated the wall separating it from the fossa bridgei, and the two fossae became confluent. This modification has been linked to the anterior expansion of the epaxial musculature [63].

Spiracular fossa This fossa (=anterior fossa bridgei [58]) lies anterolaterally to the fossa bridgei and contains the dorsal opening of the spiracular canal, and is present when the latter is developed. The spiracular fossa can be partially confluent with the fossa bridgei. Examples can be seen in †*Lawrenciella*, †*Pteronisculus*, †*Boreosomus*, †*Australosomus*, *Acipenser*, †*Dorsetichthys* and *Amia* [58, 59, 63, 67, 70].

Prespiracular fossa This term corresponds to a depression situated anteromedial to the spiracular fossa, on the postorbital process. It has only been described in †*Lawrenciella* [67, 82], but topologically equivalent depressions are also seen in the reconstructions of †*Boreosomus*, and putatively †*Pteronisculus* [58]. Its function is unknown, but this feature might prove to have phylogenetic value.

Hyoopercular retractor muscle origin The origins of the hyoopercular retractors and the branchial levator muscles of actinopterygians can often be identified in the form of fossae on the neurocranium. The hyoopercular fossae of most actinopterygians differ significantly from those of †*Saurichthys* and the acipenseriforms. In most Paleozoic–early Mesozoic actinopterygians such as †*Mimipiscis*, †*Moythomasia*, †*Raynerius*, †*Kentuckia*, †*Lawrenciella* and †*Australosomus*, the hyoid and opercular retractors, and potentially parts of the branchial levators, originated in a laterally-facing shallow fossa (=fossa parampullaris [93]) on the dorsolateral–lateral part of the otic region,

immediately posterodorsally to the hyomandibular facet, lateral to the posterior semicircular canal, and always dorsal to the jugular depression [44, 58, 67, 69, 78, 82]. The same arrangement was likely present in †*Kansasiella*, †*Pteronisculus* and †*Boreosomus*, but the origin of the hyoopercular constrictors is not well-delineated in these taxa [58, 65]. In modern acipenseriforms, a fossa situated lateral to the posterior semicircular canal hosts part of the hyoid constrictor [73, 76, 77] (Additional Fig. 3). The same fossa is putatively also developed in †*Saurichthys*, but in the latter it became confluent with the fossa bridgei. In *Polypterus*, the branchial levators attach to the lateral wall of the opisthotic ridge, though the hyoid and opercular retractors are accommodated in a fossa dorsal to the opisthotic ridge, shared between the opisthotic and the parietal [79]. In actinopterygians with a subvertical suspensorium, like †*Australosomus* and early neopterygians, the hyoid musculature migrated ventrally and was hosted in the subtemporal fossa, which, when developed, lies ventral to posteroventral to the hyomandibular facet [59, 63]. Given our phylogenetic scheme, this condition must have appeared more than once. The subtemporal fossa is not developed in *Amia*, but the hyoid retractor originates from a topologically homologous location on the lateral wall of the otic region [70, 85]. In gars, due to the peculiar morphology of the hyomandibula, the dorsal hyoid and opercular constrictors originate from the dorsal otic region [140].

Conclusions

The employment of μCT for the detailed study of three-dimensionally preserved crania of †*Saurichthys* cf. *ornatus* and †*S. nepalensis*, as well as a re-evalution of the dermal anatomy of other †saurichthyids, uncovered a large number of anatomical features (e.g., cryptic oticooccipital fissure; patterns of basicranial circulation; brain and inner ear endocast; nasobasal canals; fused dermohyal on hyomandibula; reduction of the opercle; identification of the subopercle as the principal component of the opercular series). New information from †saurichthyids, and modern sturgeons, allowed us to test their long-proposed affinities within a broad osteichthyan context. The historical chondrostean topology of †saurichthyiforms is not confirmed by our analyses. Instead, the latter cluster with †*Birgeria*, forming the immediate sister group to crown actinopterygians. However, given the low nodal support near the base of the actinopterygian crown, the recovered tree topology might be challenged by future discoveries. Still, †*Saurichthys*, which may now be considered as one of the very few Permian–Triassic ray-fins whose endoskeletal anatomy is known in sufficient detail, constitutes a valuable model for morphological comparison with not only other penecontemporaneous fossils, but also with recent taxa. The herein described character complex is essential for understanding

character transformations that characterize early members of the actinopterygian crowngroup.

The discrepancies between our interpretation, and those of previous workers [23, 29, 39], highlight the need for revision of many classical works of actinopterygian endoskeletal anatomy. The Permian–Triassic actinopterygian diversity, which is currently dominated by classical and largely authoritative interpretations of anatomy [29, 39, 58, 59, 63, 132, 141], is an ideal target for μCT-aided anatomical reinvestigations. Special emphasis should be given to systematically volatile forms like †*Birgeria*. As in the case of †*Saurichthys,* older interpretations are limited by the use of traditional methodologies. Future work and addition of new fossils is expected to help us achieve some better resolution of stem and early crown actinopterygian interrelationships. On a concluding note, we would like to stress the importance of directing future research efforts towards the detailed investigation of the endocranial anatomy (e.g., brain and osseus labyrinth endocast morphology) of extant taxa that remains surprisingly poorly known.

Institutional abbreviations

FMNH: Field Museum of Natural History, Chicago, Illinois, USA

MNHN: Muséum national d'Histoire naturelle, Paris, France

PIMUZ: Paleontological Institute and Museum of the University of Zurich, Zurich, Switzerland

UMMP: University of Michigan Museum of Paleontology, Ann Arbor, Michigan, USA

UMMZ: University of Michigan Museum of Zoology, Ann Arbor, Michigan, USA

NHMD: Natural History Museum of Denmark, University of Copenhagen, Copenhagen, Denmark.

Anatomical abbreviations

I, olfactory nerve; **II,** optic nerve; **III,** oculomotor nerve; **IV,** trochlear nerve; **V,** trigeminal nerve; **Vmand,** openings for mandibular canal; **Vmx,** maxillary ramus of trigeminal nerve; **Vopts,** superficial ophthalmic ramus of trigeminal nerve; **VI,** abducens nerve; **VII,** facial nerve; **VIIhm,** hyomandibular trunk of facial nerve; **IX,** glossopharyngeal nerve; **X,** vagus nerve; **aamp,** ampulla of anterior semicircular canal; **aci,** common branch of internal carotid artery; **acv,** anterior cerebral vein; **addf,**

mandibular adductor fossa; **ang,** angular; **aon,** aortic notch; **aorb,** orbital artery; **apal,** palatine artery; **aps,** pseudobranchial artery; **art,** articular; **asc,** anterior semicircular canal; **asp,** ascending process of parasphenoid; **au,** autopalatine; **auf,** autopalatine fossa; **aur,** cerebellar auricle; **bb,** bony bar (dorsum sellae); **bbr,** basibranchial; **bhc,** buccohypophyseal canal; **bhf,** buccohypophyseal opening; **cbr1,** ceratobranchial 1; **cbr2,** ceratobranchial 2; **cc,** crus communis; **ccar,** common carotid artery; **chy,** ceratohyal; **clav,** clavicle; **crsf,** craniospinal fossa; **crsp,** craniospinal process; **d,** dentary; **damy,** dorsal anterior myodome; **dhy,** dermohyal; **dlf,** likely origin of dilatator and/or hyomandibular protractor muscles; **dpal,** dermopalatine; **dpt,** dermopterotic; **dsph,** dermosphenotic; **ep,** epiphysis; **epi,** epibranchial; **epo?,** epiotic-like ossification; **eps,** efferent pseudobranchial artery; **exsc,** median extrascapular; **fb,** fossa bridgei; **fm,** foramen magnum; **fr,** frontal; **hamp,** ampulla of horizontal semicircular canal; **hh,** hypohyal; **hbr1,** hypobranchial 1; **hbr2,** hypobranchial 2; **hm,** hyomandibula; **hmf,** hyomandibular facet; **hpc,** hypophyseal chamber; **hsc,** horizontal semicircular canal; **hyp,** hypophyseal chamber; **ica,** ascending branch of internal carotid artery; **id,** intramural diverticulum; **io,** infraorbital; **ioc,** infraorbital canal; **iof,** interorbital fenestra; **ios,** interorbital septum; **jc,** jugular canal; **ju,** jugal; **jv,** jugular vein; **la,** lachrymal; **lacp,** potential origin of levator arcus palatine muscle; **latg,** lateral gular; **lcc,** lateral cranial canal; **mcv,** mid-cerebral vein; **mdc,** mandibular canal; **mk,** Meckel's cartilage; **mpt,** metapterygoid; **mx,** maxilla; **nao,** nasal opening; **n?,** putative dorsal ramus of IX or X; **nbc,** nasobasal canal; **nocc,** spinooccipital nerve; **nocc/aocc,** spinooccipital nerve or occipital artery; **not,** notochord; **nsao,** nasalo-antorbital; **occ,** occipital crest; **oph,** ophthalmic artery; **otp,** otic process; **pa,** parietal; **pals,** palatal shelf; **pamp,** ampulla of posterior semicircular canal; **paop,** palatal opening of nasobasal canals; **papl,** parietal pit line; **part,** prearticular; **partr,** prearticular ridge; **pbr,** pharyngobranchial; **pl?,** putative pit line on dermopterotic; **pmy,** posterior myodome; **pop,** preopercle; **popc,** preopercular canal; **porp,** postorbital process; **prof?,** putative course of profundus nerve; **psc,** posterior semicircular canal; **psp,** parasphenoid; **pspk,** parasphenoid keel; **pt-sc?,** putative posttemporal-supracleithrum; **q,** quadrate; **qj,** quadratojugal; **rbr,** branchiostegal ray; **rpmx,** rostropremaxilla; **sac,** saccular recess; **sang,** surangular; **sang?,** putative surangular; **scla,** sclera; **sclt,** sclerotic ring; **so,** suborbital; **soc,** (trace of) supraorbital canal; **sop,** subopercle; **spig,** spiracular groove; **supo,** supraorbital; **tel,** telencephalon; **tmpc,** temporal canal; **to,** optic tectum; **tsf,** tectosynotic fossa; **utr,** utricular recess; **vamy,** ventral anterior myodome; **vamy+prof?,** ventral anterior myodome and potential course of profundus nerve; **vl,** vagal lobe; **vo,** vomer.

Declarations

Ethics approval and consent to participate

Not applicable

Consent for publication

Not applicable

Availability of data and materials

Digital reconstructions (in .ply format) are available in Dryad (doi:10.5061/dryad.42qj362).

Competing interests

The authors declare that they have no competing interests

Funding

This research (study, data collection, analyses, interpretation and writing) was made possible by the P1ZHP3_168253 Swiss National Science Foundation doctoral mobility grant to T.A. The scanning costs of †*S. nepalensis* were covered by a SYNTHESYS-funded MNHN stay of I.K. in 2011. I.K.'s work was performed according to the Russian Government Program of Competitive Growth of Kazan Federal University. Data collection, analyses, interpretation and writing performed by S.G. were supported by a L'Oréal-UNESCO For Women in Science Fellowship and a Junior Research Fellowship from Christ Church, Oxford. Data collection, analyses, interpretation and writing performed by M. F. were supported by funds from the College of Literature, Science, and the Arts and the Department of Earth and Environmental Sciences, University of Michigan. The CTEES facility, where most of the scans were conducted, is supported by funds from the College of Literature, Science, and the Arts and the Department of Earth and Environmental Sciences, University of Michigan.

Authors' contributions

T.A. and C.R. designed the study. T.A. analyzed the µCT data, produced the digital models,

performed the analyses, created the figures and led the writing of this manuscript. S.G. scanned NHMD_157546_A, contributed to the analyses, the creation of figures, and produced the earlier, published, version of the phylogenetic matrix, which was modified by T.A. and S.G. I.K. provided the scan of MNHN F 1980-5. M.F. and M.S.-V. supervised this work. All authors were involved in the discussion and interpretation of the results, have contributed to the writing of the manuscript, and have read and approved the final version.

Acknowledgements

Kristian M. Gregersen and Bent E. K. Lindow (NHMD) greatly facilitated this study by loaning East Greenland material to T.A. The scan of †*S. nepalensis* was performed by Florent Goussard and colleagues (MNHN). Tiago Simões, Oksana Vernygora (both University of Alberta) and Gabriel Aguirre-Fernández (PIMUZ) are thanked for discussions on phylogenetics and the use of TNT. The Willi Hennig Society is thanked for making TNT available free of charge. Two anonymous reviewers and editor Diego Pol provided useful comments that enhanced the quality of this work.

Authors' information

[1]Palaeontological Institute and Museum, University of Zurich, Karl Schmid-Strasse 4, 8006 Zurich, Switzerland. [2]Department of Earth Sciences, University of Oxford, South Parks Road, Oxford, OX1 3AN, UK. [3]Museum of Paleontogy and Department of Earth and Environmental Sciences, University of Michigan, 1109 Geddes Ave, Ann Arbor, Michigan, 48109, USA. [4]TU Bergakademie Freiberg, Geological Institute, Dept. of Palaeontology, Bernhard-von-Cotta-Str. 2, 09599 Freiberg, Germany and Kazan Federal University, 18 Kremlyovskaya, Kazan 420008, Russia.

References

1. Nelson JS, Grande TC, Wilson MVH: Fishes of the world, 5th edn. Hoboken, New Jersey, USA: John Wiley & Sons, Inc.; 2016.
2. Zhu M, Zhao W, Jia L, Lu J, Qiao T, Qu Q: The oldest articulated osteichthyan reveals mosaic gnathostome characters. *Nature* 2009, 458(7237):469-474.
3. Lu J, Giles S, Friedman M, den Blaauwen Jan L, Zhu M: The Oldest Actinopterygian Highlights the Cryptic Early History of the Hyperdiverse Ray-Finned Fishes. *Current Biology* 2016, 26(12):1602-1608.
4. Betancur-R R, Broughton RE, Wiley EO, Carpenter K, López JA, Li C, Holcroft NI, Arcila D, Sanciangco M, Cureton Ii JC *et al*: The Tree of Life and a New Classification of Bony Fishes. *PLoS*

Currents 2013, 5:ecurrents.tol.53ba26640df26640ccaee26675bb26165c26648c26288.

5. Near TJ, Eytan RI, Dornburg A, Kuhn KL, Moore JA, Davis MP, Wainwright PC, Friedman M, Smith WL: Resolution of ray-finned fish phylogeny and timing of diversification. *Proceedings of the National Academy of Sciences* 2012, 109(34):13698-13703.

6. Grande L, Bemis W: Osteology and phylogenetic relationships of fossil and recent paddlefishes (Polyodontidae) with comments on the interrelationships of Acipenseriformes. *Society of Vertebrate Paleontology Memoir* 1991, 11(S1):1 - 121.

7. Grande L, Bemis WE: A Comprehensive Phylogenetic Study of Amiid Fishes (Amiidae) Based on Comparative Skeletal Anatomy. an Empirical Search for Interconnected Patterns of Natural History. *Journal of Vertebrate Paleontology* 1998, 18(sup001):1-696.

8. Otero O, Likius A, Vignaud P, Brunet M: A new polypterid fish: *Polypterus faraou* sp. nov. (Cladistia, Polypteridae) from the Late Miocene, Toros-Menalla, Chad. *Zoological Journal of the Linnean Society* 2006, 146(2):227-237.

9. Grande L: An empirical synthetic pattern study of gars (Lepisosteiformes) and closely related species, based mostly on skeletal anatomy: the resurrection of Holostei. *American Society of Ichthyologists and Herpetologists Special Publication 6 Copeia Suppl* 2010, 10(2A):871.

10. López-Arbarello A: Phylogenetic Interrelationships of Ginglymodian Fishes (Actinopterygii: Neopterygii). *PLoS ONE* 2012, 7(7):e39370.

11. Hilton EJ, Forey PL: Redescription of †*Chondrosteus acipenseroides* Egerton, 1858 (Acipenseriformes, †Chondrosteidae) from the Lower Lias of Lyme Regis (Dorset, England), with comments on the early evolution of sturgeons and paddlefishes. *Journal of Systematic Palaeontology* 2009, 7(04):427-453.

12. Giles S, Xu G-H, Near TJ, Friedman M: Early members of 'living fossil' lineage imply later origin of modern ray-finned fishes. *Nature* 2017, 549(7671):265-268.

13. Friedman M: The early evolution of ray-finned fishes. *Palaeontology* 2015, 58(2):213-228.

14. Romano C, Koot MB, Kogan I, Brayard A, Minikh AV, Brinkmann W, Bucher H, Kriwet J: Permian–Triassic Osteichthyes (bony fishes): diversity dynamics and body size evolution. *Biological Reviews* 2016, 91(1):106-147.

15. Sallan LC: Major issues in the origins of ray-finned fish (Actinopterygii) biodiversity. *Biological Reviews* 2014, 89(4):950-971.

16. Gardiner B, Schaeffer B, Masserie J: A review of the lower actinopterygian phylogeny. *Zoological Journal of the Linnean Society* 2005, 144:511 - 525.

17. Gardiner BG, Schaeffer B: Interrelationships of lower actinopterygian fishes. *Zoological Journal of the Linnean Society* 1989, 97(2):135-187.

18. Coates MI: Endocranial preservation of a Carboniferous actinopterygian from Lancashire, UK, and the interrelationships of primitive actinopterygians. *Philosophical Transactions of the Royal Society B: Biological Sciences* 1999, 354(1382):435-462.

19. Xu G-H, Gao K-Q: A new scanilepiform from the Lower Triassic of northern Gansu Province, China, and phylogenetic relationships of non-teleostean Actinopterygii. *Zoological Journal of the Linnean Society* 2011, 161(3):595-612.

20. Xu G-H, Gao K-Q, Finarelli JA: A revision of the Middle Triassic scanilepiform fish *Fukangichthys longidorsalis* from Xinjiang, China, with comments on the phylogeny of the Actinopteri. *Journal of Vertebrate Paleontology* 2014, 34(4):747-759.

21. Liu X, Wei F: A new saurichthyid from the Upper Permian of Zhejiang, China. *Vertebrata Palasiatica* 1988, 4:77-89 + I,II pls.

22. Maxwell EE, Stumpf S: Revision of *Saurorhynchus* (Actinopterygii: Saurichthyidae) from the Early Jurassic of England and Germany. *European Journal of Taxonomy* 2017, 321:1-29.

23. Rieppel O: Die Triasfauna der Tessiner Kalkalpen XXV: die Gattung *Saurichthys* (Pisces, Actinopterygii) aus der mittleren Trias des Monte San Giorgio, Kanton Tessin. *Schweizerische Paläontologische Abhandlungen* 1985, 108:1 - 103.

24. Rieppel O: A new species of the genus Saurichthys (Pisces: Actinopterygii) from the Middle Triassic of Monte San Giorgio (Switzerland), with comments on the phylogenetic interrelationships of the genus. *Palaeontographica Abt A* 1992, 221(1-3):63 - 94.

25. Kogan I, Romano C: Redescription of *Saurichthys madagascariensis* Piveteau, 1945 (Actinopterygii, Early Triassic), with implications for the early saurichthyid morphotype. *Journal of Vertebrate Paleontology* 2016, 36(4):e1151886.

26. Maxwell EE, Furrer H, Sanchez-Villagra MR: Exceptional fossil preservation demonstrates a new mode of axial skeleton elongation in early ray-finned fishes. *Nature Communications* 2013, 4:2570.

27. Maxwell EE, Romano C, Wu F, Furrer H: Two new species of *Saurichthys* (Actinopterygii: Saurichthyidae) from the Middle Triassic of Monte San Giorgio, Switzerland, with implications for character evolution in the genus. *Zoological Journal of the Linnean Society* 2015, 173(4):887-912.

28. Romano C, Kogan I, Jenks J, Jerjen I, Brinkmann W: *Saurichthys* and other fossil fishes from the late Smithian (Early Triassic) of Bear Lake County (Idaho, USA), with a discussion of saurichthyid palaeogeography and evolution. *Bulletin of Geosciences* 2012, 87(3):543-570.

29. Stensiö EA: Triassic fishes from Spitzbergen, vol. 2. Stockholm: Almqvist & Wiksells Boktryckeri-A.-B.; 1925.

30. Wu F, Sun Y, Xu G, Hao W, Jiang D: New saurichthyid actinopterygian fishes from the Anisian (Middle Triassic) of southwestern China. *Acta Palaeontologica Polonica* 2011, 56(3):581 - 614.

31. Agassiz L: Abgerissene Bemerkungen über fossile Fische. *Neues Jahrbuch für Mineralogie, Geognosie, Geologie und Petrefaktenkunde* 1834, 1834:379–390.

32. Wu F, Chang M-m, Sun Y, Xu G: A new saurichthyiform (Actinopterygii) with a crushing feeding mechanism from the Middle Triassic of Guizhou (China). *PloS one* 2013, 8(12):e81010.

33. Bürgin T: Reproduction in Middle Triassic actinopterygians; complex fin structures and evidence of viviparity in fossil fishes. *Zoological Journal of the Linnean Society* 1990, 100(4):379-391.

34. Renesto S, Stockar R: Exceptional preservation of embryos in the actinopterygian *Saurichthys* from the Middle Triassic of Monte San Giorgio, Switzerland. *Swiss Journal of Geosciences* 2009, 102(2):323-330.

35. Maxwell EE, Argyriou T, Stockar R, Furrer H: Re-evaluation of the ontogeny and reproductive biology of the Triassic fish *Saurichthys* (Actinopterygii, Saurichthyidae). *Palaeontology* 2018.

36. Wu F-X, Sun Y-L, Hao W-C, Jiang D-Y, Sun Z-Y: A new species of *Saurichthys* (Actinopterygii; Saurichthyiformes) from the Middle Triassic of southwestern China, with remarks on pattern of the axial skeleton of saurichthyid fishes. *Neues Jahrbuch für Geologie und Paläontologie - Abhandlungen* 2015, 275(3):249-267.

37. Kogan I, Pacholak S, Licht M, Schneider JW, Brücker C, Brandt S: The invisible fish: hydrodynamic constraints for predator-prey interaction in fossil fish *Saurichthys* compared to recent actinopterygians. *Biology Open* 2015.

38. Argyriou T, Clauss M, Maxwell EE, Furrer H, Sánchez-Villagra MR: Exceptional preservation reveals gastrointestinal anatomy and evolution in early actinopterygian fishes. *Scientific Reports* 2016, 6:18758.

39. Beltan L: La faune ichthyologique de l'Eotrias du N.W. Madagascar: le neurocrâne. *Cahiers de paléontology* 1968:7-135+131-135+I-Lpl.

40. Lehman JP: Etude complémentaire des poissons de l'Eotrias de Madagascar. *Kungliga Svenska Vetenskapsakademiens Handlingar* 1952, 2(6):1-201+201-248pl.

41. Patterson C: Morphology and Interrelationships of Primitive Actinopterygian Fishes. *American Zoologist* 1982, 22(2):241-259.

42. Bemis WE, Findeis EK, Grande L: An overview of Acipenseriformes. *Environ Biol Fish* 1997, 48:25-71.

43. Patterson C, Rosen DE: Review of ichthyodectiform and other Mesozoic teleost fishes and the theory and practice of classifying fossils. *Bulletin of the American Museum of Natural History* 1977, 158(2):81-172.

44. Gardiner BG: The relationships of the palaeoniscid fishes, a review based on new specimens of *Mimia* and *Moythomasia* from the Upper Devonian of Western Australia. *Bulletin of the British Museum (Natural History), Geology series* 1984, 37(4):173-428.

45. Maddison W, Maddison D: Mesquite: a modular system for evolutionary analysis. In., 3.31 edn; 2017.

46. Romano C: A redescription and a new Reconstruction of *Birgeria stensioei* ALDINGER 1931 (Birgeriidae, Actinopterygii) from the Middle Triassic of Monte San Giorgio (Canton Ticino, Switzerland) with comments on its ontogeny and the interrelationships of the genus *Birgeria* STENSIÖ 1919. Paläontologisches Institut und Museum, Universität Zürich; 2007.

47. Romano C, Brinkmann W: Reappraisal of the lower actinopterygian *Birgeria stensioei* Aldinger, 1931 (Osteichthyes; Birgeriidae) from the Middle Triassic of Monte San Giorgio (Switzerland) and Besano (Italy). *Neues Jahrbuch für Geologie und Paläontologie - Abhandlungen* 2009, 252(1):17-31.

48. Goloboff PA, Farris JS, Nixon KC: TNT, a free program for phylogenetic analysis. *Cladistics* 2008, 24(5):774-786.

49. Simões TR, Caldwell MW, Kellner AWA: A new Early Cretaceous lizard species from Brazil, and the phylogenetic position of the oldest known South American squamates. *Journal of Systematic Palaeontology* 2015, 13(7):601-614.

50. Cope ED: Zittel's Manual of Palaeontology. *American Naturalist* 1887, 21:1014–1019.

51. Rosen DE, Forey PL, Gardiner BG, Patterson C: Lungfishes, tetrapods, paleontology, and plesiomorphy. *Bulletin of the American Museum of Natural History* 1981, 167(4):159-275.

52. Aldinger H: Permische Ganoidfische aus Östgrönland. *Meddelelser om Grønland* 1937, 102(3):1-392 + 344 tabs.

53. Owen R: Palaeontology or a systematic summary of extinct animals and their geological relations. Edinburgh: A. and C. Black; 1860.

54. Mutter RJ, Cartanyà J, Basaraba SA: New evidence of Saurichthys from the Lower Triassic with an evaluation of early saurichthyid diversity. In: *Mesozoic fishes.* Edited by Arratia G, Schultze H-P, Wilson M, vol. 4. München: Verlag Dr. Friedrich Pfeil; 2008: 103-127.

55. Bjerager M, Seidler L, Stemmerik L, Surlyk F: Ammonoid stratigraphy and sedimentary evolution across the Permian–Triassic boundary in East Greenland. *Geological Magazine* 2006, 143(5):635-656.

56. Nielsen E: The Permian and Eotriassic vertebrate-bearing beds at Godthaab Gulf (East Greenland), vol. 98. Copenhagen: C. A. Reitzels Forlag; 1935.

57. Nielsen E: Some few preliminary remarks on Triassic fishes from East Greenland, vol. 112. Copenhagen: C. A. Reitzels Forlag; 1936.

58. Nielsen E: Studies on the Triassic fishes from East Greenland I. *Glaucolepis* and *Boreosomus*. Copenhagen: C.A. Reitzels; 1942.

59. Nielsen E: Studies on Triassic fishes II. *Australosomus* and *Birgeria*, vol. 3. Copenhagen: Universitetets zoologiske museum og universitetes mineralogisk-geologiske museum; 1949.

60. Nielsen E: On the Eotriassic fish faunas of central East Greenland. In: *Geology of the Arctic.* Edited by Raasch GO, vol. 1. Toronto: University of Toronto press; 1961: 255-257.

61. Stensiö EA: Triassic fishes from East Greenland, vol. 83. Copenhagen: Bianco Lunos Bogtrykkeri A/S; 1932.

62. Kogan I: Remains of *Saurichthys* (Pisces, Actinopterygii) from the Early Triassic Wordie Creek Formation of East Greenland. *Bulletin of the Geological society of Denmark* 2011, 59:93-100.

63. Patterson C: The braincase of Pholidophorid and Leptolepid fishes, with a review of the Actinopterygian braincase. *Philosophical Transactions of the Royal Society of London B, Biological Sciences* 1975, 269(899):275-579.

64. Bradley-Dyne M: The skull of *Amphicentrum granulosum*. *Journal of Zoology* 1939, 109(2):195-210.

65. Poplin C: Étude de quelques paléoniscidés pennsylvaniens du Kansas. *Cahiers de paléontology* 1974:1-148+I-XL pl.

66. Poplin C, Véran M: A revision of the actinopterygian fish *Coccocephalus wildi* from the Upper Carboniferous of Lancashire. *Special Papers in Palaeontology* 1996, 52:7-30.

67. Hamel M-H, Poplin C: The braincase anatomy of *Lawrenciella schaefferi*, actinopterygian from the Upper Carboniferous of Kansas (USA). *Journal of Vertebrate Paleontology* 2008, 28(4):989-1006.

68. Giles S, Coates MI, Garwood RJ, Brazeau MD, Atwood R, Johanson Z, Friedman M: Endoskeletal structure in *Cheirolepis* (Osteichthyes, Actinopterygii), An early ray-finned fish. *Palaeontology* 2015, 58(5):849-870.

69. Giles S, Darras L, Clément G, Blieck A, Friedman M: An exceptionally preserved Late Devonian actinopterygian provides a new model for primitive cranial anatomy in ray-finned fishes. *Proceedings of the Royal Society of London B: Biological Sciences* 2015, 282(1816).

70. Allis EP: The cranial muscles and cranial and first spinal nerves in *Amia calva*. *Journal of Morphology* 1897, 7(3):487-809.

71. Allis EP: The skull, and the cranial and first spinal muscles of and nerves in *Scomber*. *Journal of Morphology* 1903, 18(2):45-329.

72. Danforth CH: The heart and arteries of *Polyodon*. *Journal of morphology* 1912, 23(3):409-454.

73. Marinelli W, Strenger A: Vergleichende Anatomie und Morphologie der Wirbeltiere. IV. Lieferung. Wien: Franz Deuticke; 1973.

74. Hilton E, Grande L, Bemis W: Skeletal anatomy of the shortnose sturgeon *Acipenser brevirostrum* Lesueur, 1818, and the systematics of sturgeons (Acipenseriformes, Acipenseridae). *Fieldiana: Life and Earth Sciences* 2011, 3:1 - 168.

75. Britz R, Johnson GD: Occipito-vertebral fusion in actinopterygians: conjecture, myth and reality. Part 1: Non-teleosts. In: *Origin and phylogenetic interrelationships of teleosts.* Edited by Nelson JS, Schultze HP, Wilson MVH. Munich: Dr. Friedrich Pfeil; 2010: 77-93.

76. Danforth CH: The myology of *Polyodon*. *Journal of Morphology* 1913, 24(1):107-146.

77. Edgeworth FH: The cranial muscles of vertebrates: Cambridge University Press; 1935.

78. Rayner DH: III.—On the Cranial Structure of an Early Palæoniscid, *Kentuckia*, gen. nov. *Transactions of the Royal Society of Edinburgh* 1952, 62(1):53-83.

79. Allis EP: The Cranial Anatomy of *Polypterus*, with Special Reference to *Polypterus bichir*. *Journal of Anatomy* 1922, 56(Pt 3-4):189-294.143.

80. Jollie M: Development of the head and pectoral skeleton of *Polypterus* with a note on scales (Pisces: Actinopterygii). *Journal of Zoology* 1984, 204(4):469-507.

81. Claeson KM, Hagadorn JW: The occipital region in the basal bony fish *Erpetoichthys calabaricus* (Actinopterygii: Cladistia). *Journal of Fish Biology* 2008, 73(4):1075-1082.

82. Pradel A, Maisey JG, Mapes RH, Kruta I: First evidence of an intercalar bone in the braincase of "palaeonisciform" actinopterygians, with a virtual reconstruction of a new braincase of *Lawrenciella* Poplin, 1984 from the Carboniferous of Oklahoma. *Geodiversitas* 2016, 38(4):489-504.

83. Rayner DH: The structure of certain Jurassic holostean fishes with special reference to their neurocrania. *Philosophical Transactions of the Royal Society of London Series B, Biological Sciences* 1948, 233(601):287-345.

84. Bridge TW: On the osteology of *Polyodon folium*. *Philosophical Transactions of the Royal Society of London* 1878, 169:683-733.

85. Jarvik E: Basic structure and evolution of vertebrates, vol. 1. London: Academic Press; 1980.

86. Basden AM, Young GC: A primitive actinopterygian neurocranium from the Early Devonian of Southeastern Australia. *Journal of Vertebrate Paleontology* 2001, 21(4):754-766.

87. Giles S, Friedman M: Virtual reconstruction of endocast anatomy in early ray-finned fishes (Osteichthyes, Actinopterygii). *Journal of Paleontology* 2014, 88(4):636-651.

88. Kotrschal K, Van Staaden MJ, Huber R: Fish Brains: Evolution and Environmental Relationships. *Reviews in Fish Biology and Fisheries* 1998, 8(4):373-408.

89. Bjerring HC: Two Intracranial Ligaments Supporting the Brain of the Brachiopterygian Fish Polypterus senegalus. *Acta Zoologica* 1991, 72(1):41-47.

90. Werneburg R, Kogan I, Sell J: *Saurichthys* (Pisces: Actinopterygii) aus dem Buntsandstein des Germanischen Beckens. *Semana* 2014, 29:3-35.

91. Giles S, Rogers M, Friedman M: Bony labyrinth morphology in early neopterygian fishes (Actinopterygii: Neopterygii). *Journal of Morphology* 2016:n/a-n/a.

92. Clement AM, Nysjö J, Strand R, Ahlberg PE: Brain – Endocast Relationship in the Australian Lungfish, *Neoceratodus forsteri*, Elucidated from Tomographic Data (Sarcopterygii: Dipnoi). *PLoS ONE* 2015, 10(10):e0141277.

93. Bjerring HC: The Term 'Fossa Bridgei' and Five Endocranial Fossae in Teleostome Fishes. *Zoologica Scripta* 1984, 13(3):231-238.

94. Nieuwenhuys R: An Overview of the Organization of the Brain of Actinopterygian Fishes. *American Zoologist* 1982, 22(2):287-310.

95. Lu J, Zhu M, Ahlberg PE, Qiao T, Zhu Ya, Zhao W, Jia L: A Devonian predatory fish provides insights into the early evolution of modern sarcopterygians. *Science Advances* 2016, 2(6).

96. Long J: New palaeoniscoid fishes from the Late Devonian and Early Carboniferous of Victoria. *Memoirs of the Association of Australasian Palaeontologists* 1988, 7:1-64.

97. Coates MI: Actinopterygians from the Namurian of Bearsden, Scotland, with comments on early actinopterygian neurocrania. *Zoological Journal of the Linnean Society* 1998, 122(1-2):27-59.

98. Olsen PE: The skull and pectoral girdle of the parasemionotid fish *Watsonulus eugnathoides* from the Early Triassic Sakamena Group of Madagascar, with comments on the relationships of the holostean fishes. *Journal of Vertebrate Paleontology* 1984, 4(3):481-499.

99. Watson DMS: On some Points in the Structure of Palæoniscid and allied Fish. *Proceedings of the Zoological Society of London* 1928, 98(1):49-70.

100. Stamberg S: Actinopterygians of the central bohemian Carboniferous basins. *Acta Musei Nationalis Pragae B, Hist naturalis* 1991, 47(1-4):25-104 + I-XXIV pl.

101. Bürgin T: Basal ray-finned fishes (Osteichthyes; Actinopterygii) from the Middle Triassix of Monte San Giorgio (Canton Tessin, Switzerland). *Schweizerische Paläontologische Abhandlungen* 1992, 114:1-164.

102. Arratia G: Morphology, taxonomy, and phylogeny of Triassic pholidophorid fishes (Actinopterygii, Teleostei). *Journal of Vertebrate Paleontology* 2013, 33(sup1):1-138.

103. Pearson DM, Westoll TS: The Devonian actinopterygian *Cheirolepis* Agassiz. *Earth and Environmental Science Transactions of the Royal Society of Edinburgh* 1979, 70(13-14):337-399.

104. Arratia G, Schultze H-P: Palatoquadrate and its ossifications: Development and homology within osteichthyans. *Journal of Morphology* 1991, 208(1):1-81.

105. Arratia G, Cloutier R: Reassessment of the morphology of *Cheirolepis canadensis* (Actinopterygii). In: *Devonian Fishes and Plants of Miguasha, Quebec, Canada.* Edited by Schultze H-P. München: Verlag Dr. Friedrich Pfeil; 1996: 165-197.

106. Lund R, Poplin C: The rhadinichthyids (paleoniscoid actinopterygians) from the Bear Gulch Limestone of Montana (USA, Lower Carboniferous). *Journal of Vertebrate Paleontology* 1997, 17(3):466-486.

107. Mickle KE, Lund R, Grogan ED: Three new palaeoniscoid fishes from the Bear Gulch Limestone (Serpukhovian, Mississippian) of Montana (USA) and the relationships of lower actinopterygians. *Geodiversitas* 2009, 31(3):623-668.

108. Poplin C, Lund R: Two Carboniferous fine-eyed palaeoniscoids (Pisces, Actinopterygii) from Bear Gulch (USA). *Journal of Paleontology* 2002, 76(6):1014-1028.

109. Marramà G, Lombardo C, Tintori A, Carnevale G: Redescription of '*Perleidus*' (Osteichthyes, Actinopterygii) from the Early Triassic of Northwestern Madagascar. *Rivista Italiana di Paleontologia e Stratigrafia* 2017, 123(2):219-242.

110. Gardiner BG: A revision of certain actinopterygian and coelacanth fishes, chiefly from the Lower Lias. *Geology* 1960, 4(7):241–384.

111. Griffith J, Patterson C: The structure and relationships of the Jurassic fish *Ichthyokentema purbeckensis*. *Bulletin of the British Museum (Natural History), Geology series* 1963, 8(1):1-43 + 44pl.

112. Lund R: The new actinopterygian order Guildayichthyiformes from the Lower Carboniferous of Montana (USA). *Geodiversitas* 2000, 22(2):171-206.

113. Taverne L: *Osorioichthys marginis*,''paléonisciforme''du Famennien de Belgique, et la phylogénie des Actinoptérygiens dévoniens (Pisces). *Bulletin de l'institut Royal des Sciences Naturelles de Belgique* 1997, 67:57-78.

114. Poplin C, Lund R: Two new deep-bodied palaeoniscoid actinopterygians from Bear Gulch (montana, USA, Lower Carboniferous). *Journal of Vertebrate Paleontology* 2000, 20(3):428-449.

115. Choo B, Long JA, Trinajstic K: A new genus and species of basal actinopterygian fish from the Upper Devonian Gogo Formation of Western Australia. *Acta Zoologica* 2009, 90:194-210.

116. Germain D, Meunier FJ: Teeth of extant Polypteridae and Amiidae have plicidentine organization. *Acta Zoologica* 2017:1-7.

117. Wilson L, Furrer H, Stockar R, Sanchez-Villagra M: A quantitative evaluation of evolutionary patterns in opercle bone shape in *Saurichthys* (Actinopterygii: Saurichthyidae). *Palaeontology* 2013, 56(4):901 - 915.

118. Grande L, Bemis WE: Interrelationships of Acipenseriformes, with comments on "Chondrostei". In: *In Interrelationships of Fishes.* Edited by Stiassny M, Parenti L, Johnson GD: Academic Press; 1996: 85-115.

119. Moy-Thomas JA, Dyne MB: XVII.—The Actinopterygian Fishes from the Lower Carboniferous of Glencartholm, Eskdale, Dumfriesshire. *Transactions of the Royal Society of Edinburgh* 1938, 59(2):437-480.

120. Sallan LC, Coates MI: Styracopterid (Actinopterygii) ontogeny and the multiple origins of post-Hangenberg deep-bodied fishes. *Zoological Journal of the Linnean Society* 2013, 169(1):156-199.

121. Beckett H, Giles S, Friedman M: Comparative anatomy of the gill skeleton of fossil Aulopiformes (Teleostei: Eurypterygii). *Journal of Systematic Palaeontology* 2017:1-25.

122. Britz R, Johnson GD: On the homology of the posteriormost gill arch in polypterids (Cladistia, Actinopterygii). *Zoological Journal of the Linnean Society* 2003, 138(4):495-503.

123. Watson DMS: The Structure of Certain Palæoniscids and the Relationships of that Group with other Bony Fish. *Proceedings of the Zoological Society of London* 1925, 95(3):815-870.

124. Nelson GJ: Gill arches and the phylogeny of fishes, with notes on the classification of vertebrates. *Bulletin of the American Museum of Natural History* 1969, 141(4):475-552 + 479-492pl.

125. Olsen PE, McCune AR: Morphology of the *Semionotus elegans* species group from the Early Jurassic part of the Newark Supergroup of eastern North America with comments on the Family Semionotidae (Neopterygii). *Journal of Vertebrate Paleontology* 1991, 11(3):269-292.

126. Beltan L, Janvier P: Un nouveau Saurichthyidae (Pisces, Actinopterygii), *Saurichthys nepalensis* n. sp. du Trias inférieure des Annapurnas (Thakkhola, Nepal) et sa significations paléobiogéographique. *Cybium* 1978, 4:17-28.

127. Romano C, Ware D, Brühwiler T, Bucher H, Brinkmann W: Marine Early Triassic Osteichthyes from Spiti, Indian Himalayas. *Swiss Journal of Palaeontology* 2016, 135(2):275-294.

128. Garzanti E, Nicora A, Tintori A: Triassic stratigraphy and sedimentary evolution of the Annapurna Tethys Himalaya (Manang area, central Nepal). *Rivista Italiana di Paleontologia e Stratigrafia* 1994, 100(2):195-226 + 193 tabs.

129. Chang MM: The braincase of *Youngolepis*, a Lower Devonian crossopterygian from Yunnan, south-western China. Stockholm; 1982.

130. Holland T: The endocranial anatomy of *Gogonasus andrewsae* Long, 1985 revealed through micro CT-scanning. *Earth and Environmental Science Transactions of the Royal Society of Edinburgh* 2014, 105(1):9-34.

131. Campbell K, Barwick R, Senden T: Perforations and tubules in the snout region of Devonian dipnoans. In: *Morphology, Phylogeny and Paleobiogeography of Fossil Fishes.* Edited by Elliott DK, Maisey JG, Yu X, Miao D: Verlag Dr Friedrich Pfeil; 2010: 325–361.

132. Stensiö EA: Triassic fishes from Spitzbergen (Part 1). Vienna: Adolf Holzhausen; 1921.

133. Cloutier R, Arratia G: Early diversification of actinopterygians. In: *Recent advances in the origin and early radiation of vertebrates.* Edited by Arratia G, Wilson MVH, Cloutier R. München, Germany: Dr. Friedrich Pfeil; 2004: 217-270.

134. Sallan LC, Coates MI: End-Devonian extinction and a bottleneck in the early evolution of modern jawed vertebrates. *Proceedings of the National Academy of Sciences* 2010, 107(22):10131-10135.

135. Friedman M, Sallan LC: Five hundred million years of extinction and recovery: a phanerozoic survey of large-scale diversity patterns in fishes. *Palaeontology* 2012, 55(4):707-742.

136. Broughton RE, Betancur-R R, Li C, Arratia G, Ortí G: Multi-locus phylogenetic analysis reveals the pattern and tempo of bony fish evolution. *PLoS Currents* 2013, 5:ecurrents.tol.2ca8041495ffafd8041490c8092756e75247483e.

137. Hurley IA, Mueller RL, Dunn KA, Schmidt EJ, Friedman M, Ho RK, Prince VE, Yang Z, Thomas MG, Coates MI: A new time-scale for ray-finned fish evolution. *Proceedings of the Royal Society of London B: Biological Sciences* 2007, 274(1609):489-498.

138. Nielsen E: A preliminary note on *Bobasatrania groenlandica*. *Meddelelser fra Dansk Geologisk Förening* 1952, 12:197–204.

139. Campbell KSW, Phuoc LD: A Late Permian actinopterygian fish from Australia. *Palaeontology* 1983, 26(1):33-70.

140. Konstantinidis P, Warth P, Naumann B, Metscher B, Hilton EJ, Olsson L: The Developmental Pattern of the Musculature Associated with the Mandibular and Hyoid Arches in the Longnose Gar, *Lepisosteus osseus* (Actinopterygii, Ginglymodi, Lepisosteiformes). *Copeia* 2015, 103(4):920-932.

141. Schaeffer B, Dalquest WW: A palaeonisciform braincase from the Permian of Texas, with comments on cranial fissures and the posterior myodome. *American Museum Novitates* 1978, 2658:1-15.

Additional files

Additional file 1: List of new and modified characters and scoring changes (PDF)

Additional file 2: Additional figures (PDF)

Additional file 3: Phylogenetic matrix and trees (ZIP folder containing matrix and trees in NEX and matrix in TNT format)

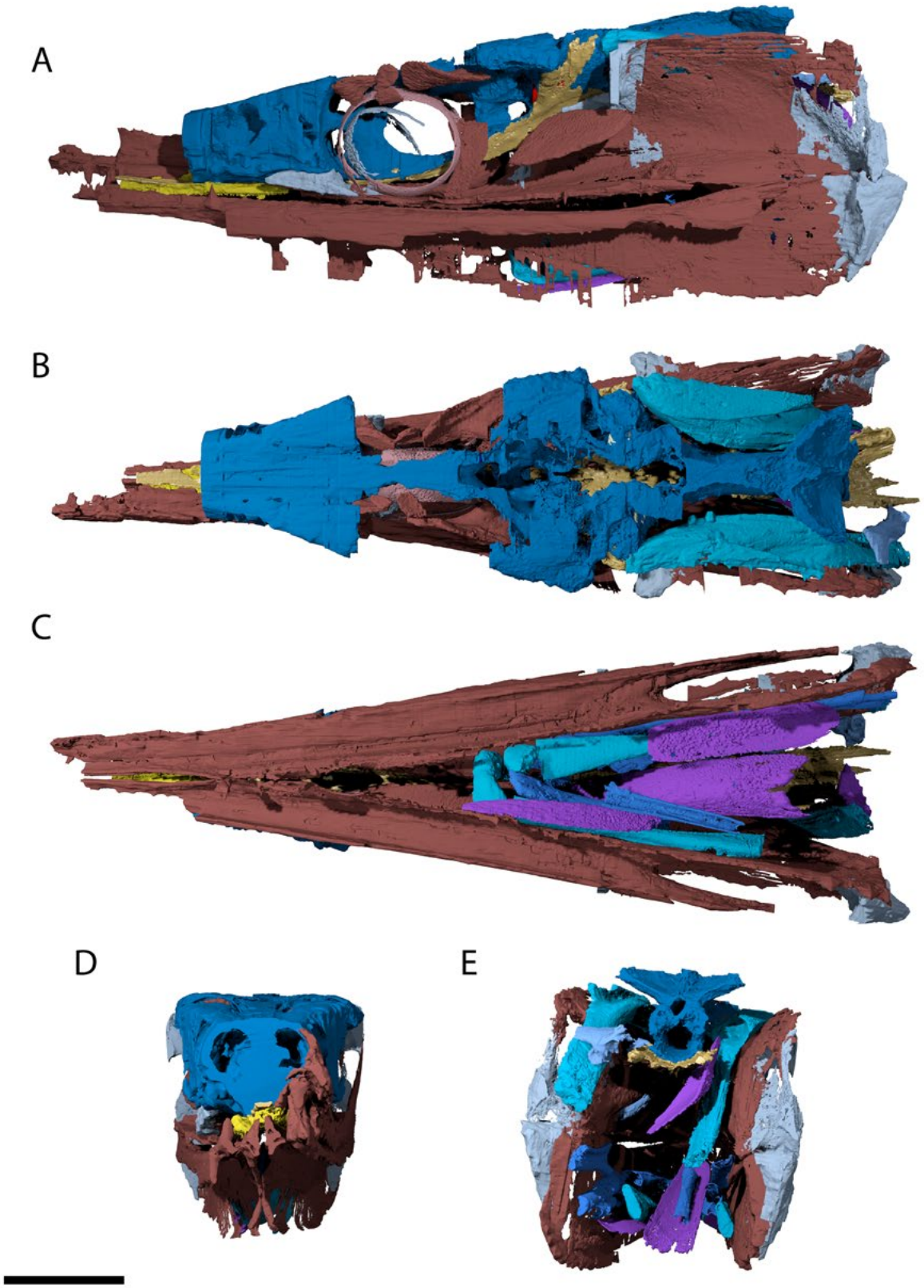
A
B
C
D
E

Figure 1. Tomographic renderings of endoskeletal anatomy of †*Saurichthys* sp. (NHMD_157546_A); **A)** right lateral (mirrored) view; **B)** dorsal view; **C)** ventral view; **D)** anterior view; **E)** posterior view. Blue shades indicate elements of likely endochondral origin (except dermohyal). Earthy–purple shades indicate elements of likely dermal origin. Scale bar equals 1cm.

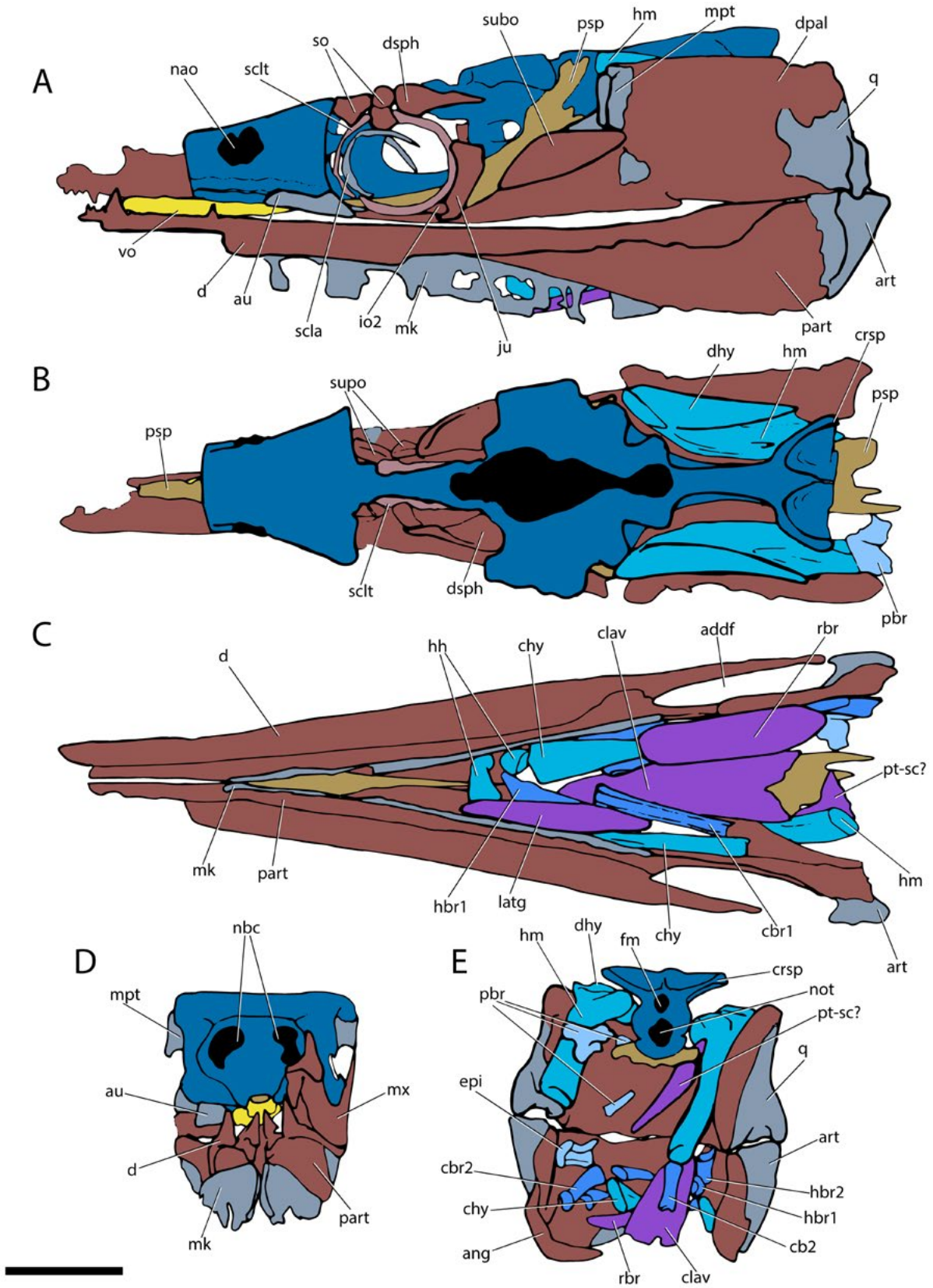
A
nao
sclt
so
dsph
subo
psp
hm
mpt
dpal
q
vo
d
au
scla
io2
mk
ju
part
art
B
supo
psp
dhy
hm
crsp
psp
sclt
dsph
pbr
C
d
hh
chy
clav
addf
rbr
pt-sc?
hm
mk
part
hbr1
latg
chy
cbr1
art
D
nbc
mpt
au
d
mx
part
mk
E
hm
dhy
fm
chy
crsp
pbr
not
pt-sc?
q
epi
art
cbr2
hbr2
chy
hbr1
cb2
ang
rbr
clav

Figure 2. Interpretative drawing of endoskeletal anatomy of †*Saurichthys* sp. (NHMD_157546_A); **A)** right lateral (mirrored) view; **B)** dorsal view; **C)** ventral view; **D)** anterior view; **E)** posterior view. Blue shades indicate elements of likely endochondral origin (except dermohyal). Earthy–purple shades indicate elements of likely dermal origin. Abbreviations: **addf,** mandibular adductor fossa; **ang,** angular; **art,** articular; **au,** autopalatine; **cbr1,** ceratobranchial 1; **cbr2,** ceratobranchial 2; **chy,** ceratohyal; **clav,** clavicle; **crsp,** craniospinal process; **d,** dentary; **dhy,** dermohyal; **dpal,** dermal palate; **dsph,** dermoshenotic; **epi,** epibranchial; **fm,** foramen magnum; **hh,** hypohyal; **hbr1,** hypobranchial 1; **hbr2,** hypobranchial 2; **hm,** hyomandibula; **io,** infraorbital; **ju,** jugal; **latg,** lateral gular; **mpt,** metapterygoid; **mk,** Meckel's cartilage; **mx,** maxilla; **nao,** nasal opening; **nbc,** nasobasal canal; **not,** notochordal canal; **part,** prearticular; **pbr,** pharyngobranchial; **psp,** parasphenoid; **pt-sc?,** putative posttemporal-supracleithrum; **q,** quadrate; **rbr,** branchiostegal ray; **scla,** sclera; **sclt,** sclerotic ring; **so,** suborbital; **supo,** supraorbital; **vo,** vomer. Scale bar equals 1cm.

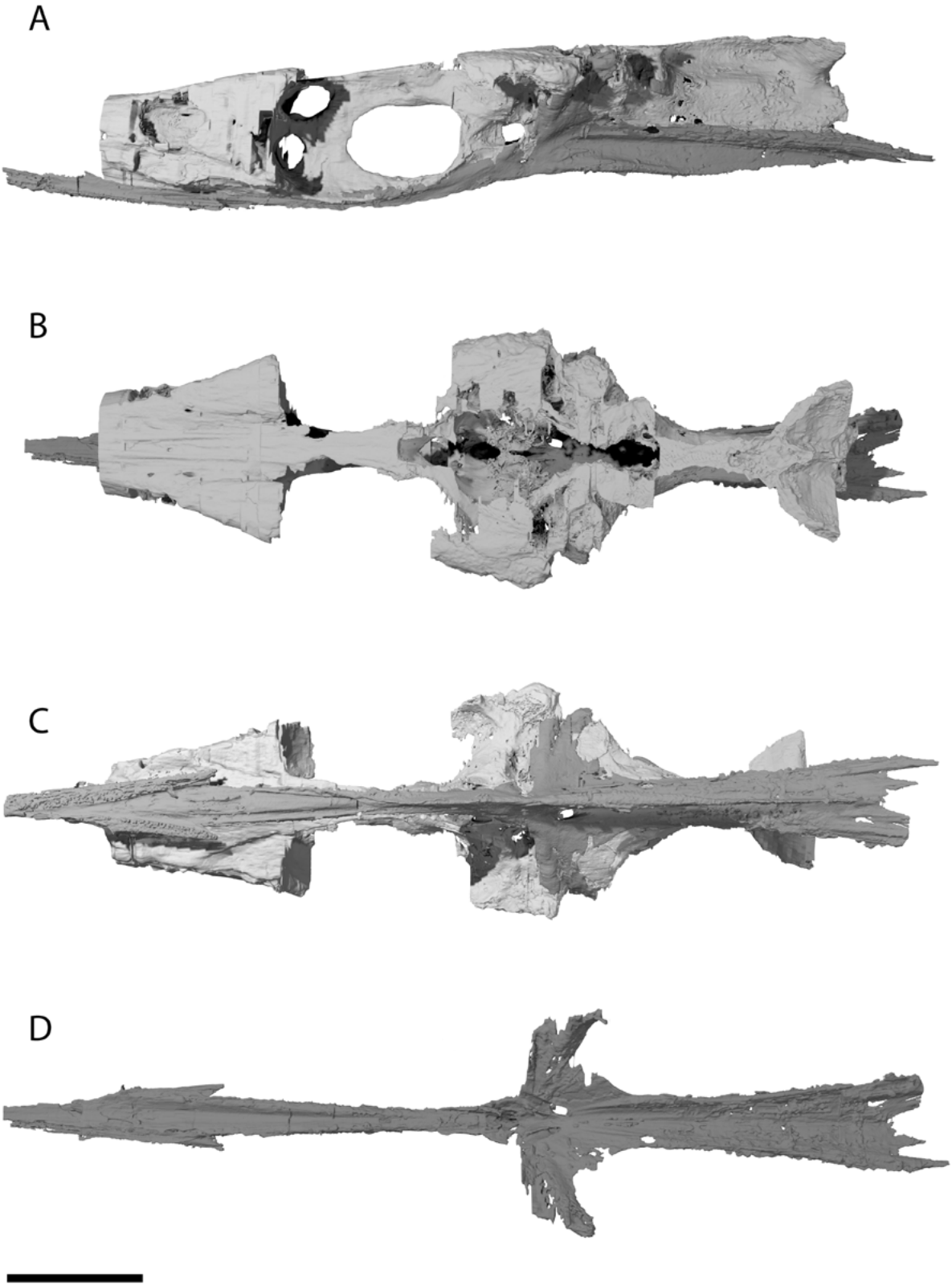
A
B
C
D

Figure 3. Tomographic renderings of braincase and parasphenoid of †*Saurichthys* sp. (NHMD_157546_A); **A)** left lateral view; **B)** dorsal view; **C)** ventral view; **D)** dorsal view of parasphenoid; dark gray shade indicates elements of dermal origin. Scale bar equals 1cm.

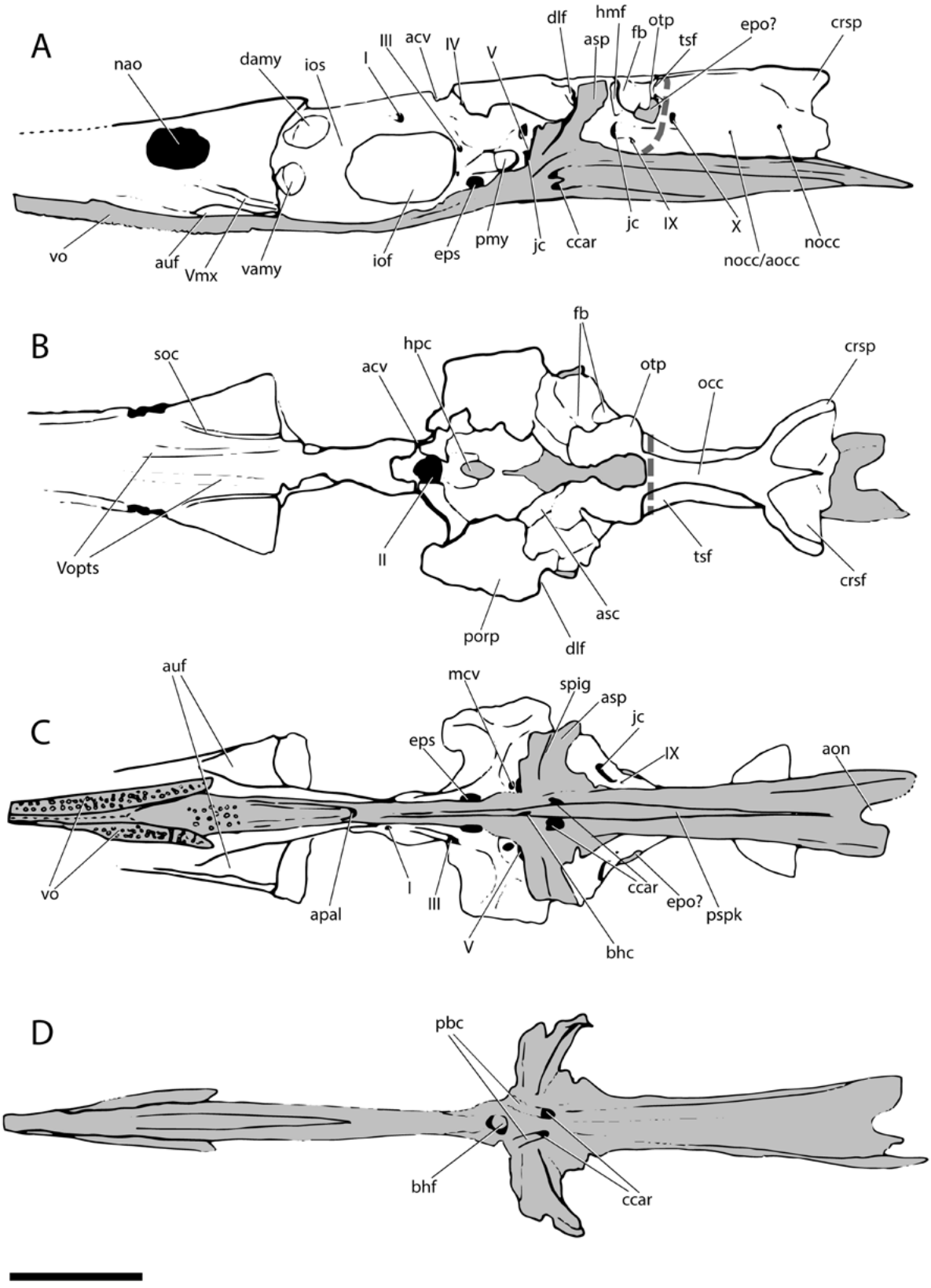
A
nao
damy
ios
I
III
acv
IV
V
dlf
hmf
asp
fb
otp
tsf
epo?
crsp
vo
auf
Vmx
vamy
iof
eps
pmy
jc
ccar
jc
IX
X
nocc
nocc/aocc
B
soc
hpc
acv
fb
otp
occ
crsp
Vopts
II
tsf
crsf
asc
porp
dlf
C
auf
mcv
spig
asp
jc
eps
IX
aon
vo
apal
I
III
V
ccar
epo?
pspk
bhc
D
pbc
bhf
ccar

Figure 4. Interpretative drawing of braincase and parasphenoid anatomy of †*Saurichthys* sp. (NHMD_157546_A); **A)** left lateral view; **B)** dorsal view; **C)** ventral view; **D)** dorsal view of parasphenoid; gray shade indicates elements of dermal origin. Dashed gray line indicates cryptic oticooccipital fissure. Abbreviations: **I,** olfactory nerve; **II,** optic nerve; **III,** oculomotor nerve; **IV,** trochlear nerve; **V,** trigeminal nerve; **Vmx,** maxillary ramus of trigeminal nerve; **Vopts,** superficial ophthalmic ramus of trigeminal nerve; **IX,** glossopharyngeal nerve; **X,** vagus nerve; **acv,** anterior cerebral vein; **aon,** aortic notch; **apal,** palatine artery; **aps,** pseudobranchial artery; **asc,** anterior semicircular canal; **asp,** ascending process of parasphenoid; **auf,** autopalatine fossa; **bhf,** buccohypophyseal opening; **ccar,** common carotid artery; **crsf,** craniospinal fossa; **crsp,** craniospinal process; **damy,** dorsal anterior myodome; **dlf,** likely origin of dilatator and/or hyomandibular protractor muscles; **epo?,** epiotic-like ossification; **fb,** fossa bridgei; **hmf,** hyomandibular facet; **hpc,** hypophyseal chamber; **iof,** interorbital fenestra; **ios,** interorbital septum; **jc,** jugular canal; **mcv,** mid-cerebral vein; **nao,** nasal opening; **nocc,** spinooccipital nerve; **nocc/aocc,** spinooccipital nerve or occipital artery; **occ,** occipital crest; **otp,** otic process; **pmy,** posterior myodome; **porp,** postorbital process; **pspk,** parasphenoid keel; **soc,** trace of supraorbital canal; **spig,** spiracular groove; **tsf,** tectosynotic fossa; **vamy,** ventral anterior myodome; **vo,** vomer. Scale bar equals 1cm.

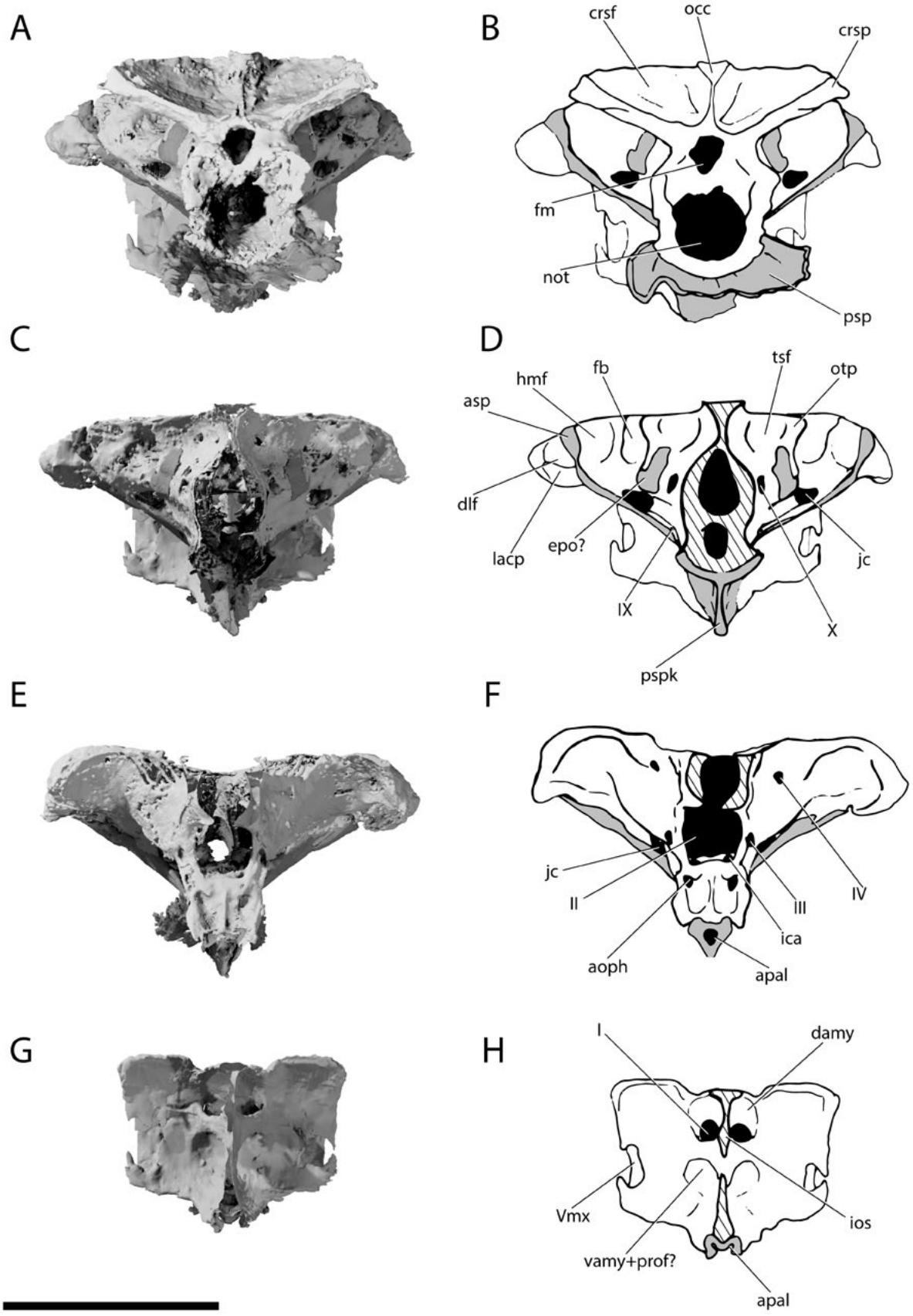
A
B
crsf
occ
crsp
fm
not
psp
C
D
hmf
fb
tsf
otp
asp
dlf
lacp
epo?
jc
IX
X
pspk
E
F
jc
II
III
IV
ica
aoph
apal
G
H
I
damy
Vmx
ios
vamy+prof?
apal

Figure 5. Coronal views of tomographic renderings of different regions of the braincase and parasphenoid of †*Saurichthys* sp. (NHMD_157546_A); **A)** posterior view of occipital region; **B)** interpretative drawing of **A**; **C)** posterior view of otic region; **D)** interpretative drawing of **C**; **E)** anterior view of orbitotemporal region; **F)** interpretative drawing of **E**; **G)** posterior view of ethmoidal region; **H)** interpretative drawing of **G**; gray shade indicates elements of dermal origin. Abbreviations: **I,** olfactory nerve; **II,** optic nerve; **III,** oculomotor nerve; **IV,** trochlear nerve; **Vmx,** maxillary ramus of trigeminal nerve; **IX,** glossopharyngeal nerve; **X,** vagus nerve; **apal,** palatine artery (parabasal canal); **aps,** pseudobranchial artery; **asc,** anterior semicircular canal; **asp,** ascending process of parasphenoid; **crsf,** craniospinal fossa; **crsp,** craniospinal process; **damy,** dorsal anterior myodome; **dlf,** likely origin of dilatator and/or hyomandibular protractor muscles; **epo?,** epiotic-like ossification; **fb,** fossa bridgei; **hmf,** hyomandibular facet; **ica,** ascending branch of internal carotid artery; **ios,** interorbital septum; **jc,** jugular canal; **lacp,** potential origin of levator arcus palatini muscle; **occ,** occipital crest; **oph,** opthalmic artery; **otp,** otic process; **psp,** parasphenoid; **pspk,** parasphenoid keel; **tsf,** tectosynotic fossa; **vamy+prof?,** ventral anterior myodome and potential course of profundus nerve. Scale bar equals 1cm.

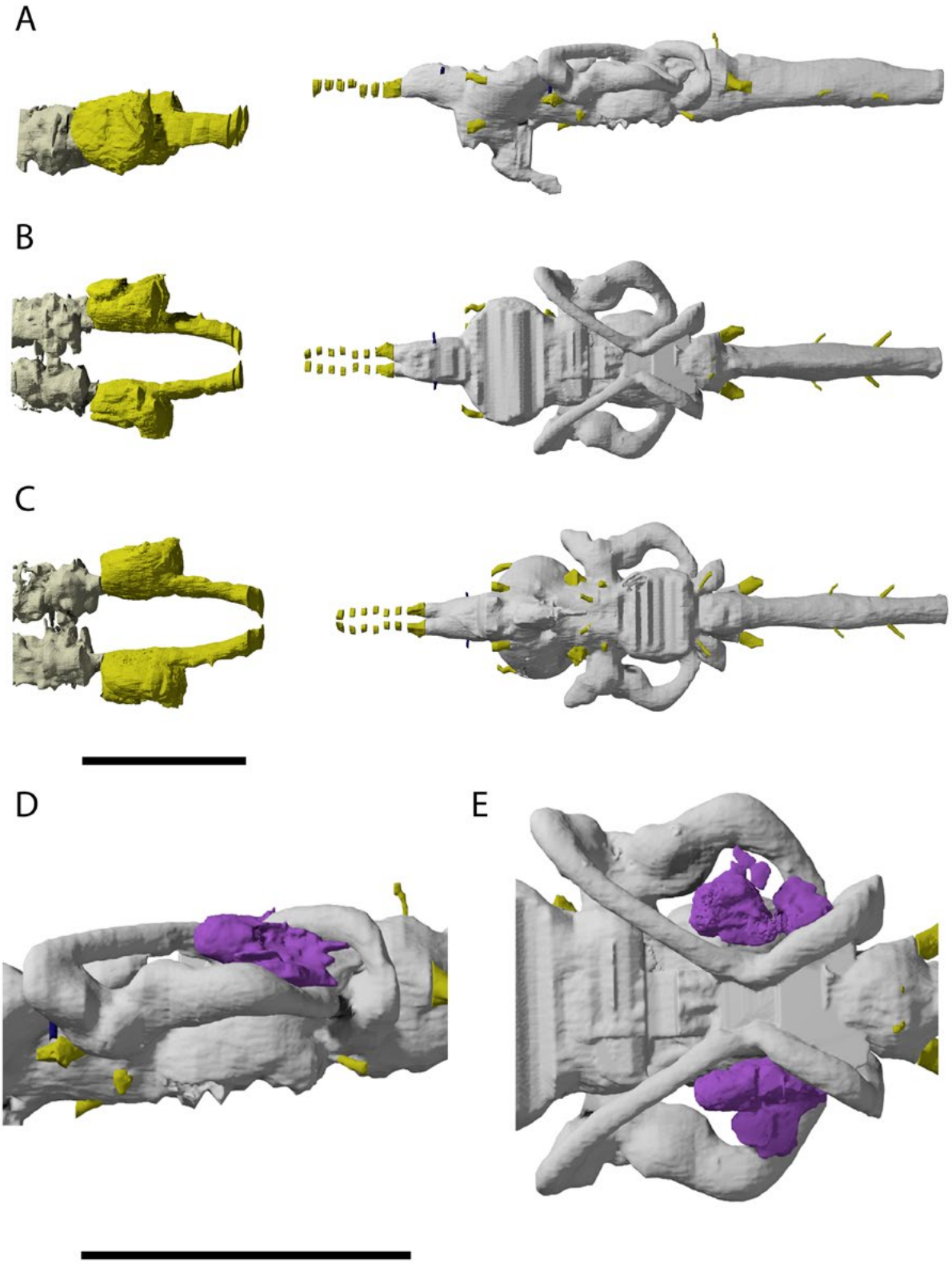
A
B
C
D
E

Figure 6. Tomographic renderings of brain, osseus labyrinth and nasobasal canal endocasts of †*Saurichthys* sp. (NHMD_157546_A); **A)** left lateral view; **B)** dorsal view; **C)** ventral view; **D)** left lateral closeup of bony labyrinth and intramural diverticula; **E)** closeup of dorsal view of bony labyrinth and intramural diverticula. Origin of major cranial nerve canals in yellow, canals for veins in blue, intramural diverticula in purple, nasobasal canals in beige. Scale bars equal 1cm.

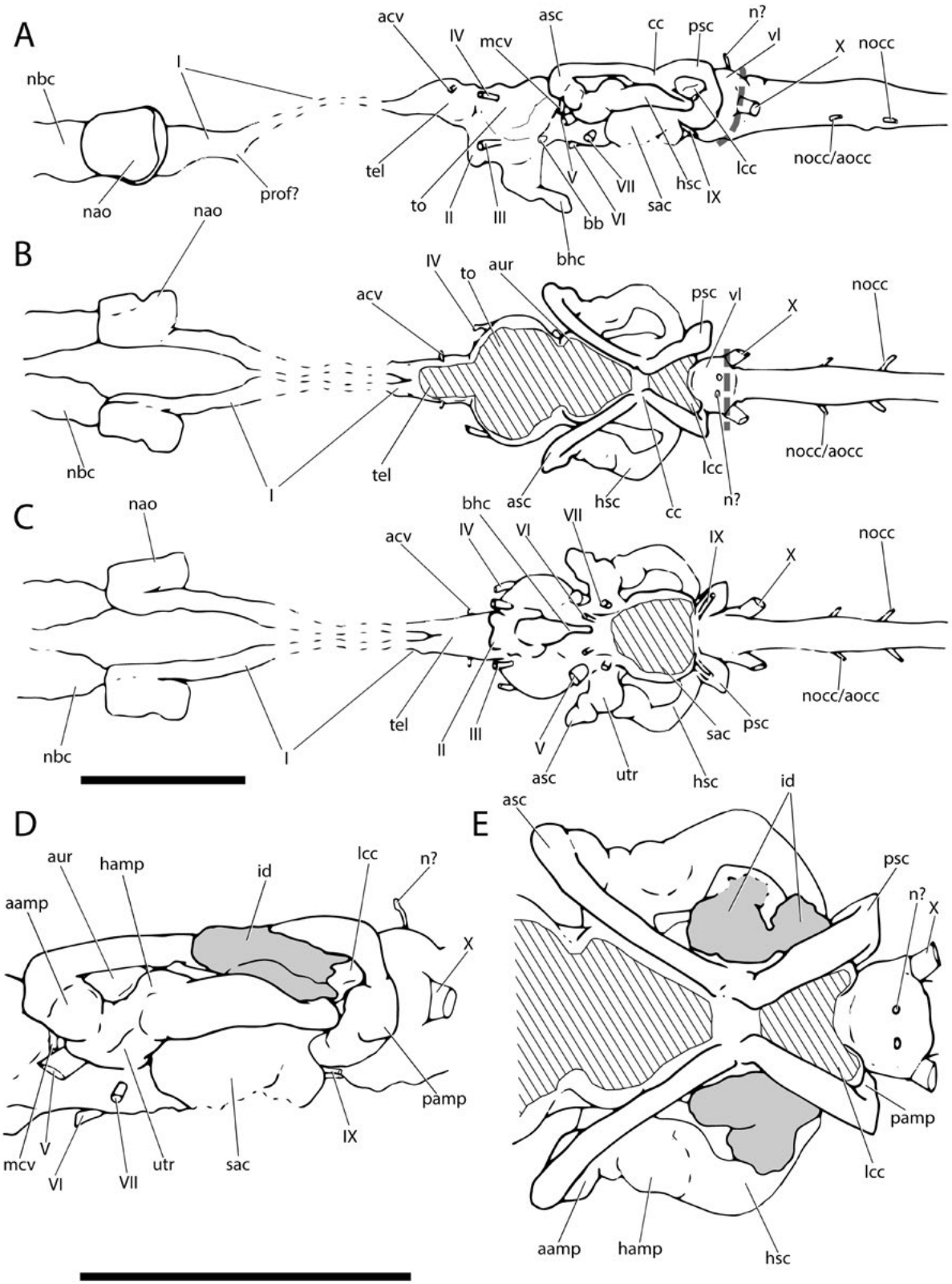
A
nbc
I
prof?
nao
nao
acv
IV
mcv
asc
cc
psc
n?
vl
X
nocc
tel
to
II
III
V
bb
VI
VII
sac
hsc
IX
lcc
nocc/aocc
bhc
B
IV
to
aur
acv
psc
vl
X
nocc
nbc
I
tel
asc
hsc
cc
n?
lcc
nocc/aocc
C
nao
bhc
VII
acv
IV
VI
IX
X
nocc
nbc
I
tel
II
III
V
asc
utr
hsc
sac
psc
nocc/aocc
D
aur
hamp
id
lcc
n?
aamp
X
pamp
IX
mcv
V
VI
VII
utr
sac
E
asc
id
psc
n?
X
pamp
lcc
aamp
hamp
hsc

Figure 7. Interpretative drawings of brain, osseus labyrinth and nasobasal canal endocasts of †*Saurichthys* sp. (NHMD_157546_A); **A)** left lateral view; **B)** dorsal view; **C)** ventral view; **D)** left lateral closeup of bony labyrinth and intramural diverticula; **E)** closeup of dorsal view of bony labyrinth and intramural diverticula. Dashed gray line indicates cryptic oticooccipital fissure. Abbreviations: **I,** olfactory nerve; **II,** optic nerve; **III,** oculomotor nerve; **IV,** trochlear nerve; **V,** trigeminal nerve; **VI,** abducens nerve; **VII;** facial nerve; **IX,** glossopharyngeal nerve; **X,** vagus nerve; **aamp,** ampulla of anterior semicircular canal; **acv,** anterior cerebral vein; **asc,** anterior semicircular canal; **aur,** cerebellar auricle; **bb,** bony bar (dorsum sellae); **bhc,** buccohypophyseal canal; **cc,** crus communis; **hamp,** ampulla of horizontal semicircular canal; **hsc,** horizontal semicircular canal; **id,** intramural diverticulum; **lcc,** lateral cranial canal; **mcv,** mid-cerebral vein; **n?,** putative dorsal ramus of IX or X; **nbc,** nasobasal canal; **nocc;** spinooccipital nerve; **nocc/aocc;** spinooccipital nerve or occipital artery; **pamp,** ampulla of posterior semicircular canal; **prof?,** putative course of profundus nerve; **psc,** posterior semicircular canal; **sac,** saccular recess; **tel,** telencephalon; **to,** optic tectum; **utr,** utricular recess; **vl,** vagal lobe. Scale bars equal 1cm.

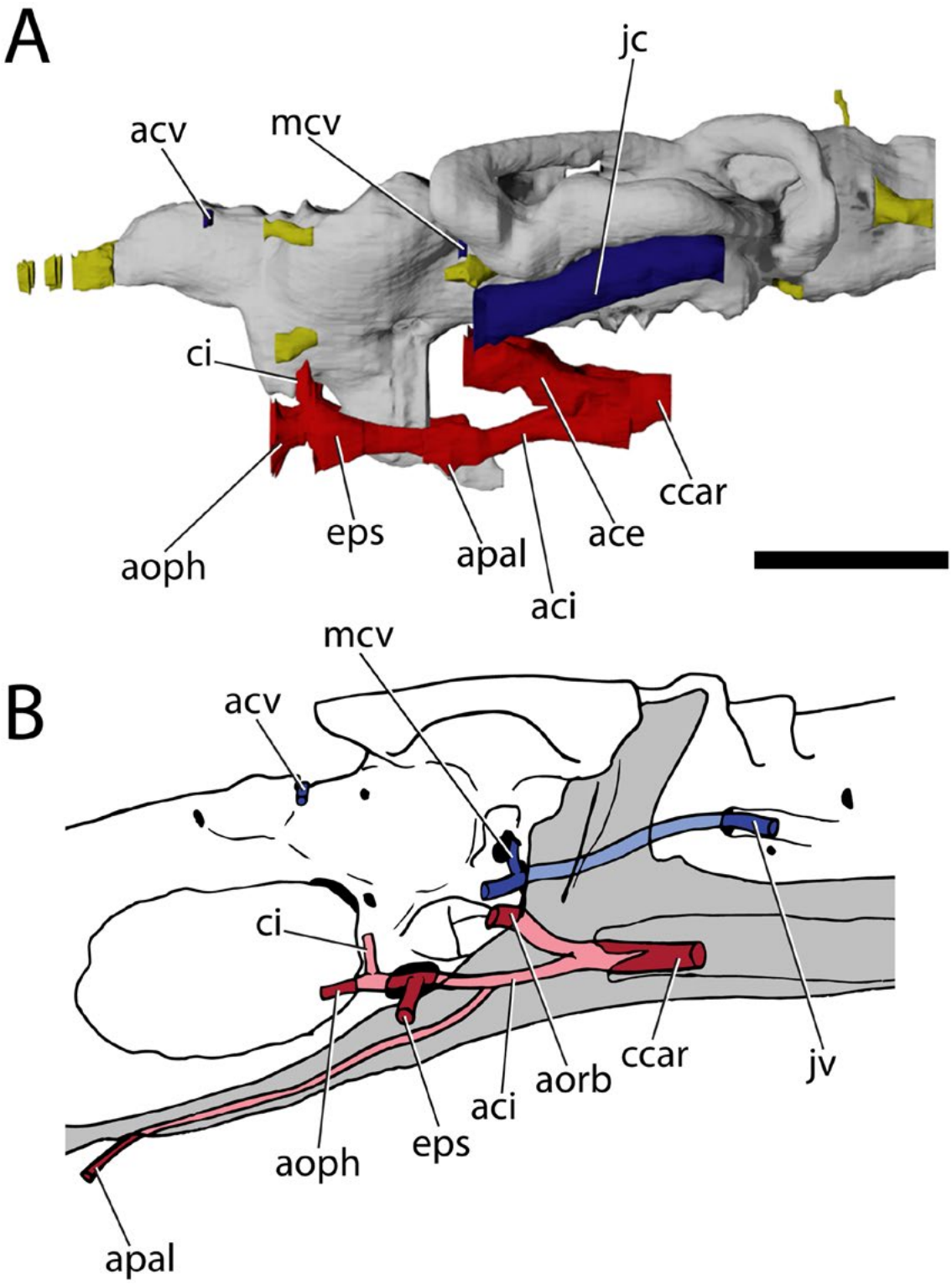
A
jc
acv
mcv
ci
ccar
eps
apal
ace
aoph
aci
B
mcv
acv
ci
ccar
jv
aorb
aci
eps
aoph
apal

Figure 8. Basicranial circulation of †*Saurichthys* sp. (NHMD_157546_A); **A)** digital rendering of brain and osseus labyrinth endocasts, with major cranial nerves in yellow, arterial canals in red and venal canals in blue; **B)** Simplified schematic of skull in lateroventral view showing the passage of major blood vessels. Abbreviations: **aci,** common branch of internal carotid artery; **acv,** anterior cerebral vein; **aorb,** orbital artery; **apal,** palatine artery (parabasal canal); **eps,** efferent pseudobranchial artery; **ccar,** common carotids; **ica,** ascending branch of internal carotid; **jc,** jugular canal; **jv,** jugular vein; **mcv,** mid-cerebral vein; **oph,** ophthalmic artery. Scale bars equal 0.5cm.

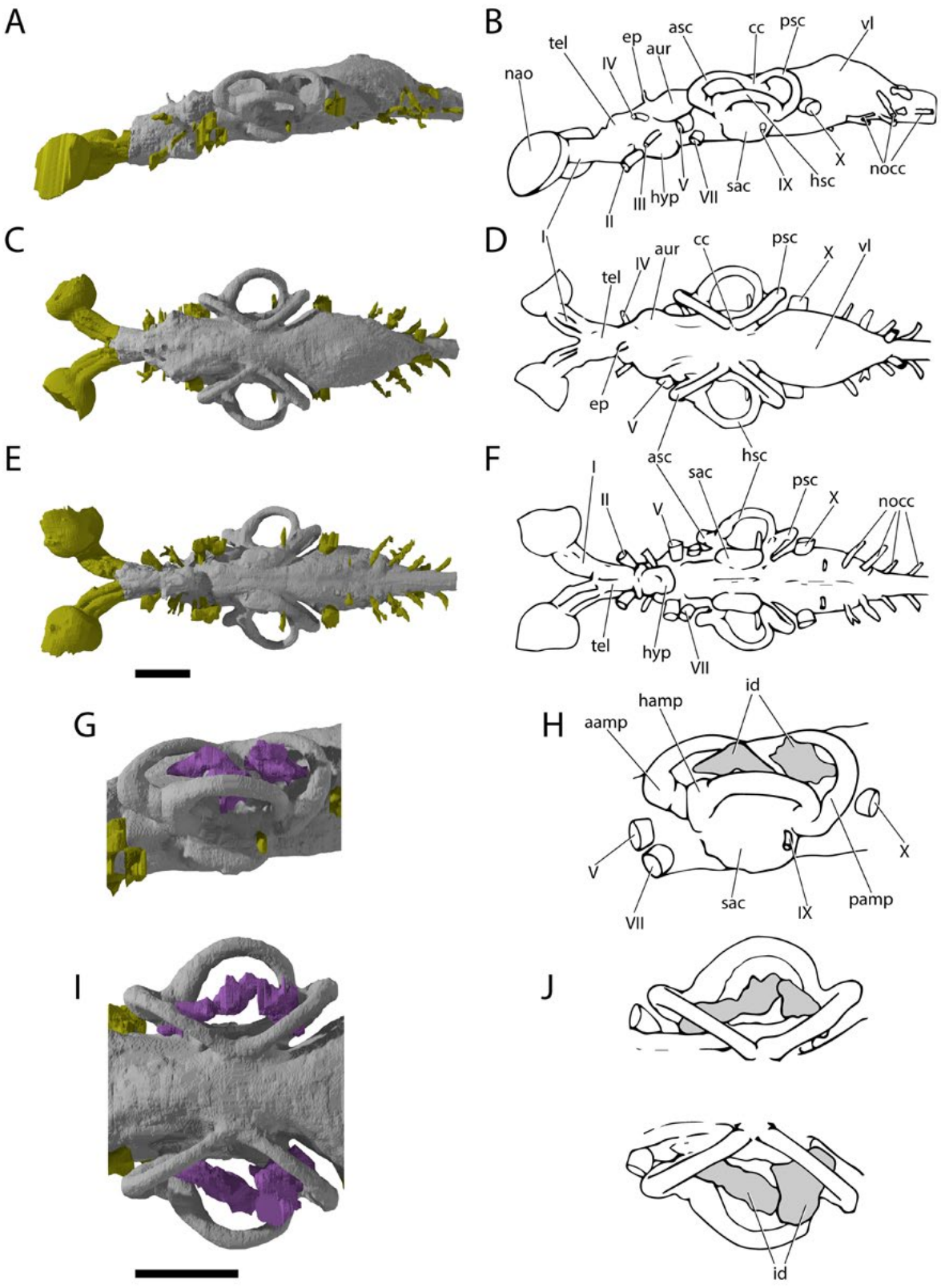
A
B
tel
ep
asc
aur
cc
psc
vl
nao
IV
X
nocc
III
hyp
V
VII
sac
IX
hsc
II
I
C
D
aur
cc
psc
X
vl
tel
IV
ep
V
asc
hsc
E
F
I
sac
psc
X
nocc
II
V
tel
hyp
VII
G
H
id
hamp
aamp
X
V
sac
IX
pamp
VII
I
J
id

Figure 9. Brain and osseus labyrinth endocast anatomy of *Acipenser brevirostrum* (FMNH 113538). **A)** lateral view; **B)** interpretative drawing of **A**; **C)** dorsal view; **D)** interpretative drawing of **C**; **E)** ventral view; **F)** interpretative drawing of **E**; **G)** left lateral closeup of bony labyrinth and intramural diverticula; **H)** interpretative drawing of **G**; **I)** closeup of dorsal view of bony labyrinth and intramural diverticula; **J)** interpretative drawing of **I**. Major cranial nerves in yellow, intramural diverticula in purple. Abbreviations: **I,** olfactory nerve; **II,** optic nerve; **III,** oculomotor nerve; **IV,** trochlear nerve; **V,** trigeminal nerve; **VII,** facial nerve; **IX,** glossopharyngeal nerve; **X,** vagus nerve; **asc,** anterior semicircular canal; **aur,** cerebellar auricle; **cc,** crus communis; **ep,** epiphysis; **hsc,** horizontal semicircular canal; **hyp,** hypophyseal chamber; **nao,** nasal opening; **nocc,** spinooccipital nerve; **psc,** posterior semicircular canal; **sac,** saccular recess; **tel,** telencephalon; **vl,** vagal lobe. Scale bar equals 2cm.

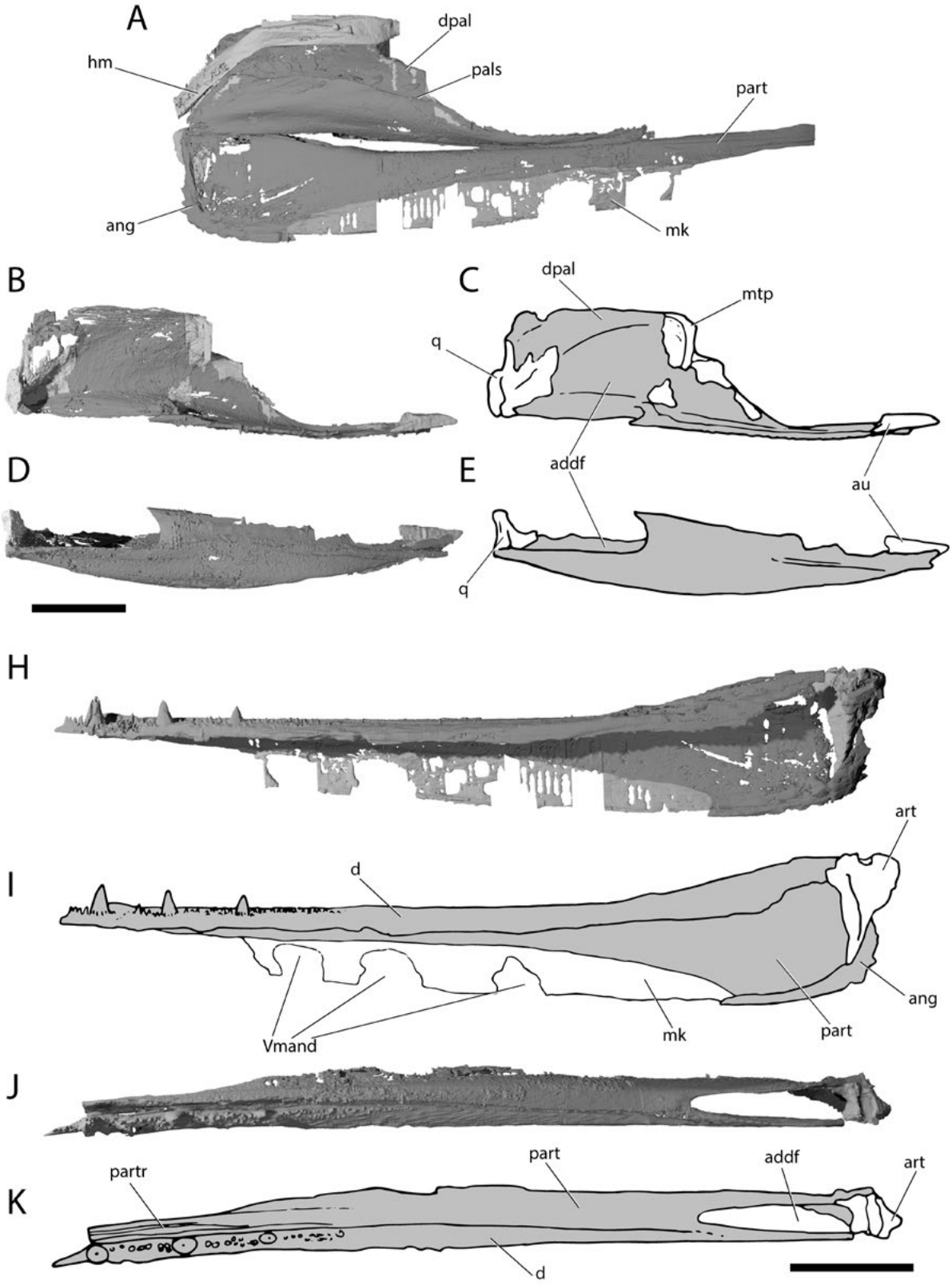
A
dpal
hm
pals
part
ang
mk
B
C
dpal
mtp
q
D
E
addf
au
q
H
art
I
d
ang
Vmand
mk
part
J
K
partr
part
addf
art
d

Figure 10. Palatal and lower jaw anatomy of †*Saurichthys* sp. (NHMD_157546_A); **A)** digital rendering of left palate, lower jaw and hyomandibula in life association, medial view; **B)** digital rendering of right palate in lateral view; **C)** interpretative drawing of **B**; **D)** digital rendering of right palate in ventral view; **E)** interpretative drawing of **D**; **H)** digital rendering of left mandible in lateral view; **I)** interpretative drawing of **H**; **J)** digital rendering of left mandible in dorsal view; **K)** interpretative drawing of **J**. Gray shades indicate elements of dermal origin. Abbreviations: **Vmand,** openings for mandibular trunk of trigeminal; **addf,** adductor fossa; **ang,** angular; **au,** autopalatine; **d,** dentary; **dpal,** dermal palate; **hm,** hyomandibula; **mk,** meckel's cartilage; **mpt,** metapterygoid; **pals,** palatal shelf; **part,** prearticular; **partr,** prearticular ridge; **q,** quadrate. Scale bars equal 1cm.

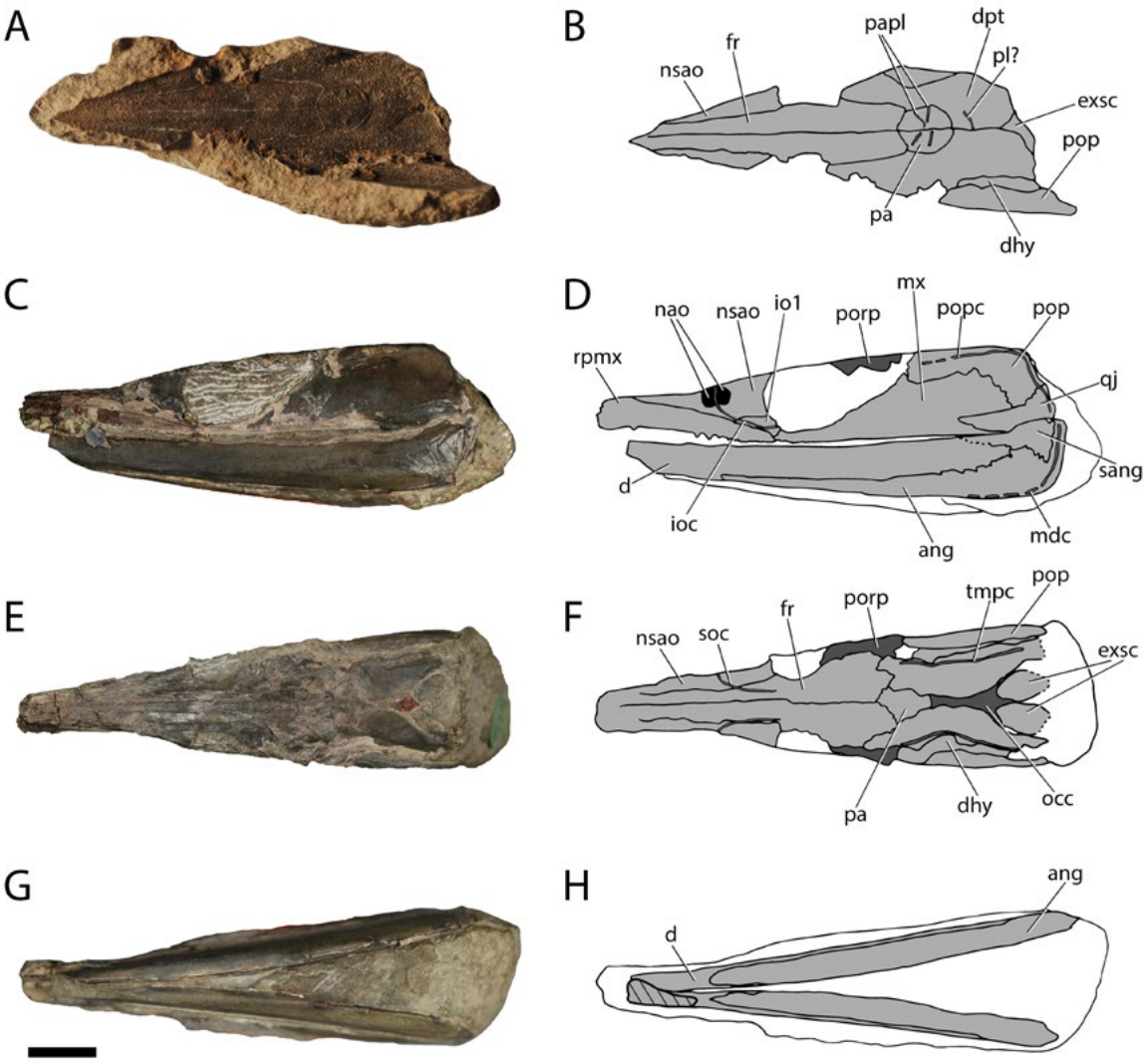
A
B
papl
dpt
fr
pl?
nsao
exsc
pop
pa
dhy
C
D
mx
nao
nsao
io1
porp
popc
pop
rpmx
qj
sang
d
ioc
ang
mdc
E
F
pop
tmpc
porp
fr
nsao
soc
exsc
pa
dhy
occ
G
H
ang
d

Figure 11. External anatomy of †*Saurichthys* sp. (NHMD_157546_A). **A)** partial counterpart showing dorsal dermatocranium; **B)** interpretative drawing of **A**; **C)** skull and mandible in lateral view; **D)** interpretative drawing of **C**; **E)** skull and mandible in dorsal view; **F)** interpretative drawing of **E**; **G)** skull and mandible in ventral view; **H)** interpretative drawing of **G**. Light gray shade indicates elements of dermal origin, dark gray shade indicates exposed regions of the chondrocranium. Abbreviations: **ang,** angular; **d,** dentary; **dhy,** dermohyal; **dpt,** dermopterotic; **exsc,** median extrascapular; **fr,** frontal; **ioc,** infraorbital canal; **la,** lachrymal; **mdc,** mandibular canal; **mx,** maxilla; **nao,** nasal opening; **nsao,** nasalo-antorbital; **occ,** occipital crest; **pa,** parietal; **papl,** parietal pit line; **pl?,** putative pit line on dermopterotic; **pop,** preopercle; **popc,** preopercular canal; **porp,** postorbital process; **qj,** quadratojugal; **rpmx,** rostropremaxilla; **sang,** surangular; **soc,** supraorbital canal; **tmpc,** temporal canal. Scale bar equals 1cm.

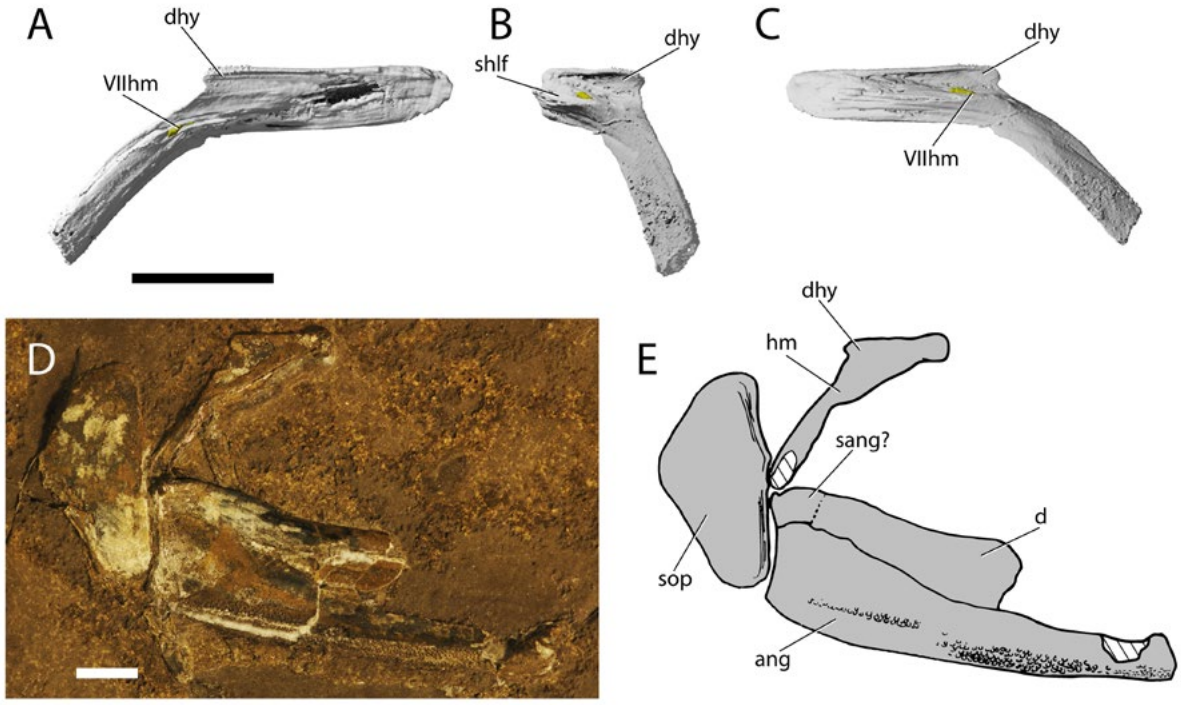
A
dhy
VIIhm
B
dhy
shlf
C
dhy
VIIhm
D
E
dhy
hm
sang?
d
sop
ang

Figure 12. Hyomandibular and opercular anatomy of †saurichthyids. Digital rendering of right hyomandibula of †*Saurichthys* sp. (NHMD_157546_A) in: **A)** lateral view; **B)** posteromedial view; **C)** medial view; **D)** right hyomandibula, subopercle and mandible of an unidentified †saurichthyid (PIMUZ A/I 4648) from Prosanto Formation in life position; **E)** interpretative drawing of **D**. Gray shade indicates elements of dermal origin. Abbreviations: **VIIhm,** hyomandibular trunk of facial nerve; **d,** dentary; **dhy,** dermohyal; **hm,** hyomandibula; **sang?,** putative surangular; **sop,** subopercle. Scale bar equals 1cm.

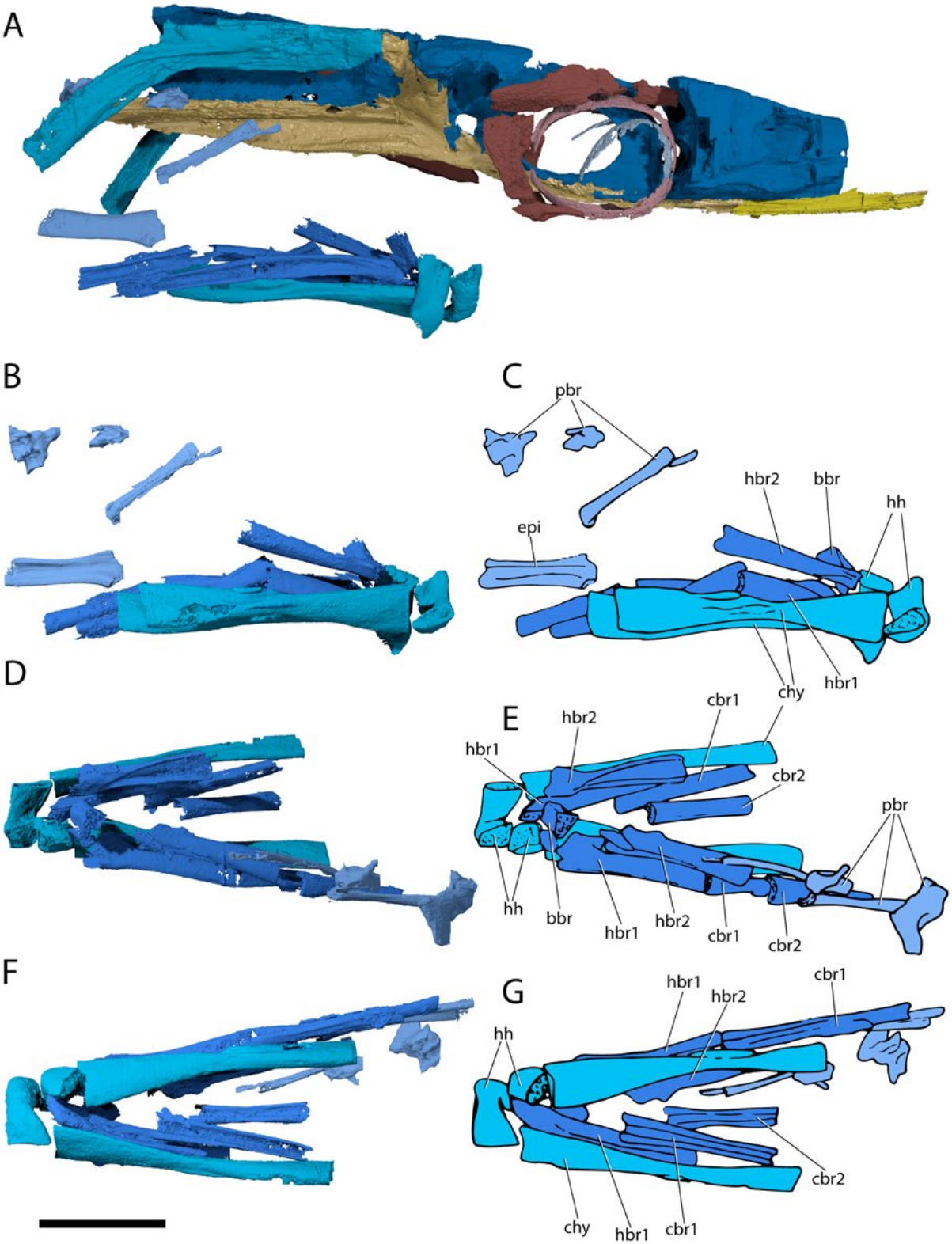
A
B
C
pbr
hbr2
bbr
hh
epi
chy
hbr1
D
E
cbr1
hbr2
hbr1
cbr2
pbr
hh
bbr
hbr1
hbr2
cbr1
cbr2
F
G
hbr1
hbr2
cbr1
hh
cbr2
chy
hbr1
cbr1

Figure 13. Hyoid and gill skeleton of †*Saurichthys* sp. (NHMD_157546_A). **A)** Digital rendering of braincase and associated hyoid and branchial ossifications in left lateral view (mirrored); **B)** ventral hyoid and gill ossifications in right lateral view; **C)** interpretative drawing of **B**; **D)** ventral hyoid and gill ossifications in dorsal view; **E)** interpretative drawing of **D**; **F)** ventral hyoid and gill ossifications in ventral view; **G)** interpretative drawing of **F**. Abbreviations: **bbr,** basibranchial; **cbr1,** ceratobranchial 1; **cbr2,** ceratobranchial 2; **chy,** ceratohyal; **epi,** epibranchial; **hbr1,** hypobranchial 1; **hbr2,** hypobranchial 2; **hh,** hypobranchial; **pbr,** pharyngobranchial. Scale bar equals 1cm.

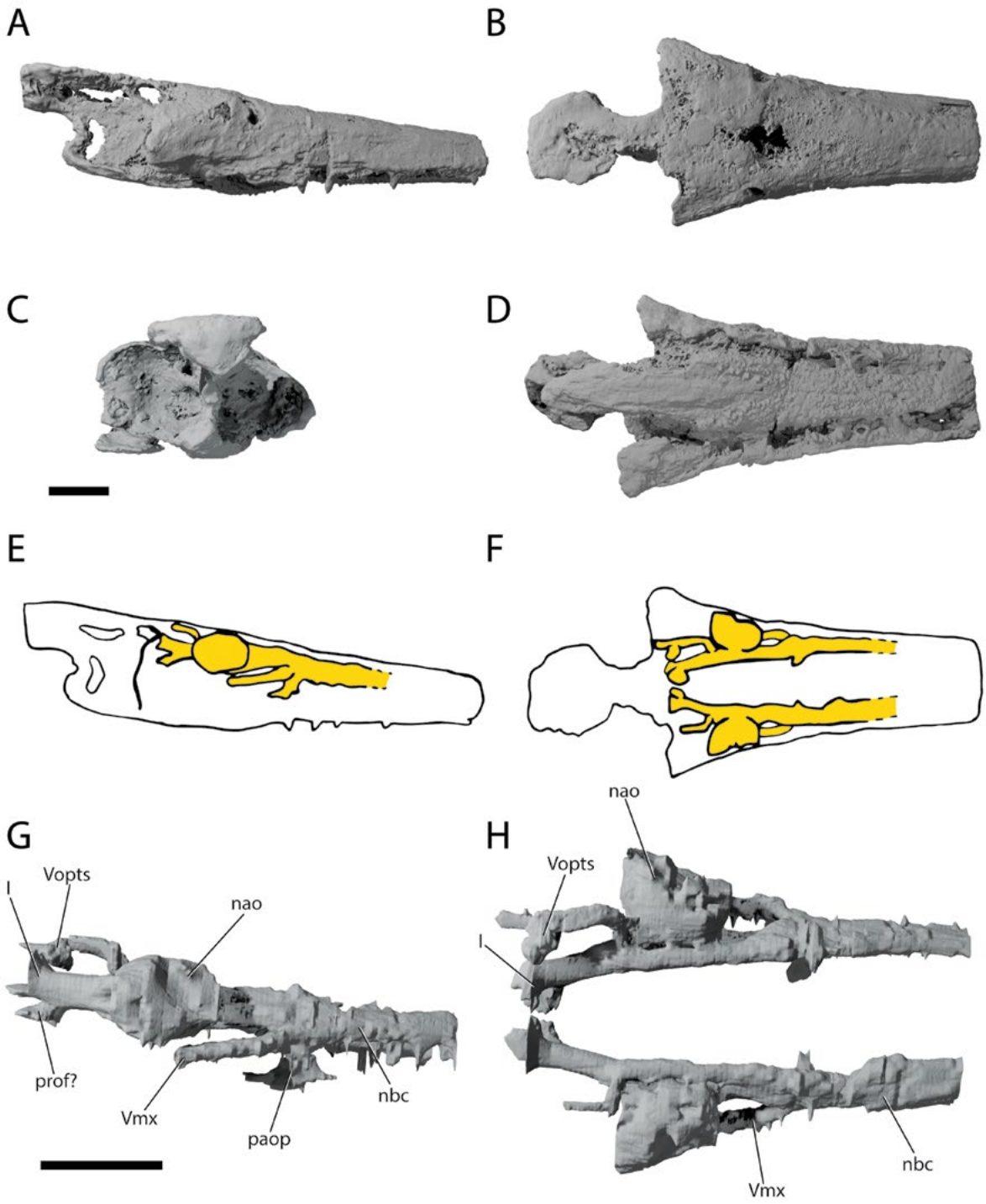
A
B
C
D
E
F
G
Vopts
l
nao
prof?
Vmx
paop
nbc
H
nao
Vopts
l
Vmx
nbc

Figure 14. Ethmoid region of †*Saurichthys nepalensis* (MNHN F 1980-5). Digital rendering of complete specimen in: **A)** right lateral view; **B)** dorsal view; **C)** posterior view; **D)** ventral view; schematic exhibiting the arrangement of rostral canals (in yellow) in: **E)** lateral view; **F)** dorsal view; digital rendering of rostral canals in: **G)** lateral view; **H)** dorsal view. Abbreviations: **I,** olfactory nerve; **Vmx,** maxillary ramus of trigeminal nerve; **Vopts,** superficial ophthalmic ramus of trigeminal nerve; **nao,** nasal opening; **nbc,** nasobasal canal; **paop,** palatal opening of nasobasal canals; **prof?,** putative course of profundus nerve. Scale bars equal 1cm.

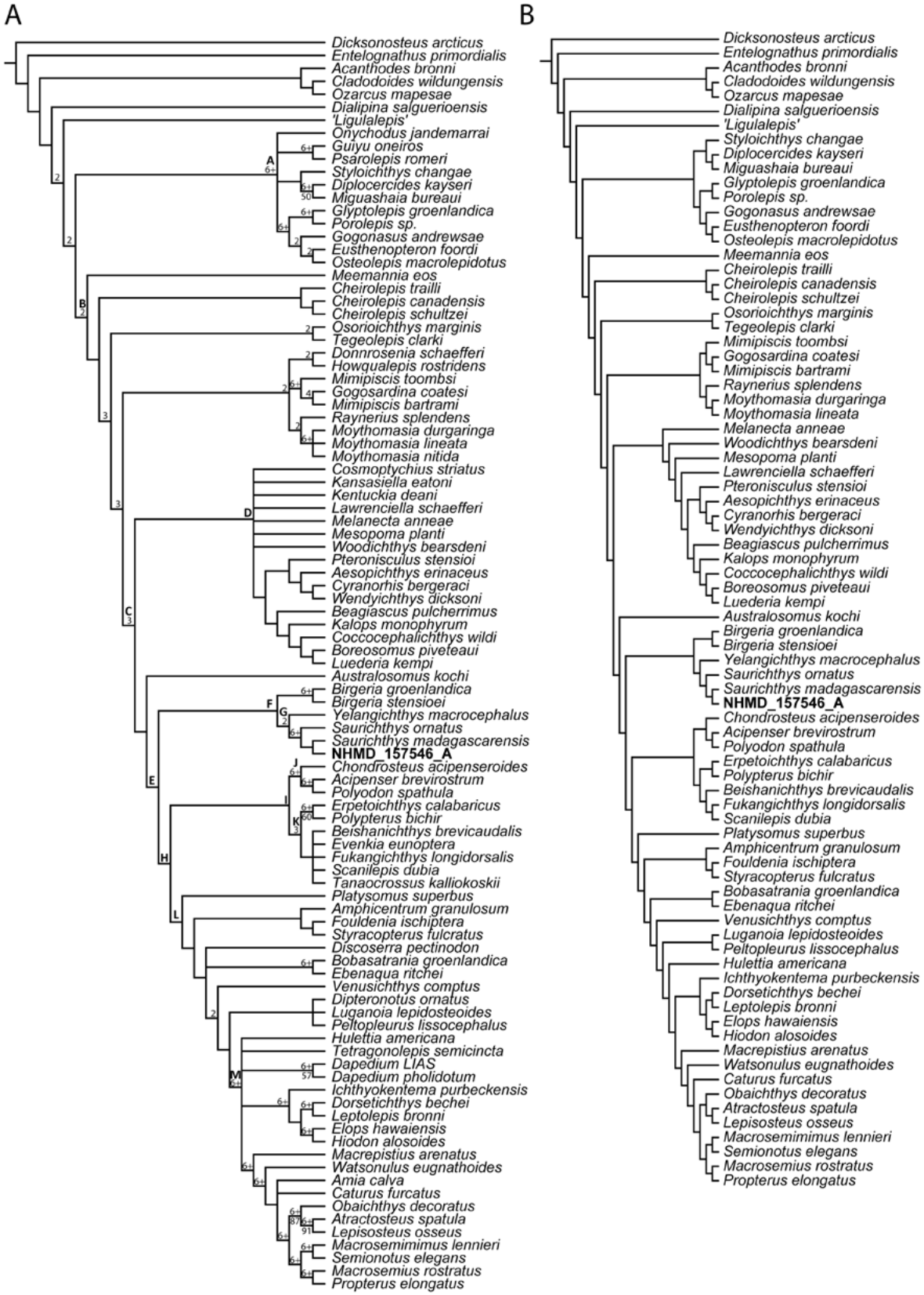
A
Dicksonosteus arcticus
Entelognathus primordialis
Acanthodes bronni
Cladodoides wildungensis
Ozarcus mapesae
Dialipina salguerioensis
'Ligulalepis'
Onychodus jandemarrai
Guiyu oneiros
Psarolepis romeri
Styloichthys changae
Diplocercides kayseri
Miguashaia bureaui
Glyptolepis groenlandica
Porolepis sp.
Gogonasus andrewsae
Eusthenopteron foordi
Osteolepis macrolepidotus
Meemannia eos
Cheirolepis trailli
Cheirolepis canadensis
Cheirolepis schultzei
Osorioichthys marginis
Tegeolepis clarki
Donnrosenia schaefferi
Howqualepis rostridens
Mimipiscis toombsi
Gogosardina coatesi
Mimipiscis bartrami
Raynerius splendens
Moythomasia durgaringa
Moythomasia lineata
Moythomasia nitida
Cosmoptychius striatus
Kansasiella eatoni
Kentuckia deani
Lawrenciella schaefferi
Melanecta anneae
Mesopoma planti
Woodichthys bearsdeni
Pteronisculus stensioi
Aesopichthys erinaceus
Cyranorhis bergeraci
Wendyichthys dicksoni
Beagiascus pulcherrimus
Kalops monophyrum
Coccocephalichthys wildi
Boreosomus piveteaui
Luederia kempi
Australosomus kochi
Birgeria groenlandica
Birgeria stensioei
Yelangichthys macrocephalus
Saurichthys ornatus
Saurichthys madagascarensis
NHMD_157546_A
Chondrosteus acipenseroides
Acipenser brevirostrum
Polyodon spathula
Erpetoichthys calabaricus
Polypterus bichir
Beishanichthys brevicaudalis
Evenkia eunoptera
Fukangichthys longidorsalis
Scanilepis dubia
Tanaocrossus kalliokoskii
Platysomus superbus
Amphicentrum granulosum
Fouldenia ischiptera
Styracopterus fulcratus
Discoserra pectinodon
Bobasatrania groenlandica
Ebenaqua ritchei
Venusichthys comptus
Dipteronotus ornatus
Luganoia lepidosteoides
Peltopleurus lissocephalus
Hulettia americana
Tetragonolepis semicincta
Dapedium LIAS
Dapedium pholidotum
Ichthyokentema purbeckensis
Dorsetichthys bechei
Leptolepis bronni
Elops hawaiensis
Hiodon alosoides
Macrepistius arenatus
Watsonulus eugnathoides
Amia calva
Caturus furcatus
Obaichthys decoratus
Atractosteus spatula
Lepisosteus osseus
Macrosemimimus lennieri
Semionotus elegans
Macrosemius rostratus
Propterus elongatus
B
Dicksonosteus arcticus
Entelognathus primordialis
Acanthodes bronni
Cladodoides wildungensis
Ozarcus mapesae
Dialipina salguerioensis
'Ligulalepis'
Styloichthys changae
Diplocercides kayseri
Miguashaia bureaui
Glyptolepis groenlandica
Porolepis sp.
Gogonasus andrewsae
Eusthenopteron foordi
Osteolepis macrolepidotus
Meemannia eos
Cheirolepis trailli
Cheirolepis canadensis
Cheirolepis schultzei
Osorioichthys marginis
Tegeolepis clarki
Mimipiscis toombsi
Gogosardina coatesi
Mimipiscis bartrami
Raynerius splendens
Moythomasia durgaringa
Moythomasia lineata
Melanecta anneae
Woodichthys bearsdeni
Mesopoma planti
Lawrenciella schaefferi
Pteronisculus stensioi
Aesopichthys erinaceus
Cyranorhis bergeraci
Wendyichthys dicksoni
Beagiascus pulcherrimus
Kalops monophyrum
Coccocephalichthys wildi
Boreosomus piveteaui
Luederia kempi
Australosomus kochi
Birgeria groenlandica
Birgeria stensioei
Yelangichthys macrocephalus
Saurichthys ornatus
Saurichthys madagascarensis
NHMD_157546_A
Chondrosteus acipenseroides
Acipenser brevirostrum
Polyodon spathula
Erpetoichthys calabaricus
Polypterus bichir
Beishanichthys brevicaudalis
Fukangichthys longidorsalis
Scanilepis dubia
Platysomus superbus
Amphicentrum granulosum
Fouldenia ischiptera
Styracopterus fulcratus
Bobasatrania groenlandica
Ebenaqua ritchei
Venusichthys comptus
Luganoia lepidosteoides
Peltopleurus lissocephalus
Hulettia americana
Ichthyokentema purbeckensis
Dorsetichthys bechei
Leptolepis bronni
Elops hawaiensis
Hiodon alosoides
Macrepistius arenatus
Watsonulus eugnathoides
Caturus furcatus
Obaichthys decoratus
Atractosteus spatula
Lepisosteus osseus
Macrosemimimus lennieri
Semionotus elegans
Macrosemius rostratus
Propterus elongatus

Figure 15. Results of phylogenetic analysis (maximum parsimony). **A)** strict consensus of the 2430 MPTs (1421 steps, C.I: 0.217, R.I: 0.645) for 97 taxa and 275 characters of equal weight. Bremer decay indices above 1 are placed above nodes. Bootstrap values above 50% are placed below nodes. Synapomorphies common to all MPTs for selected nodes are as follows: **A** (Sarcopterygii): C.26(1), C.36(0), C.60(1), C.134(1); **B** (Actinopterygii): C.44(1), C.46(0), C.202(1); **C** (post-Devonian Actinopterygii): C.58(0), C.72(0), C.93(2,3), C.124(1), C.133(1), C.139(2), C.141(2), C.144(1), C.146(1), C.186(0), C.191(1), C.194(1), C.201(1), C.221(1), C.243(1); **D** (generalized Carboniferous–Triassic forms): no common synapomorphies; **E** ((†Saurichthyiformes + †*Birgeria*) + crown Actinopterygii): C.68(1), C.102(1), C.148(0), C.155(0), C.159(2), C.177(2), C.184(1),C.244(0); **F** (†Saurichthyiformes + †*Birgeria*): C.53(2), C.66(1), C.213(0), C.215(0), C.240(2); **G** (†Saurichthyiformes): C.20(1), C.31(1); **H** (crown Actinopterygii): C.44(0), C.105(1), C.133(0), C.224(0); **I** (Chondrostei + Cladistia): C.34(1), C.130(0), C.139(0), C.186(1), C.218(0), C.220(0); **J** (Chondrostei): C.69(0), C.92(1), C.104(1), C.107(1), C.160(1), C.177(3), C.185(1), C.212(2), C.221(0); **K** (Cladistia): C.3(0), C.95(1), C.103(1), C.131(1), C.231(1), C.265(0), C.267(1); **L** (total group Neopterygii): C.7(0), C.29(1), C.118(1), C.142(0), C.179(0); **M** (crown Neopterygii): C.74(1), C.75(1), C.115(1), C.121(1), C.182(1). **B)** agreement subtree of 2430 MPTs containing 80 taxa.

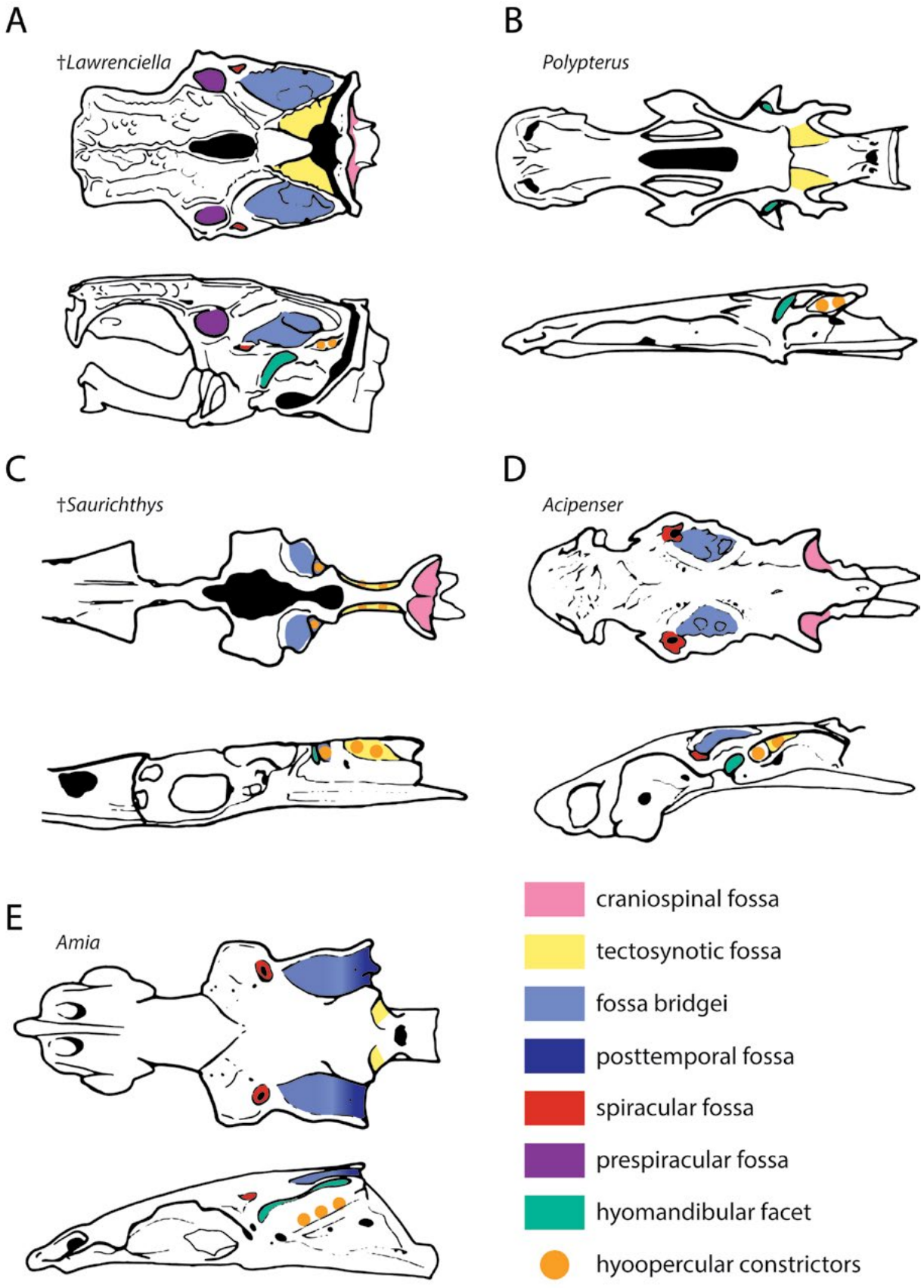
A
†Lawrenciella
B
Polypterus
C
†Saurichthys
D
Acipenser
E
Amia
craniospinal fossa
tectosynotic fossa
fossa bridgei
posttemporal fossa
spiracular fossa
prespiracular fossa
hyomandibular facet
hyoopercular constrictors

Figure 16. Cranial fossae of the occipital and otic regions of selected actinopterygians and hyoopercular muscle attachment fields. **A)** †*Lawrenciellla schaefferi* (redrawn from [67]); **B)** *Polypterus* (redrawn from [79]); **C)** †*Saurichthys* (based on NHMD_157546_A); **D)** *Acipenser brevirostrum* (based on FMNH 113538); **E)** *Amia calva* (redrawn from [70]). **Craniospinal fossa**: fossa on the posterior surface of the craniospinal processes, for the accommodation of epaxial muscle segments. Absent when craniospinal processes are absent; **Tectosynotic fossa:** paired fossae bounded laterally by the arch of the posterior semicircular canal. Non-homologous across taxa. **Fossa bridgei**: depression roughly constrained by the planes of the three semicircular canals. Absent when the dermatocranium is fused to the dorsal part of the neurocranium (e.g., in *Polypterus*); **Posttemporal fossa**: on the posterior part of the otic region, but lateral to the posterior semicircular canal. In most neopterygians it is confluent with the fossa bridgei, which opens posteriorly to receive epaxial segments; **Spiracular fossa**: depression formed around the dorsal exit of the spiracle; **Prespiracular fossa**: small fossa lateral to the spiracle and the anterior semicircular canal, dorsal to the horizontal semicircular canal and near to the dorsolateral margin of the braincase. Present in some late Paleozoic–early Mesozoic generalized actinopterygians; **Hyoopercular constrictor fields**: Origins of the hyoid and opercular constrictor muscles. Hypothesized in fossil taxa. These attachment fields migrate according to the changes in the orientation of the suspensorium. In †*Saurichthys* the hyoopercular musculature likely originated in the deeper, posterior part of the fossa bridgei and the tectosynotic fossa. In *Amia* there is no fossa developed, but the origin of the muscle corresponds topologically to the subtemporal fossa in †*Australosomus* and many fossil neopterygians. Drawings not to scale.

Internal cranial anatomy of Early Triassic species of †*Saurichthys* (Actinopterygii: Saurichthyiformes): implications for the phylogenetic placement of †saurichthyiforms

Thodoris Argyriou, Sam Giles, Matt Friedman, Carlo Romano, Ilja Kogan, and Marcelo R. Sánchez-Villagra

Additional file 1: List of new and modified characters and scoring changes

A. List of new and modified characters added to Giles et al. matrix[1]

B. List of taxon scoring changes

A. List of new and modified characters

C.20: Both nostrils accommodated within single ossification: 0=absent, 1=present (new character). In †saurichthyiforms both external nares are completely encompassed within a single ossification, historically referred to as the nasaloantorbital[2-6].

C.24: Anterior junction between supraorbital and infraorbital canal: 0=absent, 1=between external nares, 2=anterior to external nares (new character).

C.44: Bone carrying otic portion of lateral line canal extends past posterior margin of parietals: 0=absent, 1=present (new character).

C.112: Operculum: 0=absent, 1=present (new character).

C.154: Craniospinal process: 0=absent, 1=present (modified from [7])

C.159: Birfurcation of dorsal aorta into lateral dorsal aortae: 0=open in endoskeletal groove, 1=enclosed in canal, 2=below parasphenoid (state 2 added, see description in [1]). We modified this character to capture the variation in crown actinopterygians taxa that lack an aortic canal, or taxa that have an aortic canal, but whose dorsal aortae or common carotids extend ventral to the parasphenoid. In *Acipenser*, foramina for the efferent branchial arteries are variably present [8, 9], which are here accounted for similarly to the lateral dorsal aortae or common carotids, and are coded as polymorphic 1/2.

C.170: Occipital region ossification pattern: 0=basioccipital and exoccipitals as separate ossifications, 1=comineralized (new character). This character applies only to taxa with separate braincase ossifications. Acipenseriforms are coded as ?, due to the putative homologization of the occipital perichondral ossification with a compound exoccipital-epioccipital [9]. The occipital region is comineralized in polypterids [10].

C.177: [G 118] Parasphenoid: 0=terminates at/anterior to ventral otic fissure, 1=extends across ventral otic fissure, 2=extends to basioccipital, 3=extends past the occipital region, below the first 1-3 vertebrae (state 3 added).

C.181: Parasphenoid pierced by ascending common carotids: 0=absent, 1=present (new character). In †saurichthyids and likely †*Yelangichthys* the common carotids bifurcate after piercing the parasphenoid, at the level of the ascending processes (scored as present). Not to be confused with the condition in some sturgeons where the parasphenoid is pierced by the descending 1st and 2nd efferent branchial arteries, but a circulus cephalicus is absent [8, 9].

C.189: Arrangement of olfactory nerve in orbital region: 0=completely enclosed in endoskeletal olfactory canal, 1=traversing the orbit lateral to the interorbital septum, at times leaving a groove on the latter (new character).

C.204: Lateral cranial canal connects to lateral wall of braincase: 0=absent, 1=present (new character).

C.205: Intramural diverticula opening in fossa bridgei: 0=absent, 1=present (new character).

C.212: Trunk squamation: 0=complete coverage or more than six horizontal rows of scales, 1=reduced coverage (six to two scale rows), 2=trunk mostly naked (modified from [5, 7, 11]). We removed the ordering, but combined the reduced states in previous versions of this character to one. Although state 1 conflates different possible states (which need additional taxa to be accounted for), it serves test the historical hypothesis that trunk squamation reduction is homologous amongst †saurichthyiforms, †acipenseriforms and †*Birgeria* [2, 7].

C.228: Position of symplectic: 0=posterior to the posterior margin of quadrate, 1=medial to the posterior margin of quadrate. Modified from [12].

C. 268: Epineural processes: 0=absent, 1=present (from [12]). Most Paleozoic and early Mesozoic non-neopterygian actinopterygians and many teleosts bear strong posterolaterally expanding epineural processes on lateral surfaces of their neural arches.

B. List of taxon scoring changes

†*Acanthodes bronni*

C.113: ? → -

C.114: ? → -

C.115: ? → -

C.116: ? → -

Acipenser brevirostrum

C.113: 2 → -

C.130: 1 → 0

C.142: 0 → 1

C.159: - → 1/2

C.177: 2 → 3

C.198: ? → 1

C.200: ? → 0

C.201: ? → 1

C.202: ? → 0

C.203: 0 → -

C.210: - → 0

C.211: - → 1

C.213: - → 0

C.215: - → 0

C.216: - → 0

C.218: 0 → 1

C.232: 0 → 0/1

Amia calva

C.159: 0 → 2

C.177: 2 → 3

†*Amphicentrum granulosum*

C.73: 1 → 0

C.156: 1 → ?

Atractosteus spatula

C.159: 0 → 2

C.177: 2 → 3

C.188: 0 → 1

†*Birgeria groenlandica*

C.3: 0 → 1

C.4: 0 → -

C.5: 1 → -

C.7: 0 → -

C.9: 0 → -

C.10: 0 → -

C.11: 1 → -

C.12: 0 → -

C.48: 0 → 1

C.65: 0 → 1

C.66: - → ?

C.67: - → 1

C.71: 0 → 1

C.98: - → ?

C.101: 2 → 0

C.113: 1 → ?

C.159: ? → 2

C.185: 1 → ?

C.210: 1 → 0

C.213: ? → 0

C.215: ? → 0

C.222: 0 → ?

C.246: - → ?

C.245: - → ?

†*Boreosomus piveteaui*

C.190: 1 → ?

C.233: 1 → ?

†*Chondrosteus acipenseroides*

C.29: 1 → 0

C.53: 1 → 0

C.142: 0 → ?

C.143: 0 → ?

†*Cladodoides wildungensis*

C.113: ? → -

C.114: ? → -

C.115: ? → -

C.116: ? → -

C.143: 0 → -

Elops hawaiensis

C.159: 0 → 2

†*Fouldenia ischiptera*

C.44: ? → 1

†*Fukangichthys longidorsalis*

C.224: 0 → 1

†*Hulettia americana*

C.159: 0 → 2

C.177: 1 → 2

†*Ichthyokentema purbeckensis*

C.159: 0 → 2

Lepisosteus osseus

C.159: 0 → 2

C.177: 2 → 3

C.188: 0 → 1

†*Leptolepis bronni*

C.156: 1 → 0

C.159: 0 → 2

†*Luederia kempi*

C.188: ? → 0

†*Luganoia lepidosteoides*

C.53: 0 → 1

C.54: - → 0

†*Melanecta annae*

C.38: 1 → ?

†*Mesopoma planti*

C.188: ? → 0

†*Obaichthys decoratus*

C.159: 0 → 2

†*Ozarcus mapesae*

C.113: ? → -

C.115: ? → -

C.143: 0 → -

C.144: 0 → -

†*Peltopleurus lissocephalus*

C.70: 0 → 1

C.241: 1 → ?

C.266: 0 → 1

Polypterus bichir

C.155: ? → 1

C.156: ? → 0

C.157: ? → 0

C.158: ? → 1

C.159: ? → 1

†*Saurichthys madagascariensis*

C.7: 0 → -

C.14: 1 → ?

C.21: 1 → -

C.22: 1 → -

C.63: 0 → ?

C.65: 1 → ?

C.66: 1 → ?

C.67: 1 → ?

C.102: 0 → ?

C.113: - → 2

C.114: 1 → 0

C.115: - → 0

C.116: - → 0

C.133: 0 → ?

C.138: ? → 1

C.144: 0 → -

C.177: 2 → 3

C.193: 1 → ?

C.242: 0 → ?

C.244: 1 → 0

†*Semionotus elegans*

C.177: 1 → ?

†*Watsonulus eugnathoides*

C.114: 1 → 0

C.159: 0 → 2

References

1. Giles S, Xu G-H, Near TJ, Friedman M: **Early members of 'living fossil' lineage imply later origin of modern ray-finned fishes**. *Nature* 2017, **549**(7671):265-268.
2. Stensiö EA: **Triassic fishes from Spitzbergen**, vol. 2. Stockholm: Almqvist & Wiksells Boktryckeri-A.-B.; 1925.
3. Rieppel O: **Die Triasfauna der Tessiner Kalkalpen XXV: die Gattung *Saurichthys* (Pisces, Actinopterygii) aus der mittleren Trias des Monte San Giorgio, Kanton Tessin**. *Schweizerische Paläontologische Abhandlungen* 1985, **108**:1 - 103.
4. Kogan I, Romano C: **Redescription of *Saurichthys madagascariensis* Piveteau, 1945 (Actinopterygii, Early Triassic), with implications for the early saurichthyid morphotype**. *Journal of Vertebrate Paleontology* 2016, **36**(4):e1151886.
5. Wu F, Chang M-m, Sun Y, Xu G: **A new saurichthyiform (Actinopterygii) with a crushing feeding mechanism from the Middle Triassic of Guizhou (China)**. *PloS one* 2013, **8**(12):e81010.

6. Wu F, Sun Y, Xu G, Hao W, Jiang D: **New saurichthyid actinopterygian fishes from the Anisian (Middle Triassic) of southwestern China**. *Acta Palaeontologica Polonica* 2011, **56**(3):581 - 614.

7. Gardiner B, Schaeffer B, Masserie J: **A review of the lower actinopterygian phylogeny**. *Zoological Journal of the Linnean Society* 2005, **144**:511 - 525.

8. Marinelli W, Strenger A: **Vergleichende Anatomie und Morphologie der Wirbeltiere. IV. Lieferung**. Wien: Franz Deuticke; 1973.

9. Hilton E, Grande L, Bemis W: **Skeletal anatomy of the shortnose sturgeon *Acipenser brevirostrum* Lesueur, 1818, and the systematics of sturgeons (Acipenseriformes, Acipenseridae)**. *Fieldiana: Life and Earth Sciences* 2011, **3**:1 - 168.

10. Allis EP: **The Cranial Anatomy of *Polypterus*, with Special Reference to *Polypterus bichir***. *Journal of Anatomy* 1922, **56**(Pt 3-4):189-294.143.

11. Maxwell EE, Romano C, Wu F, Furrer H: **Two new species of *Saurichthys* (Actinopterygii: Saurichthyidae) from the Middle Triassic of Monte San Giorgio, Switzerland, with implications for character evolution in the genus**. *Zoological Journal of the Linnean Society* 2015, **173**(4):887-912.

12. Arratia G: **Morphology, taxonomy, and phylogeny of Triassic pholidophorid fishes (Actinopterygii, Teleostei)**. *Journal of Vertebrate Paleontology* 2013, **33**(sup1):1-138.

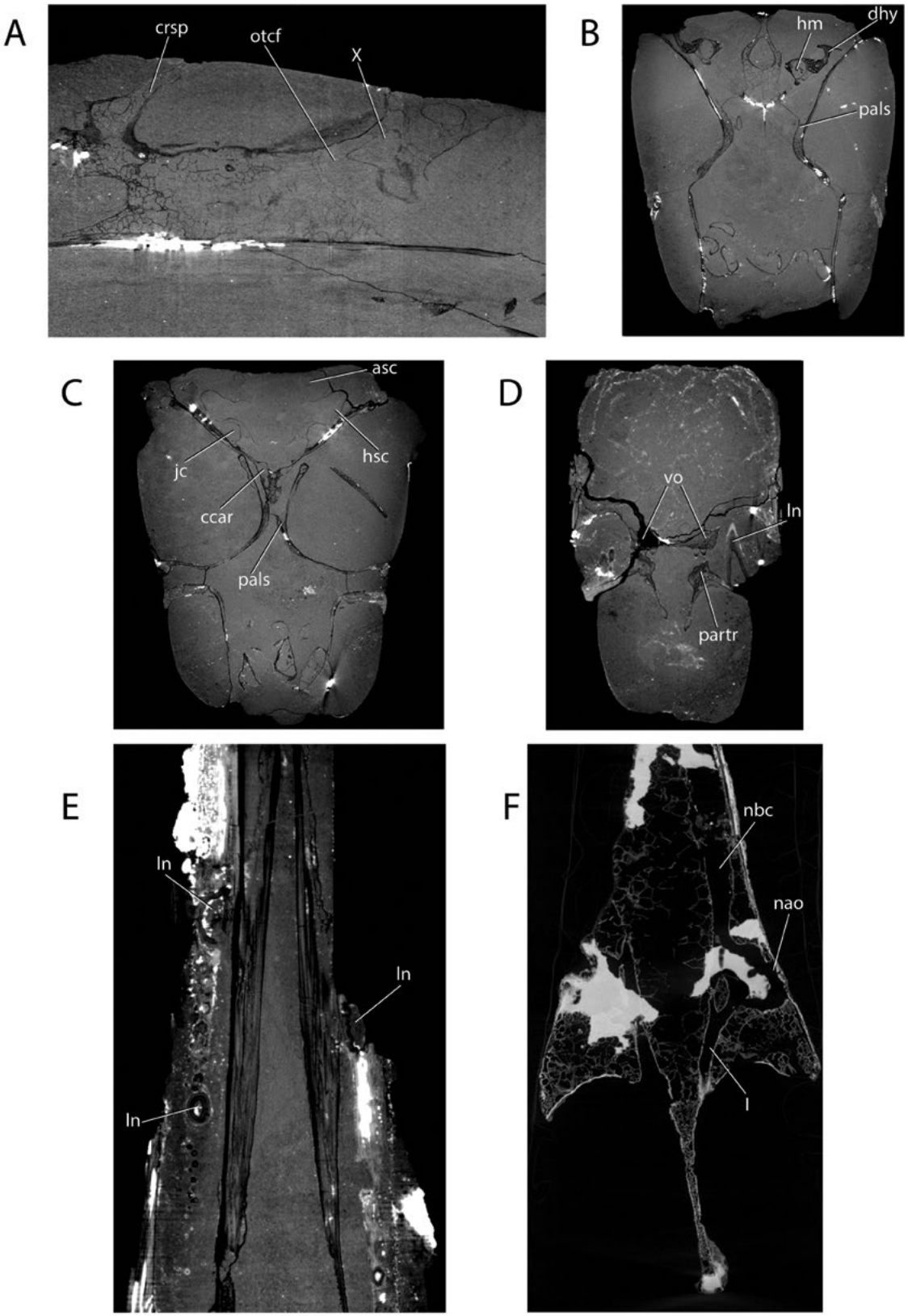
A
crsp
otcf
X
B
hm
dhy
pals
C
asc
jc
hsc
ccar
pals
D
vo
ln
partr
E
ln
ln
ln
F
nbc
nao
l

Internal cranial anatomy of Early Triassic species of †*Saurichthys* (Actinopterygii: Saurichthyiformes): implications for the phylogenetic placement of †saurichthyiforms

Thodoris Argyriou, Sam Giles, Matt Friedman, Carlo Romano, Ilja Kogan, and Marcelo R. Sánchez-Villagra

Additional file 2: Additional figures

Additional figure 1. Tomographs of †*Saurichthys* cf. *ornatus* (NHMD_157546_A) (A–E) and †*Saurichthys nepalensis* (MNHN F 1980-5) (F). **A**) Sagittal tomograph of the occipital region, showing the presence of the weakly mineralized oticooccipital fissure; **B**) Coronal tomograph of the occipital region, showing hyomandibula with fused dermohyal; **C**) Coronal tomograph of the anterior otic region, showing the semicircular canals, the jugular canal and the entrance of the common carotids; **D**) Coronal tomograph of ethmoidal region showing the paired vomers, the prearticular and a laniary of the lower jaw; **E**) Axial tomograph of ethmoidal region showing the arrangement of dentition and the presence of plicidentine in the laniaries; **F**) Axial tomograph of ethmoidal region showing the course of the olfactory and nasobasal canals. Abbreviations: **I**, olfactory nerve; **X**, vagus nerve; **asc**, anterior semicircular canal; **ccar**, entrance of common carotids; **crsp**, craniospinal process; **dhy**, dermohyal; **hm**, hyomandibula; **hsc**, horizontal semicircular canal; **jc**, jugular canal; **ln**, laniary; **nbc**, nasobasal canal; **otcf**, oticooccipital fissure; **pals**, median palatal shelf; **partr**, prearticular ridge; **vo**, vomer.

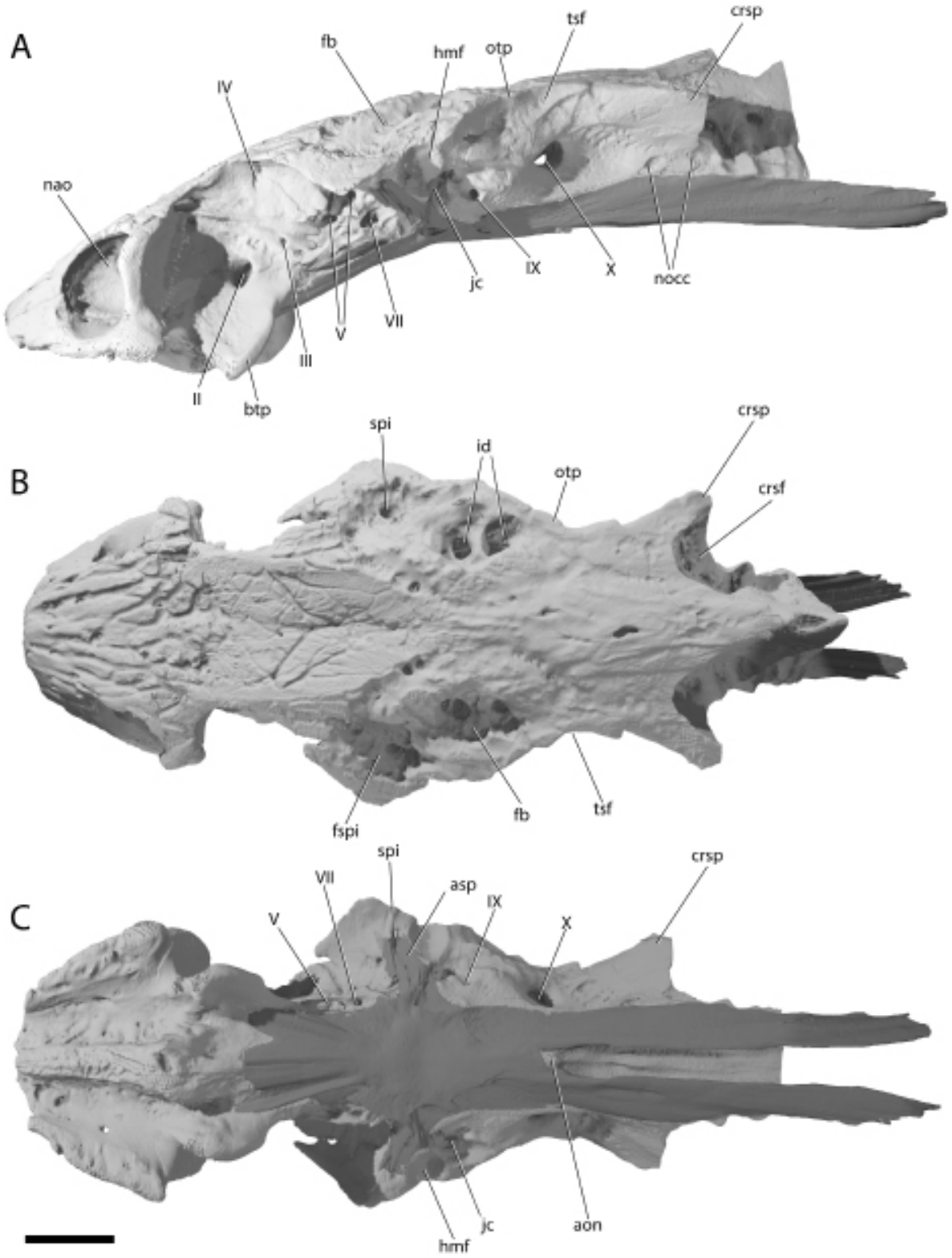
A
fb
hmf
otp
tsf
crsp
IV
nao
jc
IX
X
nocc
V
VII
III
II
btp
B
spi
id
otp
crsp
crsf
fb
tsf
fspi
C
spi
VII
asp
IX
V
X
crsp
jc
aon
hmf

Additional figure 2. Digital rendering of braincase and parasphenoid of *Acipenser brevirostrum* (FMNH 113538) in: **A**) left lateral; **B**) dorsal; **C**) ventral views. Parasphenoid in dark gray shade. Abbreviations: **II**, optic nerve; **III**, oculomotor nerve; **IV**, trochlear nerve; **V**, trigeminal nerve; **VII**, facial nerve; **IX**, glossopharyngeal nerve; **X**, vagus nerve; **aon**, aortic notch; **asp**, ascending process of parasphenoid; **btp**, basitrabecular process; **crsf**, craniospinal fossa; **crsp**, craniospinal process; **fb**, fossa bridgei; **fspi**, spiracular fossa; **hmf**, hyomandibular facet; **id**, intramural diverticulum; **jc**, jugular canal; **nao**, nasal opening; **nocc**, spinooccipital nerve; **otp**, otic process; **spi**, spiracular opening; **tsf**, tectosynotic fossa. Scale bar equals 2cm.

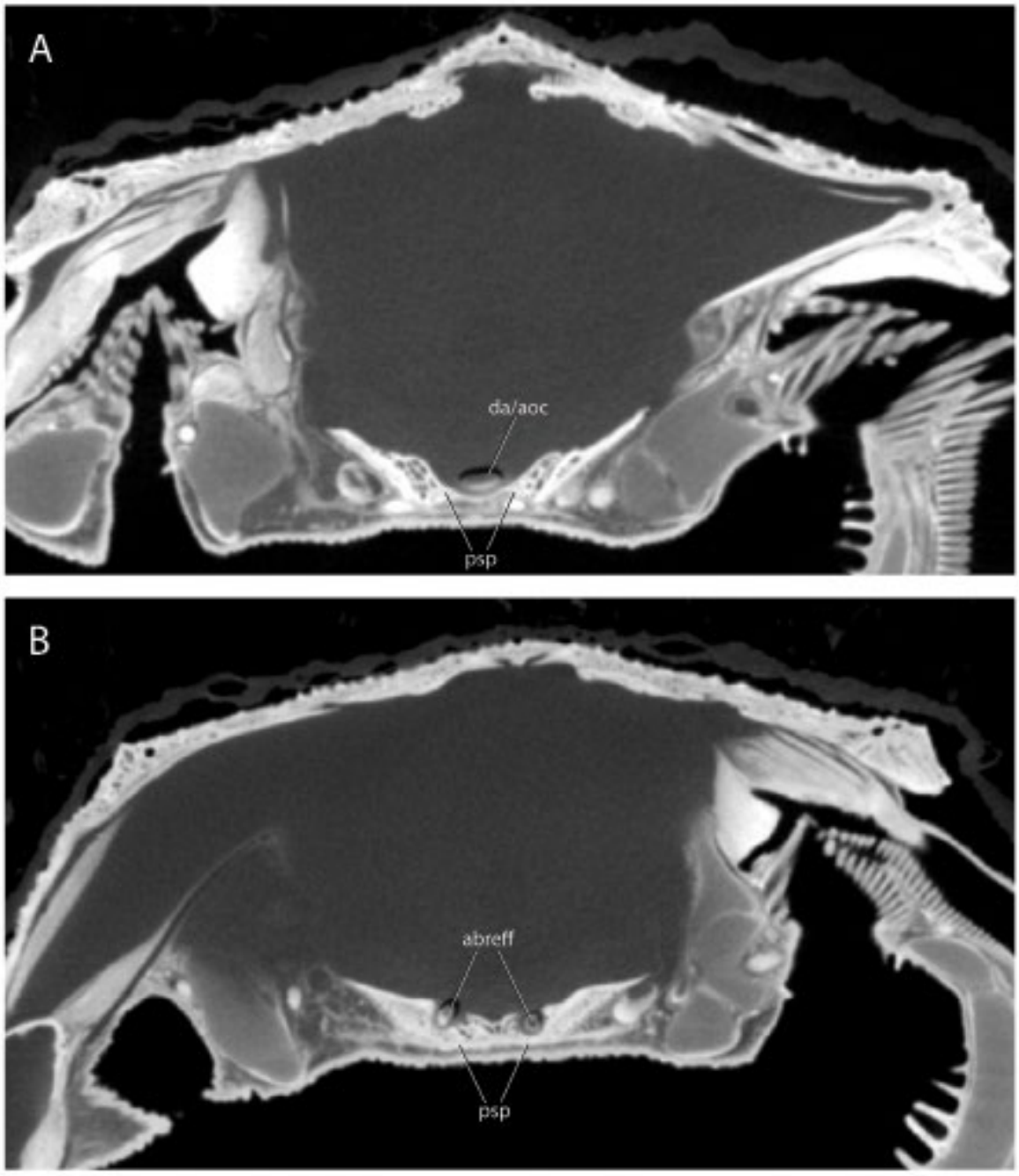
A
da/aoc
psp
B
abreff
psp

Additional figure 3. Coronal tomographs of the occipital region of PTA-stained *Acipenser brevirostrum* (UMMZ 64250), showing aspects of basicranial circulation. **A**) showing dorsal aorta enclosed in endoskeletal aortic canal; **B**) showing bifurcating efferent branchial arteries piercing parasphenoid. Abbreviations: **abreff**, efferent branchial artery; **da/aoc**, dorsal aorta/aortic canal; **psp**, parasphenoid.

CHAPTER IV

The endoskeleton of †*Brachydegma caelatum* (Cisuralian) implies earlier evolution of the sophisticated neopterygian jaw suspension

Thodoris Argyriou*, Sam Giles, Matt Friedman

Ray-finned fishes (Actinopterygii) are nowadays represented by three evolutionary lineages: the basally diverging Cladistia (bichirs and reedfish, 14 spp.), the Chondrostei (sturgeons and paddlefishes, 27 spp.), and the markedly speciose Neopterygii (Holostei [gars and bowfin], 8spp. + Teleostei, ~32,000 spp.) [1]. The success of neopterygians is often attributed to specializations related to body shape and fin structure, and also innovations in their feeding apparatus, which allowed for better prey capture and manipulation, and removed functional constraints for further anatomical and ecological diversification [2-7]. The presence of an independent symplectic in the hyoid arch, and its involvement in the lower jaw joint, have been long and weightily established as essential components of the neopterygian phylogenetic and morphofunctional hallmark [4,8-12]. Moreover, the decoupling of the interhyal from the symplectic, and the displacement of the former in the posteroventral tip of the hyoid bone is thought to have maximized jaw opening and orobranchial expansion efficiency in neopterygians[13]. The seemingly clear-cut restriction of these features in neopterygians was among the arguments mustered by Patterson to argue against the utility of fossils in tracing homologies[9]. However, the limited documentation of such accessory hyoid elements in fossils, their conflicted homology in extant actinopterygians, and a profound gap of knowledge pertaining to the endoskeletal character complex of Paleozoic crown actinopterygians, cast doubts on the actual synapomorphy value of these and other historically salient phylogenetic and functional traits.

Documentation of endoskeletal structures from rare, three dimensionally-preserved fossils is crucial for achieving much needed phylogenetic resolution stemward of the Middle–Late Triassic neopterygian radiation [7,14,15], and for understanding the distribution and the timing of origin of important morphofunctional specializations. Previous research has mostly focused on largely primitive, Devonian–Carboniferous forms [16-23], or more anatomically derived Triassic taxa [24-30]. Although fossil-informed, molecular calibrations place the origin of the actinopterygian crown group between the Silurian and the Carboniferous [28,31,32], few Paleozoic actinopterygians (e.g., †*Platysomus* [33], †*Amphicentrum* [34], †*Discoserra* [35,36], †*Ebenaqua* [37], †*Acentrophorus*[38]) have been

variably resolved at the stem of crown lineages [28,36,39,40], but their endoskeletal anatomy is poorly understood at best. Furthermore, the Permian represents a considerable gap for endoskeletal information for actinopterygians. The isolated and largely anatomically generalized braincase of †*Luederia*[41] is the best known example from this interval, with minimal information deriving from other fossils [42,43]. As a result, a morphological bridge between the early part of the actinopterygian evolutionary history and their post-Paleozoic radiations is still lacking, hampering the resolution of basal actinopterygian interrelationships.

We employ μCT to study the endoskeletal anatomy of †*Brachydegma caelatum*, which is represented by two specimens from the Cisuralian (early Permian) Red Beds of Texas, USA [44]. Previous anatomical interpretations of this taxon rested solely on the dermal skeleton of the type specimen [36,44]. Still, †*Brachydegma* has had a particularly volatile systematic history. Early, non-cladistic works have associated †*Brachydegma* with †elonichthyid [44] or †acrolepidid [45] generalized actinopterygians. A more recent anatomical and systematic reappraisal of †*Brachydegma* assigned it to crown neopterygians, and halecomorphs in particular, and proposed it as a minimum age marker for the holostean-teleost split [36]. Characters evoked to support this topology included the presence of: a large median gular; a posteriorly indented and free maxilla; an antorbital with a tapering anterior process; an neopterygian-like coronoid process [36]. However, contemporary works have challenged the halecomorph [31,40], or total-group neopterygian [28,32] affinities of †*Brachydegma*. Our work revealed, for the first time, the character-rich anatomy of the braincase, mandibular and hyoid arches, branchial skeleton, pectoral girdle and the anterior portion of the axial skeleton of †*Brachydegma* (Figs. 1–3, Suppl. Figs. 1–4). This allows for a more secure systematic assessment of the latter within the actinopterygian crown, and provides unique insights into the character complex of early crown actinopterygians. Critically, novel μCT data from †*Brachydegma* and other fossil and extant taxa shift the established paradigm for the distribution and homology of accessory hyoid elements, and relevant feeding specializations in actinopterygians.

Results

Systematic paleontology.

Actinopterygii Cope 1887[46]

†*Brachydegma caelatum* Dunkle 1939[44]

Material. MCZ_VPF_6503, †*Brachydegma caelatum*, holotype, preserving cranial and anterior postcranial skeleton; MCZ_VPF_6504, †*Brachydegma caelatum*, paratype, preserving cranial and anterior postcranial skeleton.

Locality and geological background. Both specimens of †*Brachydegma* come from the northern deposits of the Clear Fork Formation (Formerly part of Arroyo Fm, see [47]), Indian Creek, Baylor County, Texas [44]. These deposits are dated as Artinskian–Kungurian (=late Cisuralian) [47]. Clear Fork Fm is characterized by ferruginous, calcitic–sandy, terrigenous facies [44,47,48]. The deposits of Clear Fork Fm are broadly assigned to coastal floodplain environments[47]. The accompanying vertebrate fauna[48], which also includes †xenacanths, lungfishes, and emblematic tetrapods such as †*Dimetrodon*, emits a rather terrestrial signal.

Revised diagnosis. An early crown actinopterygian characterized by the unique set of: tripartite occipital region; endoskeletal aortic canal; absence of a posterior myodome; absence of a dermal or endochondral basipterygoid process; parasphenoid reaching basioccipital; lateral dorsal aortae extending below parasphenoid; cleaver-shaped, immobile maxilla; coronoid process absent; four to five suborbitals; two to three accessory opercles; unfused dermohyal on perforate hyomandibula; sub-parallel arrangement of accessory hyoid elements; four branchial arches, including a fourth hypobranchial; broad clavicles; unjointed pectoral radials; non-lobate fins.

Description of endoskeletal anatomy. The occipital region (Figs 1b–c; 2c–f) comprises three distinct ossifications, a basioccipital and a pair of exoccipitals, comparable to non-teleost neopterygians [5,30,49]. Its anterior margin is well-demarcated, putatively indicating an open oticooccipital fissure. The posteroventral part of the basioccipital projects posteriorly and forms a short endoskeletal aortic canal. The exoccipitals form the dorsal margin of the notochord foramen and surround the foramen magnum. Lateral to the foramen magnum, the exoccipitals form posteriorly expanding pads. Anteriorly, the exoccipitals gain width and flare laterally, but do not enclose the vagus nerve, unlike in most neopterygians[11,33,43]. A ridge is formed along the dorsal contact between the exoccipitals. Only non-attributable fragments remain of the otic capsule of both specimens. The anterior part of the postorbital process of MCZ_VPF_6504 exhibits a short anteroventrally–posterodorsally running spiracular canal. The basisphenoid forms two pillars that are pierced near their base by a canal, for the internal carotid and/or the efferent pseudobranchial

artery. The posterior myodome is absent. There are separate openings for the right and left optic nerves rather than a median opening. The interorbital septum is robust, but still not broad as that of polypterids and fossil relatives [28,50], and *Acipenser* (personal observations on UMMZ 64250).

The parasphenoid (Figs. 1c,d; 2c–f) forms a posterior stem, which terminates below the basioccipital, a condition present in all crown actinopterygians [27,28,30,50,51], but also in Paleozoic forms of unclear relationships like †platysomids [33], †*Amphicentrum* [34] and likely †*Sphaerolepis* [52]. The lateral dorsal aortae of †*Brachydegma* extended along the ventral surface of the parasphenoid, divided by a median keel. The posterodorsally directed ascending processes are short, and a dermal basipterygoid process is not developed. Unlike most Triassic neopterygians[26,28], and living holosteans [5,49], the parasphenoid of †*Brachydegma* is completely edentulous. It shares with †parasemionotids [27,53] and crownward holosteans [5,49,54] notches for the internal carotids and/or the efferent pseudobranchial arteries, which suggest that the basicranial circulation was largely conducted ventral to the parasphenoid. The parabasal canals on the dorsal surface of the anterior process of the parasphenoid extend anteriorly and then lateroventrally, like in e.g., *Amia* [55].

The palate (dermal and endochondral) of †*Brachydegma* (Figs. 1e,f; 2j,k) is deep along most of its length, forming a convex dorsal margin, and lacking a markedly depressed infraorbital portion, like †*Fukangichthys* [28]. There are no processes for articulation with the braincase and parasphenoid. Individual palatal ossifications could not be reconstructed. Ventrally, the palate forms flanges that abut the prominent medial shelf of the maxilla. This indicates a strong connection between the two, rendering maxillary kinesis unlikely. The adductor foramen is well-constricted by dermal bones and rather narrow, suggesting the presence of a smaller adductor muscle than that of neopterygians[3,49]. On the medial surface of the anterior portion of each palate there is a broad entopterygoid toothplate, similar to that of †*Watsonulus* [27].

The hyomandibula (Figs. 1a; 2a,h) is boomerang shaped, perforate, and forms a well-developed opercular process. An unfused dermohyal sits on the lateral surface of the dorsal limb of the hyomandibula. Two endochondral elements (Fig. 3a–c) are associated with the ventral tip of the hyomandibula, and lie in a subparallel manner to each other, on the left side of the type specimen. A more robust, subquadrangular symplectic articulates with the anteroventral tip of the hyomandibula. Its anterior surface forms a keel, which articulates with a groove on the

posterior surface of the quadrate. The anteroventral tip of the symplectic forms a condyle, which inserts in a facet on the posterior surface of the articular, while its posteroventral tip forms a thin, ventrally directed process, which contacted the posterior surface of the articular. Dorsolaterally, the symplectic bears a faint groove, likely for the passage of the afferent mandibular artery. The interhyal is rod-shaped, and issues from the posteroventral tip of the hyomandibula. The arrangement of the two intermediate hyoid ossifications is remarkably similar to that of Triassic neopterygians [4,27,53,56] (Fig. 2d–f). A single, laterally grooved, plate-like ceratohyal is ossified on each side of the suspensorium (Fig. 1h; 2i), like in e.g., †*Fukangichthys* [28].

The branchial skeleton of the type specimen is nearly complete. Only four branchial arches are developed (Fig. 1h; Suppl. Fig. 4a–e). The first two basibranchial ossifications are preserved in the type specimen, while a putative third basibranchial is seen in the paratype. The basibranchials are subtriangular in cross section, with a flat dorsal surface. The first basibranchial is the smallest of the series. The second basibranchial bears a mid-length constriction. The ceratobranchials are curved, potentially conforming to the deeper shape of the head. Their posteroventral surface is grooved, whereas anterodorsally they accommodate a series of small, multicuspidate rakers. The dorsal gill arches are partially disarticulated. The epibranchials form uncinate processes, with the first two being markedly well-developed, like in †*Australosomus*[26]. The uncinate processes of the second and third epibranchials are bent medially. The fourth epibranchial is short and wide and forms a long and thin anterior process, and a laterally extending plate for the passage of the efferent branchial artery. Unlike in holosteans [5,49], no toothplates are associated with the epibranchials. The first infrapharyngobranchial is rod-shaped and edentulous. The second infrapharyngobranchial is wider and plate-like, and bears teeth on its ventral surface. Additional rod- or plate-like elements are preserved more posteriorly must correspond to supra- or infrapharyngobranchials. Among them is a conspicuously curved and stout element, which might be a second suprapharyngobranchial.

The dentary (Figs. 1g; 2g; Suppl. Fig. 4f) is the principal bone of the lateral surface of the jaw, and bears a single row of caniniform teeth. The prearticular forms the mesial surface of the lower jaw, but no teeth were apparent in the tomograms. The presence or absence of coronoids could not be ascertained. A surangular on the posterodorsal corner of the jaw and an angular on the posteroventral are visible externally in MCZ_VPF_6503, but sutures are not apparent in

tomograms. There is no coronoid process. The deep adductor fossa is surrounded by the articular posteriorly, the prearticular medially, and the surangular and dentary laterally. Apart from the two depressions for the quadrate, the articular bears a posterior facet for the insertion of the condyle of the symplectic.

The pectoral girdle (Fig. 1i) is incompletely preserved in †*Brachydegma*. The clavicles are broad triangular plates covering the anterior process of the massive cleithra, resembling the primitive [18,25], and non-neopterygian condition [51,57], retained in †*Watsonulus* [27] and stem-teleosts[56]. Little can be said about the endochondral portions of the girdle. A single series of rod-like radials lie subparallelly to each other. A short, stocky, and likely imperforate propterygium is present.

The notochord is unconstricted, and only arcual elements are observed (Suppl. Fig. 4g,h). We did not observe supraneurals in the anterior vertebral segments. Dorsally, the first abdominal vertebral segment comprises a stout, paired basidorsal bearing a short neural spine and a prezygapophysis. More posterior basidorsals exhibit thinner but longer neural spines and thinner prezygapophyses. Comparably to most crown actinopterygians, excluding teleosts [58], epineural processes are not developed. The basiventrals of the first arch are fused to form a median hemi-cylindrical element, which lacks parapophyses. However, all remaining basiventrals are paired and bear short, lateroventrally expanding parapophyses, though no ossified ribs were observed. The rhomboid scales (Suppl. Fig. 4i) of †*Brachydegma* exhibit a dorsal articular peg and a small anterodorsal process. Their posterior scale margin forms acute serrations.

Phylogenetic results

Our parsimony analysis recovered 1211 trees of 1434 steps (Fig. 5). In our strict consensus, †*Brachydegma* falls on a basal polytomy with †scanilepiforms and polypterids on the basis of: presence of three or more suborbitals (C.56); absence of a posterior myodome (C.139); presence of four ceratobranchials (C.230); anterior fin rays not embracing propterygium (C.245). This topology receives low nodal support (Bremer Decay Index [BDI]=1). We confidently reject an association with either the neopterygian crown or total group [36,40], or even the actinopteran stem [28]. In our phylogenetic hypothesis, the neopterygian total group (BDI=1) loses resolution from analyses conducted with earlier versions of this matrix and a similar taxonomic sample [28] (Argyriou et al. submitted). It forms a large basal polytomy, reflecting uncertainty in the placement

of the deep-bodied †*Platysomus* and †*Eurynotiforms* (sensu[59]) at its stem. The neopterygian total group is diagnosed on the basis of: angular being the only infradentary in the lower jaw (though a surangular is present in crown neopterygians) (C.91); presence of a basipterygoid process (C.142); presence of a posttemporal fossa (C.173). None of these states was observed in †*Brachydegma*. The neopterygian crown is supported by eight synapomorphies: i) mobile maxilla (C.74); ii) peg-like process on maxilla (C.75); iii) presence of two infradentaries on lower jaw (C.91); iv) subopercle with an anterodorsal process (C115); v) preopercle with pronounced ventral limb (C.118); vi) interopercle present (C.121); vii) ascending internal carotids piercing parasphenoid (C.182); viii) two ceratohyal ossifications (C.221). For all these characters, †*Brachydegma* shows the primitive condition.

Discussion

The morphological character complex of early crown actinopterygians remained largely hypothetical, up until now. The rich dermal and endoskeletal anatomical information now available for †*Brachydegma*, establishes it as the oldest adequately known crown actinopterygian, and provides a much needed basis for comparison with Paleozoic forms. Our reappraisal of the systematic affinities of †*Brachydegma* contrasts previous hypotheses of close relationships with either the neopterygians [31,36,40], or even actinopterans [28,32]. Instead, it recovers †*Brachydegma* nested within polypteriforms + †scanilepiforms. Despite obvious similarities with polypterids and fossil relatives (e.g., presence of more than three suborbitals, absence of a posterior myodome, presence of only four ceratobranchials)[28,50], †*Brachydegma* exhibits features that are best explained as reflecting the crown actinopterygian bauplan. Chief among them is the presence of a double jaw joint, involving a symplectic, and the subparallel arrangement of symplectic and interhyal. These conditions are for the first time documented, in conjuction, in a non-neopterygian actinopterygian. Their occurrence in †*Brachydegma* helps illuminate the homology of the accessory hyoid elements of actinopterygians, which has been debated for decades [4,8,10,12,13,57,60,61]. Moreover, it suggests that some of the feeding specializations, which likely contributed to the meteoric radiation of neopterygians in the Triassic[7,13,15], were inherited from a generalized crown actinopterygian ancestor.

In †parasemionotids, holosteans and stem teleosts, the symplectic articulates with the

anteroventral head of the hyomandibula, extends behind the posterior surface of the quadrate, and articulates with the lower jaw, forming a double jaw joint [4,5,8,10-13,18,27,49,53,56] (Fig. 3). Ontogenetically, the symplectic starts as an anteroventral outgrowth of the hyosymplectic cartilage, but later detaches to form an independent element [62-64]. The neopterygian symplectic functions largely as a brace for the mandibular arch, while compensating for the movement of palate and jaws relative to the hyomandibula [3,13]. In polypterids, a symplectic does not develop [57]. In acipenseriforms, a hypertrophied cartilage lies in close association with the anteroventral tip of the hyomandibula and suspends the mandibular arch. Due to its topology and ontogenetic history, this cartilage has been homologized with the symplectic [13,60,65]. It was later reassigned to the interhyal, following the attribution of the small, globular cartilage, which lies immediately ventral to it, to the posterior ceratohyal [8,10,12,61]. The neopterygian interhyal articulates with the posteroventral tip of the hyomandibula, and suspends the ventral hyoid elements from the latter [4,5,8,10-13,18,27,49,53,56]. It is cartilaginous in holosteans [5,49]. The interhyal is likely of compound embryonic origin, deriving from both the hyoid arch and the pharyngeal epithelium [62,63], but is thought to be embryologically linked with the ceratohyal(s) [66]. The interhyal helps decouple the movement of the ventral hyoid elements from the mandibular arch, aiding in jaw depression [3,13]. The interhyal of polypterids is arranged in a similar manner to that of the neopterygians [28,50,57]. In acipenseriforms, the small globular cartilage intercalated between the ceratohyal and the hypertrophied cartilage that suspends the jaws has been variably considered an interhyal, on topological grounds [13,65], or a posterior ceratohyal, due to its association with a branchiostegal ray in paddlefishes [8,10,12,60,61,67].

The presence of a symplectic, in close association with the ventral–anteroventral tip of the hyomandibula and the palatoquadrate, was reported by early 20th century workers in some Paleozoic–Triassic anatomically generalized actinopterygians, but evidence was scant [25,26,68]. Additional documentation was provided by Véran, who hypothesized the linear arrangement of different hyoid arch elements as the primitive actinopterygian condition, retained in modern acipenseriforms [13]. However, given the scarcity of data from fossils, infuential paleoichthyologists dismissed previous reports of a symplectic in non-neopterygian ray-fins as misidentifications, and homologized the symplectic of previous authors with the interhyal [8-12,18]. Their main argument for fossils was the absence of a break in the perichondral lining of the so-called symplectic, which would imply the presence of a cartilaginous cap and, thus, a functional joint between the symplectic

and its adjacent jaw structures [9,11]. †*Pteronisculus* was used as a fossil example to support these views [8]. The symplectic was established as a neopterygian neomorph, and its involvement in the lower jaw joint as a key halecomorph synapomorphy [4,8-12]. The symplectic and double jaw joint of coelacanths [13] were deemed homoplasic. These ideas have gained much traction in the literature, and were followed in subsequent phylogenetic works [10,12,19,28,36,40,69,70] (but see [27]).

Our novel data (Fig. 3) from †*Brachydegma*, †*Pteronisculus*, *Acipenser*, and a †parasemionotid (early neopterygian), demonstrate that the presence of a symplectic and a double jaw joint are widespread in actinopterygians. This reinforces historically dismissed notions that such features are primitive for actinopterygians, or even osteichthyans [13,27]. By comparison with fossil and extant forms, we suggest that the symplectic can be identified across a large part of the actinopterygian phylogeny on the basis of: i) its position, being anteroventral to the hyomandibula, posterior to the palatoquadrate, and posterodorsal to the lower jaw; ii) the presence of an anterior–ventral condyle for articulation with the articular; iii) the presence of a dorsolateral groove for the passage of the afferent mandibular artery [13]. These three criteria apply to all taxa we examined, except *Acipenser*, and agree with overlooked assessments in fossils [13,25]. The involvement of the symplectic in the jaw joint of †*Brachydegma*, and the presence of an interhyal, lying sub-parallel to the symplectic, are reminiscent of the generalized neopterygian condition [4,8,27,49,56], exemplified by †parasemionotids. The only notable difference between the two is the presence of a ventral process on the symplectic of †*Brachydegma*, which abutted the posterior surface of the articular, potentially limiting the jaw gape. The posteroventral process of the symplectic is plesiomorphic for crown actinopterygians [13], as it is present in generalized actinopterygians like †*Pteronisculus*[13,25], but it is absent in neopterygians[4,5,27,49,53,56].

We consider the hypertrophied cartilage of acipenseriforms (Fig. 3j–l) homologous to the symplectic of other actinopterygians. In addition to comparable ontogenetic history, topology and relationship with neighboring skeletal elements [13,60,65], its relationship to the afferent hyoidean artery in *Polyodon* [71] is similar to that of other actinopterygians[13]. The homologization of the cartilage connecting the symplectic and the ceratohyal in acipenseriforms with the interhyal of other actinopterygians constitutes the most parsimonious option, because it: i) is the only element connecting the derivates of the hyosymplectic anlage with the ventral hyoidean

elements; ii) lacks a ligamentous connection with the lower jaw (the mandibulohyoid ligament attaches to the ceratohyal)[13,61]; iii) mineralizes independently from the ceratohyals [61]. The association of the interhyal of paddlefishes with a branchiostegal ray[8,10,12,60,61,67] is conceivably secondary, as suggested by the independent origin of this condition in some modern teleosts[72], and the tight ontogenetic relationship between interhyal and ceratohyals[66]. It remains uncertain whether the linear arrangement of acipenseriform hyoidean elements reflects the hypothesized plesiomorphic condition[13]. The documentation of blastematic connections between the symplectic and the interhyal at an early ontogenetic stage of neopterygians [62] could hint at heterochronic control (paedomorphism) over the symplectic/interhyal linear geometry of acipenseriforms. Alternatively, the acipenseriform condition might relate to function. Following the reappraisal of the acipenseriform hyoidean anatomy, we suggest that the presence of two ceratohyal ossifications is a neopterygian synapomorphy.

In †*Brachydegma*, polypterids and neopterygians, the position of the interhyal, posteroventrally to the hyomandibula and posteriorly to the symplectic (when present), maximizes its lever properties relative to the hypothesized plesiomorphic serial arrangement of generalized actinopterygians[13]. This allows for more efficient jaw depression and larger expansion of the oropharyngeal cavity, which, in turn, aids in prey manipulation and conceivably in suction feeding[2,3,13,73]. This sophisticated anatomical modification is better explained as a crown actinopterygian trait, although the possibility of an independent acquisition due to the evolution of a subvertical suspensorium cannot be ruled out. The strikingly long interhyal of †*Brachydegma*, relative to that of e.g., †parasemionotids, could imply a hyper-piscivorous lifestyle[73], or could constitute a compensation for the lack of an interopercle, which contributes to the auxiliary jaw depression mechanism of neopterygians[2,3].

†*Brachydegma* is characterized by a peculiar mosaic of braincase and parasphenoid characters, which could hint at generalized crown actinopterygian conditions, or alternatively reflect systematic uncertainties. It hosts the oldest occurrence of differentiated endochondral ossifications in the occipital region, resembling neopterygians [5,30,49]. However, the co-ossified occiput of polypterids[50], †saurichthyiforms (Argyriou et al. submitted), and †parasemionotids[27], and the highly apomorphic occiput of acipenseriforms [51], imply a complex evolutionary

and developmental history for this region of the actinopterygian skull. The bifurcation of the dorsal aorta into lateral dorsal aortae occurs below the posterior stem of the parasphenoid in †*Brachydegma*, resembling the condition seen in actinopterans [30,55] (Argyriou et al. in prep) and not polypterids[50]. The endoskeletal spiracular canal of †*Brachydegma* supports the secondary loss of spiracular constriction in polypterids [28]. The absence of any form of basipterygoid process is also explained as a generalized crown actinopterygian feature, as it is widespread around the base of the actinopterygian crown (see †*Australosomus* [26], †*Brachydegma*, †*Birgeria*[26], †saurichthyids[24], polypterids[50] and acipenseriforms[51]). The posterior parasphenoid stem that reaches the basioccipital, clearly differentiates †*Brachydegma* from generalized Paleozoic–early Mesozoic actinopterygians [17,18,25,26,41]. The occurrence of this feature in Carboniferous taxa like †*Sphaerolepis* [52], †*Platysomus* [33] and †*Amphicentrum* [34] could indicate crown membership.

Reconstructions of branchial skeletons of Paleozoic–early Mesozoic ray-fins are scarce in the literature, since this part of the skeleton is rarely preserved in an identifiable state [17,18,24-26,28,68] (Argyriou et al. submitted). As a result, hypotheses on the evolution of gill arches rely largely on data from living taxa [5,49,50,74]. The nearly complete branchial skeleton of the holotype of †*Brachydegma* represents one of the best examples from the Paleozoic. Although it shares multiple (two or three) basibranchial and four hypobranchial ossifications with most Permian–Triassic actinopterygians [25,26,28] and most teleosts [74], it is completely missing elements of the fifth gill-arch. The loss of the fifth arch is characteristic for Cladistia [28,50] and potentially †*Birgeria* [68]. The four epibranchials of †*Brachydegma* reflect the generalized actinopterygian condition [5,26,49,51,74], differing from the greatly reduced epibranchial series of polypterids [50], and putatively †*Birgeria* [68]. Neopterygians exhibit enlarged tooth patches associated with the dorsal gill arches [5,49,74], which are absent in †*Brachydegma*. Additionally, suprapharyngobranchials are absent [49] or do not ossify [5] in modern holosteans, whereas only the anterior suprapharyngobranchial ossifies in modern teleosts [74]. The overall anatomy of the dorsal gill skeleton of †*Brachydegma* appears generalized, though the distribution of dorsal gill-arch characters needs to be investigated in early neopterygian fossils.

In summary, †*Brachydegma* shows conspicuous anatomical similarities with polypterids + †scanilepiforms[28] that imply a closer relationship with the latter, contrasting all previous hypotheses for its systematic placement[28,31,32,36,40,44,45]. Yet, other anatomical features related to its braincase,

hyoidean and branchial endoskeleton show a wider distribution across the actinopterygian crown and its immediate stem, hinting at their likely presence in generalized crown actinopterygians. This new information will be pivotal for the recognition of crown actinopterygians in the Paleozoic. Our re-appraisal of the distribution and homology of a symplectic and a double jaw joint in actinopterygians weakens historical arguments for placing Early Triassic forms, like †parasemionotids, to crown neopterygians[4,8,9,11]. The neopterygian-like arrangement of accessory hyoidean elements in †*Brachydegma* implies a gradual rather than saltatory evolution of the complex, suction feeding-aided neopterygian feeding apparatus[2,3,6,13]. The hyoid-arch related morphological groundwork underpinning the latter was conceivably established in early crown actinopterygians, but was further furnished with a mobile maxilla and an interopercle in neopterygians[3,13]. Ironically, the double jaw joint of †*Brachydegma* highlights the potential of mosaic forms from the fossil record for toppling historical synapomorphies established on modern organisms. It also represents a case study for the importance of fossils in the study of homology of critical anatomical structures.

Material and Methods

Institutional abbreviations. MCZ: Museum of Comparative Zoology, Harvard University, Cambridge, Massachusetts, USA; NHMD: Natural History Museum of Denmark, University of Copenhagen, Copenhagen, Denmark; UMMZ: University of Michigan Museum of Zoology, Ann Arbor, Michigan, USA.

Comparative material. NHMD 73588 A, †*Pteronisculus gunnari*, holotype preserving cranial skeleton, Early Triassic, East Greenland; NHMD 74424 A, †Parasemionotidae indet. Early Triassic, East Greenland; UMMZ 64250, *Acipenser brevirostrum*, scan of PTA-stained head.

X-ray computed microtomography. µCT of the two specimens of †*Brachydegma* was performed with a Nikon XTEC 225 scanner at the CTEES lab of the University of Michigan. The parameters are as follows: MCZ_ VPF_6503: 200Kv, 200uA, 1.25 mm copper filter; MCZ_ VPF_6504: 215Kv, 265uA, 3.5 mm copper filter. The head of *Acipenser brevirostrum* (UMMZ 64250) was also scanned using the same facilities, and the parameters are: 75Kv, 290uA, no filtering. µCTs of †*Pteronisculus gunnari* (NHMD 73588 A) and the †parasemionotid (NHMD 74424 A) were performed at the University of Bristol using a XX scanner. The parameters are as

follows: NHMD_XXX: XXXKv, XXuA, XX copper filter; NHMD_XXX: XXXKv, XXuA, XX copper filter. The resulting tomograms were processed in Mimics (biomedical.materialise.com/mimics; Materialise, Leuven, Belgium) for the creation of three-dimensional, digital anatomical models. The reconstruction process of the two †*Brachydegma* specimens was challenging, since the accommodating matrix is particularly rich in metallic content. In the case of MCZ_VPF_6503, the external surfaces of endoskeletal elements are lined with a dense mineral layer, hampering beam penetration and resolution of smaller structures, such as nerve foramina. However, we were able to reconstruct the gross morphology of the endoskeleton. The completed models where exported in .ply format, and processed in Blender (blender.org) for imaging.

Phylogenetic analysis. For analyzing the interrelationships of †*Brachydegma* in a broader osteichthyan context, we modified an already existing, large-scale phylogenetic matrix[28](Argyriou et al. submitted). The matrix was edited in Mesquite[75], and the parsimony analyses were performed with 'New Technology Search' implemented in TNT[76]. We placed an outgroup constraint, to ensure the monophyly of Osteichthyes. Initial trees were created by 1000 random addition sequences using all four algorithms. The following 2x3 rounds of analyses were conducted using an alternation of 1000 iterations of 'Ratchet' and 'Sectorial Search' algorithms, and were always complemented by the 1000 iterations of 'Tree Fusing'. Suboptimal trees up to 10 steps longer were kept during each round of analysis, and were used at the end to calculate Bremer supports. Bootstrap values were calculated by reanalyzing the matrix with 1000 iterations of the 'Traditional Search' algorithm.

Acknowledgements

S. Pierce (MCZ), D. Nelson, (UMMZ), Kristian M. Gregersen and Bent E. K. Lindow (both NHMD) are thanked for kindly providing access to fossil and/or recent material. M. R. Sánchez-Villagra, C. Romano (both PIMUZ), T. Simoes, O. Vernygora and T. Miyashita (all three University of Alberta) are thanked for useful discussions. The Willi Hennig Society is acknowledged for making TNT available free of charge. This research was supported by P1ZHP3_168253 Swiss National Science Foundation doctoral mobility grant to T.A.

References

1 Nelson, J. S., Grande, T. C. & Wilson, M. V. H. *Fishes of the world*. 5th edn, (John Wiley & Sons, Inc., 2016).

2 Lauder, G. V. Pattern of evolution in the feeding mechanism of actinopterygian fishes. *American Zoologist* **22** (1982).

3 Lauder, G. V. Evolution of the feeding mechanism in primitive actinopterygian fishes: a functional anatomical analysis of *Polypterus*, *Lepisosteus*, and *Amia*. *Journal of Morphology* **163**, 283-317 (1980).

4 Patterson, C. in *Interrelationships of fishes* (eds P H Greenwood, R S Miles, & Colin Patterson) 233-305 (Academic Press, 1973).

5 Grande, L. An empirical synthetic pattern study of gars (Lepisosteiformes) and closely related species, based mostly on skeletal anatomy: the resurrection of Holostei. *American Society of Ichthyologists and Herpetologists Special Publication 6 Copeia Suppl* **10**, 871 (2010).

6 Schaeffer, B. & Rosen, D. E. Major Adaptive Levels in the Evolution of the Actinopterygian Feeding Mechanism. *American Zoologist* **1**, 187-204 (1961).

7 Tintori, A. Fish biodiversity in the marine Norian (Late Triassic) of northern Italy: The first Neopterygian radiation. *Italian Journal of Zoology* **65**, 193-198, doi:10.1080/11250009809386812 (1998).

8 Patterson, C. Morphology and Interrelationships of Primitive Actinopterygian Fishes. *American Zoologist* **22**, 241-259 (1982).

9 Patterson, C. Bony Fishes. *Short Courses in Paleontology* **7**, 57-84, doi:10.1017/S2475263000001264 (1994).

10 Gardiner, B., Schaeffer, B. & Masserie, J. A review of the lower actinopterygian phylogeny. *Zoological Journal of the Linnean Society* **144**, 511 - 525 (2005).

11 Gardiner, B. G., Maisey, J. G. & Littlewood, D. T. J. in *Interrelationships of fishes* (eds MLJ Stiassny, LR Parenti, & G. David Johnson) 117-146 (Academic Press, 1996).

12 Gardiner, B. G. & Schaeffer, B. Interrelationships of lower actinopterygian fishes. *Zoological Journal of the Linnean Society* **97**, 135-187, doi:10.1111/j.1096-3642.1989.tb00550.x (1989).

13 Véran, M. Les éléments accessoires de l'arc hyoïdien des poissons téléostomes (Acanthodiens et Osteichthyens) fossiles et actuels. *Mémoires du museum national d'histoire naturelle* **54**, 1-98 + I-VII pl (1988).

14 Friedman, M. & Sallan, L. C. Five hundred million years of extinction and recovery: a phanerozoic survey of large-scale diversity patterns in fishes. *Palaeontology* **55**, 707-742, doi:10.1111/j.1475-4983.2012.01165.x (2012).

15 Romano, C. *et al.* Permian–Triassic Osteichthyes (bony fishes): diversity dynamics and body size evolution. *Biological Reviews* **91**, 106-147, doi:10.1111/brv.12161 (2016).

16 Giles, S. *et al.* Endoskeletal structure in *Cheirolepis* (Osteichthyes, Actinopterygii), An early ray-finned fish. *Palaeontology* **58**, 849-870, doi:10.1111/pala.12182 (2015).

17 Giles, S., Darras, L., Clément, G., Blieck, A. & Friedman, M. An exceptionally preserved Late Devonian actinopterygian provides a new model for primitive cranial anatomy in ray-finned fishes. *Proceedings of the Royal Society of London B: Biological Sciences* **282**, doi:10.1098/rspb.2015.1485 (2015).

18 Gardiner, B. G. The relationships of the palaeoniscid fishes, a review based on new specimens of *Mimia* and *Moythomasia* from the Upper Devonian of Western Australia. *Bulletin of the British Museum (Natural History), Geology series* **37**, 173-428 (1984).

19 Coates, M. I. Endocranial preservation of a Carboniferous actinopterygian from Lancashire, UK, and the interrelationships of primitive actinopterygians. *Philosophical Transactions of the Royal Society B: Biological Sciences* **354**, 435-462, doi:10.1098/rstb.1999.0396 (1999).

20 Poplin, C. Étude de quelques paléoniscidés pennsylvaniens du Kansas. *Cahiers de paléontology*, 1-148+I-XL pl (1974).

21 Rayner, D. H. III.—On the Cranial Structure of an Early Palæoniscid, *Kentuckia*, gen. nov. *Transactions of the Royal Society of Edinburgh* **62**, 53-83, doi:10.1017/S0080456800009248 (1952).

22 Hamel, M.-H. & Poplin, C. The braincase anatomy of *Lawrenciella schaefferi*, actinopterygian from the Upper Carboniferous of Kansas (USA). *Journal of Vertebrate Paleontology* **28**, 989-1006, doi:10.1671/0272-4634-28.4.989 (2008).

23 Poplin, M. & Véran, M. A revision of the actinopterygian fish *Coccocephalus wildi* from the Upper Carboniferous of Lancashire. *Special Papers in Palaeontology* **52**, 7-30 (1996).

24 Stensiö, E. A. *Triassic fishes from Spitzbergen*. Vol. 2 1-261 (Almqvist & Wiksells Boktryckeri-A.-B., 1925).

25 Nielsen, E. *Studies on the Triassic fishes from East Greenland I. Glaucolepis and Boreosomus*. 394 + 30 pl. (C.A. Reitzels, 1942).

26 Nielsen, E. *Studies on Triassic fishes II. Australosomus and Birgeria*. Vol. 3 1 - 309 + 20pl. (Universitetets zoologiske museum og universitetes mineralogisk-geologiske museum, 1949).

27 Olsen, P. E. The skull and pectoral girdle of the parasemionotid fish *Watsonulus eugnathoides* from the Early Triassic Sakamena Group of Madagascar, with comments on the relationships of the holostean fishes. *Journal of Vertebrate Paleontology* **4**, 481-499, doi:10.1080/02724634.1984.10012024 (1984).

28 Giles, S., Xu, G.-H., Near, T. J. & Friedman, M. Early members of 'living fossil' lineage imply later origin of modern ray-finned fishes. *Nature* **549**, 265-268, doi:10.1038/nature23654 http://www.nature.com/nature/journal/v549/n7671/abs/nature23654.html#supplementary-information (2017).

29 Beltan, L. La faune ichthyologique de l'Eotrias du N.W. Madagascar: le neurocrâne. *Cahiers de paléontology*, 7-135+131-135+I-Lpl (1968).

30 Patterson, C. The braincase of Pholidophorid and Leptolepid fishes, with a review of the Actinopterygian braincase. *Philosophical Transactions of the Royal Society of London. B, Biological Sciences* **269**, 275-579, doi:10.1098/rstb.1975.0001 (1975).

31 Near, T. J. *et al.* Resolution of ray-finned fish phylogeny and timing of diversification. *Proceedings of the National Academy of Sciences* **109**, 13698-13703, doi:10.1073/pnas.1206625109 (2012).

32 Broughton, R. E., Betancur-R, R., Li, C., Arratia, G. & Ortí, G. Multi-locus phylogenetic analysis reveals the pattern and tempo of bony fish evolution. *PLoS Currents* **5**, ecurrents.tol.2ca8041495ffafd8041490c8092756e75247483e, doi:10.1371/currents.tol.2ca8041495ffafd0c92756e75247483e (2013).

33 Moy-Thomas, J. A. & Dyne, M. B. XVII.—The Actinopterygian Fishes from the Lower Carboniferous of Glencartholm, Eskdale, Dumfriesshire. *Transactions of the Royal Society of Edinburgh* **59**, 437-480, doi:10.1017/S0080456800009170 (1938).

34 Bradley-Dyne, M. The skull of *Amphicentrum granulosum*. *Journal of Zoology* **109**, 195-210 (1939).

35 Lund, R. The new actinopterygian order Guildayichthyiformes from the Lower Carboniferous of Montana (USA). *Geodiversitas* **22**, 171-206 (2000).

36 Hurley, I. A. *et al.* A new time-scale for ray-finned fish evolution. *Proceedings of the Royal Society of London B: Biological Sciences* **274**, 489-498, doi:10.1098/rspb.2006.3749 (2007).

37 Campbell, K. S. W. & Phuoc, L. D. A Late Permian actinopterygian fish from Australia. *Palaeontology* **26**, 33-70 (1983).

38 Gill, E. L. The Permian fishes of the genus *Acentrophorus*. *Proceedings of the Zoological Society of London* **93**, 19-40, doi:10.1111/j.1096-3642.1923.tb02170.x (1923).

39 Cloutier, R. & Arratia, G. in *Recent advances in the origin and early radiation of vertebrates* (eds G Arratia, M V H Wilson, & R Cloutier) 217-270 (Dr. Friedrich Pfeil, 2004).

40 Xu, G.-H., Gao, K.-Q. & Finarelli, J. A. A revision of the Middle Triassic scanilepiform fish *Fukangichthys longidorsalis* from Xinjiang, China, with comments on the phylogeny of the Actinopteri. *Journal of Vertebrate Paleontology* **34**, 747-759, doi:10.1080/02724634.2014.837053 (2014).

41 Schaeffer, B. & Dalquest, W. W. A palaeonisciform braincase from the Permian of Texas, with comments on cranial fissures and the posterior myodome. *American Museum Novitates* **2658**, 1-15 (1978).

42 Dunkle, D. H. A new palaeoniscoid fish from the Lower Permian of Texas. *Journal of the Washington Academy of Sciences* **36** (1946).

43 Aldinger, H. Permische Ganoidfische aus Östgrönland. *Meddelelser om Grønland* **102**, 1-392 + 344 tabs (1937).

44 Dunkle, D. H. A new paleoniscid fish from the Texas Permian. *American Journal of Science* **237**, 262-274 (1939).

45 Schaeffer, B. in *Interrelationships of fishes* (eds P H Greenwood, R H Miles, & Colin Patterson) 207-226 (Academic Press Inc, 1973).

46 Cope, E. D. Zittel's Manual of Palaeontology. *American Naturalist* **21**, 1014–1019 (1887).

47 Nelson, W. J., Hook, R. W. & Chaney, D. S. in *The Carboniferous-Permian transition* Vol. 60 *New Mexico Museum of Natural History and Science, Bulletin* (eds S G Lucas *et al.*) 286-311 (New Mexico Museum of Natural History & Science, 2013).

48 Olson, E. C. The Arroyo Formation (Leonardian: Lower Permian) and its vertebrate fossils. *Texas Memorial Museum bulletin* **35**, 1-25 (1989).

49 Grande, L. & Bemis, W. E. A Comprehensive Phylogenetic Study of Amiid Fishes (Amiidae) Based on Comparative Skeletal Anatomy. an Empirical Search for Interconnected Patterns of Natural History. *Journal of Vertebrate Paleontology* **18**, 1-696, doi:10.1080/02724634.1998.10011114 (1998).

50 Allis, E. P. The Cranial Anatomy of *Polypterus*, with Special Reference to *Polypterus bichir*. *Journal of Anatomy* **56**, 189-294.143 (1922).

51 Hilton, E., Grande, L. & Bemis, W. Skeletal anatomy of the shortnose sturgeon *Acipenser brevirostrum* Lesueur, 1818, and the systematics of sturgeons (Acipenseriformes, Acipenseridae). *Fieldiana: Life and Earth Sciences* **3**, 1 - 168 (2011).

52 Stamberg, S. Actinopterygians of the central bohemian Carboniferous basins. *Acta Musei Nationalis Pragae. B, Hist. naturalis* **47**, 25-104 + I-XXIV pl (1991).

53 Stensiö, E. A. *Triassic fishes from East Greenland*. Vol. 83 (Bianco Lunos Bogtrykkeri A/S, 1932).

54 Olsen, P. E. & McCune, A. R. Morphology of the *Semionotus elegans* species group from the Early Jurassic part of the Newark Supergroup of eastern North America with comments on the Family Semionotidae (Neopterygii). *Journal of Vertebrate Paleontology* **11**, 269-292, doi:10.1080/02724634.1991.10011398 (1991).

55 Allis, E. P. The cranial muscles and cranial and first spinal nerves in *Amia calva*. *Journal of Morphology* **7**, 487-809 (1897).

56 Arratia, G. Morphology, taxonomy, and phylogeny of Triassic pholidophorid fishes (Actinopterygii, Teleostei). *Journal of Vertebrate Paleontology* **33**, 1-138, doi:10.1080/02724634.2013.835642 (2013).

57 Jollie, M. Development of the head and pectoral skeleton of *Polypterus* with a note on scales (Pisces: Actinopterygii). *Journal of Zoology* **204**, 469-507, doi:10.1111/j.1469-7998.1984.tb02382.x (1984).

58 Arratia, G., Schultze, H. P. & Casciotta, J. Vertebral column and associated elements in dipnoans and comparison with other fishes: development and homology. *Journal of Morphology* **250**, 101-172 (2001).

59 Sallan, L. C. & Coates, M. I. Styracopterid (Actinopterygii) ontogeny and the multiple origins of post-Hangenberg deep-bodied fishes. *Zoological Journal of the Linnean Society* **169**, 156-199, doi:10.1111/zoj.12054 (2013).

60 Jollie, M. Development of Head and Pectoral Girdle Skeleton and Scales in Acipenser. *Copeia* **1980**, 226-249, doi:10.2307/1444000 (1980).

61 Warth, P., Hilton, E. J., Naumann, B., Olsson, L. & Konstantinidis, P. Development of the skull and pectoral girdle in Siberian sturgeon, *Acipenser baerii*, and Russian sturgeon, *Acipenser gueldenstaedtii* (Acipenseriformes: Acipenseridae). *Journal of Morphology* **278**, 418-442, doi:10.1002/jmor.20653 (2017).

62 Bertmar, G. On the ontogeny of the chondral skull in Characidae, with a discussion on the chondrocranial base and the visceral chondrocranium in fishes. *Acta Zoologica* **40**, 204-364 (1959).

63 Holmgren, N. Studies on the head of fishes. An embryological, morphological and phyogenetical study. Part IV. General morphology of the head in fish. *Acta Zoologica* **24**, 1-188 (1943).

64 Pehrson, T. Some points in the cranial development of teleostomian fishes. *Acta Zoologica* **3**, 1-63 (1922).

65 Sewertzoff, A. N. The head skeleton and muscles of *Acipenser ruthenus*. *Acta Zoologica* **9**, 1-127 + I-IX pl (1928).

66 Bockmann, F. A., Carvalho, M., Carvalho, M. R. & Rizatto, P. P. in *11th International Congress of Vertebrate Morphology.* 129.

67 Grande, L. & Bemis, W. Osteology and phylogenetic relationships of fossil and recent paddlefishes (Polyodontidae) with comments on the interrelationships of Acipenseriformes. *Society of Vertebrate Paleontology Memoir* **11**, 1 - 121 (1991).

68 Stensiö, E. A. *Triassic fishes from Spitzbergen (Part 1)*. 1-307+35 plates (Adolf Holzhausen, 1921).

69 Xu, G.-H. & Gao, K.-Q. A new scanilepiform from the Lower Triassic of northern Gansu Province, China, and phylogenetic relationships of non-teleostean Actinopterygii. *Zoological Journal of the Linnean Society* **161**, 595-612, doi:10.1111/j.1096-3642.2010.00645.x (2011).

70 López-Arbarello, A. Phylogenetic Interrelationships of Ginglymodian Fishes (Actinopterygii: Neopterygii). *PLoS ONE* **7**, e39370, doi:10.1371/journal.pone.0039370 (2012).

71 Danforth, C. H. The heart and arteries of *Polyodon*. *Journal of morphology* **23**, 409-454 (1912).

72 McAllister, D. A. The evolution of branchiostegals and associated opercular, gular, and hyoid bones, and the classification of teleostome fishes, living and fossil. *National Museum of Canada Bulletin* **221**, 1–239 (1968).

73 Anker, G. C. The Morphology of Joints and Ligaments in the Head of a Generalized Haplochromis Species: H. Elegans Trewavas 1933 (Teleostei, Cichlidae). *Netherlands Journal of Zoology* **39**, 1-40, doi:doi:https://doi.org/10.1163/156854289X00011 (1988).

74 Nelson, G. J. Gill arches and the phylogeny of fishes, with notes on the classification of vertebrates. *Bulletin of the American Museum of Natural History* **141**, 475-552 + 479-492pl (1969).

75 Mesquite: a modular system for evolutionary analysis. v. 3.31 (2017).

76 Goloboff, P. A., Farris, J. S. & Nixon, K. C. TNT, a free program for phylogenetic analysis. *Cladistics* **24**, 774-786, doi:10.1111/j.1096-0031.2008.00217.x (2008).

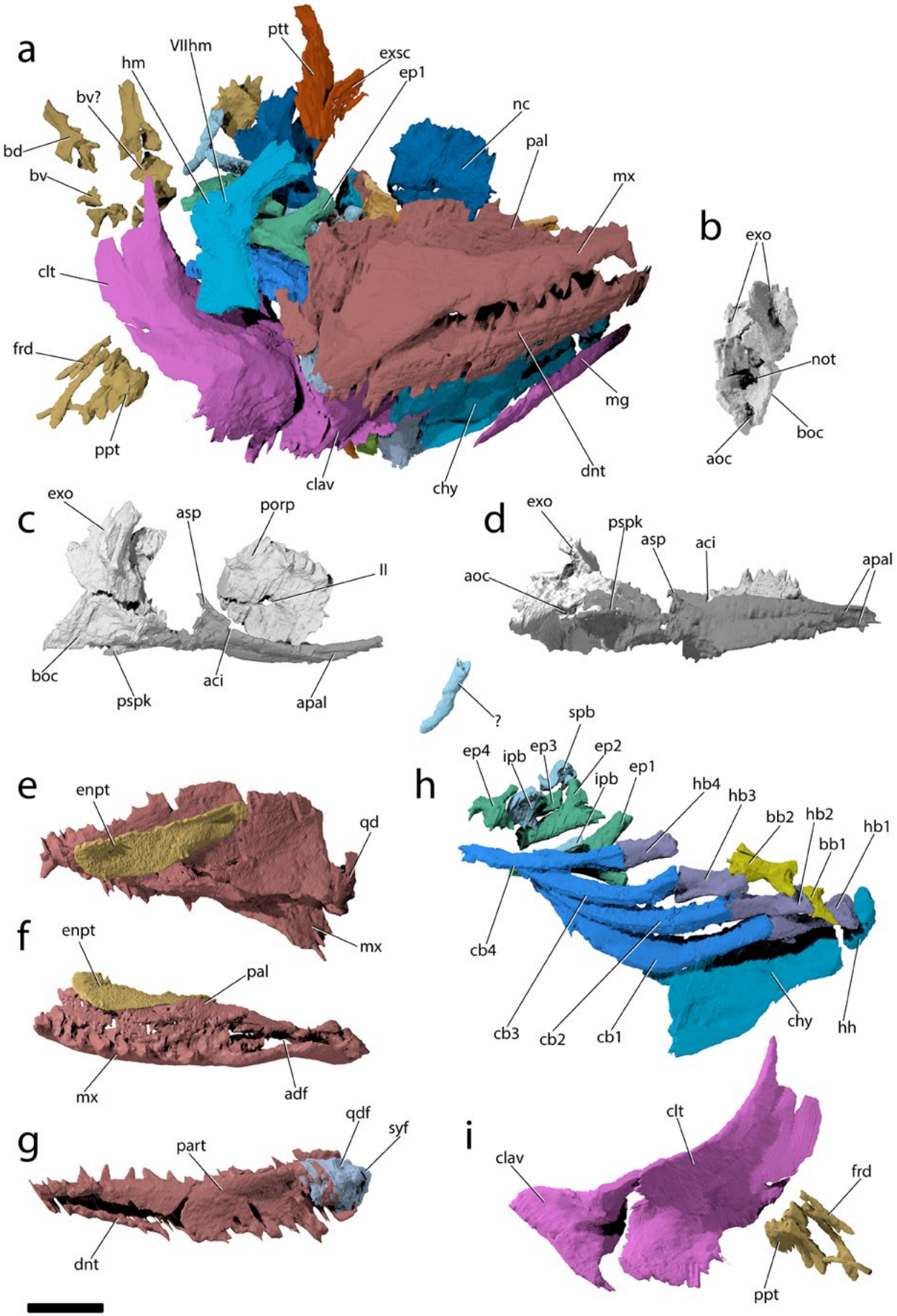
a
ptt
VIIhm
hm
exsc
ep1
bv?
nc
pal
bd
bv
mx
clt
frd
mg
ppt
clav
chy
dnt
b
exo
not
boc
aoc
c
exo
asp
porp
ll
boc
pspk
aci
apal
d
exo
pspk
asp
aci
apal
aoc
?
e
enpt
qd
mx
f
enpt
pal
mx
adf
g
qdf
syf
part
dnt
h
spb
ep4
ipb
ep3
ep2
ipb
ep1
hb4
hb3
bb2
hb2
hb1
bb1
cb4
cb3
cb2
cb1
chy
hh
i
clt
clav
frd
ppt

Fig. 1 Endoskeletal anatomy of †*Brachydegma caelatum* holotype (MCZ_VPF_6503). (**a**) complete reconstruction in lateral view; (**b**) occipital region of braincase in posterior view; (**c**) braincase and parasphenoid in right lateral view; (**d**) braincase and parasphenoid in ventral view; right palate in (**e**) medial, (**f**) ventral view; (**g**) right lower jaw in medial view; (**h**) left branchial and ventral hyoid arches in medial view; (**i**) right pectoral girdle in medial view. **II**, optic nerve; **VIIhm**, hyomandibular trunk of facial nerve; **aci**, notch for internal carotid; **adf**, adductor fossa; **asp**, ascending process of parasphenoid; **apal**, grooves for palatine artery; **aoc**, aortic canal; **bb 1,2**, basibranchial 1,2; **bd**, basidorsal; **boc**, basioccipital; **bv**, basiventral; **cb 1–4**, ceratobranchial 1–4; **chy**, ceratohyal; **clav**, clavicle; **clt**, cleithrum; **dnt**, dentary; **enpt**, endopterygoid toothplate; **ep 1–4**, epibranchial 1–4; **exo**, exoccipital; **exsc**, extrascapular; **frd**, fin radials; **hb 1–4**, hypobranchial 1–4; **hh**, hypohyal; **hm**, hyomandibula; **ipb**, infrapharyngobranchial; **mg**, median gular; **mx**, maxilla; **nc**, neurocranium; **not**, notochord; **pal**, palatal complex; **part**, prearticular; **porp**, postorbital process; **ppt**, propterygium; **pspk**, parasphenoid keel; **ptt**, posttemporal; **qd**, quadrate; **qdf**, quadrate facet; **spb**, suprapharyngobranchial; **syf**, symplectic facet. Scale bar equals 1 cm.

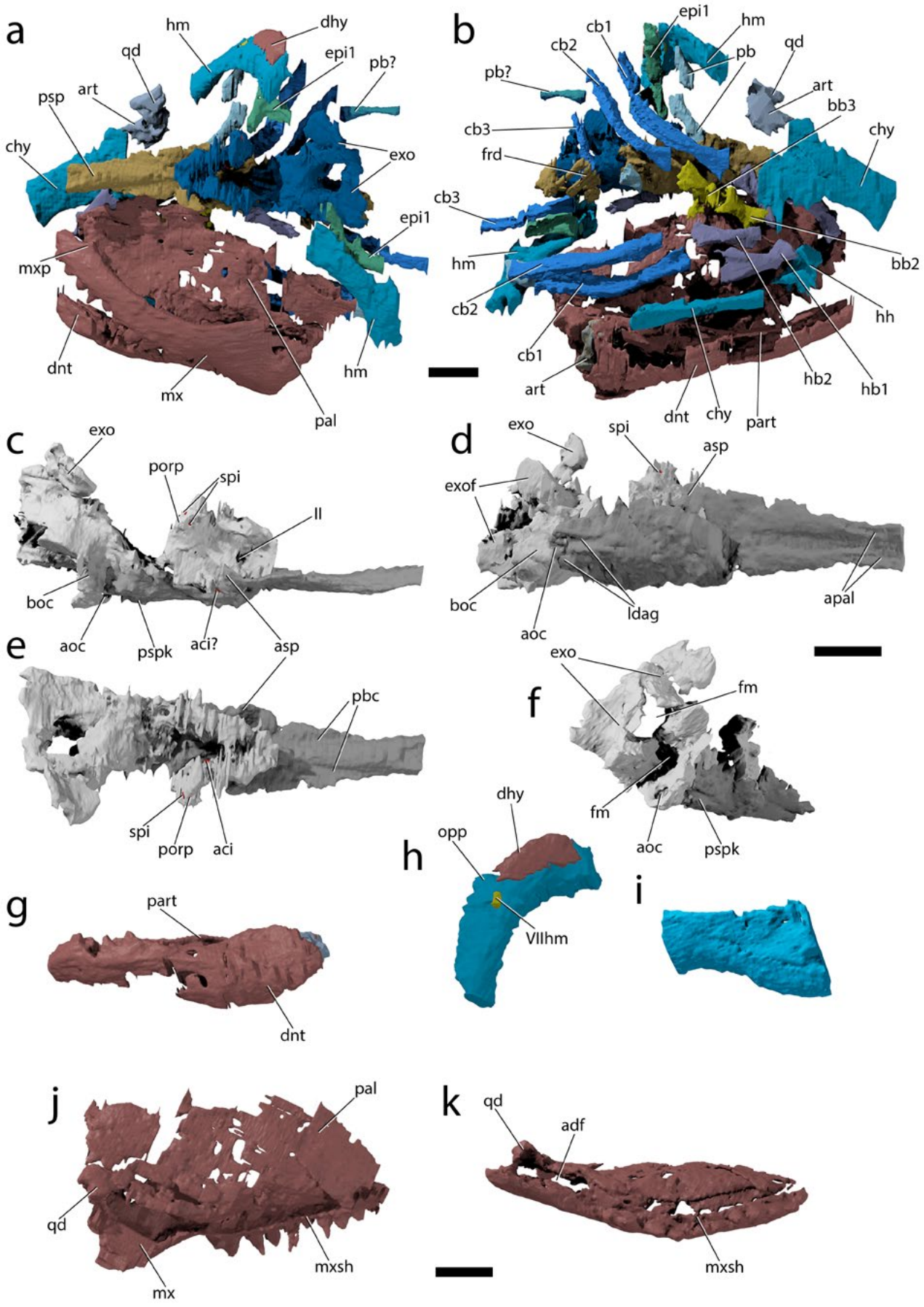
a
hm
dhy
qd
epi1
pb?
psp
art
chy
exo
epi1
mxp
dnt
mx
hm
pal
b
epi1
cb1
hm
cb2
pb
qd
pb?
art
bb3
cb3
chy
frd
cb3
bb2
hm
hh
cb2
cb1
art
hb2
hb1
dnt
chy
part
c
exo
porp
spi
II
boc
aoc
pspk
aci?
asp
d
exo
spi
asp
exof
boc
aoc
ldag
apal
e
asp
pbc
spi
porp
aci
f
exo
fm
fm
aoc
pspk
h
dhy
opp
VIIhm
i
g
part
dnt
j
pal
qd
mxsh
mx
k
qd
adf
mxsh

Fig. 2 Endoskeletal anatomy of †*Brachydegma caelatum* paratype (MCZ_VPF_6504). complete reconstruction in (**a**) dorsal–dorsolateral and (**b**) ventral views; braincase and parasphenoid in (**c**) lateral (**d**) ventral, (**e**) dorsal, and (**f**) posterolateral views; (**g**) lower jaw in lateral view; (**h**) right hyomandibula in lateral view; (**i**) left ceratohyal in lateral view; left palatal complex in (**j**) medial, (**i**) ventral views. **II**, optic nerve; **VIIhm**, hyomandibular trunk of facial nerve; **aci**, internal carotid; **adf**, adductor fossa; **aoc**, aortic canal; **art**, articular; **asp**, ascending process of parasphenoid; **apal**, grooves for palatine artery; **bb 2,3**, basibranchial 2,3; **boc**, basioccipital; **cb 1–3**, ceratobranchial 1–3; **chy**, ceratohyal; **dhy**, dermohyal; **dnt**, dentary; **epi**, epibranchial; **exo**, exoccipital; **exof**, exoccipital facets; **fm**, foramen magnum; **frd**, fin radials; **hb 1,2**, hypobranchial 1,2; **hm**, hyomandibula; **ldag**, grooves for lateral dorsal aortae; **mx**, maxilla; **mxp**, maxillary process; **mxsh**, median maxillary shelf; **opp**, opercular process; **pal**, palatal complex; **part**, prearticular; **pb**, pharyngobranchial; **pbc**, parabasal canal; **porp**, postorbital process; **psp**, parasphenoid; **pspk**, parasphenoid keel; **qd**, quadrate; **spi**, spiracular canal. Scale bars equal 1 cm.

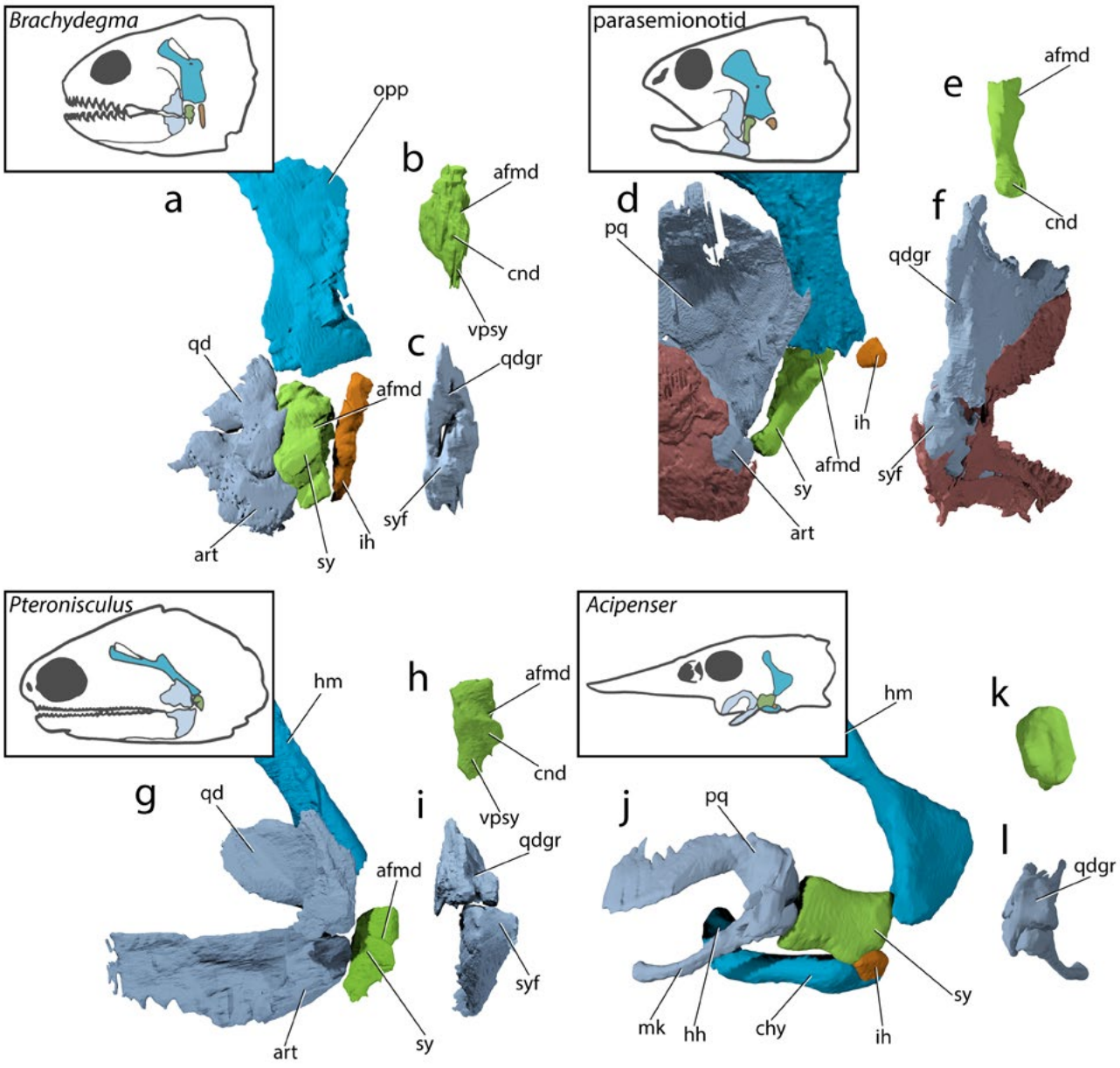
Brachydegma
opp
a
b
afmd
cnd
vpsy
c
qdgr
qd
afmd
syf
art
sy
ih
parasemionotid
d
pq
afmd
sy
art
ih
e
afmd
cnd
f
qdgr
syf
Pteronisculus
hm
g
qd
afmd
art
sy
h
afmd
cnd
vpsy
i
qdgr
syf
Acipenser
hm
j
pq
mk
hh
chy
ih
sy
k
l
qdgr

Fig. 3 Tomographic reconstructions of intermediate hyoid elements and associate ossifications in actinopterygians. †*Brachydegma caelatum* (MCZ_VPF_9503), (**a**) hyoid arch and posterior mandibular arch in lateral view, (**b**) symplectic in anterior view, (**c**) quadrate and articular in posterior view; †parasemionotidae indet. (NHMD_74424_A), (**d**) hyoid arch and posterior mandibular arch in lateral view, (**e**) symplectic in anterior view, (**f**) quadrate and articular in posteroventral view; †*Pteronisculus gunnari* (NHMD_73588_A), (**g**) hyoid arch and posterior mandibular arch in lateral view, (**h**) symplectic in anterior view, (**i**) quadrate and articular in posterior view; *Acipenser brevirostrum* (UMMZ_64250), (**j**) hyoid arch and mandibular arch in lateral view, (**k**) symplectic in anterior view, (**l**) palatoquadrate and meckel's cartilage in posterior view. **afmd**, groove for afferent mandibular artery; **art**, articular; **chy**, ceratohyal; **cnd**, condyle for articulation with lower jaw; **hh**, hypohyal; **hm**, hyomandibula; **ih**, interhyal; **mk**, meckel's cartilage; **opp**, opercular process; **pq**, palatoquadrate; **qd**, quadrate; **qdgr**, posterior groove on quadrate; **sy**, symplectic; **syf**, facet for symplectic; **vpsy**, ventral process of symplectic.

A

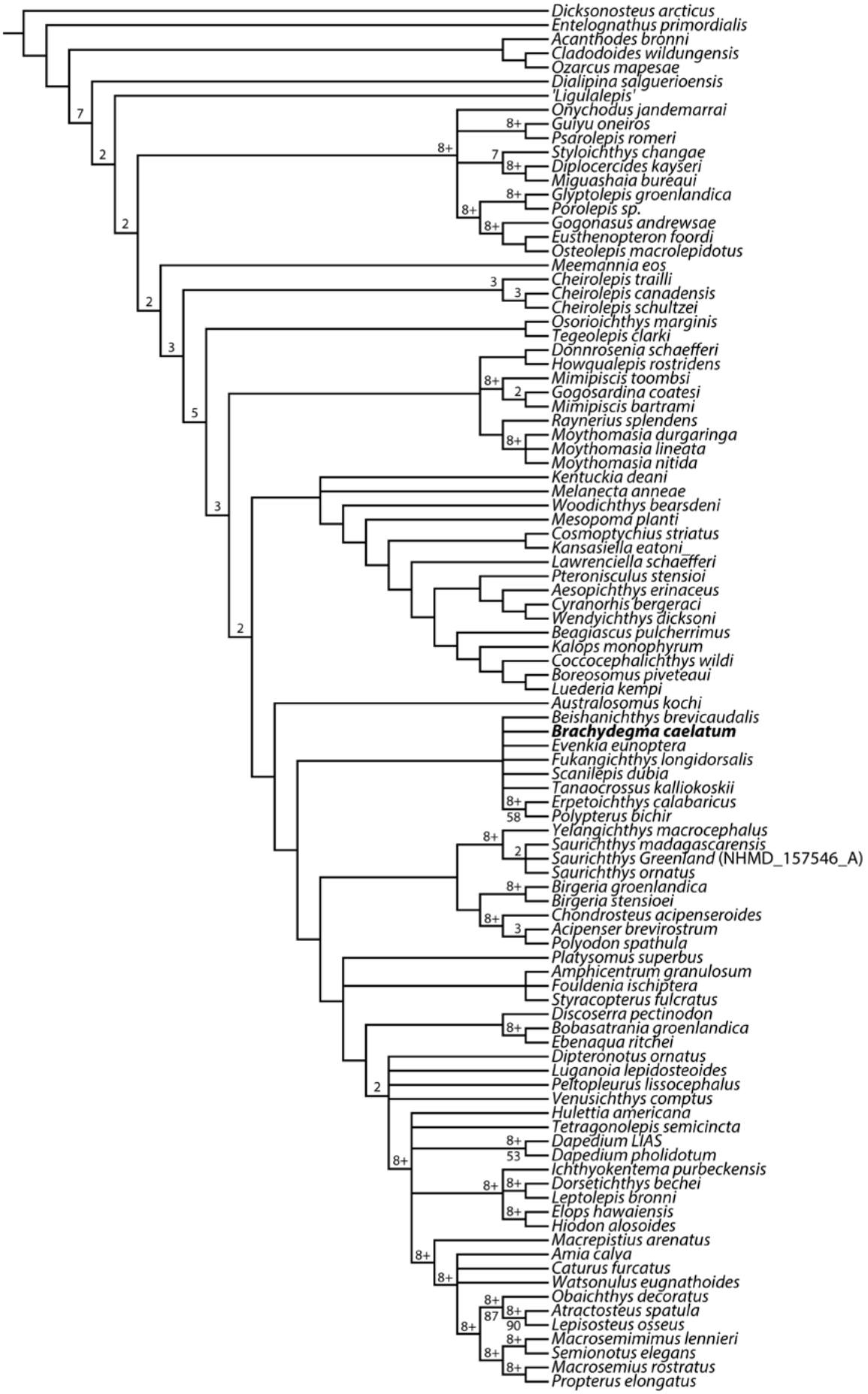
Dicksonosteus arcticus
Entelognathus primordialis
Acanthodes bronni
Cladodoides wildungensis
Ozarcus mapesae
Dialipina salguerioensis
'Ligulalepis'
Onychodus jandemarrai
Guiyu oneiros
Psarolepis romeri
Styloichthys changae
Diplocercides kayseri
Miguashaia bureaui
Glyptolepis groenlandica
Porolepis sp.
Gogonasus andrewsae
Eusthenopteron foordi
Osteolepis macrolepidotus
Meemannia eos
Cheirolepis trailli
Cheirolepis canadensis
Cheirolepis schultzei
Osorioichthys marginis
Tegeolepis clarki
Donnrosenia schaefferi
Howqualepis rostridens
Mimipiscis toombsi
Gogosardina coatesi
Mimipiscis bartrami
Raynerius splendens
Moythomasia durgaringa
Moythomasia lineata
Moythomasia nitida
Kentuckia deani
Melanecta anneae
Woodichthys bearsdeni
Mesopoma planti
Cosmoptychius striatus
Kansasiella eatoni
Lawrenciella schaefferi
Pteronisculus stensioi
Aesopichthys erinaceus
Cyranorhis bergeraci
Wendyichthys dicksoni
Beagiascus pulcherrimus
Kalops monophyrum
Coccocephalichthys wildi
Boreosomus piveteaui
Luederia kempi
Australosomus kochi
Beishanichthys brevicaudalis
Brachydegma caelatum
Evenkia eunoptera
Fukangichthys longidorsalis
Scanilepis dubia
Tanaocrossus kalliokoskii
Erpetoichthys calabaricus
Polypterus bichir
Yelangichthys macrocephalus
Saurichthys madagascarensis
Saurichthys Greenland (NHMD_157546_A)
Saurichthys ornatus
Birgeria groenlandica
Birgeria stensioei
Chondrosteus acipenseroides
Acipenser brevirostrum
Polyodon spathula
Platysomus superbus
Amphicentrum granulosum
Fouldenia ischiptera
Styracopterus fulcratus
Discoserra pectinodon
Bobasatrania groenlandica
Ebenaqua ritchei
Dipteronotus ornatus
Luganoia lepidosteoides
Peltopleurus lissocephalus
Venusichthys comptus
Hulettia americana
Tetragonolepis semicincta
Dapedium LIAS
Dapedium pholidotum
Ichthyokentema purbeckensis
Dorsetichthys bechei
Leptolepis bronni
Elops hawaiensis
Hiodon alosoides
Macrepistius arenatus
Amia calva
Caturus furcatus
Watsonulus eugnathoides
Obaichthys decoratus
Atractosteus spatula
Lepisosteus osseus
Macrosemimimus lennieri
Semionotus elegans
Macrosemius rostratus
Propterus elongatus

Fig. 4 Strict consensus of 1211 most parsimonious trees of 1434 steps. Consistency Index=0.215, Retention Index=0.643. Numbers above nodes indicate Bremer values. Numbers below nodes indicate bootstrap percentages.

Supplemental information

Re-description of external cranial anatomy of †*Brachydegma*.

We hereby provide a short re-description of †*Brachydegma caelatum*, mostly based on the better-preserved typed specimen MCZ_ VPF_6503 (for previous interpretations see[1,2]). We only refer to the paratype MCZ_ VPF_6504 when it shows features absent from the type specimen. Our anatomical interpretations are in in broad agreement with the original description[1], and are largely based on direct observations of the fossils, since superficial ossifications were poorly resolved in the µCT data. The rostrum and the anterior part of the skull roof are incompletely preserved. The paired premaxillae bear strong teeth, but it is unclear if they were in contact on the mid-line. The frontals are longer than wide, with their posteroventral margin bearing an indentation for the insertion of the dermopterotics. The parietals are quadrate-shaped. The midline suture between the bilateral counterparts of the frontals and parietals is strongly zigzag. An additional and tiny anamestic bone is wedged between the parietal and the dermopterotic, on the left side of the specimen. The dermopterotics are longer than wide. The left dermopterotic appears divided in two parts, but this separation may be a result of breakage. On the right side of the skull, the anterior and posterior portions of the dermopterotic are clearly bridged by a ventral bony bridge, allowing us to treat them collectively as a single ossification. A pair of lateromedially elongate extrascapulars lies posterior to the parietals.

The dermosphenotic (postorbital in[1]) is sub-rectangular, forming a posterior ramus. Its anterior end is fragmented, but it likely did not reach far anteriorly above the orbit. Three infraorbitals (jugal, infraorbital 2, lachrymal) line the posterior and ventral margins of the orbit, with the lachrymal bearing an anterior thickening. Three or four anamestic suborbitals, form a dorsoventral series, separating the infraorbitals from the preopercle. A supramaxilla is absent. The maxilla is cleaver-shaped, forming a distinct posterior plate, with its posterodorsal margin fitting in a notch on the preopercle. On the left side of the specimen, the maxilla is slightly disarticulated from the preopercle, which likely gave the impression of maxillary kinesis (hereby deemed absent) to previous authors[2]. The maxilla of MCZ_VPF_6504 does not form a posterior notch, contrasting a previous reconstruction of this feature[2]. The preopercle is higher than wide, and sits almost upright in the cheek. The pronounced ventral limb of the preopercle leads to a putative, small

quadratojugal. Four splint-shaped anamestic bones separate the preopercle from the opercular series. The dorsal most lies anteriorly to the other three, and must constitute a spiracular bone. The remaining anamestic bones (accessory opercles) form a dorsoventrally expanding series, with the dorsal-most constituting the dermohyal, and are broadly comparable to those of the †Acrolepidids (s.l.)[3,4]. The opercle is rhomboidal and is of almost equal size to the more quadrate subopercle. Nine branchiostegal rays are present. The two lateral gulars are rostrocaudally elongate and underlie the posterior half of the lower jaw. The median gular is longer than wide, and of subequal length to the lateral gulars.

The posttemporal is subquadrate and seems to form an anterolateral ramus, likely excluding the extrascapular from the lateral margin of the skull roof. An additional dermal ossification lies ventrally to the posttemporal. Although the presence or absence of sensory canals in the shoulder girdle cannot be ascertained, we tentatively identify the latter as a presupracleithrum. The supracleithrum is larger than the posttemporal, reaches further posteriorly than the cleithrum, and forms a strongly convex posterior margin. A small postcleithrum lies posteriorly to the dorsal third of the cleithrum. Fringing fulcra line the anterior margin of the pectoral fin.

References

1 Dunkle, D. H. A new paleoniscid fish from the Texas Permian. *American Journal of Science* **237**, 262-274 (1939).

2 Hurley, I. A. *et al.* A new time-scale for ray-finned fish evolution. *Proceedings of the Royal Society of London B: Biological Sciences* **274**, 489-498, doi:10.1098/rspb.2006.3749 (2007).

3 Aldinger, H. Permische Ganoidfische aus Östgrönland. *Meddelelser om Grønland* **102**, 1-392 + 344 tabs (1937).

4 Nielsen, E. *Studies on the Triassic fishes from East Greenland I. Glaucolepis and Boreosomus*. 394 + 30 pl. (C.A. Reitzels, 1942).

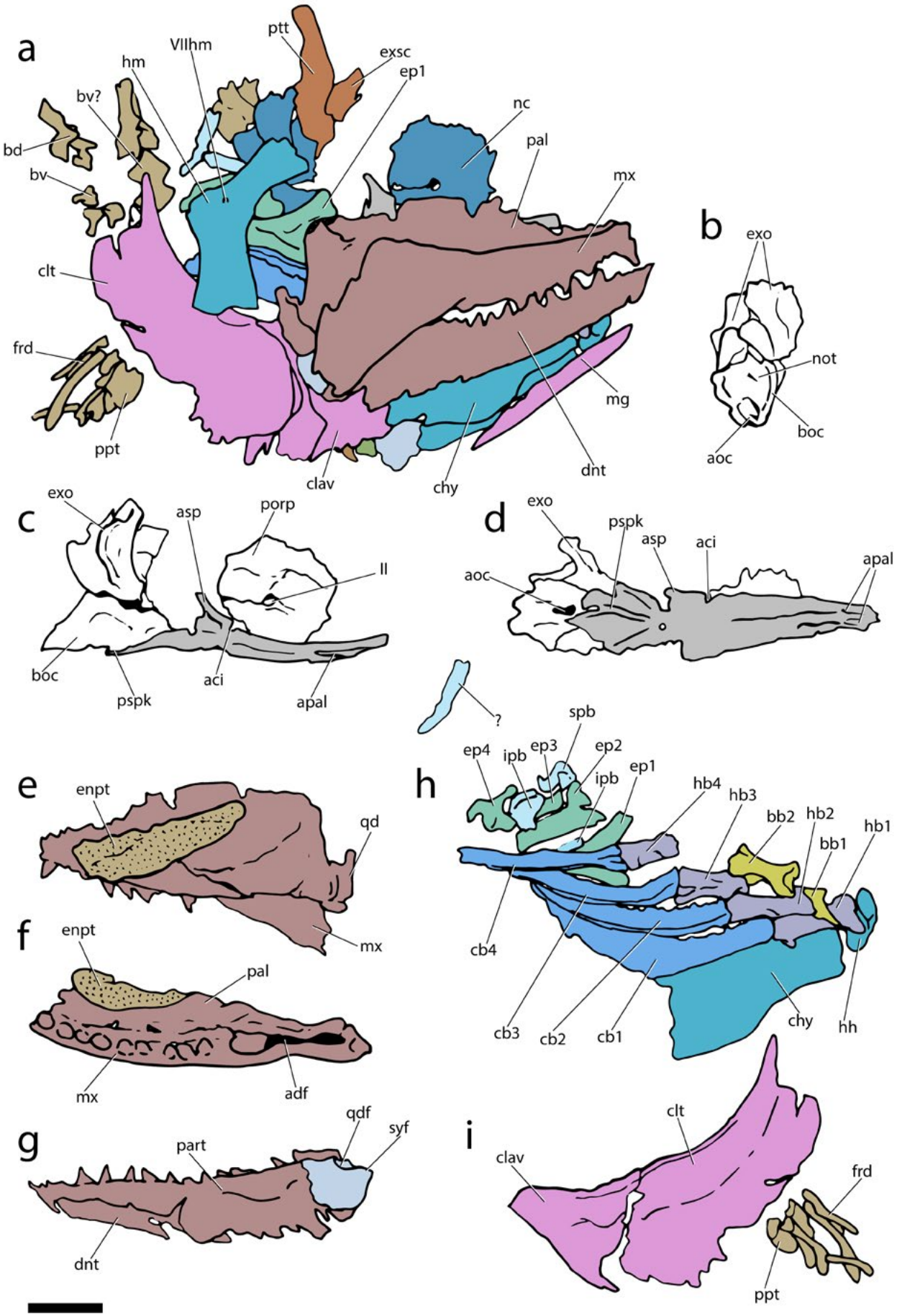
a
ptt
VIIhm
hm
exsc
ep1
bv?
nc
pal
bd
bv
mx
clt
frd
mg
ppt
clav
chy
dnt
b
exo
not
boc
aoc
c
exo
asp
porp
II
boc
pspk
aci
apal
d
exo
pspk
asp
aci
apal
aoc
?
e
enpt
qd
mx
f
enpt
pal
mx
adf
h
spb
ep4
ipb
ep3
ep2
ipb
ep1
hb4
hb3
bb2
hb2
hb1
bb1
cb4
cb3
cb2
cb1
chy
hh
g
qdf
syf
part
dnt
i
clt
clav
frd
ppt

Supplementary Figure 1 Interpretative drawing of Fig. 1. (**a**) complete reconstruction in lateral view; (**b**) occipital region of braincase in posterior view; (**c**) braincase and parasphenoid in right lateral view; (**d**) braincase and parasphenoid in ventral view; right palate in (**e**) medial, (**f**) ventral view; (**g**) right lower jaw in medial view; (**h**) left branchial and ventral hyoid arches in medial view; (**i**) right pectoral girdle in medial view. **II**, optic nerve; **VIIhm**, hyomandibular trunk of facial nerve; **aci**, notch for internal carotid; **adf**, adductor fossa; **asp**, ascending process of parasphenoid; **apal**, grooves for palatine artery; **aoc**, aortic canal; **bb 1,2**, basibranchial 1,2; **bd**, basidorsal; **boc**, basioccipital; **bv**, basiventral; **cb 1–4**, ceratobranchial 1–4; **chy**, ceratohyal; **clav**, clavicle; **clt**, cleithrum; **dnt**, dentary; **enpt**, endopterygoid toothplate; **ep 1–4**, epibranchial 1–4; **exo**, exoccipital; **exsc**, extrascapular; **frd**, fin radials; **hb 1–4**, hypobranchial 1–4; **hh**, hypohyal; **hm**, hyomandibula; **ipb**, infrapharyngobranchial; **mg**, median gular; **mx**, maxilla; **nc**, neurocranium; **not**, notochord; **pal**, palatal complex; **part**, prearticular; **porp**, postorbital process; **ppt**, propterygium; **pspk**, parasphenoid keel; **ptt**, posttemporal; **qd**, quadrate; **qdf**, quadrate facet; **spb**, suprapharyngobranchial; **syf**, symplectic facet. Scale bar equals 1 cm.

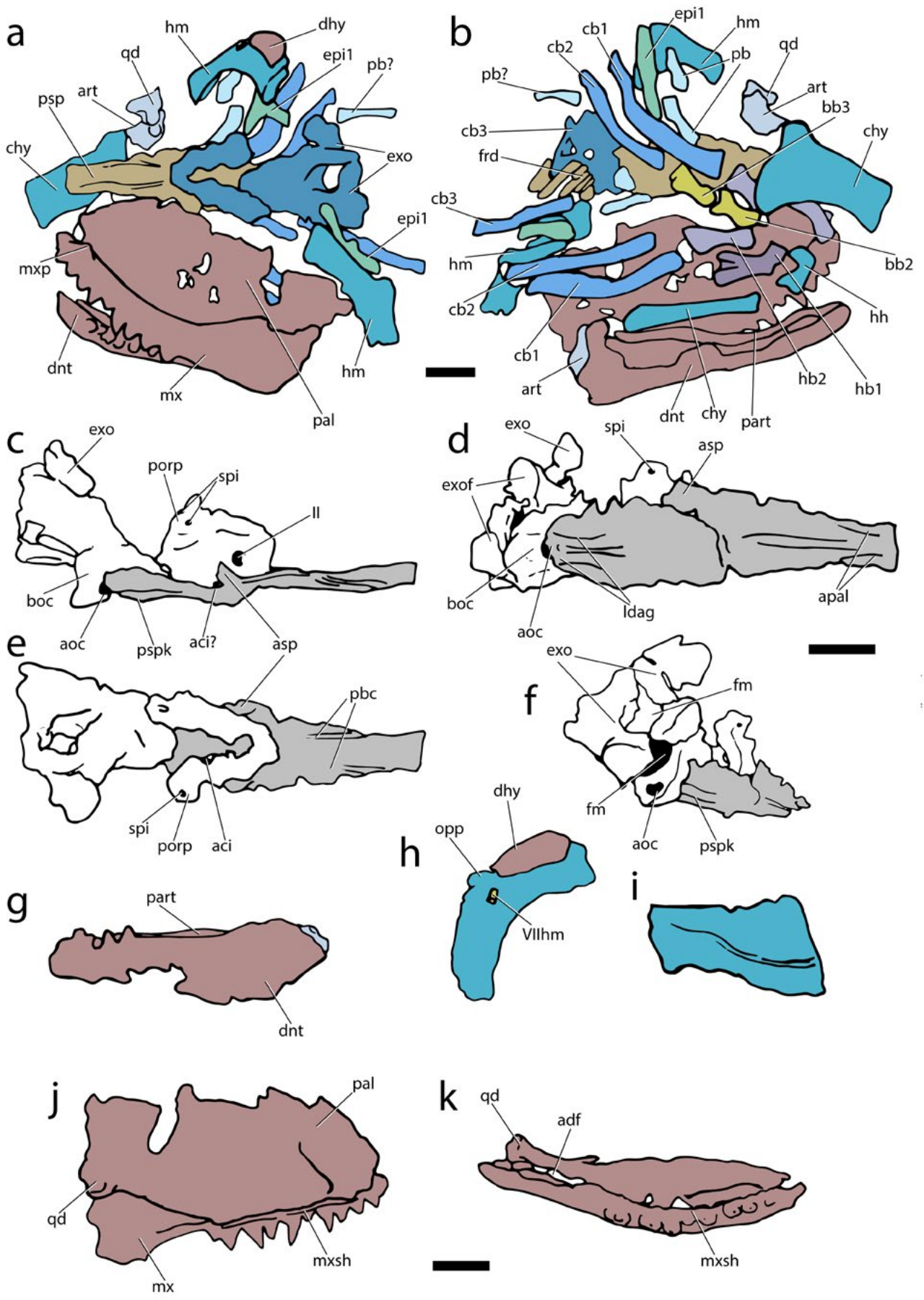
a
hm
dhy
qd
epi1
pb?
psp
art
chy
exo
epi1
mxp
dnt
mx
hm
pal
b
epi1
cb1
hm
cb2
pb
qd
pb?
art
bb3
cb3
chy
frd
cb3
bb2
hm
hh
cb2
cb1
art
hb2
hb1
dnt
chy
part
c
exo
porp
spi
ll
boc
aoc
pspk
aci?
asp
d
exo
spi
asp
exof
boc
aoc
ldag
apal
e
asp
pbc
spi
porp
aci
f
exo
fm
fm
aoc
pspk
h
dhy
opp
VIIhm
i
g
part
dnt
j
pal
qd
mxsh
mx
k
qd
adf
mxsh

Supplementary figure 2 Interpretative drawing of Fig. 2. complete reconstruction in (**a**) dorsal–dorsolateral and (**b**) ventral views; braincase and parasphenoid in (**c**) lateral (**d**) ventral, (**e**) dorsal, and (**f**) posterolateral views; (**g**) lower jaw in lateral view; (**h**) right hyomandibula in lateral view; (**i**) left ceratohyal in lateral view; left palatal complex in (**j**) medial, (**i**) ventral views. **II**, optic nerve; **VIIhm**, hyomandibular trunk of facial nerve; **aci**, internal carotid; **adf**, adductor fossa; **aoc**, aortic canal; **art**, articular; **asp**, ascending process of parasphenoid; **apal**, grooves for palatine artery; **bb 2,3**, basibranchial 2,3; **boc**, basioccipital; **cb 1–3**, ceratobranchial 1–3; **chy**, ceratohyal; **dhy**, dermohyal; **dnt**, dentary; **epi**, epibranchial; **exo**, exoccipital; **exof**, exoccipital facets; **fm**, foramen magnum; **frd**, fin radials; **hb 1,2**, hypobranchial 1,2; **hm**, hyomandibula; **ldag**, grooves for lateral dorsal aortae; **mx**, maxilla; **mxp**, maxillary process; **mxsh**, median maxillary shelf; **opp**, opercular process; **pal**, palatal complex; **part**, prearticular; **pb**, pharyngobranchial; **pbc**, parabasal canal; **porp**, postorbital process; **psp**, parasphenoid; **pspk**, parasphenoid keel; **qd**, quadrate; **spi**, spiracular canal. Scale bars equal 1 cm.

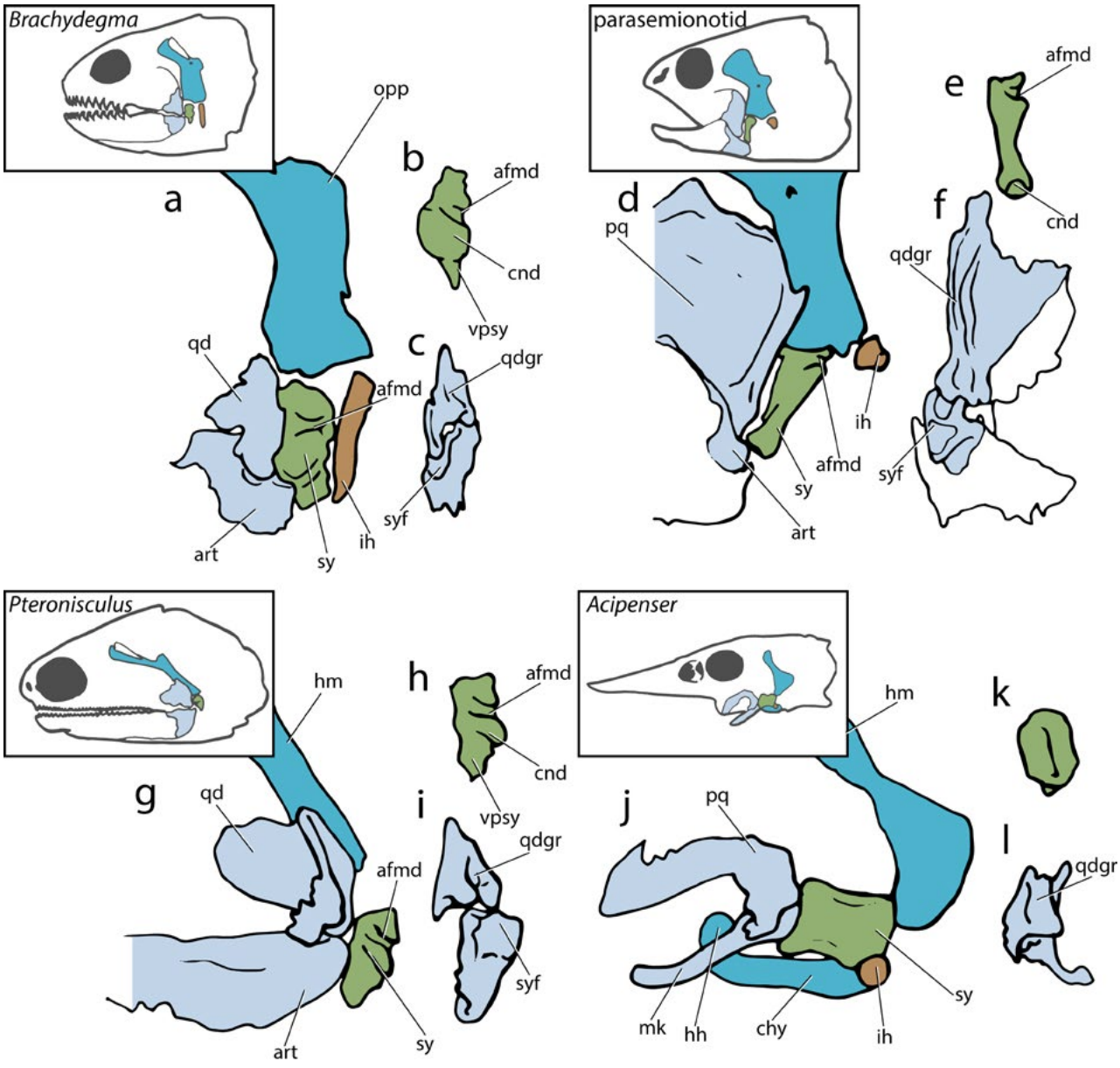
Brachydegma
a
opp
qd
art
sy
ih
b
afmd
cnd
vpsy
c
qdgr
afmd
syf
parasemionotid
d
pq
afmd
sy
art
ih
e
afmd
cnd
f
qdgr
syf
Pteronisculus
g
hm
qd
afmd
art
sy
h
afmd
cnd
vpsy
i
qdgr
syf
Acipenser
j
hm
pq
mk
hh
chy
ih
sy
k
l
qdgr

Supplementary figure 3 Interpretative drawing of Fig. 3. †*Brachydegma caelatum* (MCZ_VPF_9503), (**a**) hyoid arch and posterior mandibular arch in lateral view, (**b**) symplectic in anterior view, (**c**) quadrate and articular in posterior view; †parasemionotidae indet. (NHMD_74424_A), (**d**) hyoid arch and posterior mandibular arch in lateral view, (**e**) symplectic in anterior view, (**f**) quadrate and articular in posteroventral view; †*Pteronisculus gunnari* (NHMD_73588_A), (**g**) hyoid arch and posterior mandibular arch in lateral view, (**h**) symplectic in anterior view, (**i**) quadrate and articular in posterior view; *Acipenser brevirostrum* (UMMZ_64250), (**j**) hyoid arch and mandibular arch in lateral view, (**k**) symplectic in anterior view, (**l**) palatoquadrate and meckel's cartilage in posterior view. **afmd**, groove for afferent mandibular artery; **art**, articular; **chy**, ceratohyal; **cnd**, condyle for articulation with lower jaw; **hh**, hypohyal; **hm**, hyomandibula; **ih**, interhyal; **mk**, meckel's cartilage; **opp**, opercular process; **pq**, palatoquadrate; **qd**, quadrate; **qdgr**, posterior groove on quadrate; **sy**, symplectic; **syf**, facet for symplectic; **vpsy**, ventral process of symplectic.

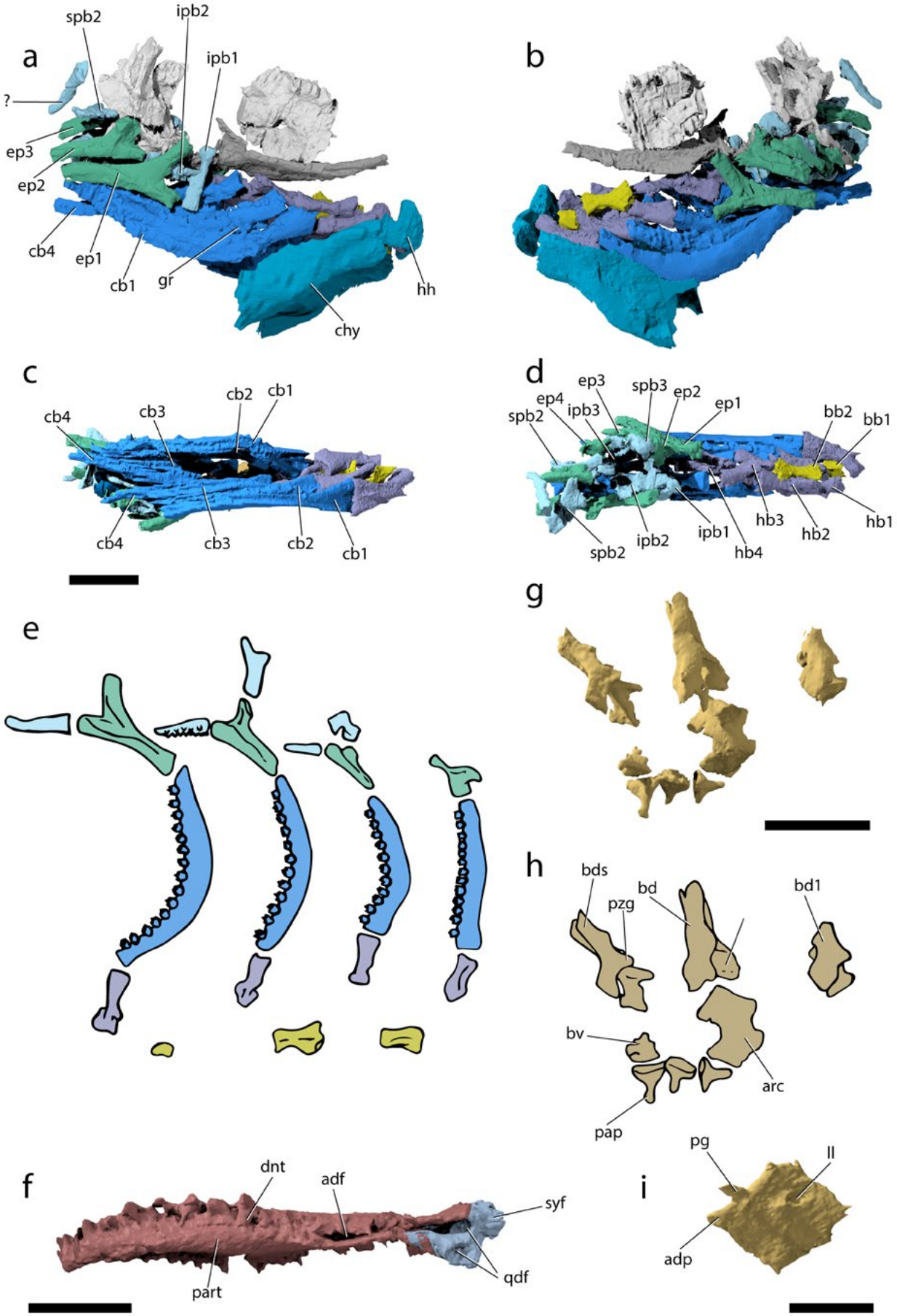
a
spb2
ipb2
ipb1
?
ep3
ep2
cb4
ep1
cb1
gr
hh
chy
b
c
cb2
cb1
cb4
cb3
cb4
cb3
cb2
cb1
d
ep3
spb3
ep4
ep2
ipb3
ep1
spb2
bb2
bb1
hb3
hb1
hb2
spb2
ipb2
ipb1
hb4
e
g
h
bds
pzg
bd
bd1
bv
arc
pap
f
dnt
adf
syf
qdf
part
i
pg
ll
adp

Supplementary figure 4 Details of branchial skeleton, lower jaw and axial skeleton of †*Brachydegma caelatum* holotype (MCZ_VPF_6503). Tomographic renderings of branchial and ventral hyoid skeleton in association with braincase and parasphenoid in (**a**) right and (**b**) left lateral views; Tomographic renderings of branchial skeleton with ventral hyoid elements removed in (**c**) ventral and (**d**) dorsal views; (**e**) schematic reconstruction of left branchial ossifications in lateral view, disarticulated and spaced, and not to scale; (**f**) tomographic rendering of lower jaw in dorsal view; (**g**) tomographic rendering of anterior axial elements; (**h**) interpretative drawing of (g); (**i**) lateral line scale in medial view. **adf**, adductor fossa; **adp**, anterodorsal process; **arc**, median arcual element; **bb 1,2**, basibranchial 1,2; **bd**, basidorsal; **bds**, basidorsal spine; **bv**, basiventral; **cb 1–4**, ceratobranchial 1–4; **chy**, ceratohyal; **dnt**, dentary; **ep 1–4**, epibranchial 1–4; **gr**, gill rakers; **hh**, hypohyal; **ipb 1–3**, infrapharyngobranchial 1–3; **ll**, lateral line pore; **qdf**, quadrate facets; **part**, prearticular; **pap**, parapophyses; **pg**, dorsal peg; **pzg**, prezygapophysis; **spb 2,3**, suprapharyngobranchial 2,3; **syf**, symplectic facet. Scale bars equal 1cm, except for (i) where scale bar equals 0.5 cm.

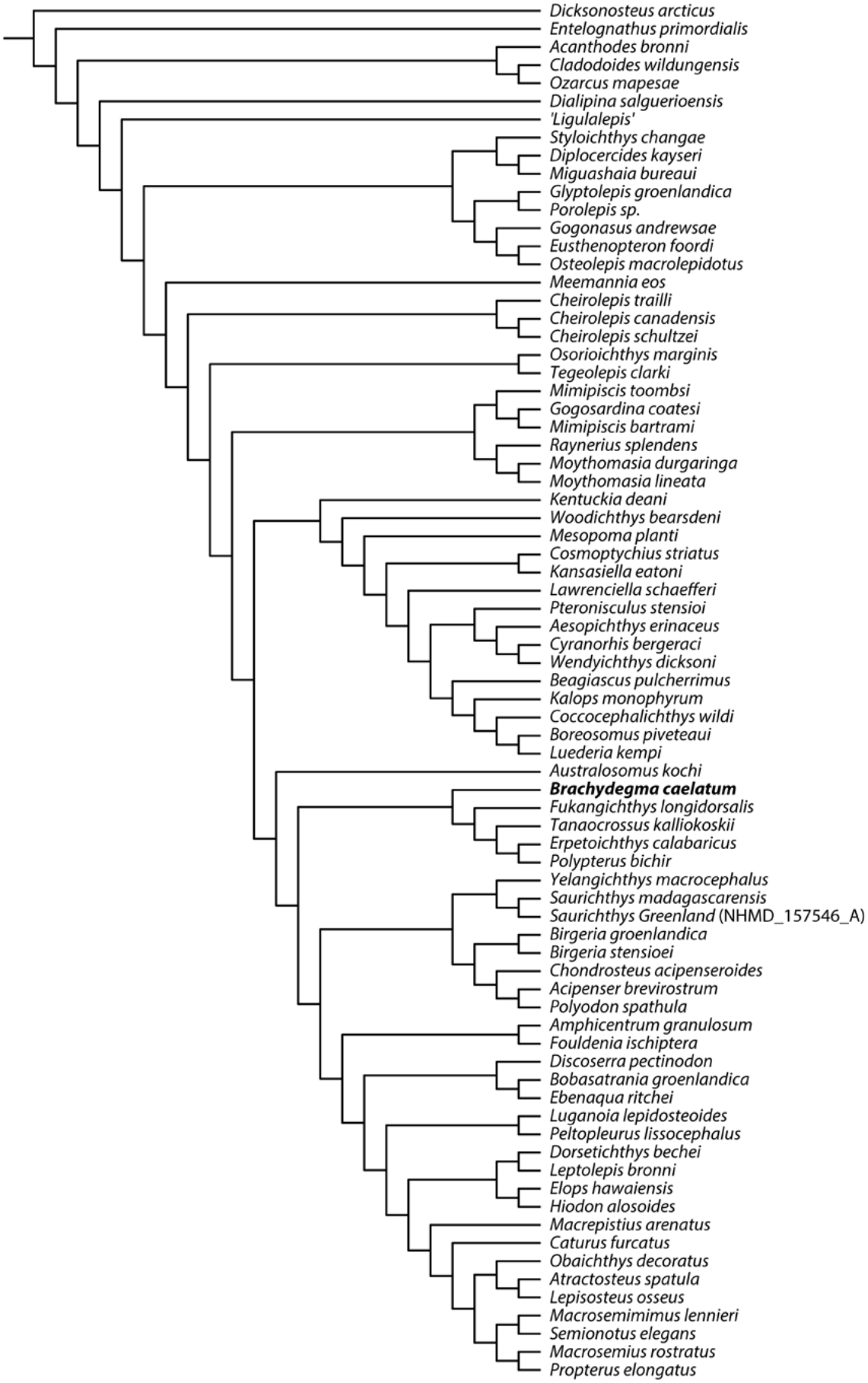
Dicksonosteus arcticus
Entelognathus primordialis
Acanthodes bronni
Cladodoides wildungensis
Ozarcus mapesae
Dialipina salguerioensis
'Ligulalepis'
Styloichthys changae
Diplocercides kayseri
Miguashaia bureaui
Glyptolepis groenlandica
Porolepis sp.
Gogonasus andrewsae
Eusthenopteron foordi
Osteolepis macrolepidotus
Meemannia eos
Cheirolepis trailli
Cheirolepis canadensis
Cheirolepis schultzei
Osorioichthys marginis
Tegeolepis clarki
Mimipiscis toombsi
Gogosardina coatesi
Mimipiscis bartrami
Raynerius splendens
Moythomasia durgaringa
Moythomasia lineata
Kentuckia deani
Woodichthys bearsdeni
Mesopoma planti
Cosmoptychius striatus
Kansasiella eatoni
Lawrenciella schaefferi
Pteronisculus stensioi
Aesopichthys erinaceus
Cyranorhis bergeraci
Wendyichthys dicksoni
Beagiascus pulcherrimus
Kalops monophyrum
Coccocephalichthys wildi
Boreosomus piveteaui
Luederia kempi
Australosomus kochi
Brachydegma caelatum
Fukangichthys longidorsalis
Tanaocrossus kalliokoskii
Erpetoichthys calabaricus
Polypterus bichir
Yelangichthys macrocephalus
Saurichthys madagascarensis
Saurichthys Greenland (NHMD_157546_A)
Birgeria groenlandica
Birgeria stensioei
Chondrosteus acipenseroides
Acipenser brevirostrum
Polyodon spathula
Amphicentrum granulosum
Fouldenia ischiptera
Discoserra pectinodon
Bobasatrania groenlandica
Ebenaqua ritchei
Luganoia lepidosteoides
Peltopleurus lissocephalus
Dorsetichthys bechei
Leptolepis bronni
Elops hawaiensis
Hiodon alosoides
Macrepistius arenatus
Caturus furcatus
Obaichthys decoratus
Atractosteus spatula
Lepisosteus osseus
Macrosemimimus lennieri
Semionotus elegans
Macrosemius rostratus
Propterus elongatus

Supplementary figure 5 Agreement subtree containing 76 out of 98 taxa.


a
Type
b
c
Type
d

Supplementary figure 6 †*Brachydegma caelatum* holotype (MCZ_VPF_6503) in (**a**) left lateral, (**b**) right lateral, (**c**) dorsal, (**d**) ventral views. Scale bar equals 1 cm.

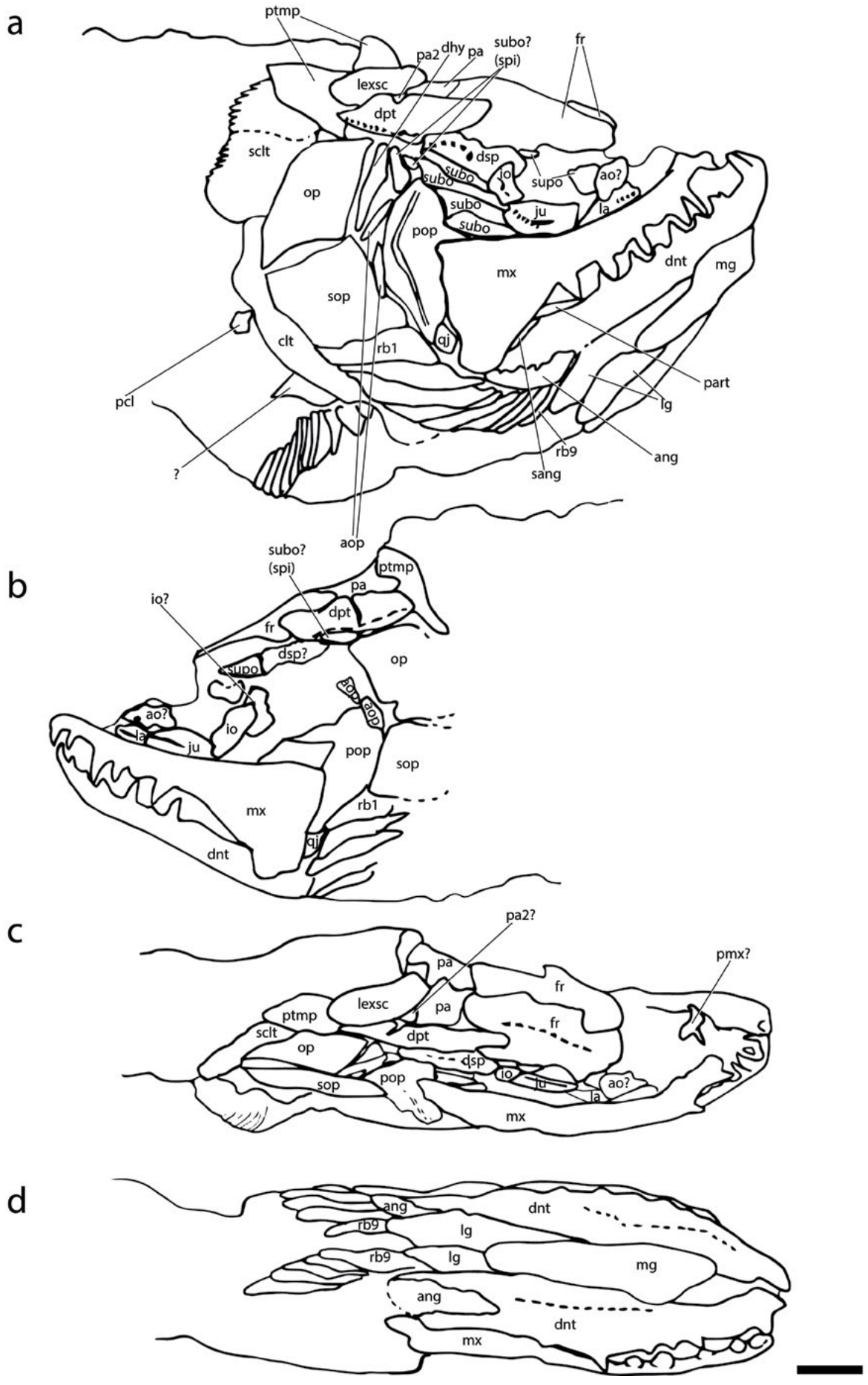
a
ptmp
pa2
dhy
pa
subo?
(spi)
fr
lexsc
dpt
sclt
dsp
subo
jo
supo
ao?
op
la
ju
pop
mx
dnt
mg
sop
clt
rb1
qj
part
pcl
lg
rb9
ang
?
sang
aop
b
subo?
(spi)
ptmp
pa
io?
dpt
fr
dsp?
op
supo
pop
aop
ao?
la
ju
io
pop
sop
mx
rb1
qj
dnt
c
pa2?
pa
pmx?
fr
lexsc
pa
ptmp
fr
sclt
dpt
op
dsp
io
pop
ju
ao?
sop
la
mx
d
ang
dnt
rb9
lg
rb9
lg
mg
ang
dnt
mx

Supplementary figure 7 Interpretative drawing of Suppl. Fig. 6. Scale bar equals 1 cm. L **ao?**, putative antorbital; **aop**, accessory opercles; **clt**, cleithrum; **dhy**, dermohyal; **dnt**, dentary; **dpt**, dermopterotic; **dsph**, dermosphenotic; **fr**, frontal; **io**, infraorbital; **ju**, jugal; **la**, lachrymal; **lexsc**, lateral extrascapular; **lg**, lateral gular; **mg**, median gular; **mx**, maxilla; **op**, opercle; **pa**, parietal; **pa2**, accessory parietal; **part**, prearticular; **pcl**, postcleithrum; **pmx?**, putative premaxilla; **pop**, preopercle; **ptmp**, posttemporal; **qj**, quadratojugal; **rb**, branchiostegal ray; **sang**, surangular; **sclt**, supracleithrum; **sop**, subopercle; **subo(spi)**, spiracular; **subo**, suborbital; **supo**, supraorbital. Scale bar equals 1 cm.

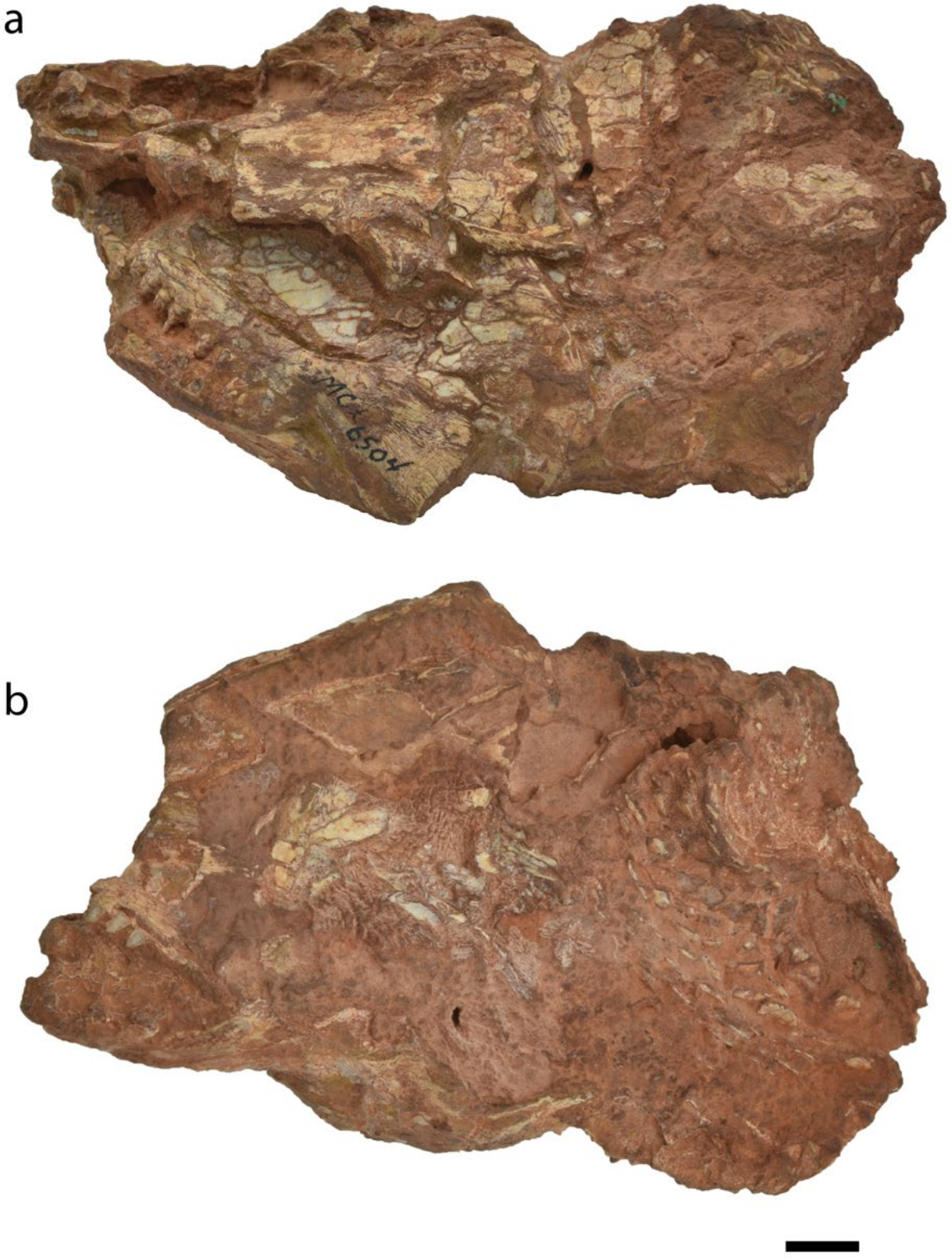
a
MCA 6504
b

Supplementary figure 8 †*Brachydegma caelatum* paratype (MCZ_VPF_6504) in (**a**) dorsolateral, (**b**) ventral views. Scale bar equals 1 cm.

Conclusions and future directions

Conclusion

This thesis was initially designed to explore aspects of paleobiology of †*Saurichthys*, based on exceptionally well-preserved material recovered from the Middle Triassic deposits of Monte San Giorgio. However, it soon became apparent that †*Saurichthys* fossils preserved information that could be compared with a broader actinopterygian, or even piscine gnathostome, sample and provide a basis for discussion on the evolution of anatomical structures within a much broader context.

In Chapter 1 (Argyriou *et al.* 2016), we described, for the first time, the anatomy of the gastrointestinal tract of †*Saurichthys*, on the basis of in situ preserved cololite material. After this work, †*Saurichthys* is established as the first Mesozoic actinopterygian the gross gastrointestinal anatomy of which is known in detail, and provides a useful model for comparison with fossil and recent forms. Our work gave a deep time perspective into the evolution of actinopterygian gastrointestinal tracts, and uncovered additional morphological diversity in non-teleostean forms, which would otherwise remain untraced. The markedly developed spiral intestine, forming more than 28 turns, is the most conspicuous feature of the gastrointestinal anatomy of †*Saurichthys*, setting it apart from living non-teleostean actinopterygians, which exhibit fewer than ten turns. The similarity of the high spiral valve turn count of †*Saurichthys* with modern large-size and high metabolism chondrichthyans is noted. Our phylogenetically-informed statistical analysis of the distribution of spiral valve turn counts across gnathostomes showed that the latter is controlled by body size and phylogeny, and not by diet, as previously hypothesized. We concluded that the small-sized Middle Triassic †saurichthyiforms inherited their well-developed spiral intestine from a large-sized ancestor. In addition, we highlighted the possibility that spiral valve turn count multiplication is linked with high metabolic rates and the energetically expensive lifestyle of †*Saurichthys*.

In Chapter 2 (Maxwell *et al.* 2018), we explored the early life history and reproductive biology of live-bearing Middle Triassic †*Saurichthys*, and again, uncovered new features unknown in other actinopterygians. We focused on two species from Monte San Giorgio, which are represented by largely complete ontogenetic series, ranging from embryos to juveniles and adults. We showed that a larval stage is absent in these species. As dictated by the formed cranial ossifications and dentition, embryos were born as largely precocial juveniles, capable of exogenous feeding. A larval stage was absent. We detected the delayed onset of parietal bone and mid-lateral scale row ossification. These features along, with the presence of open sensory grooves and pit organs in the head, as well as the strong negative allometry of skull growth relative to postcranium, can now be used as criteria for distinguishing between †*Saurichthys* juveniles and miniature species in the fossil record. A list of topological criteria for distinguishing between cannibalized prey and embryos in †*Saurichthys* is also provided, which can be conceivably employed in other actinopterygian fossils. When placed within a †saurichthyiform phylogenetic context, viviparity seems to have not been primitively present in the clade, but could have been among the biological properties that influenced the success of the clade during the Middle Triassic.

In chapter 3, we utilized modern μCT-aided imaging methods to explore the craniosensory anatomy of †saurichthyids, and reappraise classical anatomical models for the genus (Stensiö 1925), which remained the chief source of morphological characters used in phylogenies for many decades. Particular attention was paid to comparing †saurichthyiforms with modern acipenseriforms, in order to test the historical hypotheses of a close phylogenetic relationship between the two clades. Numerous new structures were recognized, which remained undetected or misidentified by previous workers, but which added a lot to our understanding of the phylogenetic position of the genus, and of crownward early actinopterygians in general. Some of the newly discovered features pertain to: i) the persistence of a cryptic oticooccipital fissure; ii) the reappraisal of the basicranial circulation, which contrasts previous interpretations that considered it similar to that of acipenseriforms; iii) brain and inner ear endocast; iv) the presence of nasobasal canals, suggesting that such structures are not restricted in Devonian actinopterygians; v) the presence of a fused dermohyal on the hyomandibula, which is for the first time recorded in a Mesozoic taxon. Among the major contributions of this work, is the reassessment of the homology of the components of the saurichthyid opercular series. We show that the bone historically attributed as an opercle is actually a subopercle, whereas a vestigial opercle must have only been present in some Early Triassic representatives of the genus. Our phylogenetic analysis of Osteichthyes suggested that †saurichthyiforms are not closely related to acipenseriforms, but form a clade with †*Birgeria*. This clade is resolved as the immediate sister group to crown actinopterygians, though overall nodal support around the base of the actinopterygian crown is very low. The inclusion of new fossils is required for achieving better resolution for this part of the tree, but it might also alter the topology of †saurichthyiforms. Our work indicated the deficiencies of historical works conducted with analogue, destructive techniques such as serial grinding, and highlighted the importance of revisiting older authoritative models of endoskeletal anatomy for bettering our understanding of early actinopterygian interrelationships.

Information from Chapter 4 helps ameliorate the lack of resolution around the actinopterygian crown, this time by providing new information from a poorly-known actinopterygian, †*Brachydegma caelatum*. The latter taxon comes from an inadequately sampled time interval, the Permian, and helps build a bridge between the better-studied Devonian and Triassic forms. We provide, for the first time, anatomical models and descriptions of the endoskeletal anatomy of †*Brachydegma*, which shed light on its long contested systematic affinities. μCT revealed a character mosaic comprising features that are encountered in distantly related crown group lineages. These include, among others, the presence of only four branchial arches, which is nowadays seen in polypterids, and the presence of a double jaw joint, involving a symplectic. The latter constituted one of the most well-established neopterygian synapomorphies. Following the discovery of a symplectic involvement in the jaw joint of †*Brachydegma* and other forms, we suggest that this is better treated as an actinopterygian, or even an osteichthyan synapomorphy. Still, the sub-parallel arrangement of symplectic and interhyal of †*Brachydegma* resembles the condition in parasemionotids and early neopterygians, suggesting that this is a crown actinopterygian synapomorphy. Based on

our anatomical observations and a new phylogenetic analysis, we reject its previously proposed affiliation with neopterygians, and halecomorphs in particular. Instead, †*Brachydegma* is resolved as an early member of the actinopterygian crown. Its inclusion in our taxonomic sample expands the membership of the crown group, to also include †saurichthyiforms and †*Birgeria*. This work provided a valuable new anatomical model for understanding the early crown actinopterygian character complex. Moreover, information from †*Brachydegma* is expected to aid in the recognition of Paleozoic members of the crown group, which are otherwise scarce and poorly known. Finally, this work shows that historical synapomorphies of modern clades, most of which were erected by prominent paleontologists before the widespread adoption of cladistics and 3D imaging methods, can be questioned with new fossils and study techniques.

The results of this thesis emphasize the importance of multidisciplinary approaches in the study of fossils. The paleobiological information contained in fossils, not only offers the deep time perspective in the study of evolution, but can also provide inspiration on how to study evolution of different anatomical structures, and what evolutionary, or even functional morphology related questions one should or could address. Like in the case of the spiral valve, the biological context of soft tissue anatomical systems can sometimes be hidden from neontologists, who often treat anatomical differences solely as means to for taxomonic assessment. Moreover, the results of the chapters 3 and 4 are a testimony to the indispensable value of character information from fossils, for reconstructing the tree of life of modern organisms, and identifying its problematic sectors (contra e.g., (Patterson 1994).

Future perspectives

As every scientific work, this thesis resulted in a large number of questions to be addressed and opened new avenues for future research. Some ideas are outlined below.

While studying the gastrointestinal anatomy of non-teleostean fishes, and especially their spiral intestines, I came to realize that there is no clear way to compare the potential digestive efficiency and the effects of diet, metabolism and habitat among a large taxonomic sample. In teleosts and tetrapods, which do not possess a spiral intestine, this can be achieved by measuring gut length, while accounting for the role of phylogeny (Wilson & Castro 2011). As far as I am aware, there is no stable formula that accounts for spiral valve turns and effective digestive surface in spiral intestine-bearing forms.

Studying life history parameters, such as life span, age of sexual maturity and growth rates of fossil actinopterygians, could further aid in understanding the mode of life of these long extinct animals, and give insights into the dynamic ecosystems they lived in. It can also provide a much needed basis for attempting larger scale comparisons with other modern and extinct forms. Bone histology is a powerful tool for extracting skeletochronological information from fossils, but previous implementation in †saurichthyids has proven challenging (Scheyer *et al.* 2014). However, endochondral bones of circular cross-section, such as the ceratohyal, appear to give reliable age results (Scheyer *et al.* 2014), and a comparative study of these and other

elements of circular cross-section among †saurichthyids, or at an even broader actinopterygian scale could prove pivotal for determining how life history properties influenced species diversity through time and morphological disparity. There are still tremendous limitations associated with such histological work, pertaining to e.g., the availability of material, or the need for recourse to destructive study methods. However, non-invasive microhistological imaging techniques are being developed (Sanchez *et al.* 2012; Sanchez *et al.* 2016), and are expected to become more easily available for the study of fossils in the near future. On a similar note, important ontogenetic and functional anatomical information, as well as phylogenetic signals, can be extracted by directing such methods to the study of tooth attachment/replacement patterns in actinopterygians. There has been a long hiatus in the study of such structures (Fink 1981), but recent works, utilizing modern imaging techniques, are providing promising results that can act as foundations for broader studies (Germain & Meunier 2017).

The endoskeletal anatomy and phylogenetic investigations I conducted underlined several areas of instability in the early actinopterygian tree of life. This issue can be addressed with the use of μCT on already available three-dimensionally preserved fossils. One major cause of instability is the limited understanding of the endocranial anatomy of potential late Paleozoic crown actinopterygians. Although the study of †*Brachydegma* added a lot to our knowledge, lack of data from phylogenetically fluid forms, such as the deep-bodied †eurynotiforms or †platysomoids, still contributes to the uncertainty regarding early crown actinopterygian character complexes. In the emerging phylogenetic picture, Carboniferous–Triassic generalized actinopterygian forms are being removed from the actinopterygian crown group and are being resolved forming a poorly supported clade (Giles *et al.* 2017); Chapters 3, 4). Among these, †*Pteronisculus* and †*Boreosomus* from the Early Triassic of East Greenland are known from more complete specimens, but, like in the case of †*Saurichthys,* their endoskeletal anatomy was last studied half a century ago by serial grinding (Nielsen 1942). An investigation of this potential clade of generalized animals would greatly benefit from having a solid comparative base, in the form of modern digital models of †*Pteronisculus* and †*Boreosomus*. Information from understudied fossils, like the iconic †*Palaeoniscum* (Müller 1962), will further help resolve the problematic interrelationships of generalized forms (also known as 'palaeoniscoids'), and can potentially provide synapomorphies for their grouping. Finally, the removal of †*Brachydegma* from the neopterygian or halecomorph stem, and the reconsideration of characters that constituted historical neopterygian synapomorphies, act as reminders for how little is known about the character transformations underpinning the largest clade of ray-finned fishes, the neopterygians. Again, this gap of knowledge can be partially bridged by modern studies of the stem neopterygian '†*Perleidus*' *stoschiensis* and the likely stem holostean †parasemionotids from the Early Triassic of East Greenland (Stensiö 1932).

References

Argyriou, T., Clauss, M., Maxwell, E.E., Furrer, H. & Sánchez-Villagra, M.R. 2016. Exceptional preservation reveals gastrointestinal anatomy and evolution in early actinopterygian fishes. *Scientific Reports*, **6**: 18758.

Fink, W.L. 1981. Ontogeny and phylogeny of tooth attachment modes in actinopterygian fishes. *Journal of Morphology*, **167**: 167-184.

Germain, D. & Meunier, F.J. 2017. Teeth of extant Polypteridae and Amiidae have plicidentine organization. *Acta Zoologica*: 1-7.

Giles, S., Xu, G.-H., Near, T.J. & Friedman, M. 2017. Early members of 'living fossil' lineage imply later origin of modern ray-finned fishes. *Nature*, **549**(7671): 265-268.

Maxwell, E.E., Argyriou, T., Stockar, R. & Furrer, H. 2018. Re-evaluation of the ontogeny and reproductive biology of the Triassic fish *Saurichthys* (Actinopterygii, Saurichthyidae). *Palaeontology*.

Müller, A.H. 1962. Körperlich erhaltene Fische (Palaeoniscoidea) aus dem Zechstein (Kupferschiefer) von Ilmenau (Thuringen). *Geologie*, **11**: 845-856.

Nielsen, E. 1942. *Studies on the Triassic fishes from East Greenland I.* Glaucolepis *and* Boreosomus. C.A. Reitzels, Copenhagen, 394 + 330 pl. pp.

Patterson, C. 1994. Bony Fishes. *Short Courses in Paleontology*, **7**: 57-84.

Sanchez, S., Ahlberg, P.E., Trinajstic, K.M., Mirone, A. & Tafforeau, P. 2012. Three-Dimensional Synchrotron Virtual Paleohistology: A New Insight into the World of Fossil Bone Microstructures. *Microscopy and Microanalysis*, **18**(5): 1095-1105.

Sanchez, S., Tafforeau, P., Clack, J.A. & Ahlberg, P.E. 2016. Life history of the stem tetrapod Acanthostega revealed by synchrotron microtomography. *Nature*, **537**: 408.

Scheyer, T.M., Schmid, L., Furrer, H. & Sánchez-Villagra, M.R. 2014. An assessment of age determination in fossil fish: the case of the opercula in the Mesozoic actinopterygian Saurichthys. *Swiss Journal of Palaeontology*, **133**(2): 243-257.

Stensiö, E.A. 1925. *Triassic fishes from Spitzbergen*. Almqvist & Wiksells Boktryckeri-A.-B., Stockholm.

Stensiö, E.A. 1932. *Triassic fishes from East Greenland*. Bianco Lunos Bogtrykkeri A/S, Copenhagen, 305 + XXXIX pl. pp.

Wilson, J. & Castro, L. 2011. Morphological diversity of the gastrointestinal tract in fishes. Pp. 1-55 in M. Grosell, A. Farrell and C. Brauner (eds) *The multifunctional gut of fish*. Academic Press, U.S.A.

APPENDIX A

AMEGHINIANA
A GONDWANAN PALEONTOLOGICAL JOURNAL

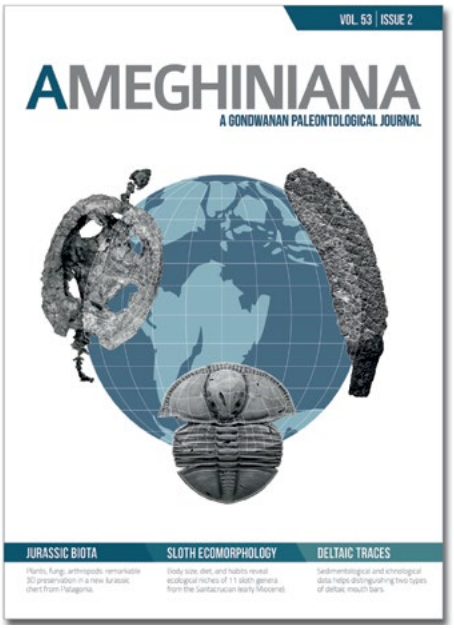

A NEW EARLY MIOCENE (AQUITANIAN) ELASMOBRANCHII ASSEMBLAGE FROM THE LA GUAJIRA PENINSULA, COLOMBIA

JORGE D. CARRILLO-BRICEÑO[1]
THODORIS ARGYRIOU[1]
VLADIMIR ZAPATA[2]
RENÉ KINDLIMANN[1]
CARLOS JARAMILLO[3]

[1]Paleontological Institute and Museum, University of Zurich, Karl-Schmid-Strasse 4, 8006 Zürich, Switzerland.
[2]Ecopetrol S.A Edificio Colgas, Calle 37 N° 8-43 Piso 8 costado occidental, 11001000 Bogotá, Colombia.
[3]Smithsonian Tropical Research Institute, Av. Gorgas, Ed. 235, 0843- 03092 Balboa, Ancón, Panamá.

Submitted: July 1st, 2015 - **Accepted:** October 26th, 2015

To cite this article: Jorge D. Carrillo-Briceño, Thodoris Argyriou, Vladimir Zapata, René Kindlimann, and Carlos Jaramillo (2016). A new early Miocene (Aquitanian) Elasmobranchii assemblage from the La Guajira Peninsula, Colombia. *Ameghiniana* 53: 77–99.

To link to this article: http://dx.doi.org/10.5710/AMGH.26.10.2015.2931

AMEGHINIANA - 2016 - Volume 53 (2): 77 – 99 ARTICLES

ISSN 0002-7014

A NEW EARLY MIOCENE (AQUITANIAN) ELASMOBRANCHII ASSEMBLAGE FROM THE LA GUAJIRA PENINSULA, COLOMBIA

JORGE D. CARRILLO-BRICEÑO[1], THODORIS ARGYRIOU[1], VLADIMIR ZAPATA[2], RENÉ KINDLIMANN[1], AND CARLOS JARAMILLO[3]

[1]Paleontological Institute and Museum, University of Zurich, Karl-Schmid-Strasse 4, 8006 Zürich, Switzerland. *jorge.carrillo@pim.uzh.ch*; *thodoris.argyriou@pim.uzh.ch*; *mad_design@gmx.ch*

[2]Ecopetrol S.A Edificio Colgas, Calle 37 N° 8-43 Piso 8 costado occidental, 11001000 Bogotá, Colombia. *vladimir.zapata@ecopetrol.com.co*

[3]Smithsonian Tropical Research Institute, Av. Gorgas, Ed. 235, 0843- 03092 Balboa, Ancón, Panamá. *jaramilloc@si.edu*

Abstract. Recent field expeditions have led to the discovery of a selachian assemblage from the earliest Miocene (Aquitanian) deposits of the Uitpa Formation in the La Guajira Peninsula, Colombia. This elasmobranch assemblage provides a unique glimpse into the Caribbean biodiversity at the onset of the Neogene. The assemblage consists of 13 taxa, of which some are reported from Miocene deposits for the very first time. There are also new records of taxa the in southern Caribbean region. The taxonomic composition of the selachian assemblage was used to conduct a paleoenvironmental and paleobathymetric analysis of the lower Uitpa Formation. The maximum likelihood estimation of paleobathymetry suggests that the lower part of the Uitpa Formation was probably accumulated at a water depth of 100 to 200 m. This indicates a rapid increase in relative sea level or basin deepening, providing new insights into the possible causes of marine biota changes in the Cocinetas Basin during the Oligocene/Miocene transition.

Key words. Neogene. Tropical America. Caribbean. Sharks. Rays. Paleobathymetry. Paleoenvironments.

Resumen. UN NUEVO ENSAMBLE DE ELASMOBRANCHII DEL MIOCENO TEMPRANO (AQUITANIANO) DE LA PENÍNSULA DE LA GUAJIRA, COLOMBIA. Recientes trabajos de campo han llevado al descubrimiento de un conjunto de seláceos procedente del Mioceno temprano (Aquitaniano) en los depósitos más antiguos de la Formación Uitpa en la Península de La Guajira, Colombia. Este conjunto de elasmobranquios provee una visión única de la paleobiodiversidad del Caribe a inicios del Período Neógeno. El conjunto aquí descrito se compone de 13 taxones, algunos de los cuales son reportados por vez primera para el Mioceno. Esta fauna también incluye nuevos registros para la región sur del Caribe. La composición taxonómica del nuevo ensamble permitió realizar un análisis paleoambiental y paleobatimétrico en la sección más inferior de la Formación Uitpa. La estimación de paleobatimetría usando *maximum likelihood* sugiere que la parte inferior de la Formación Uitpa fue probablemente depositada a profundidades entre los 100 y 200 m. Esto indica un rápido incremento en el nivel relativo del mar o en la profundización de la cuenca, proveyendo nueva información sobre las posibles causas que dieron origen a los cambios en la biota marina de la Cuenca de Cocinetas durante la transición del Oligoceno/Mioceno.

Palabras clave. Neógeno. América Tropical. Caribe. Tiburones. Rayas. Paleobatimetría. Paleoambientes.

THE beginning of the Neogene was a time when world climate was warmer and sea level was higher than at present (Zachos *et al.*, 2001). Large scale geological processes, including the closure of the Central American Seaway and the rise of the Panamanian Isthmus, had not yet been completed (Woodburne, 2010; Montes *et al.*, 2012a,b; Coates and Stallard, 2013; Montes *et al.*, 2015). Large areas of the northern margin of South America were submerged during the early Miocene (see Iturralde-Vinent and MacPhee, 1999 and references therein). This was also the case in the southern Caribbean Cocinetas Basin, where there are widespread early Miocene marine sedimentary deposits that have yielded a rich record of invertebrate (Becker and Dusenbury, 1958; Lockwood, 1965; Rollins, 1965; Thomas, 1972; Hendy *et al.*, 2015) and vertebrate fossils of which most are chondrichthyans (Lockwood, 1965; Moreno *et al.*, 2015).

Early Miocene marine chondrichthyan faunas from Tropical America are still poorly known with only a few relevant reports from Barbados (Casier, 1958), Brazil (Santos and Travassos, 1960; Santos and Salgado, 1971; Reis, 2005; Costa *et al.*, 2009), Cuba (Iturralde-Vinent *et al.*, 1996), Mexico (Gonzales-Barba and Thies, 2000), Panama (Pimiento *et al.*, 2013a), Trinidad (Leriche, 1938), the Grenadines (Portell *et al.*, 2008) and Venezuela (Leriche, 1938; Sánchez-Villagra *et*

AMEGHINIANA - 2016 - Volume 53 (2): 77 – 99

al., 2000; Aguilera and Rodrigues de Aguilera, 2004; Aguilera, 2010; Aguilera and Lundberg, 2010) available. These studies depict the composition of marine vertebrate Caribbean faunas before the complete closure of the Central American Seaway (Woodburne, 2010; Montes *et al.*, 2012a,b; Coates and Stallard, 2013; Montes *et al.*, 2015). Reports on marine chondrichthyans from the Miocene of Colombia are scarce in the literature and previous works on the Cocinetas Basin (La Guajira Peninsula) only include a brief mention of elasmobranch fossils with no accompanying taxonomic description by Lockwood (1965) and a list of 14 families presented in Moreno *et al.* (2015).

The Cocinetas Basin is located in the eastern flank of La Guajira Peninsula, northern Colombia (Fig. 1), and provides an extensive and well-exposed sedimentary and paleontological record of the last 30 million years (**Ma**) (Jaramillo *et al.*, 2015; Moreno *et al.* 2015). Recent expeditions to the La Guajira Peninsula (Cocinetas Basin) brought about the extensive surface collection of vertebrate fossils, including the chondrichthyan assemblage from the early Miocene (Aquitanian) Uitpa Formation reported here. We studied the taxonomic composition of this assemblage and its paleobiogeographical and chronostratigraphic significance. Additionally, we conducted a paleoenvironmental and paleobathymetric analysis of the data to explore possible causes related to the marine biota changes that occurred in the Cocinetas Basin during the Oligocene/Miocene transition (**OMT**). Furthermore, we compared the Uitpa Formation chondrichthyans to other coetaneous faunas from Tropical America such as the Venezuela and Trinidad collection described by Leriche (1938). The new assemblage reported herein, which includes taxa previously unreported from the Caribbean region, is one of the oldest shark-ray associations known from the Neogene of Tropical America.

Figure 1. Location map of the fossiliferous locality.

GEOLOGICAL AND STRATIGRAPHICAL SETTING

The Uitpa Formation and its type section were described by Renz (1960, p. 340) and named after the water spring of the Uitpa village, located to the SE of the Serranía de Jarara. The formation was re-described by Rollins (1965). The Uitpa Formation is one of the most extensive Cenozoic units in the La Guajira Peninsula and boasts a thickness of approximately 230 m. It conformably overlies the Siamana Formation while conformably underlying the Jimol Formation (Fig. 2). While an Oligocene to early Miocene age was proposed by Becker and Dusenbury (1958) based on benthic foraminifera, Lockwood (1965) and Rollins (1965) suggested an early Miocene age (Aquitanian) based on foraminifera and ostracods. More recently, an early Miocene to earliest middle Miocene age was proposed by Hendy *et al.* (2015) based on mollusks and stratigraphic relations. The outcrop studied herein is located close to the Uitpa village (Fig. 1) and the chondrichthyan-bearing strata (Fig. 2) lie at 0.5 to 10 m fom the base of the Uitpa Formation. The lower part of the Uitpa Formation comprises well-differentiated layers of soft light brown shales and calcareous bioturbated silty-sandstones presenting thin selenite layers. We have also observed abundant mollusks, echinoids, crustaceans and bony fish fragmentary remains.

MATERIALS AND METHODS

The fossils studied herein (Figs. 3–5) were collected from the base of the Uitpa Formation in the course of three field trips conducted between 2008 and 2014. Fossil specimens came from stratigraphic meters 0.5 to 10 (Fig. 2) in the Arroyo Uitpa locality, ID locality: 360181, 12° 1′ 32.73″

N, 71° 25′ 4.94″ W, ~0.9 km SW of the Uitpa village. Photographs of the fossils were taken with a Leica MZ16F and multifocal stereomicroscope. As for the imaging of small teeth, a Scanning Electronic Microscope was used. We identified all fossil chondrichthyan teeth and narrowed their classification down to the lowest possible taxonomic level. This material is deposited at the Mapuka Museum of Universidad del Norte (**MUN-STRI**), Barranquilla, Colombia. While the dental terminology utilized herein is the one coined by Cappetta (2012), the systematics applied for fossil and recent taxa are consistent with Compagno (2005) and Cappetta (2012). The sole exception to this approach is the extinct genus *Carcharocles* Jordan and Hannibal, 1923, whose assignment in this study has prolonged the discussion presented by Pimiento *et al.* (2010). Measurements taken refer to the entire tooth, including the root, and consist of height, width and length. For incomplete teeth we used only crown measurements. In addition to MUN-STRI materials, specimens housed at the Natural History Museum of Basel (**NMB**), Basel, Switzerland, were also included here. Taxonomic identification involved an extensive bibliographical review and comparative studies concerning fossil and extant specimens from other collections such as the Fossil Vertebrate Section of the Museum für Naturkunde, Berlin, Germany; the Museu Paraense Emilio Goeldi, Belem, Brazil; the Paleontological collections of the Alcaldía Bolivariana de Urumaco, Urumaco, Venezuela; the Palaeontological Institute and Museum at the University of Zurich, Zurich, Switzerland; the René Kindlimann private collection, Uster, Switzerland; and the Universidad Nacional Experimental Francisco de Miranda, Coro, Venezuela.

In this work, the term "Tropical America" (Neotropics) refers to the geographical area of the western hemisphere located between the Tropic of Cancer (23° 27′ N) and the Tropic of Capricorn (23° 27′ S). "Southern South America" is a region composed of the southernmost areas of South

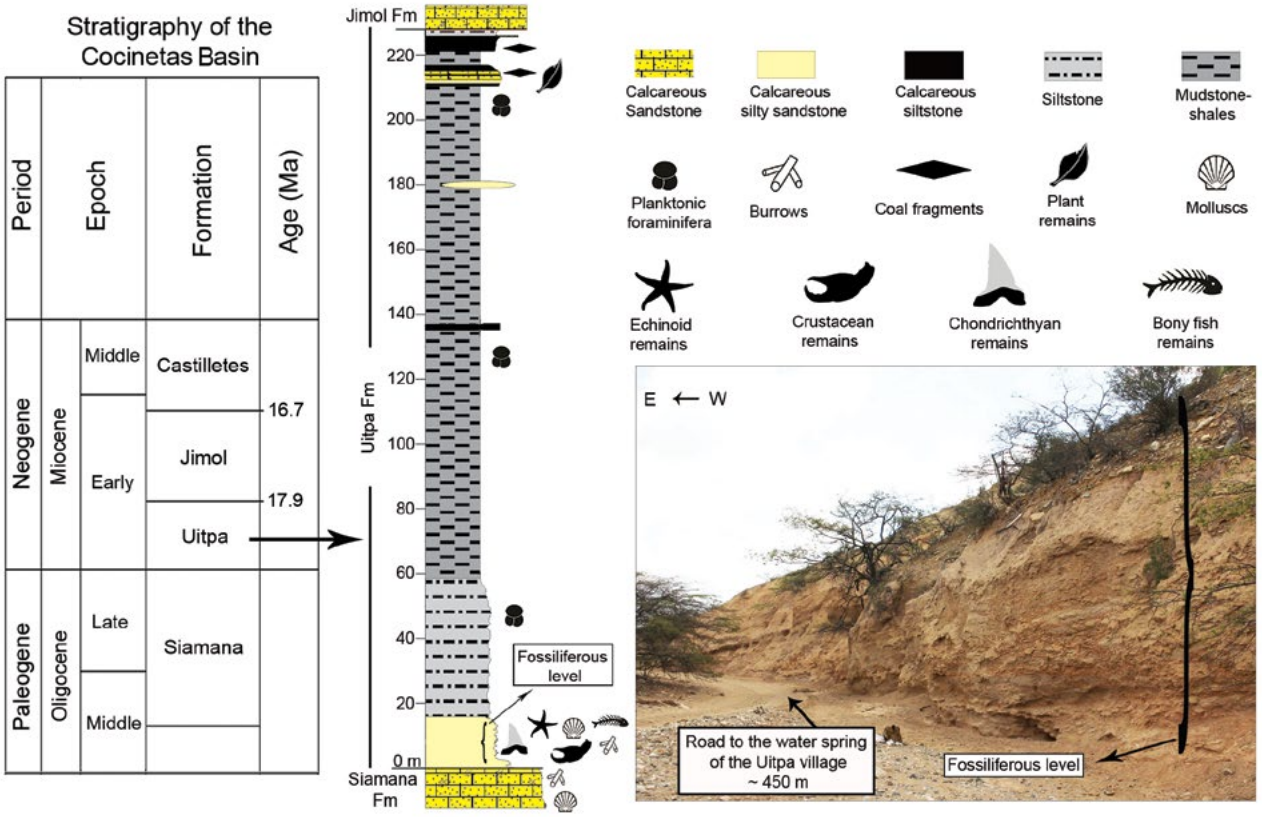

Figure 2. Generalized stratigraphy of the Cocinetas Basin (after Moreno *et al.*, 2015), including a complete stratigraphic section of the Uitpa Formation and an illustration of the studied outcrop, that corresponds to the lowest 10 stratigraphic meters of the formation.

AMEGHINIANA - 2016 - Volume 53 (2): 77 – 99

America; namely, Argentina, Chile, Paraguay and Uruguay (south of the Tropic of Capricorn). We refer to Canada, the USA and the northern part of Mexico as "North America" (north of the Tropic of Cancer).

We compiled information on the paleodistribution of all chondrichthyan taxa known from the Neogene of the Americas (Appendix 1) [*e.g.*, Tropical America (Leriche,1938; Casier, 1958, 1966; Santos and Travassos, 1960; Gillette, 1984; De Muizon and Devries, 1985; Kindlimann, 1990; Kruckow and Thies, 1990; Iturralde-Vinent *et al.*, 1996; Laurito, 1999; Donovan and Gunter, 2001; Reis, 2005; Portell *et al.*, 2008; Aguilera and Lundberg, 2010; Pimiento *et al.*, 2010, 2013a, b; Aguilera *et al.*, 2011; Carrillo-Briceño *et al.*, 2014, 2015), Southern South America (Long, 1993a; Arratia and Cione, 1996; Suárez and Marquardt, 2003; Suárez *et al.*, 2006; Cione *et al.*, 2011; Carrillo-Briceño *et al.*, 2013) and North America (Case, 1980; Kruckow and Thies, 1990; Long, 1993b; Müller, 1999; Gonzales-Barba and Thies, 2000; Purdy *et al.*, 2001; Boessenecker, 2011)]. For conducting the paleoenvironmental interpretation, we used Compagno (1984a,b), Compagno and Last (1999), Compagno *et al.* (2005), Musick *et al.* (2004), Kiraly *et al.* (2003), Cao *et al.* (2011), Voigt and Weber (2011) and the FishBase website (Froese and Pauly, 2015) for collecting bathymetric and habitat information for both the taxa present in the Uitpa Formation and their extant relatives. In addition, we performed a maximum likelihood estimation of paleobathymetry following the method developed and extensively described in Punyasena *et al.* (2011), with which the probability that a fossil assemblage is derived from a given depth can be calculated. Drawing on information that was compiled from the literature (Fig. 6), all species with extant relatives were individually modeled with normal probability densities to replicate each species abundance distribution along a depth gradient. Probability density reflects the likelihood of finding a given species at a given point along a depth gradient. For the analysis put forth herein, we use the function *rtruncnorm* in the package *truncnorm* in R (R-Development-Core-Team, 2012) to simulate the probability density. Likelihood values for the depth estimates are the sum of the log likelihoods of the species found within a fossil sample (identical to the joint product of the probability densities of these families). The likelihood estimation was performed using the software package developed by Punyasena *et al.* (2011) that can be downloaded at https://www.life.illinois.edu/punyasena-download/. The R-code used to run the analysis can be found in Appendix 2.

RESULTS

Elasmobranch taxonomical composition

The elasmobranch assemblage described herein comprises 13 taxa attributed to 12 genera, 11 families and six orders (Appendix 1).

SYSTEMATIC PALEONTOLOGY

Chondrichthyes Huxley, 1880
Neoselachii Compagno, 1977
Squalomorphii Compagno, 1973
Hexanchiformes Buen, 1926
Heptranchidae Barnard, 1925

Heptranchias Rafinesque, 1810

Type species. *Squalus cinereus* Gmelin, 1789.

†***Heptranchias*** cf. ***howellii*** (Reed, 1946)
Figure 3.1–7

1938 *Notidanion tenuidens* Leriche, p. 3–4, fig. 2, pl. 1, figs. 1–4.
1946 *Notidanion howellii* Reed, p. 1–2, figs. 1–3, p. 3, fig. 4.
1971 *Heptranchias* Waldman, p. 166, pl. 1, figs. 1–2.
1968 *Heptranchias ezoensis* Applegate and Uyeno, p. 197–198, pl. 1A.
1974 *Heptranchias howellii* (Reed), Welton, p. 3, fig. 1 A–B, p. 7, pl. 2.
1981 *Heptranchias howellii* (Reed), Cappetta, p. 568, pl. 1, fig. 1–1'.
2015 *Heptranchias howellii* (Reed), Adolfssen and Ward, p. 319–320, fig. 2K–L.

Referred material. Five lower teeth (MUN-STRI-34777, MUN-STRI-34784a and MUN-STRI-39926) and one upper tooth (MUN-STRI-34784b).

Geographic and stratigraphic occurrence. See Remarks.

Description. The five lower teeth, of which two correspond to the mesial part of the tooth (Fig. 3.1–3.2) while the remaining three to the distal part (Fig. 3.3–3.4), are incomplete. All specimens are strongly compressed labiolingually. The mesial specimens present a developed acrocone, which is larger than the distal cusplets, with two small but well differentiated mesial cusps preserving the first two distal cusplets (accessory conules). The other specimens that correspond to the distal part of the teeth only preserve between three and four distal cusplets. In these

specimens, the acrocone and distal cusplets are smooth and inclined distally while their root is poorly preserved. The upper antero-lateral tooth (Fig. 3.5) preserves only the crown, which is tall and narrow with sigmoidal contour.

Remarks. *Heptranchias howellii* ranges from the early Paleocene to the late Oligocene with records from Africa (Morocco), Asia (Japan), Australia, Europe, North America and South America (Venezuela) (Leriche, 1938; Reed, 1946; Applegate and Uyeno, 1968; Welton, 1974; Kemp, 1978; Cappetta, 1981, 2012; Bieńkowska-Wasiluk and Radwański, 2009; Adolfssen and Ward, 2015). The teeth of *Heptranchias howellii* are very similar to those of the extant *Heptranchias perlo* Bonnaterre, 1788. However, the teeth of *H. howellii* tend to be larger, reaching up to 25 mm in length, and exhibit a broader and less attenuated acrocone than that of *H. perlo* (Kemp, 1978). According to Cappetta (1981), the acrocone of the *H. howellii* teeth is much less developed in comparison with their distal cusplets. The specimens of *Heptranchias* (*Notidanion*) *tenuidens* (Fig. 3.6–3.7) described from the locality of Mene de Acosta in Venezuela (Menecito Member of the San Lorenzo Formation: early to middle Miocene) by Leriche (1938, pl. 1, figs. 1–3), exhibit clear morphological similarities to the teeth of *Heptranchias* cf. *howellii* from both the Uitpa Formation described herein and those referred to the latter species found in African, European and North American deposits (Welton, 1974; Cappetta, 1981, 2012; Bieńkowska-Wasiluk and Radwański, 2009; Adolfssen and Ward, 2015). This resemblance suggests that *Heptranchias* (*Notidanion*) *tenuidens* could be a synonym of *H. howellii*. The merging of the two species was previously suggested by Cappetta (1981, 2012); nevertheless, the aforementioned author did not provide a direct comparison between the *H. tenuidens* specimens of the Leriche collection and *H. howellii*. It should also be noted that one of the specimens referred to as *H. tenuidens* by Leriche (1938, pl. 1, fig. 4) most likely corresponds to an upper anterior tooth of cf. *Centrophorus* (Fig. 3.16–3.17).

SQUALIFORMES Goodrich, 1909

CENTROPHORIDAE Bleeker, 1859

Centrophorus Müller and Henle, 1837

Type species. *Squalus acanthias* Linnaeus, 1758.

Centrophorus sp.

Figure 3.8–15

Referred material. Five poorly preserved lower teeth (MUN-STRI-39927).

Geographic and stratigraphic occurrence. See Remarks.

Description. These specimens exhibit ranges in height of about 3 to 4 mm and, in width, between 3.5 to 5 mm. The teeth are labio-lingually compressed and taller than broad, with a distally inclined triangular cusp. The mesial cutting edge of the main cusp is convex and markedly serrated. Such disposition contrasts with the distal cutting edge, which is straight to convex and presents finer serrations. The distal heel is high, convex and very weakly serrated. The apron is prominent and long but ends before reaching the base of the root. The uvula is less prominent and short. The labial face of the root is short and presents a well-defined external depression. On the lingual face, a large infundibulum opens below the tip of the uvula.

Remarks. *Centrophorus* ranges from the Late Cretaceous to the present (Adnet *et al.*, 2008; Kriwet and Klug, 2009). Extant *Centrophorus* comprises at least 12 species characterized by complex interspecific morphological variations. Additionally, their dentition also displays ontogenetic changes and sexual dimorphism (White *et al.*, 2008). The teeth described herein are not adequately preserved and consequently, although they do resemble the *Centrophorus* sp. teeth referred by Carrillo-Briceño *et al.* (2014) from the middle to late Miocene of Ecuador, they cannot be assigned to any known species. The specimen illustrated as *Acanthias stehlini* by Leriche (1938, pl. 1, fig. 5) from the locality of Mene de Acosta in Venezuela (San Lorenzo Formation: early–middle Miocene) is, instead, a lower tooth of *Centrophorus* (Fig. 3.14–3.15), as previously suggested by Cappetta (2012, p. 116). The poorly preserved single isolated and fragmented tooth used by Leriche (1938) to erect *Acanthias stehlini* (*Centrophorus stehlini*) does not exhibit any diagnostic features that may distinguish it from the specimens from the Uitpa Formation or any other known fossil or recent species. We consider Leriche's species a *nomen dubium* of questionable taxonomical validity.

DALATIIDAE Gray, 1851

AMEGHINIANA - 2016 - Volume 53 (2): 77 – 99

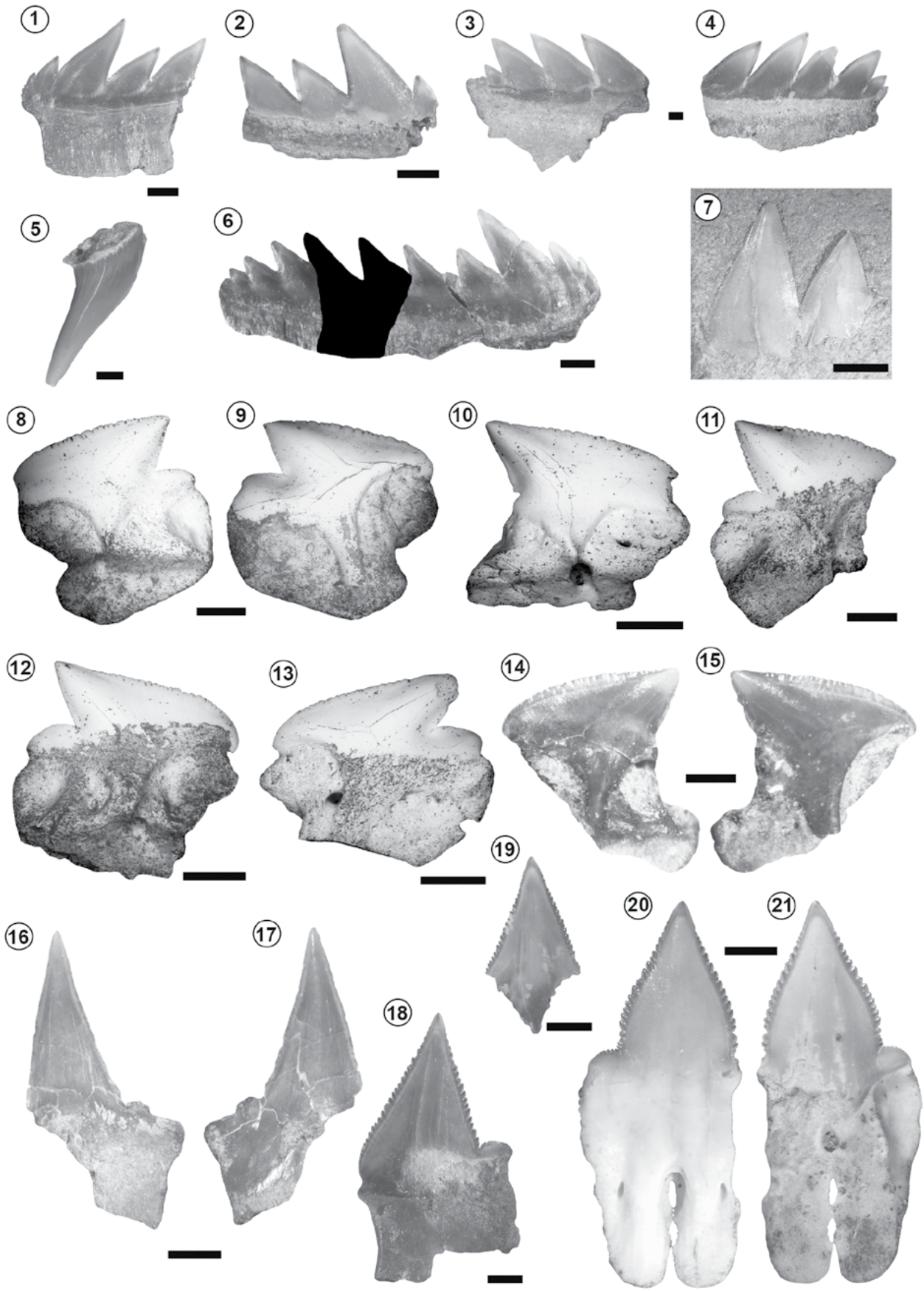

Dalatias Rafinesque, 1810

Type species. *Dalatias sparophagus* Rafinesque, 1810.

Dalatias cf. ***licha*** (Bonnaterre, 1788)
Figure 3.18–21

1788 *Squalus licha* Bonnaterre, p. 2.
1948 *Dalatias licha* (Bonnaterre), Bigelow and Schroeder, p. 502, figs. 96, 97.
1970 *Scymnorhinus licha* (Bonnaterre), Ledoux, p. 353, figs. 20, 21.
1975 *Dalatias licha* (Bonnaterre), Uyeno and Matsushima, p. 46, pl. 2, fig. 2a–b.

Referred material. Three lower teeth, one symphyseal (MUN-STRI-39928) and two laterals (MUN-STRI-39929).

Geographic and stratigraphic occurrence. See Remarks.

Description. The symphyseal tooth is complete and displays a height of 9.5 mm and a width of 4.1 mm. The tooth is labio-lingually compressed and bears an upright and triangular crown with strongly serrated cutting edges. The serrations are directed apically. Two short, narrow, weakly convex and finely serrated heels flank the main cusp. In labial view, the apron is flat and markedly deep, reaching the base of the tooth. A transverse slit divides the basal half of the apron in two. The root is high and presents convex distal and mesial edges. There is a well-developed medio-lingual foramen and a broad elliptical button hole with a broad channel-shaped depression. The lateral teeth are incomplete, lacking parts of their roots. Their main cusps are similar to those of the symphyseal tooth yet slightly inclined distally. Only one distal heel is observed in the lateral teeth but it is similar to that of the symphyseal. The root is high and resembles that of the symphyseal tooth though presenting a convex distal and a concave medial edge.

Remarks. *Dalatias* ranges from the early Paleocene to the Recent (see Kriwet and Klug, 2009; Cappetta, 2012), with the oldest record of *Dalatias licha* known from the middle Eocene of New Zealand (Keyes, 1984; Kriwet and Klug, 2009). The tooth morphology of the Neogene species is identical to that of the recent *D. licha* (Cappetta, 2012). Its fossil record includes occurrences in the Caribbean, Europe, Japan and New Zealand (Kriwet and Klug, 2009; Cappetta, 2012). A specimen previously referred to *Hemipristis serra* Agassiz, 1843, by Casier (1958, pl. 2, fig. 1; 1966, pl. 1, fig. 9), from the early Miocene of Barbados, is hereby identified as a crown of a *Dalatias*. The fossil record of *Dalatias* from the Americas is shown in Appendix 1.

PRISTIOPHORIFORMES Berg, 1958
PRISTIOPHORIDAE Bleeker, 1859

Pristiophorus Müller and Henle, 1837

Type species. *Pristis cirratus* Latham, 1794.

Pristiophorus sp.
Figure 4.1–3

Referred material. Thirteen rostral teeth (MUN-STRI-39930; MUN-STRI-39931).

Geographic and stratigraphic occurrence. See Remarks.

Description. The root is missing in all specimens. The crowns, which measure between 4 and 17 mm in length, are long and slender while dorso-ventrally compressed and bearing smooth edges. The fairly flat enameled cusp is slightly inclined distally.

Remarks. *Pristiophorus* ranges from the Late Cretaceous to the Recent and its rostral teeth are readily distinguishable from those of *Pliotrema* Regan, 1906 since the latter present a barbed posterior cutting edge (Cappetta, 2012). The *Pristiophorus* specimens from the Uitpa Formation described herein constitute the oldest known record of the genus from Tropical America. Other records from the Americas are shown in Appendix 1.

Figure 3. 1–7, ***Heptranchias*** cf. ***howellii***; **1–4,** lower teeth (**1: MUN-STRI**-34777, **2–4: MUN-STRI**-34784a); **5,** upper tooth (**MUN-STRI**-34784b); **6–7,** lower *Heptranchias* teeth referred by Leriche (1938) as ***Notidanion tenuidens*** (**6: NMB** S.a.1314, **7: NMB** S.a.1315). **8–15,** ***Centrophorus*** sp.; **8–13,** lower teeth (**MUN-STRI**-39927); **14–15,** lower ***Centrophorus*** sp. tooth referred by Leriche (1938) as ***Acanthias stehlini*** (**NMB** S.a.1314). **16–17,** upper tooth of cf. ***Centrophorus*** referred by Leriche (1938) as ***Notidanion tenuidens*** (**NMB** S.a.1316). **18–21,** ***Dalatias*** cf. ***licha*** lower teeth (**18–19: MUN-STRI**-39929, **20–21: MUN-STRI**-39928). Views: labial (**1, 2, 9, 12, 15, 17, 18, 20**), lingual (**3, 4, 6, 8, 10, 11, 12, 13, 14, 16, 19, 21**), lateral (**5**), indet. (**7**). Scale bar= 1 mm.

AMEGHINIANA - 2016 - Volume 53 (2): 77 – 99

GALEOMORPHII Compagno, 1973

LAMNIFORMES Berg, 1937

LAMNIDAE Müller and Henle, 1838

Isurus Rafinesque, 1810

Type species. *Isurus oxyrinchus* Rafinesque, 1810.

Isurus cf. ***oxyrinchus*** Rafinesque, 1810

Figure 4.4–11

1810 *Isurus oxyrinchus* Rafinesque, p. 12, pl. 13, fig. 1.

2001 *Isurus oxyrinchus* Rafinesque, Purdy *et al.* p. 114–116, figs. 25, 26.

Referred material. Seven teeth. Two upper teeth (MUN-STRI-39932), five lateral teeth of indeterminate position (MUN-STRI-39933).

Geographic and stratigraphic occurrence. See Remarks.

Description. All teeth are incomplete and present damaged roots. The crown height measures between 9 and 45 mm. The upper anterior tooth exhibits a wide, asymmetrical and distally inclined crown. Both the lingual and the labial sur-

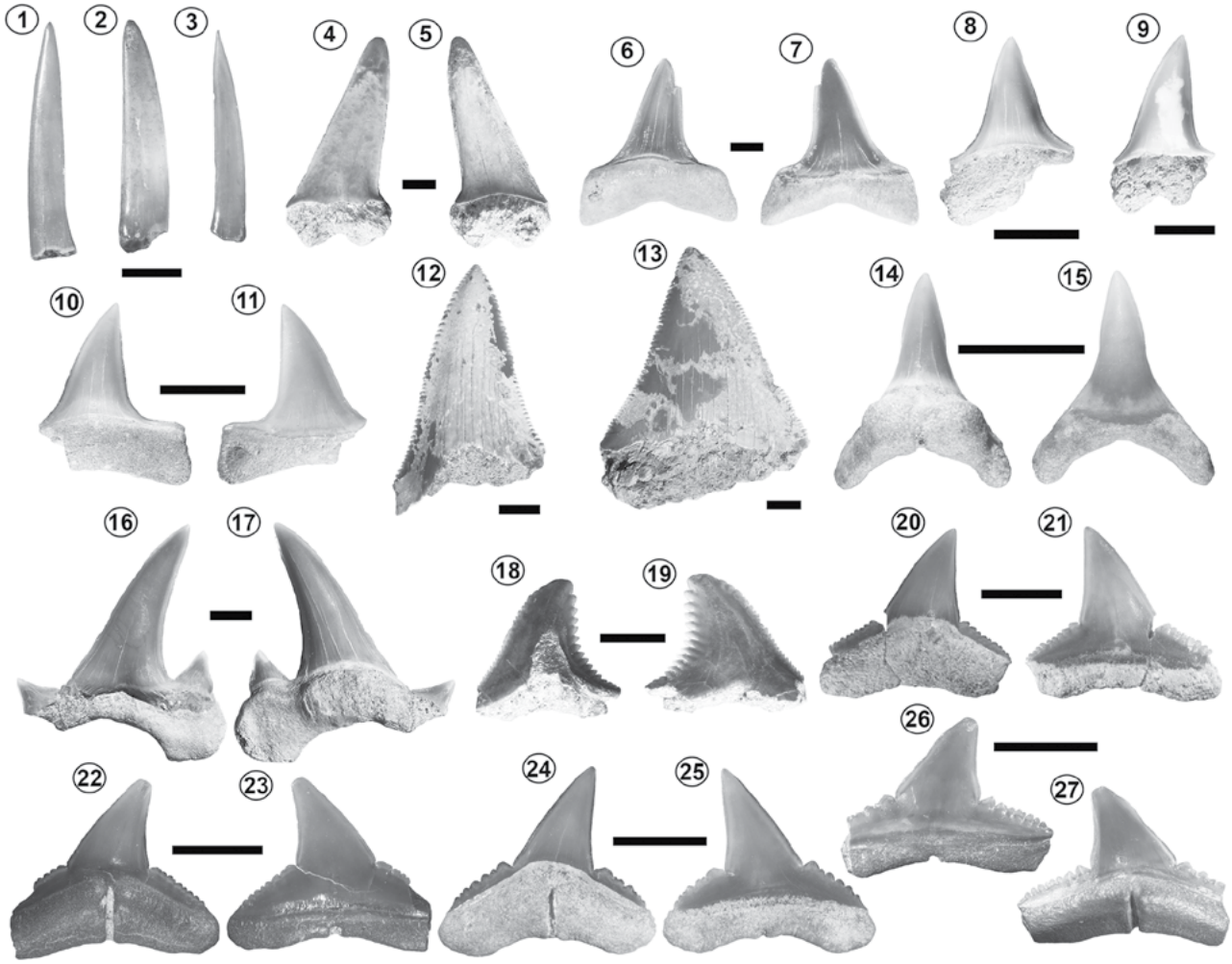

Figure 4. 1–3, ***Pristiophorus*** sp.; **1–3** rostral teeth (**MUN-STRI**-39930). **4–11,** ***Isurus*** cf. ***oxyrinchus***; **4–5,** upper tooth (**MUN-STRI**-39932); **6–11,** indet. position (**6–7: MUN-STRI**-39932, **8–11: MUN-STRI**-39933). **12–13,** ***Carcharocles*** sp.; **12,** lower tooth (**MUN-STRI**-39934); **13,** upper tooth (**MUN-STRI**-39934). **14–15,** ***Alopias*** cf. ***superciliosus*** lower tooth (**MUN-STRI**-39936). **16–17,** Lamniformes gen. et sp. indet. upper tooth (**MUN-STRI**-39937). **18–19,** ***Hemipristis serra*** upper tooth (**MUN-STRI**-39938). **20–27,** ***Carcharhinus gibbesii***; **20–25,** upper teeth (**MUN-STRI**-39945); **26–27,** upper tooth referred by Leriche (1938) as ***Hypoprion*** sp. (**NMB** S.a.1389). Views: labial (**4, 7, 11, 15, 16, 19, 21, 23, 25, 26**), lingual (**5, 6, 8, 9, 10, 12, 13, 14, 17, 18, 20, 22, 24, 27**), dorsal (**1, 2, 3**). Scale bar= 5 mm.

faces are smooth. The upper lateral tooth displays a slightly inclined triangular crown marked by smooth cutting edges. Its root is rather low with an obtuse V-shaped basal surface. Similarly, the teeth of indeterminate jaw position, of which some even preserve fragments of the eroded root, also exhibit a triangular crown with smooth cutting edges. In all seven teeth, the crown presents a flat labial face and a moderately convex lingual one.

Remarks. *Isurus oxyrinchus* ranges from the late Oligocene (middle Chattian) to the present (see Reinecke *et al.*, 2011 for an excellent summary of the fossil record of the genus). Although the specimens from the Uitpa Formation are mostly incomplete, the fact that their teeth do exhibit a close resemblance to teeth of the extant *Isurus oxyrinchus* allows us to associate them with this taxon. We adopt the taxonomic proposal suggested by Purdy *et al.* (2001) and ratified by Reinecke *et al.* (2011) by which narrow-cusped *Isurus* teeth from Miocene–Pliocene deposits referred by other authors (see Purdy *et al.*, 2001) to *Isurus desori* Agassiz, 1843, should be assigned to *Isurus oxyrinchus*. The tooth referred to *Oxyrhina* cf. *desori* by Leriche (1938, pl. 1, fig.15) from the northeast of the Mene de Acosta locality in Venezuela (San Lorenzo Formation *sensu* Leriche, 1938) is hereby reattributed to a lower lateral-posterior tooth of *Isurus oxyrinchus*. The fossil record of *Isurus oxyrinchus* in the Americas is shown in Appendix 1.

†Otodontidae Glikman, 1964

†***Carcharocles*** Jordan and Hannibal, 1923

Type species. *Carcharodon megalodon* Agassiz, 1835.

†***Carcharocles*** sp.

Figure 4.12–13

Referred material. Three incomplete teeth. Two upper teeth (MUN-STRI-39934; MUN-STRI-39935) and one lower tooth (MUN-STRI-39934).

Geographic and stratigraphic occurrence. See Remarks.

Description. The teeth are incomplete and only preserve the crown, which is triangular in shape and strongly serrated while presenting a pointed apex. Lateral cusplets are not preserved and the crowns of the upper teeth are broader than those of the lower ones. The crown height measures between ~31 and 45 mm.

Remarks. In the Neogene deposits, *Carcharocles* are mainly represented by *Carcharocles chubutensis* Ameghino, 1901 and *Carcharocles megalodon* Agassiz, 1843 (*e.g.*, Pimiento *et al.*, 2010, 2013a,b; Pimiento and Clements, 2014; Pimiento and Balk, 2015). While *Carcharocles chubutensis* ranges from the early to the middle Miocene, *Carcharocles megalodon* ranges from the middle Miocene to the late Pliocene (Pimiento and Balk, 2015). However, other authors have suggested that *C. megalodon* also occurs in the early Miocene (Burdigalian) of Europe and North America (*e.g.*, Leriche, 1938; Purdy *et al.*, 2001; Visaggi and Godfrey, 2010; Reinecke *et al.*, 2011). The generic assignment of *C. chubutensis*, *C. megalodon* and the other species of the lineage has been debated over the years and hitherto there is no consensus among paleoichthyologists concerning the different taxonomical approaches that are still in use (*e.g.*, Cappetta, 2012; Pimiento *et al.*, 2010, 2013b; Reinecke *et al.*, 2011; Bor *et al.*, 2012). According to Pimiento *et al.* (2013a), the teeth of sub-adult and adult specimens of *C. chubutensis* differ morphologically from those of *C. megalodon* by possessing a pair of lateral cusplets that are not separated from the main cusp. Although the teeth of *Carcharocles chubutensis* from the early Miocene exhibit/retain lateral cusplets, these were lost in the adult stage of *C. megalodon* during the late Miocene. This phenomenon is a heterochronic process by which the ontogenetic changes mimic the changes in the *Carcharocles* clade throughout geologic time (Applegate and Espinosa-Arrubarrena, 1996; Ward and Bonavia, 2001; Pimiento *et al.*, 2010, 2013a,b; Pimiento and Balk, 2015). According to Pimiento *et al.* (2013a) *Carcharocles chubutensis* can be distinguished from *C. megalodon* based on the age of the fossils, *e.g.*, an early Miocene specimen would be *C. chubutensis* while a late Miocene specimen would be *C. megalodon*. However, *C. megalodon* is present in Burdigalian deposits (Leriche, 1938; Purdy *et al.*, 2001; Visaggi and Godfrey, 2010; Reinecke *et al.*, 2011). The specimens from the Uitpa Formation correspond to an early Miocene (Aquitanian) age, which could justify an assignment to *Carcharocles chubutensis*, but their poor preservation does not allow us to identify any species-diagnostic elements. Thus, we prefer to keep those specimens in open nomenclature. The fossil record of *Carcharocles* in the Americas is shown in Appendix 1.

AMEGHINIANA - 2016 - Volume 53 (2): 77 – 99

ALOPIIDAE Bonaparte, 1838

Alopias Rafinesque, 1810

Type species. *Alopias macrourus* Rafinesque, 1810.

Alopias cf. ***superciliosus*** (Lowe, 1841)
Figure 4.14–15

1958 *Alopias acutidens* Casier, p. 39, pl. 1, fig. 20.
1970 *Alopias* cf. *superciliosus* (Lowe), Antunes and Jonet, p. 150, pl. 7, 8, fig. 4.
1988 *Alopias superciliosus* (Lowe), Cigala-Fulgosi, p. 95, pl. 1, figs. 1–2.
2001 *Alopias* aff. *superciliosus* (Lowe), Aguilera and Rodrigues de Aguilera, p. 740, fig. 6.22–6.23.

Referred material. One lower anterior tooth (MUN-STRI-39936).

Geographic and stratigraphic occurrence. See Remarks.

Description. The tooth is complete and is 8 mm high and 6.5 mm wide. The crown, which exhibits smooth cutting edges, is upright, elongated and inclined lingually. The root is low and the basal surface is U-shaped. The lingual protuberance is prominent and bears a shallow nutrient groove.

Remarks. *Alopias superciliosus* ranges from the early Miocene to the present and occurs in deposits in Asia, Europe and North-South America (Antunes and Jonet, 1970; Case, 1980; Laurito, 1999; Aguilera and Rodriguez de Aguilera, 2001; Purdy *et al*., 2001; Antunes and Balbino, 2003; Cigala-Fulgosi *et al*., 2009; Nazarkin and Malyshkina, 2012). *Alopias superciliosus* is characterized by sexual dimorphism as the teeth of the males are considerably higher and thinner with more slanted crowns than those of the females (Gruber and Compagno, 1981). The tooth from the Uitpa Formation is similar to the lower anterior teeth of a male *A. superciliosus* illustrated by Herman *et al*. (2004). The fossil record of *Alopias superciliosus* in the Americas is shown in Appendix 1. Additionally, a tooth from the early Miocene of Barbados erroneously referred to *Alopias acutidens* by Casier (1958), is also tentatively included in the living species.

LAMNIFORMES Berg, 1937

LAMNIFORMES gen. et sp. indet.
Figure 4.16–17

Referred material. One upper tooth (MUN-STRI-39937).

Geographic and stratigraphic occurrence. See Remarks.

Description. The tooth measures 28 mm in height and 27 mm in width and, bearing a main cusp flanked by a cusplet on each side, is of typical lamniform morphology. The lateral cusplets are sharp, broad and present tiny accessory cusps. The crown is slim, biconvex and bent distally while its cutting edges are smooth and reach the base of the crown. The latter clearly overhangs the root, labially. The root is short with rounded and flattened lobes while the lingual collaret is narrow and the median bulge is prominent. There is a small lingual nutritive foramen.

Remarks. This very rare, medium sized lamniform shark is only represented by a few isolated teeth from several regions of the world. It is found in the Paratethyan deposits in Austria, Switzerland and Germany (all in private collections, pers. obs. RK) while similar finds are also known from Sardinia (Tethyan/ Mediterranean deposits) (private collection RK). Records outside Europe include Peru and the east coast of North America (Atlantic), particularly the Miocene deposits of the Calvert Cliffs in Maryland (pers. obs. RK). Its distribution was cosmopolitan and it likely inhabited cold to subtropical waters. It is only abundant in the ichthyofauna of the Miocene Calvert Formation of Maryland. This taxon might be closely related to the otodontids and most likely represents an unknown member of this group that coexisted with the other known large otodontid shark *Carcharocles*. Alternatively, this tooth belongs to a yet unnamed lamnid shark. Both a study of the relevant material in private collections and a comparison with other taxa are required before naming and properly assigning this new shark to a family. This, however, remains beyond the scope of the present work and will be presented separately in the future.

CARCHARHINIFORMES Compagno, 1973

HEMIGALEIDAE Hasse, 1879

Hemipristis Agassiz, 1835

Type species. *Hemipristis serra* Agassiz, 1835.

†***Hemipristis serra*** Agassiz, 1835
Figure 4.18–19

1835 *Hemipristis serra* Agassiz, p. 237, pl. 27, figs. 18–30.
1970 *Hemipristis serra* Agassiz, Antunes and Jonet, p. 167, pl. 11, figs. 63–64, pl. 12. figs. 65–67.
2012 *Hemipristis serra* Agassiz, Cappetta, p. 296, fig. 279g–i.

Referred material. One upper, lateral tooth (MUN-STRI-39938).

Geographic and stratigraphic occurrence. See Remarks.

Description. The single specimen recovered exhibits a crown 40 mm high and 30 mm wide. The tooth is labio-lingually compressed with a triangular crown curved distally. The mesial cutting edge is strongly concave and bears fine serrations that end shortly before reaching the apex. The distal edge is concave and coarsely serrated with the serrated part also terminating before reaching the apex. Even though the lingual face of the crown is damaged and the root is mostly missing, there is evidence for the presence of a strong lingual protuberance near the crown-root margin.

Remarks. *Hemipristis serra* is one of the most common fossil elasmobranch species around the world. It is particularly abundant in Neogene tropical to subtropical neritic deposits. Most of the records of this taxon come from Miocene and Pliocene deposits (see Cappetta, 2012). This taxon has also been found in the middle–late Oligocene of Baja California, Mexico (González-Barba and Thies, 2000), and the Oligocene–early Miocene deposits in the Atlantic Coastal Plain, USA (Müller, 1999; Chandler *et al.*, 2006; Cicimurri and Knight, 2009). The fossil record of *Hemipristis serra* in the Americas is shown in Appendix 1.

CARCHARHINIDAE Jordan and Evermann, 1896

Carcharhinus Blainville, 1816

Type species. *Carcharhinus melanopterus* Quoy and Gaimard, 1824.

†***Carcharhinus gibbesii*** Woodward, 1889
Figure 4.20–27

1889 *Carcharias* (*Aprionodon*) *gibbesii* Woodward, p. 437.
1938 *Hypoprion* sp. Leriche, p. 29, pl. 4, fig. 27.
1956 *Negaprion gibbesii* (Woodward), White, p.139, figs. 77–86, pl. 2, fig. 9.
1980 *Negaprion gibbesii* (Woodward), Case, p. 88, pl. 5, figs. 9a–9b, 10a–10b.
1999 *Carcharhinus gibbesii* Woodward, Müller, p. 49.
2009 *Carcharhinus gibbesii* Woodward, Cicimurri and Knight, p. 632, fig. 5A–D.

Referred material. Seven teeth. Six upper ones and a lower one (MUN-STRI-39945; MUN-STRI-39946).

Geographic and stratigraphic occurrence. See Remarks.

Description. The teeth range between 7 and 9.5 mm in height and between 9 and 11 mm in width. The upper teeth present low triangular crowns that are slightly inclined distally. While their mesial cutting edges are slightly convex, their distal ones are slightly concave. Both cutting edges are smooth and well differentiated from the heels by a notch. The mesial and distal heels are rather straight and strongly serrated. These serrations increase in size towards the base of the main cusp. The root is low, the lobes are slightly rounded and flattened, the lingual surface of the root is slightly inflated and the transverse medial lingual groove is narrow and reaches the base of the root forming a basal notch. The lower tooth presents a triangular crown marked by smooth cutting edges. There is no notch between the main cusp and the lateral heels, which bear completely smooth cutting edges. The root is low and its lobes rounded with a narrow medial lingual groove.

Remarks. *Carcharhinus gibbesii* is well known from the Oligocene of the Gulf and Atlantic Coastal Plains, USA (Case, 1980; Kruckow and Thies, 1990; Müller, 1999; Manning, 2006; Cicimurri and Knight, 2009), and the late Oligocene of Germany (Reinecke *et al.*, 2014). According to White (1956) and Cicimurri and Knight (2009), the upper teeth of *C. gibbesii* present a smooth cusp flanked by serrated mesial and distal heels while the lower teeth exhibit a cusp flanked by low and smooth-edged heels. The upper teeth of *C. gibbesii* are similar to those of *Carcharhinus elongatus* Leriche, 1910, but the latter species can be distinguished by possessing more weakly serrated or smoother lateral heels (*e.g.*, Génault 1993; Baut and Génault, 1999; Reinecke *et al.*, 2001, 2005; Haye *et al.*, 2008). In contrast, the upper teeth of *Carcharhinus gibbesii* from the Uitpa Formation display strongly serrated mesial and distal heels, which allows us to differentiate them from those of *C. elongatus* reported from the Oligocene of Europe (*e.g.*, Baut and Génault, 1999; Reinecke *et al.*, 2001, 2005; Haye *et al.*, 2008) and North America (Müller, 1999). Additionally, the tooth referred to *Hypoprion* sp. by Leriche (1938, pl. 4, fig. 27) from the Miocene of Trinidad belongs to an upper lateral tooth of *C. gibbesii* (Fig. 4.26–27).

Carcharhinus sp.
Figure 5.1–3

Referred material. Seven incomplete teeth (MUN-STRI-39947).

AMEGHINIANA - 2016 - Volume 53 (2): 77 – 99

Description. The specimens are markedly damaged and the crowns heavily eroded. Due to fragmentary conditions and bad preservation in most cases, the remaining specimens are not distinguishable to the species level. However, given that the isolated main cusps (upper and lower) bear clearly serrated cutting edges, we suggest that these specimens differ from those referred to *Carcharhinus gibbesi*, also found in this assemblage.

SPHYRNIDAE Gill, 1872

Sphyrna Rafinesque, 1810

Type species. *Squalus zygaena* Linnaeus, 1758.

†***Sphyrna laevissima*** (Cope, 1867)
Figure 5.4–5.5

1867 *Galeocerdo laevissima* Cope, p. 141–142, pl. 79–80.
1942 *Sphyrna laevissima* (Cope), Leriche, p. 84, pl. 7, figs. 23–27.
1980 *Sphyrna zygaena* (Linnaeus, 1758), Case, p. 98, pl. 8, fig. 2a–2b.
1999 *Sphyrna laevissima* (Cope), Müller, p. 54, pl. 8, figs. 5–8.
2011 *Sphyrna laevissima* (Cope), Reinecke, Louwye, Havekost, and Moths, p. 81–86, fig. 30, pl. 79, figs. 1a–7c, pl. 80, figs. 1a–5d.

Referred material. One upper lateral tooth (MUN-STRI-39948).

Geographic and stratigraphic occurrence. See Remarks.

Description. The tooth is complete and measures 8 mm high and 6.5 mm wide. The triangular crown, which is high and wide as well as distally inclined, exhibits a strongly convex lingual face and a flat labial face. Whereas the mesial edge is convex, the distal one is straight. Both cutting edges are completely smooth. The mesial cutting edge continues on the mesial heel without being interrupted by a notch. In contrast, a shallow notch separates the distal heel from the main cusp. The root is low and marked by rounded lobes and a slightly concave basal surface. The lingual protuberance is well-developed and bears a deep groove that extends to the base of the root and forms a very shallow notch.

Remarks. Some authors (*e.g.*, Purdy *et al.*, 2001; Cicimurri and Knight, 2009) noted the close morphological similarities shared by the living *Sphyrna zygaena* Linnaeus, 1758, and the extinct *Sphyrna laevissima*. They described the latter from the early Miocene of Pungo River Formation, USA, and suggested that *S. laevissima* is a synonym of *S. zygaena* (*e.g.*, Purdy *et al.*, 2001). Despite this, authors like Reinecke *et al.* (2011) and Bor *et al.* (2012) have pointed out significant morphological differences between *S. zygaena* and *S. laevissima* and considered the latter as a valid species. Teeth of *S. laevissima* differ from those of *S. zygaena* in presenting a broader and more upright cusp in their upper teeth as well as a shorter and more triangular-shaped cusp in their lower anterior and anterior-lateral teeth (Reinecke *et al.*, 2011). The morphological features observed in the specimen from the Uitpa Formation are comparable to those described by Reinecke *et al.* (2011) thus allowing us to assign this tooth to *S. laevissima*. According to Reinecke *et al.* (2011), *S. laevissima* probably first appeared in the upper Oligocene of USA (see Müller, 1999; Cicimurri and Knight, 2009), has a fossil record reaching the middle Miocene and most likely gave rise to *S. zygaena* (see Reinecke *et al.*, 2011, p. 86 for more information about the fossil record of *S. laevissima*).

BATOMORPHII Cappetta, 1980
MYLIOBATIFORMES Compagno, 1973
MOBULIDAE Gill, 1893

Mobula Rafinesque, 1810

Type species. *Mobula auriculata* Rafinesque, 1810.

Mobula sp.
Figure 5.6–5.8

Referred material. One tooth of indeterminate position (MUN-STRI-39949).

Geographic and stratigraphic occurrence. See Remarks.

Description. The tooth, 1.4 mm long and 3 mm wide, is broader than long. The crown is higher than the root and its apical part is wider than the collar between the base of the crown and the root. The occlusal section shows a rectangular shape with a coarse ornamentation. The labial visor of the crown displays some traces of reticular ornamentation. The root is low, polyaulacorhizous and presents five irregularly spaced grooves along its width.

Remarks. *Mobula* has a fossil record ranging from the Oligocene to the present (Cicimurri and Knight, 2009; Cappetta, 2012) and its dental morphology is both variable and characterized by marked sexual dimorphism (Adnet *et al.*, 2012). Our knowledge of the dental patterns in extant and fossil Mobulidae is scarce (Adnet *et al.*, 2012; Cappetta, 2012) and therefore any specific taxonomic assignment of fossil speci-

mens becomes difficult. The teeth of the specimen from the Uitpa Formation resemble those of *Mobula tarapacana* Philippi, 1892, illustrated by Adnet *et al.* (2012). However, the scarcity of this taxon in the Uitpa assemblage and the poor preservation of the single specimen recovered preclude further taxonomic identification below the genus level. The fossil record of *Mobula* in the Americas is shown in Appendix 1.

ACTINOPTERYGII Cope, 1887
TELEOSTEI Müller, 1846

TELEOSTEI gen. et spp. indet.
Figure 5.9–5.10

Referred material. Four fragmented teeth (MUN-STRI-39952).

Description. Two distinct morphologies of teleost teeth are present in our sample. The first morphology (Fig. 5.9–5.10) is represented by three specimens in which elongated and curved teeth with an elliptical basal outline can be observed. The presumed anterior face bears a cutting edge stretching from the base towards the missing apex of the teeth. Numerous striations, extending from base to apex, are present on the lateral surfaces of the teeth. The second morphology (Fig. 5.11) is represented by one low and triangular tooth with an elliptical basal outline and continuous cutting edges along its anterior and posterior surfaces. The lateral surfaces of the tooth are not ornamented.

Remarks. The small sample size and the incomplete state of preservation of the teeth preclude a more precise identification. The two morphologies correspond to two different teleost genera of marine affinities.

Elasmobranch habitat preferences and paleobathymetric analysis

The Uitpa Formation contains chondrichthyans whose extant relatives are characterized by diverse environmental and bathymetric affinities. Most taxa recognized in the assemblage, including *Carcharhinus*, *Hemipristis*, *Sphyrna* and *Mobula*, have extant representatives that are usual inhabitants of coastal environments, but can also occur in adjacent deep waters (Fig. 6). Species such as *Carcharhinus*, *Sphyrna* and *Mobula* are pelagic and are able to move along significant distances over oceanic basins (*e.g.*, Compagno, 1984b; Compagno and Last, 1999; Compagno *et al.*, 2005; Voigt and Weber, 2011; Thorrold *et al.*, 2014). The only *Carcharhinus* from the Uitpa assemblage identified to the species level is *C. gibbesii*, which has been previously reported to be associated with relatively shallow and neritic

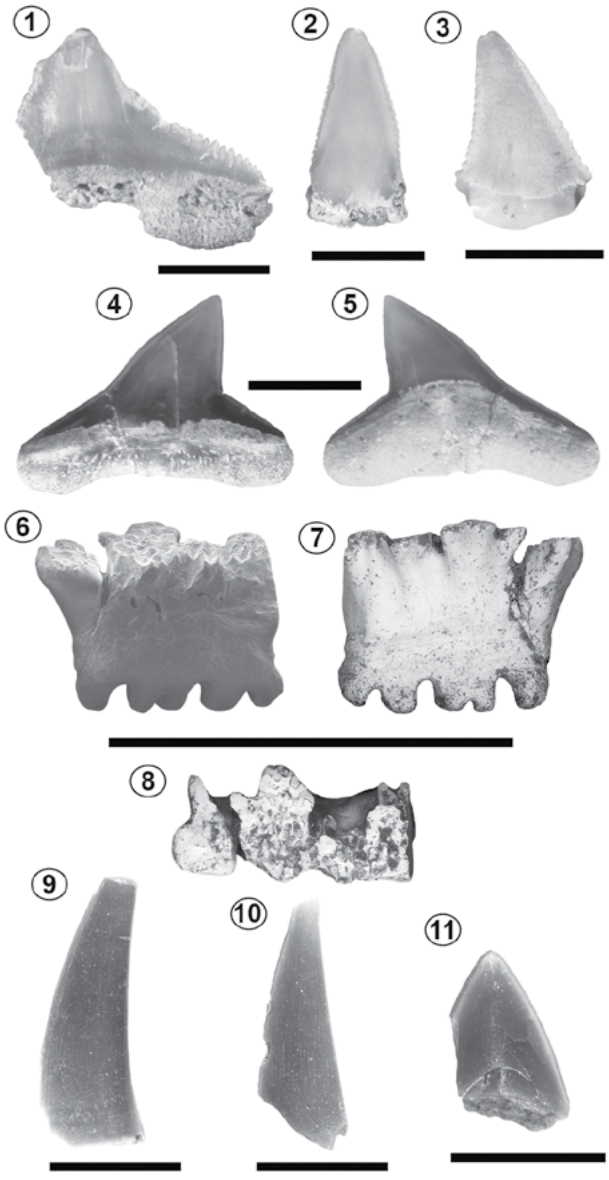

Figure 5. 1–3, ***Carcharhinus*** sp. (**MUN-STRI**-39947). **4–5,** ***Sphyrna laevissima*** upper tooth (**MUN-STRI**-39948). **6–8,** ***Mobula*** sp. (**MUN-STRI**-39949). **9–10,** teleost teeth of first morphology (**MUN-STRI**-39952). **11,** teleost tooth of the second morphology (**MUN-STRI**-39952). Views: labial (**1, 2, 3, 4, 6**), lingual (**5, 7**), oclusal (**8**), indet. view (**9–11**). Scale bar= 5 mm.

AMEGHINIANA - 2016 - Volume 53 (2): 77 – 99

environments (*e.g.*, Cicimurri and Knight, 2009). As evidenced by *C. gibbesii* fossils in European deposits (Reinecke *et al.*, 2014), the species was able to move across oceanic basins. In parallel to modern hammerheads, the extinct *S. laevissima* has been found in inner to outer shelf deposits (*e.g.*, Purdy *et al.*, 2001; Cicimurri and Knight, 2009; Reinecke *et al.*, 2011). Additionally, the extinct *Carcharocles* and the carcharhiniform *Hemipristis serra* are commonly found in coastal assemblages (*e.g.*, Pimiento *et al.*, 2010, 2013b; Cappetta, 2012) but must have also been present in open oceanic depositional environments (Carrillo-Briceño *et al.*, 2015). Their fossil record and cosmopolitan distribution (Cappetta, 2012) suggest that these large species were able to move along significant distances over oceanic basins.

Almost one third of the taxa from the Uitpa assemblage which can relate to living counterparts corresponds to benthopelagic Squalomorphii species (*Heptranchias* cf. *howellii*, *Centrophorus* sp., *Dalatias* cf. *licha* and *Pristiophorus* sp.) that prefer deep waters near the continental slope (Fig. 6). These taxa are abundant in our sample (~50%). The extant *Heptranchias perlo* Bonnaterre, 1788, together with *Dalatias licha* and many species of *Centrophorus* and *Pristiophorus*, can be found in both shallow and deep-water environments but prefer depths greater than 100 m. Also, they are frequently found on the outermost margin of the continental shelves and upper slopes (Fig. 6) (Compagno, 1984a; Castro *et al.*, 1999; Hennemann, 2001; Kiraly *et al.*, 2003; Compagno *et al.*, 2005). The only *Pristiophorus* species living in the Western Central Atlantic (Bahamas) is *Pristiophorus schroederi* Springer and Bullis, 1960, which prefers continental and insular slopes at depths of between 400 and 1000 m (Kiraly *et al.*, 2003). A small component of this assemblage corresponds to *Isurus* cf. *oxyrinchus* and *Alopias* cf. *superciliosus*. Their extant representatives inhabit open waters (Fig. 6) (Compagno *et al.*, 2005).

The maximum likelihood estimates concerning the paleobathymetric analysis (Fig. 7, Appendix 2) indicate that the most probable depth for the Uitpa assemblage is the 100 to 150 m interval (probability of 0.243) followed by the 150 to 200 m interval (probability of 0.240). Depths deeper than 200 m have probabilities <0.14 while depths shallower than 100 m have probabilities <0.17 (Fig. 7, Appendix 2 and Supplementary Online Information.

DISCUSSION

Taxonomical composition

The chondrichthyan assemblage described herein consists of 13 taxa assigned to 12 genera, 11 families and six orders (Appendix 1). While all taxa are reported for the first time from Colombian deposits, the fauna constitutes one of the earliest Miocene assemblages reported from the Caribbean and Tropical America. Other Aquitanian assemblages include the Bissex Hill, Barbados (Casier, 1958, 1966). Additional early Miocene Tropical American faunas have been reported in Barbados, Brazil, Cuba, Mexico, Panama and Venezuela (*e.g.*, Casier, 1958, 1966; Santos and Travassos, 1960; Santos and Salgado, 1971; Iturralde-Vinent *et al.*, 1996; Gonzales-Barba and Thies, 2000; Sánchez-Villagra *et al.*, 2000; Reis, 2005; Portell *et al.*, 2008; Costa *et al.*, 2009; Aguilera, 2010; Aguilera and Lundberg, 2010; Pimiento *et al.*, 2013a).

The taxa *Heptranchias* cf. *howellii*, *Carcharocles* sp., *Hemipristis serra*, *Carcharhinus gibbesii*, *Sphyrna laevissima* and the specimen referred to Lamniformes gen. et sp. indet., are extinct. Most of the remaining taxa correspond to genera or species (Appendix 1) that boast living representatives with a cosmopolitan distribution that includes Tropical America (see Compagno, 1984a,b; Compagno *et al.*, 2005; Voigt and Weber, 2011). Genera such as *Heptranchias*, *Centrophorus*, *Dalatias*, *Pristiophorus*, *Isurus*, *Carcharocles*, *Hemipristis*, *Carcharhinus*, *Sphyrna* and *Mobula* have been previously recognized in the Cenozoic fossil record of the Americas (see Appendix 1). *Heptranchias howellii* and *Carcharhinus gibbesii* had been previously reported only in North America (Welton, 1974; Case, 1980; Kruckow and Thies, 1990; Müller, 1999; Manning, 2006; Cicimurri and Knight, 2009) and herein we expand their distribution to include Tropical America. Both the specimens of *Heptranchias* cf. *howellii* from the Uitpa Formation (Aquitanian) and those reported by Leriche (1938) from the Mene de Acosta in Venezuela (Menecito Member of the San Lorenzo Formation; early–middle Miocene) represent the youngest record of the taxon. The assemblage from western Venezuela described by Leriche (1938) was originally proposed as of late Oligocene age. Yet, recent studies suggest an early to middle Miocene age (Díaz de Gamero, 1985).

Specimens of *Carcharhinus gibbesii* from the Uitpa Formation and the conspecific tooth, which had erroneously

been assigned to *Hypoprion* sp. from the Miocene of Trinidad by Leriche (1938), represent the youngest fossil record for this taxon. The previous youngest record of *C. gibbesii* is from the Chattian of the Thalberg Beds in Bavaria, Germany (Reinecke *et al.*, 2014).

Paleoenvironment and paleobathymetry

Previous studies have suggested that the Uitpa Formation was deposited in an open water environment (Becker and Dusenbury, 1958; Rollins, 1965; Thomas, 1972; Hendy *et al.*, 2015). Becker and Dusenbury (1958) proposed, based on benthic foraminifera, a depositional depth of between 100 and 300 fathoms (182 m to 549 m) for the base of the unit. Based on an invertebrate fauna that prefers outer shelf to upper bathyal waters (100–250 m), a recent and more detailed report for the Uitpa Formation by Hendy *et al.* (2015) confirms the previous paleoenvironmental interpretations for the base of the Uitpa Formation. Hendy *et al.* (2015) also note a shallowing trend towards the top of the Uitpa Formation.

Our maximum likelihood paleobathymetrical analysis indicates that the lower 10 m of the Uitpa Formation (Fig. 2) were most likely deposited in depths ranging between 100 and 200 m (Figs. 6, 7) in a middle-outer shelf environment. The Uitpa assemblage shows a predominance of benthopelagic Squalomorphii sharks (*Heptranchias* cf. *howellii*, *Centrophorus* sp., *Dalatias* cf. *licha* and *Pristiophorus* sp.). The extant species corresponding to such sharks prefer environments with deep-water near the continental slope (Fig. 6).

Oligocene/Miocene Transition in the Cocinetas Basin

The Oligocene/Miocene Transition in the Caribbean region was accompanied by a significant change in the regional biota marked by a widespread extinction of the Oligocene Tethyan reef biota and the origin of many extant

BATHYMETRIC PREFERENCES OF THE UITPA CHONDRICHTHYANS

FOSSIL TAXA	EXTANT SPECIES	n SPECIMENS	LIFESTYLE	PREFERRED HABITAT	BATHYMETRIC RANGE (m)			Inner shelf / mid-outer shelf / continental slope (50m 100m 150m 200m 250m 300m 350m 400m 450m 500m)
					MIN	MAX	COMMON	
Heptranchias cf. *howellii*	*Heptranchias perlo*	6	BP	MP/BP	0	1000	180-450	
Centrophorus sp.	*Centrophorus* spp.	5	BP	MP/BP	50	1440	180-600	
Dalatias cf. *licha*	*Dalatias licha*	6	BP	MP/BP	37	1800	200-1800	
Pristiophorus sp.	*Pristiophorus* spp.	13	BP	N/E-MP/BP	0	1000	100-300	
Isurus cf. *oxyrinchus*	*Isurus oxyrinchus*	7	P	N/E-MP/BP	0	500	100-150	
Carcharocles sp.		3	?	?	?	?	?	
Alopias cf. *superciliosus*	*Alopias superciliosus*	1	P	N/E-MP/BP	0	730	10-400	
Lamniformes indet.		1	?	?	?	?	?	
Hemipristis serra	*Hemipristis elongatus*	1	BP	N/E	0	130	inshore	
Carcharhinus gibbesii	*Carcharhinus spp.*	7	P-BP	N/E-MP/BP	0	1000	inshore	
Carcharhinus sp.	*Carcharhinus* spp.	7	P-BP	N/E-MP/BP	0	1000	inshore	
Sphyrna laevissima	*Sphyrna spp.*	1	P-BP	N/E-MP/BP	0	1000	inshore	
Mobula sp.	*Mobula* spp.	1	BP	N/E	0	>1000	less than 150	

Figure 6. Lifestyle, habitat and bathymetric preferences of the Uitpa Formation chondrichthyan taxa, based on the biology of their extant relatives (references in text). The dark gray shaded area indicates the most probable depositional depth. The horizontal bars represent the water depth inhabited by each taxon with the preferred water depths indicated by thicker bars. Only taxa with recent relatives were considered for this analysis. Abbreviations are as follows: **N,** Neritic; **E,** Epipelagic; **P,** Pelagic; **BP,** Benthopelagic; **MP,** Mesopelagic.

AMEGHINIANA - 2016 - Volume 53 (2): 77 – 99

lineages of reef corals that are characteristic of the western Atlantic at present (Johnson *et al.*, 2009). This major biotic rearrangement has been attributed to changes in the quality of the regional water (*e.g.*, Edinger and Risk, 1994; Johnson *et al.*, 2008, 2009). For example, the collapse of the San Luis coral-reef ecosystems in the northwestern Falcón Basin (Venezuela) is attributed to a decline in water quality resulting from increased sedimentary influx from the complex drainage system of the region during the OMT (Johnson *et al.*, 2009). In the nearby Cocinetas Basin, the Siamana-Uitpa sequence contains thick late Oligocene reef strata (Renz, 1960; Lockwood, 1965; Rollins, 1965; Thomas, 1972) overlain, in an abrupt transition, by the shales of the Uitpa Formation studied herein. Lockwood (1965) indicated that this fast transition could correspond to a strong environmental change from near-shore to offshore facies.

Reefs are relatively resilient to rises in sea level because corals are almost entirely subtidal and are able to accrete vertically. However, such resilience will deeply depend on the rate of rise (Hamylton *et al.*, 2014). A rapid sea-level increase will produce a collapse of the reef system (Blanchon *et al.*, 2009; Done, 2011; Hamylton *et al.*, 2014).

Our chondrichthyan data indicate that, while the lowermost Uitpa Formation was most likely deposited in the mid-outer shelf (100 to 200 m) (Fig. 6), the Siamana reef deposits probably accumulated close to sea level (*e.g.*, Rollins, 1965). These paleobathymetric changes suggest a rapid increase (100 to 200 m) in relative sea level at the Uitpa-Siamana contact during the early Aquitanian. Therefore, the collapse of coral reefs of the Guajira Siamana Formation is more likely related to a rapid increase in relative sea level than to an increase in sediment supply as proposed for the San Luis coral-reef ecosystems in the northwestern Falcón Basin (Venezuela) (Johnson *et al.*, 2009).

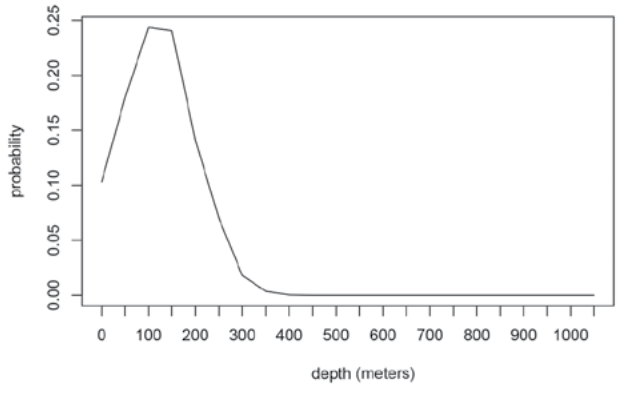

Figure 7. Maximum likelihood estimates for bathymetry of the Uitpa fossil assemblage.

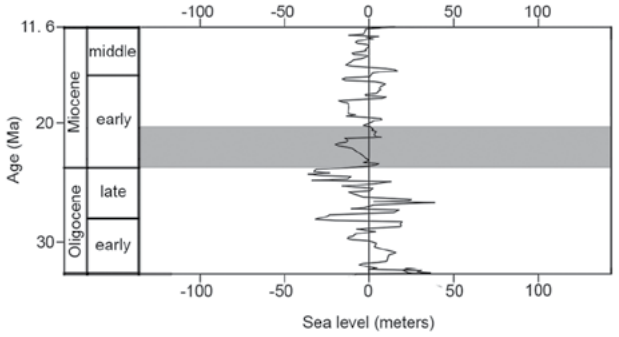

Figure 8. Cenozoic Eustatic Sea Level curve after Miller *et al.* (2005). The lower Uitpa Formation accumulated during the lower part of the early Miocene that has a ~35 m eustatic sea level rise.

A rapid increase in relative sea level could be explained by an increase in eustatic sea level and/ or an increase in tectonic subsidence. The Aquitanian begins with a brisk increase in eustatic sea level (~40 m, Miller *et al.*, 2005) (Fig. 8) that would nevertheless not be enough to account for the 100–200 m rise in relative sea level at the Uitpa-Siamana transition. An increase in regional tectonic subsidence as a result of the collision of the Panama Microplate and South America during the late Oligocene/early Miocene (Weber *et al.*, 2010; Escalona and Mann, 2011; Farris *et al.*, 2011) could also be responsible for this deepening. During the Oligocene–early Miocene, tectonic subsidence increases in western Venezuela (Falcón area) thus extending the Falcón Basin to the south and E-W (Escalona and Mann, 2011). According to Rollins (1965) and Lockwood (1965), a continuous subsidence and opening of the basins may be responsible for the marine transgression and deepening of the Cocinetas Basin in the beginning of the Miocene.

CONCLUSION

We provide descriptions of 13 selachian taxa that constitute the first fossil chondrichthyan assemblage from Colombia to be studied in detail and, also, one of the earliest Neogene occurrences of elasmobranchs in Tropical America. Our paleobathymetric and paleoenvironmental analyses suggest that the lower Uitpa Formation accumulated in waters ranging between 100 and 200 m.

ACKNOWLEDGMENTS

This project has been supported by a SENACYT APY-NI10-016A grant (National Secretary of Science and Technology of Panama) and a Swiss National Science Foundation grant 31003A-149605 (to Marcelo Sánchez-Villagra). The Smithsonian Institution, the National Geographic Society, the Anders Foundation, Gregory D. and Jennifer Walston Johnson, Universidad del Norte and the National Science Foundation (Grant EAR 0957679) helped to support this work. Thanks to the Evolutionary Morphology and Palaeobiology group of the Palaeontological Institute and Museum at the University of Zurich, Switzerland, Carlos Jaramillo's lab members (STRI) participant of fieldwork in Alta Guajira (2013–2014), the Wayuu communities of the Alta Guajira and the Colombian National Police together with the Mapuka Museum of Universidad del Norte. Thanks to the Museum für Naturkunde in Berlin, the Museu Paraense Emilio Goeldi, the Natural History Museum of Basel, Paleontological collections of the Alcaldía Bolivariana de Urumaco, Palaeontological Institute and Museum at the University of Zurich and Universidad Nacional Experimental Francisco de Miranda for their valuable assistance and permission to revise fossil collections. Special thanks to J. Ceballos for his help with the microscopic photography and to L. Costeur, L. Londoño, M. Gomez, and J. Escobar for their valuable assistance. We greatly appreciate comments and suggestions from A. López Arbarello, C. Pimiento, A. Otero and R. Vullo.

REFERENCES

Adnet, S., Cappetta, H., and Mertiniene, R. 2008. Re-evaluation of squaloid shark records from the Albian and Cenomanian of Lithuania. *Cretaceous Research* 29: 711–721.

Adnet, S., Cappetta, H., Guinot, G., and Notarbartolo Di Sciara, G. 2012. Evolutionary history of the devilrays (Chondrichthyes: Myliobatiformes) from fossil and morphological inference. *Zoological Journal of the Linnean Society* 166: 132–159.

Adolfssen, J.S., and Ward, D.J. 2015. Neoselachians from the Danian (Early Paleocene) of Denmark. *Acta Palaeontologica Polonica* 60: 313–338.

Agassiz, L. 1833–1843. *Recherches sur les poissons fossiles*. Vol. 3. Petitpierre, Neuchâtel, 390 p.

Aguilera, O. 2010. *Peces Fósiles del Caribe de Venezuela*. Gorham Printing, Washington, 258 p.

Aguilera, O., and Lundberg, J.G. 2010. Venezuelan Caribbean and Orinocoan Neogene fish. In: M.R. Sánchez-Villagra, O. Aguilera, and F. Carlini (Eds.), *Urumaco and Venezuelan Paleontology*. Indiana Press University, Bloomington, p. 129–152.

Aguilera, O., and Rodrigues de Aguilera, D. 2001. An exceptional upwelling of fish assemblages in the Caribbean Neogene. *Journal of Paleontology* 75: 732–742.

Aguilera, O., and Rodrigues de Aguilera, D. 2004. Giant-toothed White Sharks and Wide-toothed Mako (Lamnidae) from the Venezuela Neogene Their Role in the Caribbean, Shallow-water Fish Assemblage. *Caribbean Journal of Science* 40: 368–382.

Aguilera, O., Ramos, M.I., Paes, E., Costa, S., and Sánchez-Villagra, M. 2011. The Neogene Tropical America fish assemblage and the palaeobiogeography of the Caribbean region. *Swiss Journal of Palaeontology* 130: 217–240.

Ameghino, F. 1901. L'âge des formations sédimentaires de Patagonie. *Anales de la Sociedad Científica Argentina* 51: 20–39; 65–91.

Antunes, M.T., and Balbino, A.C. 2003. Uppermost Miocene Lamniform Selachians (Pisces) from the Alvalade Basin (Portugal). *Ciências da Terra (UNL)* 15: 141–154.

Antunes, M.T., and Jonet, S. 1970. Requins de l'Helvétien supérieur et du Tortonien de Lisbonne. *Revista da Faculdade de Ciências de Lisboa* 16: 119–280.

Applegate, S.P., and Espinosa-Arrubarrena, L. 1996. The fossil history of Carcharodon and its possible ancestor, Cretolamna: a study in tooth identification. In: A. Klimley, and D. Ainley (Eds.), *Great White Sharks: The Biology of Carcharodon carcharias*. San Diego Academic Press, San Diego, p. 19–36.

Applegate, S.P., and Uyeno, T. 1968. The first discovery of a fossil tooth belonging to the shark genus Heptranchias, with a new Pristiophorus spine, both from the Oligocene of Japan. *Bulletin of the National Science Museum, Series C, Geology & Paleontology* 11: 195–200.

Arratia, G., and Cione, A.L. 1996. The fish fossil record of southern South America. *Münchener Geowissenschaftliche Abhandlungen* 30: 9–72.

Barnard, K.H. 1925. A monograph of the marine fishes of South Africa. Part I (Amphioxus, Cyclostomata, Elasmobranchii, and Teleostei -Isospondyli to Heterosomata). *Annals of the South African Museum* 21: 1–418.

Baut, J.P., and Génault, B. 1999. Les élasmobranches des Sables de Kerniel (Rupélien), à Gellik, nord-est de la Belgique. *Memoirs of the Geological Survey of Belgium* 45: 1–61.

Becker, L.E., and Dusenbury, A.N. Jr. 1958. Mio-Oligocene (Aquitanian) foraminifera from the Goajira Peninsula, Colombia. *Cushman Foundation for Foraminiferal Research Special Publication* 40: 4–48.

Berg, L.S. 1937. A classification of fish-like vertebrates. *Bulletin of the Academy of Sciences of the USSR, Division of Chemical Science* 1937: 1277–1280.

Berg, L.S. 1958. *System der rezenten und fossilen Fischartigen und Fische*. Deutsche Verlag Wissenschaften, Berlin, 310 p.

Bieñkowska-Wasiluk, M., and Radwañski, A. 2009. A new occurrence of sharks in the Menilite Formation (Lower Oligocene) from the Outer (Flysch) Carpathians of Poland. *Acta Geologica Polonica* 59: 235–243.

Bigelow, H.B., and Schroeder, W.C. 1948. Fishes of the western North Atlantic. Part I. *Memoir of Sears Foundation for Marine Research* 1: 59–576.

Blainville, H.M.D. De. 1816. Prodrome d'une nouvelle distribution systematique du regne animal. *Bulletin de la Société Philomathique de Paris* 8: 105–112; 121–124.

Blanchon, P., Eisenhauer, A., Fietzke, J., and Liebetrau, V. 2009. Rapid sea-level rise and reef back-stepping at the close of the last interglacial highstand. *Nature Letters* 458: 881–885.

Bleeker, P.R. 1859. Enumeratio specierum piscium hucusque in Archipelago indico observatarum. *Acta Societatis Scientiarum Indo-Neerlandae* 6: 1–276.

Boessenecker, R.W. 2011. A New Marine Vertebrate Assemblage from the Late Neogene Purisima Formation in Central California, Part I: Fossil Sharks, Bony Fish, Birds, and Implications for the Age of the Purisma Formation West of the San Gregorio Fault: Palarch's. *Journal of Vertebrate Palaeontology* 8: 1–30.

Bonaparte, C.L. 1838. Selachorum tabula analytica. *Nuovi Annali della Science Naturali Bologna* 1: 195–214.

Bonnaterre, J.P. 1788. *Ichthyologie. Tableau encyclopédique et méthodique des trois règnes de la nature*. Panckoucke, Paris, 215 p.

Bor, T., Reinecke, T., and Verschueren, S. 2012. Miocene Chondrichthyes from Winterswijk- Miste, the Netherlands. *Palaeontos* 21: 1–136.

Buen, F. De. 1926. Catálogo ictiológico del Mediterráneo español y de Marruecos. *Resultados Campañas Internaccionale Institute Español Oceanografíá* 2: 153–161.

Cao, D.M., Song, L.M., Yu Zhang, K.KLv., and Hu, Z.X. 2011. Environ-

mental preferences of *Alopias superciliosus* and *Alopias vulpinus* in waters near Marshall Islands. *New Zealand Journal of Marine and Freshwater Research* 45: 103–119.

Cappetta, H. 1980. Modification du statut générique de quelques espèces de sélaciens crétacés et tertiares. *Palaeovertebrata* 10: 29–42.

Cappetta, H. 1981. Additions à la faune de sélaciens fossiles du Maroc. 1: Sur la présence des genres Heptranchias, Alopias et Odontorhytis dans l'Yprésien des Ouled Abdoun. *Géobios* 14: 563–575.

Cappetta, H. 2012. *Handbook of Paleoichthyology, Vol. 3E: Chondrichthyes. Mesozoic and Cenozoic Elasmobranchii: Teeth*. Verlag Dr. Friedrich Pfeil, Munich, 512 p.

Carrillo-Briceño, J.D., Aguilera, O., and Rodriguez, F. 2014. Fossil Chondrichthyes from the Central Eastern Pacific Ocean and their Paleoceanographic Significance. *Journal of South American Earth Sciences* 51: 76–90.

Carrillo-Briceño J.D., González-Barba, G., Landaeta, M.F., and Nielsen, S.N. 2013. Condrictios fósiles del Plioceno Superior de la Formación Horcón, Región de Valparaíso, Chile central. *Revista Chilena de Historia Natural* 86: 191–206.

Carrillo-Briceño, J.D., De Gracia, C., Pimiento, C., Aguilera, O.A., Kindlimann, R., Santamarina, P., and Jaramillo, C. 2015. A New Late Miocene Chondrichthyan Assemblage from the Chagres Formation, Panama. *Journal of South American Earth Science* 60: 56–70.

Case, G.R. 1980. A selachian fauna from the Trent Formation, lower Miocene (Aquitanian) of eastern North Carolina. *Palaeontographica A* 171: 75–103.

Casier, E. 1958. Contribution á l'étude des poissons fossiles des Antilles. *Mémoire Suisse de Paléontologie* 74: 1–95.

Casier, E. 1966. Sur la faune ichthyologique de la Formation de Bissex Hill et de la Série océanique, de l'Ile de la Barbade, et sur l'âge de ces formations. *Eclogae Geologicae Helvetiae* 59: 493–516.

Castro, J.I., Woodley, C.M., and Brudek, R.L. 1999. *A preliminary evaluation of the status of shark species*. FAO Fisheries Technical Paper No. 380, Rome, 72 p.

Chandler, R.E., Chiswell, K.E., and Faulkner, G.D. 2006. Quantifying a possible Miocene phyletic change in *Hemipristis* (Chondrichthyes) teeth. *Palaeontologica Electronica* 9.1.4A: 1–14.

Cicimurri, D.J., and Knight, J.L. 2009. Late Oligocene sharks and rays from the Chandler Bridge formation, Dorchester County, South Carolina, USA. *Acta Palaeontologica Polonica* 54: 627–647.

Cigala-Fulgosi, F. 1988. Additions to the Eocene and Pliocene fish fauna of Italy. Evidence of *Alopias cf. denticulatus* Cappetta, 1981 in the Bartonian-Priabonian of the Monte Piano Marl (northern Apennines) and of *A. superciliosus* (Lowe, 1840) in the Pliocene of Tuscany (Chondrichthyes, Alopiidae). *Tertiary Research* 10: 93–99.

Cigala-Fulgosi, F., Casati, S., Orlandini, A., and Persico, D. 2009. A small fossil fish fauna, rich in Chlamydoselachus teeth, from the Late Pliocene of Tuscany (Siena, central Italy). *Cainozoic Research* 6: 3–23.

Cione A.L., Cozzuol, M.A., Dozo, M.T., and Costa Hospitaleche, C. 2011. Marine vertebrate assemblages in the southwest Atlantic during the Miocene. *Biological Journal of the Linnean Society* 103: 423–440.

Coates, A.G., and Stallard, R.F. 2013. How old is the Isthmus of Panama? *Bulletin of Marine Sciences* 89: 801–813.

Compagno, L.J.V. 1973. Interrelationships of living elasmobranchs. In: P.H. Greenwood, R.S. Miles, and C. Pattterson (Eds.), *Interrelationships of fishes*. Academic Press, London, p. 15–61.

Compagno, J.L.V. 1977. Phyletic relationships of living sharks and rays. *American Zoologist* 17: 303–322.

Compagno, L.J.V. 1984a. *FAO Species Catalogue. Vol. 4: Sharks of the World. An annotated and illustrated catalogue of shark species known to date. Part 1: Hexanchiformes to Lamniformes*. Food and Agriculture Organization of the United Nations, Rome, p. 1–249.

Compagno, L.J.V. 1984b. *FAO Species Catalogue. Vol. 4: Sharks of the World. An annotated and illustrated catalogue of shark species known to date. Part 2: Carcharhiniformes*. Food and Agriculture Organization of the United Nations, Rome, p. 251–655.

Compagno, L.J.V. 2005. Checklist of living Chondrichthyes. In: W.C. Hamlett, (Ed.), *Reproductive biology and phylogeny of Chondrichthyes (sharks, batoids and chimaeras)*. Science Publishers Inc., Enfield, p. 503–548.

Compagno, L.J.V., and Last, P.R. 1999. Pristidae (Sawfishes), Rhinidae (Wedgefishes), Platyrhinidae (Thornback rays). In: K.E. Carpenter, and V.H. Niem (Eds.), *FAO Identification Guide for Fishery Purposes. The Living Marine Resources of the Western Central Pacific*. Food and Agriculture Organization, Rome, p. 1410–1432.

Compagno, L.J.V., Dando, V.M., and Flower, S. 2005. *Sharks of the World*. Princeton University Press, Princeton, 368 p.

Cope, E.D. 1867. An addition to the vertebrate fauna of the Miocene period, with a synopsis of the extinct Cetacea of the United States. *Proceedings of the Academy of Natural Sciences of Philadelphia* 19: 138–156.

Cope, E.D. 1887. Zittel's Manual of Palaeontology. *American Naturalist* 21: 1014–1019.

Costa, S.A.F., Richter, M., Toledo, P.M., and Moraes-Santos, H.M. 2009. Shark teeth from Pirabas formation (Lower Miocene), northeastern Amazonia, Brazil. *Boletin do Museo Paraense Emílio Goeldi, Ciencias Naturais* 4: 221–230.

De Muizon, C., and Devries, T.J. 1985. Geology and Paleontology of late Cenozoic marine deposits in the Sacaco area (Peru). *Geologische Rundschau* 74: 547–563.

Díaz de Gamero, M.L. 1985. Estratigrafía de Falcón nororiental. *VI Congreso Geológico Venezolano* (Caracas), *Memoria* 1: 454–502.

Done, T.J. 2011. Corals: Environmental Controls on growth. In: D. Hopley (Ed.), *Encyclopedia of Modern Coral Reefs: Structure, Form and Process*. Springer-Verlag, Berlin, p. 281–293.

Donovan, S.K., and Gunter, G.C. 2001. Fossil sharks from Jamaica. *Bulletin of the Mizunami Fossil Museum* 28: 211–215.

Edinger, E.N., and Risk, M.J. 1994. Oligocene–Miocene extinction and geographic restriction of Caribbean corals: Roles of turbidity, temperature, and nutrients. *Palaios* 9: 576–598.

Escalona, A., and Mann, P. 2011. Tectonics, basin subsidence mechanisms, and paleogeography of the Caribbean-South American plate boundary zone. *Marine and Petroleum Geology* 28: 8–39.

Farris, D.W., Jaramillo, C.A., Bayona, G.A., Restrepo-Moreno, S.A., Montes, C., Cardona, A., Mora, A., Speakman, R.J., Glasscock, M.D., Reiners, P., and Valencia, V. 2011. Fracturing of the Panamanian isthmus during initial collision with South America. *Geology* 39: 1007–1010.

Froese, R., and Pauly, D. 2015. *FishBase*. World Wide Web electronic publication. www.fishbase.org, version (2015).

Génault, B. 1993. Contribution à l'étude des élasmobranches Oligocènes du bassin de Paris 2. Découverte de deux horizons à élasmobranches dans le Stampien (Sables de Fontainebleau) de la feuille géologique de Chartres. *Cossmanniana* 2: 13–36.

Gill, T. 1872. Arrangement of the families of fishes, or classes Pisces, Marsupiobranchii, and Leptocardii. *Smithsonian Institution Miscellaneous Collection* 247: 1–49.

Gill, T. 1893. Families and subfamilies of fishes. *Memoirs of the National Academy of Sciences* 6: 125–138.

Gillette, D.D. 1984. A marine ichthyofauna from the Miocene of Panama, and the Tertiary Caribbean faunal province. *Journal of Vertebrate Paleontology* 4: 172–186.

Glikman, L.S. 1964. *Sharks of the Paleogene and their stratigraphic significance*. Nauka Press, Moscow, 229 p. [In Russian.].

Gmelin, J.F. 1789. Pisces. In: C. Linnaeus (Ed.), *Systema Naturae per regna tria naturae, secundum classes, ordines, genera, species; cum characteribus, differentiis, synonymis, locis*. 13th Ed. Beer, Leipzig, p. 1033–1516.

González-Barba, G., and Thies, D. 2000. Asociaciones faunísticas de condrictios en el Cenozoico de la Península de Baja California, México. *XVII Simposio sobre la Geología de Latinoamérica* (Stuttgart), *Resúmenes extendidos* 18: 1–4.

Goodrich, E.S. 1909. Vertebrata Craniata. Fascicule I. Cyclostomes and fishes. In: E.R. Lankester (Ed.), *A Treatise on Zoology, Part 9*. Adam and Charles Black, London, 518 p.

Gray, J. 1851. *List of the specimens of fish in the collection of the British Museum. Part 1. Chondropterygii*. British Museum (Natural History), London, 160 p.

Gruber, S.H., and Compagno, L.J.V. 1981. Taxonomic status and biology of the bigeye thresher, *Alopias superciliosus* (Lowe, 1839). *Fishery Bulletin* 79: 617–640.

Hamylton, S.M., Leon, J.X., Saunders, M.I., and Woodroffe, C.D. 2014. Simulating reef response to sea-level rise at Lizard Island: a geospatial approach. *Geomorphology* 222: 151–161.

Hasse, J.C.F. 1879. *Das nahirliche System der Elasmobranchier auf Grundlage des Baues und der Entwicklung ihrer Wirbelsaule. Eine morphologische und palaontologische Studie. Allgemeiner Theil*. Gustav Fischer Verlag, Jena, 76 p.

Haye, T., Reinecke, T., Gürs, K., and Piehl, A. 2008. Die Elasmobranchier des Neochattiums (Oberoligozän) von Johannistal, Ostholstein, und Ergänzungen zu deren vorkommen in der Ratzeburg-Formation (Neochattium) des Südöstlichen Nordseebeckens. *Palaeontos* 14: 55–95.

Hendy, A.J.W., Jones, D.S., Moreno, F., Zapata, V., and Jaramillo, C. 2015. Neogene molluscs, shallow-marine paleoenvironments and chronostratigraphy of the Guajira Peninsula, Colombia. *Swiss Journal of Paleontology* 134: 45–75.

Hennemann, R.M. 2001. *Sharks & rays: elasmobranch guide of the world*. IKAN-Unterwasserarchiv, Frankfurt, 304 p.

Herman, J., Hovestadt-Euler, M., and Hovestadt, D.C. 2004. Contributions to the odontological study of living Chondrichthyes. 1. The genus *Alopias* Rafinesque, 1810. *Bulletin de l'Institut Royal des Sciences naturelles de Belgique, Biologie* 74: 5–32.

Huxley, T.H. 1880. On the application of the laws of evolution to the arrangement of the Vertebrata, and more particularly of the Mammalia. *Proceedings of the Zoological Society of London* 43: 649–662.

Iturralde-Vinent, M.A., and MacPhee, R.D.E. 1999. Paleogeography of the Caribbean region: implications for Cenozoic biogeography. *Bulletin of the American Museum of Natural History* 238: 1–95.

Iturralde-Vinent, M.A., Gubbell, G., and Rojas, R. 1996. Catalogue of Cuban fossil Elasmobranchii (Paleocene to Pliocene) and paleogeographic implications of their lower to middle Miocene occurrence. *Boletín de la Sociedad Jamaicana de Geología* 31: 7–21.

Jaramillo, C., Moreno, F., Hendy, F., Sanchez-Villagra, M., and Marty, D. 2015. Preface: La Guajira, Colombia: a new window into the Cenozoic neotropical biodiversity and the Great American Biotic Interchange. *Swiss Journal of Paleontology* 134: 1–4.

Johnson, K.G., Budd, A.F., and Jackson, J.B.C. 2008. Coral reef development was independent of coral diversity in the Caribbean over 28 million years. *Science* 319: 1521–1522.

Johnson, K.G., Sánchez-Villagra, M.R., and Aguilera, O.S. 2009. The Oligocene–Miocene transition on coral reefs in the falcon basin (NW Venezuela). *Palaios* 24: 59–69.

Jordan, D.S., and Evermann, B.W. 1896. The fishes of North and Middle America: a descriptive catalogue of the species of fish-like vertebrates found in the waters of North America, north of the Isthmus of Panama. Part I. *Bulletin of the United States National Museum* 47: 1–1240.

Jordan, D.S., and Hannibal, H. 1923. Fossil sharks and rays of the Pacific Slope of North America. *Bulletin of the Southern California Academy of Sciences* 22: 27–63.

Kemp, N.R. 1978. Detailed comparisons of the dentitions of extant hexanchid sharks and Tertiary hexanchid teeth from South Australia and Victoria, Australia (Selachii: Hexanchidae). *Memoirs of the National Museum of Victoria* 39: 61–83.

Keyes, I.W. 1984. New records of fossil elasmobranch genera *Megascyliorhinus*, *Centrophorus*, and *Dalatias* (Order Selachii) in New Zealand. *New Zealand Journal of Geology and Geophysics* 27: 203–216.

Kindlimann, R. 1990. Selacios del Terciario Tardío de Sacaco, Departamento de Arequipa. *Boletín de Lima* 69: 91–95.

Kiraly, S.J., Moore, J.A., and Jasinski, P.H. 2003. Deepwater and other sharks of the U.S. Atlantic Ocean Exclusive Economic Zone. *Marine Fisheries Review* 65: 1–64.

Kriwet, J., and Klug, S. 2009. Fossil record and origin of squaliform sharks (Chondrichthyes, Neoselachii). In: V.F. Gallucci, G.A. MacFarlane, and G.G Bargmann (Eds), *Biology and management of dogfish sharks*. American Fisheries Society, Bethesda, p. 19–38.

Kruckow, T., and Thies, D. 1990. Die Neoselachier der Paleokaribik (Pisces: Elasmobranchii). *Courier Forschungsinstitut Senckenberg* 119: 1–102.

Latham, J. 1794. An essay on the various species of Sawfish. *Transactions of the Linnean Society of London* 2: 273–282.

Laurito, C. 1999. *Los seláceos fósiles de la localidad de Alto Guayacán (y otros ictiolitos asociados), Mioceno superior-Plioceno inferior de la Formación Uscari, provincia de Limón, Costa Rica*. Laurito, C. (Ed.), San José, 186 p.

Ledoux, J.C. 1970. Les dents des Squalidés de la Méditerranée occidentale et de l'Atlantique Nord-ouest africain. *Vie et Milieu, Serie A* 21: 309–362.

Leriche, M. 1910. Les poissons Oligocènes de la Belgique. *Mémoires du Musée Royal d'Histoire Naturelle de Belgique* 5: 233–363.

Leriche, M. 1938. Contribution à L'étude des Poissons fossiles des pays riverains de la Méditerranée américaine, Venezuela, Trinité, Antiles, Mexique. *Mémoires de la Sociéte Paléontologique Suisse* 61: 1–52.

Leriche, M. 1942 Contribution à l'étude des faunes ichthyologiques marines des terrains tertiaires de la Plaine Côtière Atlantique et du centre des Etats-Unis. Les synchronismes des formations tertiaires des deux côtés de l'Atlantique. *Mémoires de la Société géologique de France* 45: 1–110.

Linnaeus, C. 1758. *Systema Naturae per regna tria naturae, secundum classes, ordines, genera, species; cum characteribus, differentiis, synonymis, locis*. 10th Ed. Larentii Salvii, Stockholm, 824 p.

Lockwood, J.P. 1965. [*Geology of the Serranía de Jarara Area. Guajira Peninsula, Colombia*. Ph.D. Thesis., Princeton University, New Jersey, 167 p. Unpublished.].

Long, D.J. 1993a. Late Miocene and Early Pliocene fish assemblages from the north central coast of Chile. *Tertiary Research* 14: 117–126.

Long, D.J. 1993b. Preliminary list of the marine fishes and other vertebrate remains from the late Pleistocene Palos Verdes

Sand Formation at Costa Mesa, Orange County, California. *Paleo-Bios* 15: 9–13.

Lowe, R.T. 1841. A paper from the Rev. R.T. Lowe, M.A., describing certain new species of Madeiran fishes, and containing additional information relating to those already described. *Proceedings of the Zoological Society of London* 8: 36–39.

Manning, E.M. 2006. The Eocene/Oligocene transition in marine vertebrates of the Gulf Coastal Plain. In: D.R. Prothero, L.C. Ivany, and E.A. Nesbitt (Eds.), *From Greenhouse to Icehouse: The Marine Eocene–Oligocene Transition.* Columbia University Press, New York, p. 366–385.

Miller, K.G., Kominz, M.A., Browning, J.V., Wright, J.D., Mountain, G.S., Katz, M.E., Sugarman, P.J., Cramer, B.S., Christie-Blick, N., and Pekar, S.F. 2005. The Phanerozoic Record of Global Sea-Level Change. *Science* 310: 1293–1298.

Montes, C., Bayona, G.A., Cardona, A.A., Bush, D.M., Silva, C.A., Morón, S.E., Hoyos, N., Ramírez, D.A., Jaramillo, C.A., and Valencia, V. 2012a. Arc-continent collision and orocline formation: closing of the Central American seaway. *Journal of Geophysical Research* 117: B04105. Doi: 10.1029/2011JB008959.

Montes, C., Cardona, A., MacFadden, R., Morón, S.E., Silva, C.A., Restrepo-Moreno, S., Ramírez, D.A., Hoyos, N., Wilson, J., Farris, D., Bayona, G.A., Jaramillo, C.A., Valencia, V., Brian, J., and Flores, A. 2012b. Evidence for middle Eocene and younger land emergence in central Panama: implications for Isthmus closure. *Geological Society of America Bulletin* 124: 780–799.

Montes, C., Cardona, A., Jaramillo, C., Pardo, A., Silva, J.C., Valencia, V., Ayala, C., Pérez-Angel, L.C., Rodriguez-Parra, L.A., Ramirez, V., and Niño, H. 2015. Middle Miocene closure of the Central American Seaway. *Science* 348: 226–229.

Moreno, J.F., Hendy, A.J.W., Quiroz, L., Hoyos, N., Jones, D.S., Zapata, V., Zapata, S., Ballen, G.A., Cadena, E., Cárdenas, A.L., Carrillo-Briceño, J.D., Carrillo, J.D., Delgado-Sierra, D., Escobar, J., Martínez, J.I., Martínez, C., Montes, C., Moreno, J., Pérez, N., Sánchez, R., Suárez, C., Vallejo-Pareja, M.C., and Jaramillo, C. 2015. Revised Stratigraphy of Neogene strata in the Cocinetas Basin, La Guajira, Colombia. *Swiss Journal of Paleontology* 134: 5–43.

Müller, A. 1999. Ichthyofaunen aus dem atlantischen Tertiär der USA. *Leipziger Geowissenschaften* 9–10: 1–360.

Müller, J. 1846. Über den Bau und die Grenzen der Ganoiden und über das natürlichen System der Fische. *Abhandlungen Akademie der Wissenschaften* 1844: 117–216.

Müller, J., and Henle, J. 1837. Gattungen der Haifische und Rochen nach einer von ihm mit Hrn. Henle unternommenen gemeinschaftlichen Arbeit tiber die Naturgeschichte der Knorpelfische. *Akademie der Wissenschaften zu Berlin* 2: 111–118.

Müller, J., and Henle, J. 1838. Ueber die Gattungen der Plagiostomen. *Archiv für Naturgeschichte* 4: 83–85.

Musick, J.A., Harbin, M.M., and Compagno, L.J.V. 2004. Historical zoogeography of the Selachii. In: J.C. Carrier, J.A. Musick, and M.R. Heithaus (Eds.), *Biology of Sharks and their Relatives*. CRC Press, Washington DC, p. 33–78.

Nazarkin, M.V., and Malyshkina, T.P. 2012. The first reliable record of selachians from the Neogene deposits of Sakhalin Island. *Zoosystematica Rossica* 21: 180–184.

Philippi, R.A. 1892. Algunos peces de Chile. *Anales del Museo Nacional de Chile, Primera sección, Zoología* 3: 1–17.

Pimiento, C., and Balk, M.A. 2015. Body-size trends of the extinct giant shark *Carcharocles megalodon*: a deep-time perspective on marine apex predators. *Paleobiology* 41: 479–490. Doi: http://dx.doi.org/10.5061/dryad.6q5t4.

Pimiento, C., and Clements, C.F. 2014. When Did *Carcharocles megalodon* Become Extinct? A New Analysis of the Fossil Record. *PLoS ONE* 9: e111086. Doi: 10.1371/journal.pone.0111086.

Pimiento, C., Ehret, D.J., MacFadden, B.J., and Hubbell, G. 2010. Ancient Nursery Area for the Extinct Giant Shark Megalodon from the Miocene of Panama. *PLoS ONE* 5: e10552. Doi:10.1371/journal.pone.0010552.

Pimiento, C., Gonzales, G., Hendy, A., Jaramillo, C., MacFadden, B., Montes, C., Suarez, S., and Shippritt, M. 2013a. Early Miocene chondrichthyes from the Culebra Formation, Panama: a window into marine vertebrate faunas before closure the Central American Seaway. *Journal of South American Earth Sciences* 42: 159–170.

Pimiento, C., González-Barba, G., Ehret, D.J., Hendy, A.J.W., MacFadden, B.J., and Jaramillo, C. 2013b. Sharks and rays (Chondrichthyes, Elasmobranchii) from the Late Miocene Gatun Formation of Panama. *Journal of Paleontology* 87: 755–774.

Portell, R.W., Hubbell, G., Donovan, S.K., Green, J.L., Harper, D.A.T., and Pickerill, R. 2008. Miocene sharks in the Kendeace and Grand Bay formations of Carriacou, The Grenadines, Lesser Antilles. *Caribbean Journal of Science* 44: 279–286.

Punyasena, S., Jaramillo, C., de la Parra, F., and Du, Y. 2011. Probabilistic correlation of single stratigraphic samples – a generalized approach for biostratigraphic data. *American Association of Petroleum Geologists* 96: 235–244.

Purdy, R., Clellan, J.H.M., Schneider, V.P., Applegate, S.P., Meyer, R., and Slaughter, R. 2001. The Neogene sharks, rays and bony fishes from Lee Creek Mine, aurora, North Carolina. *Smithsonian Contributions to Paleobiology* 90: 71–202.

Quoy, J.R.C., and Gaimard, J.P. 1824. Description des Poissons. In: L. Freycinet (Ed.), *Voyage au tour du monde fait par ordre du roi, sur les corvettes de S. M: l'Uranie et la Physicienne pendant les années 1817, 1818, 1819 et 182.* Pillet Aïné, Paris, p. 192–401.

R Core Team. 2014. *R: A language and environment for statistical computing. R Foundation for Statistical Computing.* Vienna, Austria. Http://www.R-project.org/.

Rafinesque, C.S. 1810. *Caratteri di alcuni nuovi generi e nouve specie di Animali e Piante della Sicilia con varie osservazioni sopra I medesimi.* Sanfilippo, Palermo, 105 p.

Reed, D. 1946. New species of fossil shark from New Jersey. *Notulae Naturae of the Acadamy of Natural Sciences of Philadelphia* 172: 1–3.

Regan, C.T. 1906. A classification of the selachian fishes. *Proceedings of the Zoological Society of London* 1906: 722–758.

Reinecke, T., Stapf, H., and Raisch, M. 2001. Die Selachier und Chimären des Unteren Meeressandes und Schleichsandes im Mainzer Becken (Rupelium, unteres Oligozän). *Palaeontos* 1: 1–73.

Reinecke, T., Moths, H., Grant, A., and Breitkreutz, H. 2005. Die Elasmobranchier des Norddeutschen Chattiums, insbesondere des Sternberger Gesteins (Eochattium, Oberes Oligozän). *Palaeontos* 8: 1–135.

Reinecke, T., Louwye, S., Havekost, U., and Moths, H. 2011. The elasmobranch fauna of the late Burdigalian, Miocene, at Werder-Uesen, Lower Saxony, Germany, and its relationships with Early Miocene faunas in the North Atlantic, Central Paratethys and Mediterranean. *Palaeontos* 20: 1–170.

Reinecke, T., Balsberger, M., Beaury, B., and Pollerspoeck, J. 2014 The elasmobranch fauna of the Thalberg Beds, early Egerian (Chattian, Oligocene), in the Subalpine Molasse Basin near Siegsdorf, Bavaria, Germany. *Palaeontos* 26: 1–127.

Reis, M.A.F. 2005. Chondrichthyan fauna from the Pirabas Formation, Miocene of northern Brazil, with comments on paleobiogeography. *Anuario do Instituto de Geociencias* 28: 31–58.

Renz, O. 1960. Geología de la parte sureste de la Península de La

Guajira. *Boletín de Geología, Publicación especial III Congreso Geológico Venezolano* (Caracas)*, Ministerio de Minas e Hidrocarburos* 3: 317–347.

Rollins, J. 1965. Stratigraphy and structure of the Guajira Peninsula, northwestern Venezuela and northeastern Colombia. *University of Nebraska Studies, New Series* 30: 1–1102.

Sánchez-Villagra, M.R., Burnham, R.J., Campbell, D.C., Feldmann, R.M., Gaffney, E.S., Kay, R.F., Iozsán, R., Purdy, R.W., and Thewissen, J.G.M. 2000. A new near-shore marine fauna and flora from the early Neogene of northwestern Venezuela. *Journal of Paleontology* 74: 957–968.

Santos, R.S., and Salgado, M.S. 1971. Contribuição à paleontologia do estado do Pará. Novos restos de peixes da Formação Pirabas. *Boletim do Museu Paraense Emílio Goeldi* 16: 1–13.

Santos, R.S., and Travassos, H. 1960. Contribuição à Paleontologia do Estado do Pará. Peixes fósseis da Formação Pirabas. *Monografia da divisão de Geologia e Mineralogia, Departamento Nacional da Produção Mineral* 16: 1–35.

Springer, S., and Bullis, H.R. 1960. A new species of sawshark, *Pristiophorus schroederi*, from the Bahamas. *Bulletin of Marine Science of the Gulf and Caribbean* 10: 241–254.

Suárez, M.E., and Marquardt, C. 2003. Revisión preliminar de las faunas de peces elasmobranquios del Mesozoico y Cenozoico de Chile y comentarios sobre su valor cronoestratigráfico. *X Congreso Geológico Chileno* (Concepción), *Actas* 3: 9.

Suárez, M.E., Encinas, A., and Ward, D. 2006. An Early Miocene elasmobranch fauna from the Navidad Formation, Central Chile, South America. *Cainozoic Research* 1–2: 3–18.

Thomas, D. 1972. [*The Tertiary Geology and Systematic Paleontology (Phylum Mollusca) of the Guajira Peninsula, Colombia, South America.* Ph.D. thesis, University of New York, Binghamton, 147 p. Unpublished.].

Thorrold, S.R., Afonso, P., Fontes, J., Braun, C.D., Santos, R.S., Skomal, G.B., and Berumen, M.L. 2014. Extreme diving behaviour in devil rays links surface waters and the deep ocean. *Nature Communications* 5: 4274. Doi:10.1038/ncomms5274.

Uyeno, T., and Matsushima, Y. 1975. Pliocene shark remains of *Carcharodon*, *Carcharhinus* and *Dalatias*, from Kanagawa Prefecture, Japan. *Bulletin of the Kanagawa Prefectural Museum, natural science* 8: 41–55.

Visaggi, C.C., and Godfrey, S.J. 2010. Variation in Composition and Abundance of Miocene Shark Teeth from Calvert Cliffs, Maryland. *Journal of Vertebrate Paleontology* 30: 26–35.

Voigt, M., and Weber, D. 2011. *Field guide for sharks of the genus Carcharhinus.* Verlag Dr. Friedrich Pfeil, München, 151 p.

Waldman, M. 1971. Hexanchid and Orthacodontid Shark Teeth from the Lower Tertiary of Vancouver Island, British Columbia. *Canadian Journal of Earth Sciences* 8: 166–170.

Ward, D., and Bonavia, C. 2001. Additions to, and a review of, the Miocene shark and ray fauna of Malta. *Central Mediterranean Naturalist* 3: 131–146.

Weber, M., Cardona, A., Valencia, V., García-Casco, A., Tobón, M., and Zapata, S. 2010. U/Pb detrital zircon provenance from late cretaceous metamorphic units of the Guajira Peninsula, Colombia: Tectonic implications on the collision between the Caribbean arc and the South American margin. *Journal of South American Earth Sciences* 29: 805–816.

Welton, B.J. 1974. *Heptranchias Howellii* (Reed, 1946) (Selachii, Hexanchidae) in the Eocene of the United States and British Columbia. *Paleobios* 17: 1–15.

White, E.I. 1956. The Eocene fishes of Alabama. *Bulletins of American Paleontology* 36: 123–152.

White, W.T., Ebert, D.A., and Compagno, L.J.V. 2008. Description of two new species of gulper sharks, genus *Centrophorus* (Chondrichthyes: Squaliformes: Centrophoridae) from Australia. In: P.R. Last, W.T. White, and J.J. Pogonoski (Eds.), *Description of New Australian Chondrichthyans. CSIRO Marine and Atmospheric Research Paper* 22. CSIRO, Victoria, p. 1–21.

Woodbourne, M.O. 2010. The great American Biotic interchange: Dispersals, Tectonics, Climate, Sea Level and Holding Pens. *Journal of Mammalian Evolution* 17: 245- 264.

Woodward, A.S. 1889. *Catalogue of the fossil fishes in the British Museum. Part. I.* British Museum (Natural History), London, 474 p.

Zachos, J.C., Shackleton, N.J., Revenaugh, J.S., Pälike, H., and Flower, B.P. 2001. Climate response to orbital forcing across the Oligocene-Miocene boundary. *Science* 292: 274–278.

doi: 10.5710/AMGH.26.10.2015.2931

Submitted: July 1st, 2015

Accepted: October 26th, 2015

AMEGHINIANA - 2016 - Volume 53 (2): 77 – 99

APPENDIX 1. ***Chondrichthyan assemblage of Uitpa Formation and its fossil record in the Cenozoic of the Americas***

Taxon	*Tropical America and the Caribbean*																			*NA*		*SSA*	
	Barbados	*Bonaire*	*Brazil*	*Costa Rica*	*Cuba*	*Dominican Republic*	*Ecuador*	*Haiti*	*Jamaica*	*Martinique*	*Panama*	*Peru*	*Puerto Rico*	*Trinidad*	*The Grenadines*	*Venezuela*	*Southern Mexico*	*Northern Mexico*	*U.S.A*	*Argentina*	*Chile*	*Uruguay*
†**Heptranchias** *cf.* **howellii**				*LMi-P* ●							*LMi* ●					*EMi, LMi-P* ●	*MMi-*●	*MMi-*●	*LO*			
Centrophorus *sp.*							*MMi-LMi*				*LMi*					*LMi-P*			*LMi*			
Dalatias *cf.* **licha**	*EMi* ●										*LMi*					*LMi-P*						
Pristiophorus *sp.*							*MMi-EP*				*LMi*	*Mi*				*LMi-P*		*LO*	*LO, EMi-P*	*LO-EMi*	*EMi, LMi-P*	
†*Lamniformes gen. et sp. indet.*											*Mi*								*Mi*			
Isurus *cf.* **oxyrinchus**	*EMi ?*			*MMi*								*LMi-P*			*EMi-MMi*	*EMi*		*MO-P*	*EMi-P*			*EMi-P*
†**Carcharocles** *sp.*	*LMi*	*LMi*	*EMi*	*EMi-LMi*	*P*	*LMi-EP*	*P*	*Mi-P*	*EMi*	*EMi*	*MMi-P*	*LM*	*EMi-EP*	*EMi-MMi*	*EMi-EP*	*EMi*	*LO-P*	*LO-P*	*LO-P*	*EMi-LMi*	*LMi-P*	*LMi*
Alopias *cf.* **superciliosus**	*EMi*		*LMi-P*								*LMi*					*LMi-P*			*EMi-P*			
†**Hemipristis serra**	*EMi*	*EMi-MMi*	*MMi-EP*	*EMi-LMi*		*LMi-EP*		*Mi*		*EMi-LMi*	*LMi-P*		*EMi, EP*	*MMi*	*EMi-P*	*EMi*	*MO-P*	*LO-P*	*EMi, LMi*			
†**Carcharhinus gibbesii**														*Mi*					*LO*			
Carcharhinus *sp.*																						*LO-MMi*
†**Sphyrna laevissima**	*EMi*		*EMi*																			
Mobula *sp.*			*LMi-P*				*LMi*				*LMi*					*EMi*			*MMi-LMi*	*LO-LMi*		

E: early, M: middle, L: late, O: Oligocene, Mi: Miocene, P: Pliocene, ● *indicates presence of the genus, NA: North America, SSA: Southern South America.*

APPENDIX 2.

Code in R used to run the Maximum Likelihood Analysis

```
library(truncnorm)
perlo=rtruncnorm(n=1000, a=0, b=1000, mean=315, sd=135)
centrophorus=rtruncnorm(n=1000, a=50, b=1440,
mean=(180+(600-180)/2), sd=600-(180+(600-180)/2))
dalatia=rtruncnorm(n=1000, a=37, b=1800, mean=(200+(1800-
200)/2), sd=1800-(200+(1800-200)/2))
pristiophorus=rtruncnorm(n=1000, a=0, b=1000,
mean=(100+(300-100)/2), sd=300-(100+(300-100)/2))
isurus=rtruncnorm(n=1000, a=0, b=500, mean=(100+(150-
100)/2), sd=150-(100+(150-100)/2))
alopias=rtruncnorm(n=1000, a=0, b=730, mean=(10+(400-
10)/2), sd=400-(10+(400-10)/2))
hemipristis=rtruncnorm(n=1000, a=0, b=130, mean=(5+(128-
5)/2), sd=128-(5+(128-5)/2))
carcharhinus=rtruncnorm(n=1000, a=0, b=1000, mean=(5+(200-
5)/2), sd=200-(5+(200-5)/2))
sphyma=rtruncnorm(n=1000, a=0, b=1000, mean=(5+(200-5)/2),
sd=200-(5+(200-5)/2))
mobula=rtruncnorm(n=1000, a=0, b=1000, mean=(5+(150-5)/2),
sd=150-(5+(150-5)/2))

perlo.hist=hist(perlo,breaks = seq(0, 1800, by = 50))
centrophorus.hist=hist(centrophorus,breaks = seq(0, 1800, by = 50))
dalatia.hist=hist(dalatia,breaks = seq(0, 1800, by = 50))
pristiophorus.hist=hist(pristiophorus,breaks = seq(0, 1800, by = 50))
isurus.hist=hist(isurus,breaks = seq(0, 1800, by = 50))
alopias.hist=hist(alopias,breaks = seq(0, 1800, by = 50))
hemipristis.hist=hist(hemipristis,breaks = seq(0, 1800, by = 50))
carcharhinus.hist=hist(carcharhinus,breaks = seq(0, 1800, by = 50))
sphyma.hist=hist(sphyma,breaks = seq(0, 1800, by = 50))
mobula.hist=hist(mobula,breaks = seq(0, 1800, by = 50))

bathymet=rbind(seq(0,1750,by = 50),perlo.hist$counts,centro-
phorus.hist$counts,dalatia.hist$counts,pristiophorus.hist$count,
isurus.hist$counts,alopias.hist$counts,hemipristis.hist$counts,car
charhinus.hist$counts,sphyma.hist$counts,mobula.hist$counts)

rownames(bathymet)=c("depth","perlo","centrophorus","dalatia",
"pristiophorus","isurus","alopias","hemipristis","carcharhinus","sp
hyma","mobula")

write.table(bathymet, file="bathym.csv", quote=FALSE,
sep=",",row.names = TRUE, col.names=FALSE)

uitpa.ml=read.table("uitpaML",sep="\t", header=TRUE) #ML results

plot(uitpa.ml$depth,uitpa.ml$Probability, xlab="depth (m.)",
ylab="probability", type="l", lab=c(20,5,7))#figure

abline(v=100, col="red")
abline(v=150, col="red")
```

APPENDIX B

Palaeontologia Electronica
palaeo-electronica.org

The oldest record of gnathostome fossils from Greece: Chondrichthyes from the Lopingian of Hydra Island

Thodoris Argyriou, Carlo Romano, Jorge D. Carrillo-Briceño, Morgane Brosse, and Richard Hofmann

ABSTRACT

The Permian deposits of Hydra Island, Greece, have been known for over a century and host some of the best-studied and most diverse invertebrate assemblages of the ancient Paleotethys Ocean. However, until now, no Paleozoic fossils of jawed vertebrates had been reported from Greece. Recent fieldwork on Hydra Island brought to light rare cartilaginous fish remains, including a tooth belonging to an unknown hybodontiform shark, as well as an unidentifiable dermal denticle of an euselachian shark. Despite similarities with iconic Paleozoic and Mesozoic durophagous euselachians, the Hydriot tooth likely corresponds to a new species, but is provisionally left in open nomenclature until more material becomes available. The new chondrichthyan fossils from Hydra Island correspond to one of the few Lopingian (late Permian) occurrences known from the Paleotethys. Moreover, they constitute the oldest record of jawed-vertebrate fossils from Greece, predating younger occurrences by more than 50 million years.

Thodoris Argyriou. Paleontological Institute and Museum, University of Zurich, Karl-Schmid-Strasse 4, Zürich, 8006, Switzerland. thodoris.argyriou@pim.uzh.ch
Carlo Romano. Paleontological Institute and Museum, University of Zurich, Karl-Schmid-Strasse 4, Zürich, 8006, Switzerland. carlo.romano@pim.uzh.ch
Jorge D. Carrillo-Briceño. Paleontological Institute and Museum, University of Zurich, Karl-Schmid-Strasse 4, Zürich, 8006, Switzerland. jorge.carrillo@pim.uzh.ch
Morgane Brosse. Paleontological Institute and Museum, University of Zurich, Karl-Schmid-Strasse 4, Zürich, 8006, Switzerland. morgane.brosse@pim.uzh.ch
Richard Hofmann. Paleontological Institute and Museum, University of Zurich, Karl-Schmid-Strasse 4, Zürich, 8006, Switzerland; Leibniz Institut für Evolutions und Biodiversitätsforschung, Museum für Naturkunde, Invalidenstraße 43, Berlin, 10115, Germany. richard.hofmann@mfn-berlin.de

Keywords: late Permian; Paleotethys; fossil fish; Hybodontiformes; Hydra Island; Greece

Submission: 6 October 2016 Acceptance: 27 February 2017

Argyriou, Thodoris, Romano, Carlo, Carrillo-Briceño, Jorge D., Brosse, Morgane, and Hofmann, Richard. 2017. The oldest record of gnathostome fossils from Greece: Chondrichthyes from the Lopingian of Hydra Island. *Palaeontologia Electronica* 20.1.8A: 1-9
palaeo-electronica.org/content/2017/1769-permian-sharks-of-greece

INTRODUCTION

The Permian Period (~298–252 Ma) was a particularly important time interval for life on the planet, characterized by a series of global-scale environmental disturbances that climaxed at ~252 Ma with the most-severe end-Permian mass extinction event (Benton and Twitchett, 2003; Burgess et al., 2014). Despite the catastrophic impact of this mass extinction event for most groups (e.g., Benton and Twitchett, 2003), many osteichthyan clades as well as euselachians were less severely affected (Friedman and Sallan, 2012; Koot, 2013; Romano et al., 2016). Recent works have improved our understanding of the Permian chondrichthyan fossil record (Ginter et al., 2010; Hampe et al., 2013; Hodnett et al., 2013; Ivanov et al., 2013; Koot, 2013; Koot et al., 2013; Chahud and Petri, 2014; Ivanov and Lebedev, 2014; Ivanov et al., 2015), but the latter remains sporadic and less well known in comparison to that of the Triassic (Hampe et al., 2013; Koot, 2013; Koot et al., 2013 and references therein). This fact might bias interpretations about the timing of clade origins, impact of the end-Permian mass extinction on chondrichthyans and the hypothesized patterns of the Early Triassic biotic recovery.

The restricted occurrences of Paleozoic (Silurian–Permian) sedimentary rocks in Greece have attracted considerable scientific attention since their first discovery, more than a century ago (Renz, 1910). Several invertebrate assemblages have been described from exotic or autochthonous rocks, but until now conodonts were the only putative vertebrates reported (e.g., Nestell and Wardlaw, 1987; Groves et al., 2003; for more information on the ongoing discussion about conodont affinities see Donoghue et al., 2000; Turner et al., 2010; Murdock et al., 2013). Reif (1978) mentioned the presence of “hybodontid-type” dermal denticles in the Permian of Greece, but did not describe or figure any, nor did he provide any locality or repository information. Previous oldest ascertained gnathostome occurrences from the country include poorly preserved actinopterygian remains from the Lower Jurassic of Lefkada Island, Ionian Sea (Kottek, 1964). These are succeeded by Maastrichtian–Danian chondrichthyan and teleostean fossils from various localities around the country (Koch and Nikolaus, 1969; Trikolas, 2008; Cavin et al., 2012).

Recent fieldwork on Hydra Island by R.H. and colleagues has brought to light new invertebrate and vertebrate material. The latter, described in this work, comprises one chondrichthyan tooth and one dermal denticle, deriving from the same hand-sample. These fossils represent the oldest, unambiguous gnathostome occurrences of Greece, predating younger occurrences by more than 50 million years. Furthermore, this occurrence is a valuable addition to the poor Lopingian (late Permian) chondrichthyan record of the Paleotethys (Schaumberg, 1977; Ginter et al., 2010; Koot, 2013).

GEOLOGICAL SETTING AND AGE

Hydra Island is located in the northwestern margin of Myrtoon Basin, western Aegean Sea (Eastern Mediterranean), ~70 km to the south-southwest of Athens (Figure 1.1). The late Paleozoic outcrops, first reported by Renz (1910), are located along the southeastern coast of the island and comprise shallow water carbonate and siliciclastic successions (Figure 1.2-3), which were deposited on the northwestern Paleotethyan margin, forming the base of the “sub-Pelagonian” zone (Baud et al., 1990; Grant et al., 1991). A diverse array of fossils is known from the autochthonous Permian sedimentary successions of Hydra, including algae (Jenny et al., 2004), benthic foraminifera (Vachard et al., 1995; Jenny et al., 2004; Vachard et al., 2008), ostracods (Crasquin-Soleau and Baud, 1998; Kornicker and Sohn, 2000) and brachiopods (Grant, 1972, 1995; Shen and Clapham, 2009). Conodonts are mostly known from the upper part of the Lopingian limestone (Nestell and Wardlaw, 1987), where the successive occurrences of *Neogondolella leveni* and *Neogondolella orientalis* indicate a Wuchiapingian (early Lopingian) age (Kozur, 1975). The matrix surrounding the chondrichthyan fossils contained three conodont P_1 elements, belonging to *Hindeodus*. The best-preserved one is assignable to *Hindeodus typicalis,* which has a Lopingian–lower Induan stratigraphic range. Since Induan (earliest Triassic) deposits are unknown from Hydra, our conodonts best indicate a Lopingian age for the studied sample.

MATERIAL AND METHODS

The chondrichthyan tooth was partly exposed on the surface of a hand-sample (~1.5 kg) of silicified dark grey-colored limestone. The sample was dissolved in a 10% buffered acetic acid (Jeppsson et al., 1999) and concentrated by heavy liquid separation (Jeppsson and Anehus, 1999). The residue was handpicked under a binocular microscope, and the recovered vertebrate material was imaged

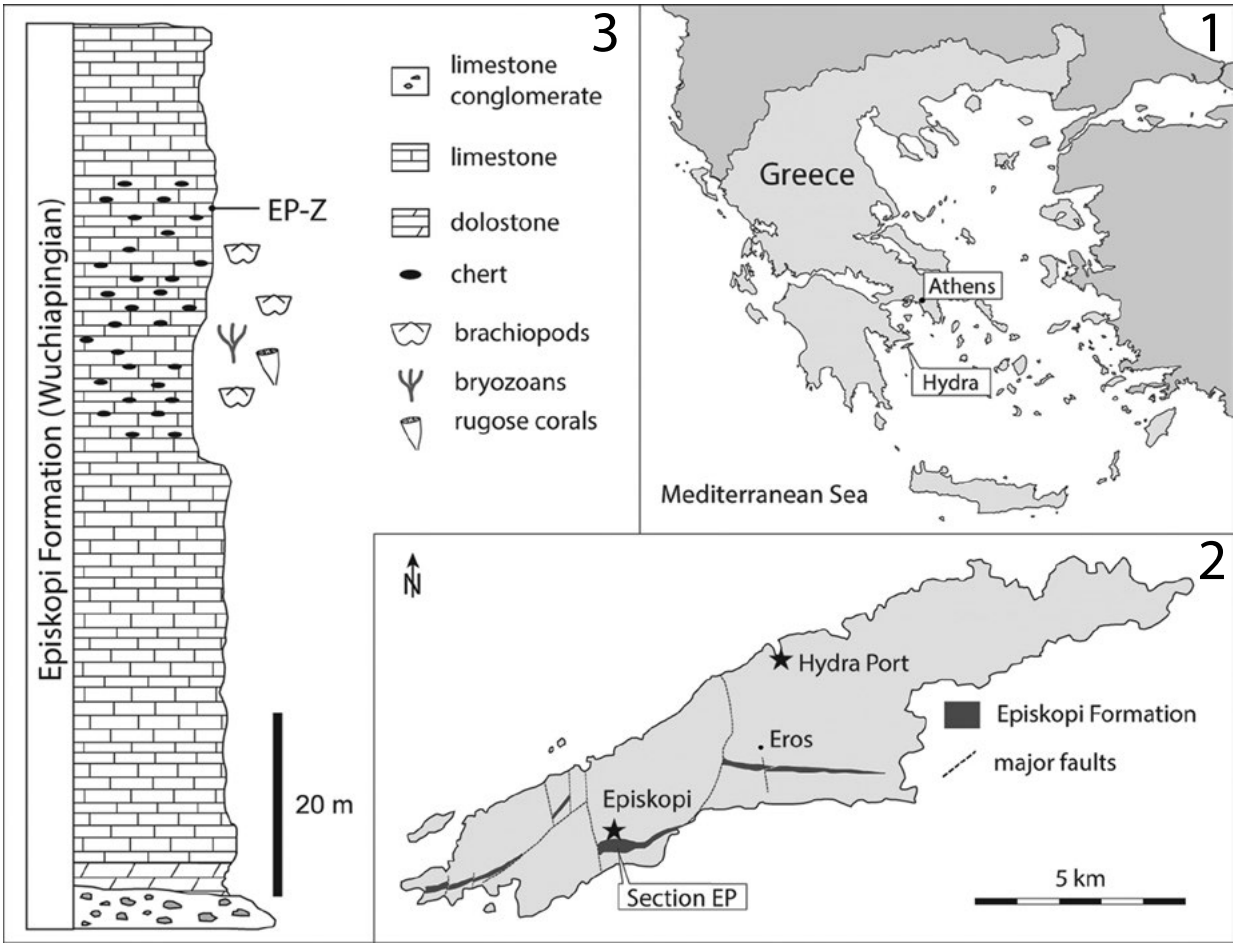

FIGURE 1. Geographical and geological context of the Hydriot chondrichthyan fossils. **1**, Map of Greece showing the location of Hydra Island; **2**, Outcrop map of Hydra Island showing the location of the sampled section "EP" south of the village of Episkopi. Outcrop map after Grant et al. (1991); **3**, Stratigraphic section of the Episkopi Formation showing the provenance ("EP-Z") of the examined gnathostome fossils.

with a JSM-6010PLUS LA Scanning Electron Microscope at the Center for Microscopy and Image Analysis, University of Zurich (ZMBUZH). Both gnathostome specimens are catalogued and housed in the vertebrate collection of the Museum of Paleontology and Geology, National and Kapodistrian University of Athens, Greece (AMPG). Tooth and dermal denticle terminology applied herein adheres to that of previous works (Reif, 1978; Ginter et al., 2010; Cappetta, 2012). For comparative purposes we examined hybodontiform and *Acronemus* material from the Middle Triassic of Monte San Giorgio (Ticino, Switzerland), housed at the Paleontological Institute and Museum, University of Zurich, Switzerland (PIMUZ). For a complete list of specimens catalogued at the PIMUZ the reader is referred to Rieppel (1981, 1982) and Mutter (1998a, 1998b).

SYSTEMATIC PALEONTOLOGY

Class CHONDRICHTHYES Huxley, 1880
Cohort EUSELACHII Hay, 1902
Order HYBODONTIFORMES Maisey, 1975
Hybodontiformes Gen. et sp. indet.
Figure 2.1-5

Material. One tooth of indeterminate jaw position, AMPG 550.

Description. The crushing-type tooth is characterized by a well-preserved crown and a somewhat damaged root. The isolated nature of the tooth allows only a tentative attribution of one of the two broad lateral surfaces to labial, based on the combination of a well-defined root sulcus accommodating a single row of foramina, as well as the lingual inclination of the underlying root surface.

The crown bears a single, low and rounded main cusp. In occlusal view (Figure 2.1) the crown

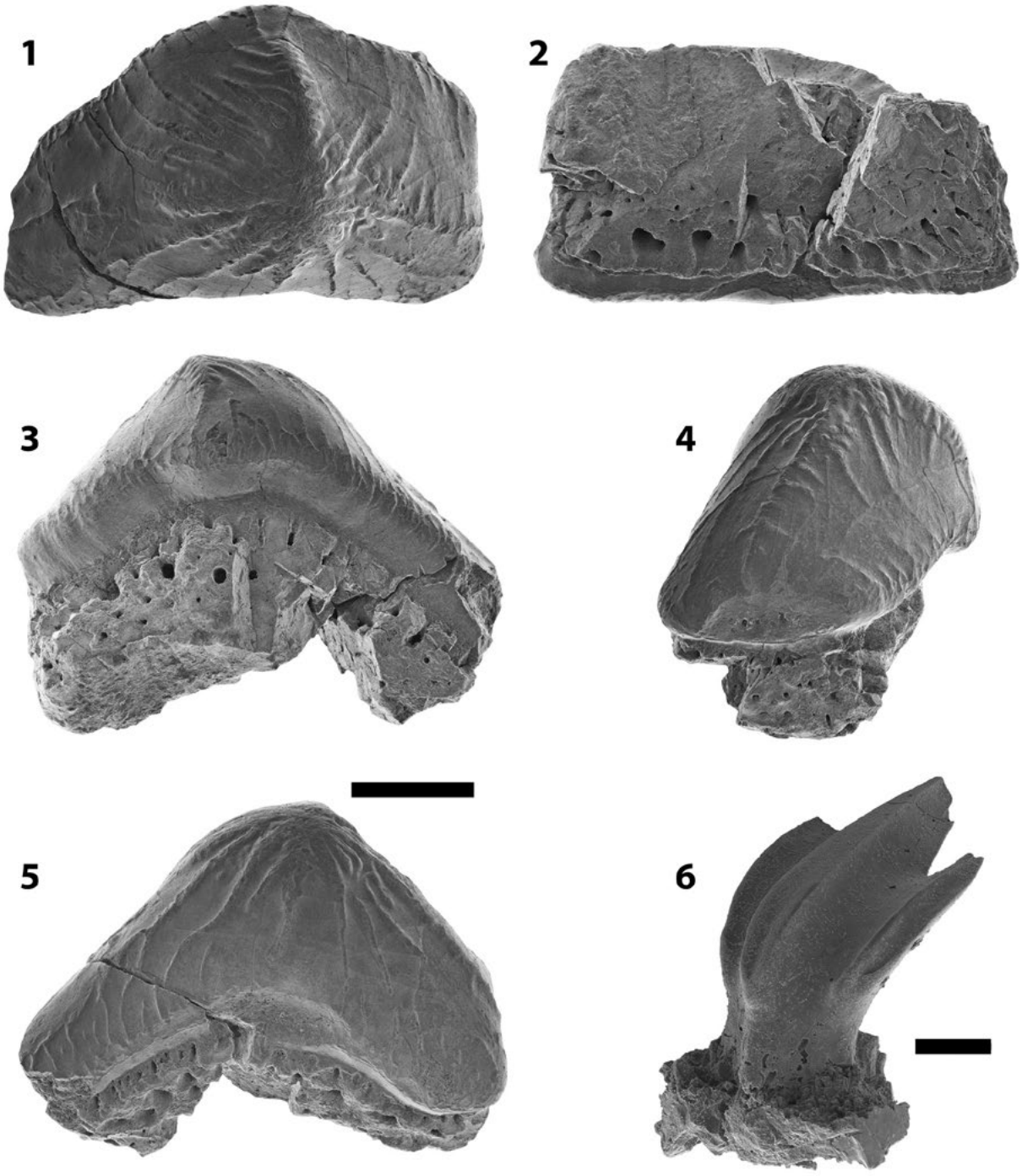

FIGURE 2. Chondrichthyan material from Hydra. **1-5,** Hybodontiformes indet. tooth (AMPG 550) in occlusal (**1**), basal (**2**), presumed lingual (**3**), profile (**4**), and presumed labial (**5**) views. Scale bar equals 5 mm. **6**, Euselachii indet. dermal denticle (AMPG 551) in anterolateral view. Scale bar equals 100 μm.

is triangular with truncated mesial and distal edges. It overhangs the root almost completely and forms a distinct presumably lingual projection. The crown bears a distinct labiolingual crest and a less distinct mesiodistal crest, the two meeting at an almost right angle, on the apex of the main cusp. The mesiodistal crest fades before reaching the edges of the crown. Most delicate secondary, crests radiate from the junction point of the two primary crests, while few originate from the labiolingual and mesiodistal crests, near their junction. Few secondary crests run continuously until the base of the crown where they might bifurcate. Others fade midway to reappear near the base of the crown. When viewed lingually or labially, the crown is boomerang-shaped. The lingual surface is convex (Figure 2.3), bearing a well-developed, median, laterobasally directed protuberance. The presumed concave labial surface bears fewer secondary crests and is characterized by a socket-like elliptical hollow (Figure 2.5), presumably for accommodating the lingual protuberance of the neighboring tooth of the same file, indicating some weak imbrication of the dentition.

The anaulacorhize root is apicobasally, mesiodistally, and labiolingually shorter than the crown and conforms to its contour. In lingual view (Figure 2.3), the root is damaged, but is populated by randomly arranged, apicobasally elongate foramina. In labial view (Figure 2.5), the root is markedly shallow, less than one fourth of the crown height. The labial face of root bears a weak sulcus along the crown-root margin, populated by a single row of well-arranged, apicobasally elongate foramina, smaller and more numerous (~20) than those of the other lateral face. The basal half of the root is slanted lingually, bearing larger, sparsely arranged, enlarged foramina. The base of the root, although damaged, appears flat and sub-rectangular, without a distinct lingual protuberance. In profile view (Figure 2.4), the crown clearly overhangs the root.

Remarks. Several Paleozoic and Mesozoic chondrichthyans have convergently evolved low crowned, crushing-type teeth. However, the presence of a single cusp, the ridged crown ornamentation and the anaulacorhize root anatomy, which includes a distinct sulcus with specialized foramina along the crown–root boundary, compare favorably to features seen in durophagous euselachians (e.g., Ginter et al., 2010; Cappetta, 2012). Isolated teeth of Paleozoic and early Mesozoic stem euselachians, hybodontiforms and stem neoselachians are often difficult to distinguish and attribute to less inclusive groups, due to their generalized and/or often homoplasic morphologies (Ginter et al., 2010; Cappetta, 2012). Despite this fact, a review of dental anatomy of Paleozoic–early Mesozoic forms can provide some information about the systematic affinities of the Hydriot tooth.

Macroscopic teeth of Paleozoic–early Mesozoic stem neoselachians exhibit crowns with well-defined median cusps and, when present, accessory cusplets and/or a median cutting edge (Ginter et al., 2010; Koot et al., 2013). Their roots are either hemiaulacorhize or pseudo-polyaulacorhize; they typically bear fewer, enlarged foramina (the median ones in particular) than other euselachians; and are somewhat arcuate in basal view, due to the presence of a lingual protuberance (Ginter et al., 2010). None of the above is seen in the examined specimen, rendering a neoselachian attribution unfavorable. Low-crowned crushing teeth without lateral cusplets, but with anaulacorhize, multiforaminate roots, which often include a labial sulcus accommodating a single row of specialized foramina, are seen in members of the Hybodontiformes (e.g., *Acrodus*; *Lissodus*; *Omanoselache*; *Onychoselache*) as well as in the stem euselachian (sensu Maisey, 2011) *Acronemus* (Johnson, 1981; Rieppel, 1982; Ginter et al., 2010; Cappetta, 2012; Koot et al., 2013, 2015).

Hybodontiformes can exhibit very disparate dental features, and are formally united as a group by means of cranial and postcranial anatomy (Maisey, 1975, 1982; Ginter et al., 2010; Cappetta, 2012). Within the Paleozoic–Triassic Hybodontiformes, dental anatomy somewhat comparable to that of our specimen occurs in *Acrodus, Lissodus, Hamiltonichthys,* and *Onychoselache* (e.g., Ginter et al., 2010; Cappetta, 2012). Despite the uncertain affinities of *Acronemus* within euselachians, its tooth morphology is hybodontiform-like (Rieppel, 1982; Maisey, 2011; Cappetta, 2012), and resemblant to that of AMPG 550. One of the most conspicuous differences among the abovementioned genera is the occurrence of a lingual crown protuberance in *Hamiltonichthys* (Maisey, 1989), *Onychoselache* (Coates and Gess, 2007) and *Acronemus* (Rieppel, 1982), rather than a labial one as in most other Hybodontiformes.

The single, blunt main cusp and the ridged ornamentation are common features of Acrodontidae (sensu Cappetta, 2012). *Acrodus* (s.l.) is the only member of the family that shows resemblances to our specimen and has Paleozoic occurrences (as ?*Acrodus*) (Johnson, 1981; Hodnett et al., 2011; Hampe et al., 2013). It is otherwise prom-

inently known from Triassic (e.g., Rieppel, 1981; Mutter, 1998a, 1998b; Cappetta, 2012) and younger Mesozoic deposits (Cappetta, 2012). *Acrodus* teeth exhibit marked monognathic heterodonty, with symphyseal, parasymphyseal and posterior teeth being mesiodistally narrower and more apicobasally arcuate than lateral teeth (Mutter, 1998a; Ginter et al., 2010; Cappetta, 2012), resembling the Hydriot tooth. However, *Acrodus* teeth bear a distinct mesiodistal crest and a less distinct or absent labiolingual crest (Johnson, 1981; Rieppel, 1981; Mutter, 1998a, 1998b; Ginter et al., 2010; Hodnett et al., 2011; Cappetta, 2012; Hampe et al., 2013). In addition, secondary crests initiate all along the horizontal crest, are tightly packed and exhibit strong bifurcation patterns, whereas a socket for tooth interlocking is absent in most species (Johnson, 1981; Rieppel, 1981; Mutter, 1998a, 1998b; Ginter et al., 2010; Hodnett et al., 2011; Cappetta, 2012; Hampe et al., 2013), except in *A. georgii*, where it is situated lingually (Mutter, 1998b). The abovementioned differences preclude the inclusion of the Hydra chondrichthyan in *Acrodus*.

Teeth of the Pennsylvanian genus *Hamiltonichthys* resemble the Hydriot tooth in terms of occlusal crown ornamentation, while they also bear a lingual protuberance and a labial scar (Maisey, 1989). Our specimen differs from *Hamiltonichthys* in exhibiting more rounded corners at the mesial and distal end of the crown in occlusal view. *Onychoselache* (Coates and Gess, 2007) exhibits teeth of more subtle crown ornamentation and higher roots than AMPG 550. Finally, unicuspidate *Lissodus* teeth have strongly lingually bent roots, whereas mesiodistal and labiolingual occlusal crests form more pronounced, sharp, and often jagged, cutting edges (Rees and Underwood, 2002; Duncan, 2004; Ginter et al., 2010). The marked labiolingual crest on the crown of AMPG 550, the lingual bulbous crown projection, along with the wider spacing between the secondary ridges are also reminiscent of characteristics of medial teeth of the ?Pennsylvanian–Middle Triassic *Acronemus* (Euselachii incertae sedis) (Rieppel, 1982; Rees and Underwood, 2002; Maisey, 2011). Despite the presence of a distinct lingual protuberance, *Acronemus* teeth do not possess a labial socket, differing in that regard from the Hydriot tooth. *Acronemus* teeth are further differentiated by their height and their shorter, strongly saddle-shaped crown (Rieppel, 1982). Unfortunately, little is known about root vascularization in *Acronemus* teeth.

A close relationship between AMPG 550 and the Triassic *Palaeobates* or *Homalodontus* (= "*Wapitiodus*"), both possessing flat-crowned teeth, is excluded based on the general tooth morphology and ornamentation (Mutter et al., 2007, 2008; Romano and Brinkmann, 2010). The potential Permian stem euselachian *Wodnika* possess a smooth crown, markedly dissimilar to that of the Hydriot specimen (Haubold and Schaumberg, 1985; Hampe in Cappetta, 2012). Finally, the unicuspidate teeth of the hybodontiform *Omanoselache* differ in ornamentation, shape, and direction of crown protuberance and exhibit fewer but larger root foramina (Koot et al., 2013, 2015).

In summary, AMPG 550 shows moderate to strong morphological affinities with *Hamiltonichthys*, *Acronemus* and moderate affinities with Paleozoic ?*Acrodus* teeth of Johnson (1981). However, conspicuous differences in crown shape and ornamentation, interlocking process and root development preclude its assignment to any of the aforementioned genera. Our small sample size does not permit the erection of a new genus and, on the basis of dental characteristics alone, we prefer to leave it in open nomenclature within Hybodontiformes until additional fossil material becomes available.

Cohort EUSELACHII Hay, 1902

Euselachii indet.

Figure 2.6

Material. One fragmented dermal denticle, AMPG 551.

Description. The relatively well-preserved crown is lanceolate and curved posteriorly. It possesses a well-developed, tricuspid distal crown, a neck and a base. Three keels can be seen on the anterodistal part of the crown. The median keel bears a shallow groove along its basal half and is distinctly higher than the two lateral keels. Its proximal end continues as a gentle ridge on the anterior surface of the neck. The lateral keels are grooved along their length and splay dorsolaterally, in anterior view. The neck is slightly narrower than the crown. The base is poorly preserved, but must have had a triangular outline and is wider than the crown, in proximal view.

Remarks. The presence of a slender crown with three keels on its anterior surface and a narrow neck are common features in scales of Paleozoic–Mesozoic ctenacanthids, but are also common in euselachian chondrichthyans (Reif, 1978; Hansen, 1986; Rieppel et al., 1996; Johns et al., 1997; Derycke-Khatir et al., 2005; Ivanov et al., 2013). The Hydriot denticle compares favorably to the par-

agenus *Moreyella* (Gunnell, 1933; Hansen, 1986), which has been tentatively affiliated with Carboniferous–Permian hybodontiform chondrichthyans (e.g., Derycke-Khatir et al., 2005). The Triassic paragenera *Fragilicorona* and *Labascicorona* (Johns et al., 1997) also display very similar, tricuspid distal crowns like the denticle in question, but their systematic affinities beyond the euselachian level have not been discussed (Ivanov et al., 2013). Hybodontiform dermal denticles can exhibit disparous morphologies, even in the same individual, ranging from somewhat stockier and shorter types with more keels and stout or undeveloped necks (Reif, 1978), to more delicate and elongate ones like AMPG 551. Denticles of the latter type cannot be effectively distinguished from those of other euselachians (Rieppel et al., 1996; Ivanov et al., 2013). Thus, it is unclear whether the Hydra denticle comes from the same genus or individual as the tooth AMPG 550.

CONCLUSION

The new chondrichthyan material from the Wuchiapingian (Early Lopingian) of Hydra Island represents the oldest gnathostome remains of Greece, and adds a new occurrence to the relatively poor late Permian fish fossil record (Koot, 2013; Romano et al., 2016). Coeval occurrences from the western Paleotethys are mainly known from Western and Central Europe (Koot, 2013). The presence of bed-controlled chondrichthyan microremains associated with conodont index fossils emphasizes the importance of the new locality and future fieldwork on Hydra could further improve our knowledge about chondrichthyan faunas a few million years before the largest mass extinction event. The Hydriot tooth presented herein shows particular resemblances to iconic Paleozoic (*Hamiltonichthys*) and Paleozoic–Mesozoic taxa (*Acrodus*, *Acronemus*), but likely belongs to a new genus and species that could prove important for the resolution of hybodontiform and euselachian phylogeny. However, additional fossil material is required for a more conclusive systematic interpretation. The discovery of Permian chondrichthyans in Hydra highlights the need for additional paleontological survey in the pre-Cenozoic, and especially the Paleozoic, deposits of Greece.

ACKNOWLEDGMENTS

The authors wish to thank the two anonymous reviewers and the editorial team of Palaeontologia Electronica for their insightful comments that improved the quality of this manuscript. Special thanks to M. Kirschmann (ZMBUZH) for assisting the SEM imaging process; R. Kindlimann (Switzerand) for providing useful comments during the early stages of the work and M. Leu (PIMUZ) for helping with acid preparation of hand samples. We are indebted to M.R. Sánchez-Villagra and M. Hautmann (both PIMUZ) for their support during the preparation of this study. M. Haas (ETH, Zürich) is thanked for field assistance and S. Roussiakis (AMPG) for providing specimen numbers. Access to the field localities and sampling permission was provided by the Hellenic Ministry of Culture and Sports, and the AMPG.

REFERENCES

Baud, A., Jenny, C., Papanikolaou, D., Sideris, C., and Stampfli, G. 1990. New observations on Permian stratigraphy in Greece and geodynamic interpretation. *Bulletin of the Geological Society of Greece,* 25(1):187-206.

Benton, M.J. and Twitchett, R.J. 2003. How to kill (almost) all life: the end-Permian extinction event. *Trends in Ecology & Evolution,* 18(7):358-365.

Burgess, S.D., Bowring, S., and Shen, S.-Z. 2014. High-precision timeline for Earth's most severe extinction. *Proceedings of the National Academy of Sciences,* 111(9):3316-3321.

Cappetta, H. 2012. Chondrichthyes II: Mesozoic and Cenozoic Elasmobranchii, p. 512. In Schultze, H.P. (ed.), *Handbook of Paleoichthyology, vol. 3B*. Dr. Friedrich Pfeil, München.

Cavin, L., Alexopoulos, A., and Piuz, A. 2012. Late Cretaceous (Maastrichtian) ray-finned fishes from the island of Gavdos, southern Greece, with comments on the evolutionary history of the aulopiform teleost *Enchodus*. *Bulletin de la Société Géologique de France,* 183(6):561-572.

Chahud, A. and Petri, S. 2014. New chondrichthyans from the Irati Formation (Early Permian, Paraná Basin), Brazil: origin, paleoenvironmental and paleogeographical considerations. *Proceedings of the Geologists' Association,* 125(4):437-445.

Coates, M.I. and Gess, R.W. 2007. A new reconstruction of *Onychoselache traquairi*, comments on early chondrichthyan pectoral girdles and hybodontiform phylogeny. *Palaeontology,* 50(6):1421-1446.

Crasquin-Soleau, S. and Baud, A. 1998. New Permian ostracods from Greece (Hydra Island). *Journal of Micropalaeontology,* 17(2):131-152.

Derycke-Khatir, C., Vachard, D., Dégardin, J.-M., Flores de Dios, A., Buitrón, B., and Hansen, M. 2005. Late Pennsylvanian and Early Permian chondrichthyan microremains from San Salvador Patlanoaya (Puebla, Mexico). *Geobios,* 38(1):43-55.

Donoghue, P.C.J., Forey, P.L., and Aldridge, R.J. 2000. Conodont affinity and chordate phylogeny. *Biological Reviews,* 75(2):191-251.

Duncan, M. 2004. Chondrichthyan genus *Lissodus* from the Lower Carboniferous of Ireland. *Acta Palaeontologica Polonica,* 49(3):417-428.

Friedman, M. and Sallan, L.C. 2012. Five hundred million years of extinction and recovery: a Phanerozoic survey of large-scale diversity patterns in fishes. *Palaeontology,* 55(4):707-742.

Ginter, M., Hampe, O., and Duffin, C. 2010. *Chondrichthyes. Paleozoic Elasmobranchii: Teeth. Handbook of Paleoichthyology,* 3D. Dr. Friedrich Pfeil, München.

Grant, R.E. 1972. The Lophophore and Feeding Mechanism of the Productidina (Brachiopoda). *Journal of Paleontology,* 46(2):213-248.

Grant, R.E. 1995. Upper Permian brachiopods of the superfamily Orthotetoidea from Hydra Island, Greece. *Journal of Paleontology,* 69(04):655-670.

Grant, R.E., Nestell, M.K., Baud, A., and Jenny, C. 1991. Permian stratigraphy of Hydra Island, Greece. *Palaios,* 6(5):479-497.

Groves, J.R., Larghi, C., Nicora, A., and Rettori, R. 2003. Mississippian (Lower Carboniferous) microfossils from the Chios Mélange (Chios Island, Greece). *Geobios,* 36(4):379-389.

Gunnell, F.H. 1933. Conodonts and fish remains from the Cherokee, Kansas City, and Wabaunsee Groups of Missouri and Kansas. *Journal of Paleontology,* 7(3):261-297.

Hampe, O., Hairapetian, V., Dorka, M., Witzman, F., Akbari, A.M., and Korn, D. 2013. A first Late Permian fish fauna from Baghuk Mountain (Neo-Tethyan shelf, central Iran). *Bulletin of Geosciences,* 88(1):1-20.

Hansen, M.C. 1986. *Microscopic chondrichthyan remains from Pennsylvanian marine rocks of Ohio and adjacent areas*, Unpublished PhD Thesis, The Ohio State University, Columbus, Ohio, USA.

Haubold, H. and Schaumberg, G. 1985. *Die Fossilien des Kupferschiefers*. A. Ziemsen, Wittenberg Lutherstadt.

Hay, O.P. 1902. Bibliography and catalogue of fossil Vertebrata of North America. *Bulletin of the United States Geological Survey,* 179:1-868.

Hodnett, J.-P., Elliott, D.K., and Olsen, T. 2011. The hybodontiform sharks (Chondrichthyes) from the marine Permian (Leonardian) Kaibab Formation of northern Arizona. *Ichthyolith Issues, Special Publication,* 12:23-24.

Hodnett, J.-P., Elliott, D.K., and Olson, T.J. 2013. A new basal hybodont (Chondrichthyes, Hybodontiformes) from the middle Permian (Roadian) Kaibab Formation, of Northern Arizona, p. 103-108. In Lucas, S.G., DiMichele, W.A., Barrick, J.E., Schneider, J.W., and Spielmann, J.A. (eds.), *The Carboniferous-Permian Transition.* New Mexico Museum of Natural History and Science, Bulletin. New Mexico Museum of Natural History, Albuquerque.

Huxley, T.H. 1880. On the application of the laws of evolution to the arrangement of the Vertebrata, and more particularly of the Mammalia. *Proceedings of the Scientific Meetings of the Zoological Society of London,* 1880:649–662.

Ivanov, A.O. and Lebedev, O.A. 2014. Permian chondrichthyans of the Kanin Peninsula, Russia. *Paleontological Journal,* 48(9):1030-1043.

Ivanov, A.O., Nestell, G.P., and Nestell, M.K. 2013. Fish assemblage from the Capitanian (Middle Permian) of the Apache Mountains, West Texas, USA, p. 152-160. In Lucas, S.G., DiMichele, W.A., Barrick, J.E., Schneider, J.W., and Spielmann, J.A. (eds.), *The Carboniferous-Permian transition*. New Mexico Museum of Natural History & Science, Albuquerque, New Mexico, USA.

Ivanov, A.O., Nestell, M.K., and Nestell, G.P. 2015. Middle Permian fish microremains from the early Capitanian of the Guadalupe Mountains,West Texas, USA. *Micropaleontology,* 61:301-312.

Jenny, C., Izart, A., Baud, A., and Jenny, J. 2004. Le Permien de l'île d'Hydra (Grèce), micropaléontologie, sédimentologie et paléoenvironnements. *Revue de Paléobiologie,* 23(1):275-312.

Jeppsson, L. and Anehus, R. 1999. A new technique to separate conodont elements from heavier minerals. *Alcheringa: An Australasian Journal of Palaeontology,* 23(1):57-62.

Jeppsson, L., Anehus, R., and Fredholm, D. 1999. The Optimal Acetate Buffered Acetic Acid Technique for Extracting Phosphatic Fossils. *Journal of Paleontology,* 73(5):964-972.

Johns, M.J., Barnes, C.R., and Orchard, M.J. 1997. *Taxonomy and Biostratigraphy of the Middle and Late Triassic elasmobranch ichthyoliths from Northeastern British Columbia* Canadian government publishing, Ottawa, Ontario, Canada.

Johnson, G.D. 1981. Hybodontoidei (Chondrichthyes) from the Wichita-Albany Group (Early Permian) of Texas. *Journal of Vertebrate Paleontology,* 1(1):1-41.

Koch, K.E. and Nikolaus, H.J. 1969. *Zur Geologie des Ostpindos – Flyschbeckens und seiner Umrandung*, Institute for Geology and Subsurface Research, Athens.

Koot, M.B. 2013. *Effects of the late Permian mass extinction on chondrichthyan palaeobiodiversity and distribution patterns*, Unpublished PhD Thesis, Plymouth University, Plymouth, UK. Available at https://pearl.plymouth.ac.uk/handle/10026.1/1584.

Koot, M.B., Cuny, G., Orchard, M.J., Richoz, S., Hart, M.B., and Twitchett, R.J. 2015. New hybodontiform and neoselachian sharks from the Lower Triassic of Oman. *Journal of Systematic Palaeontology,* 13(10):891-917.

Koot, M.B., Cuny, G., Tintori, A., and Twitchett, R.J. 2013. A new diverse shark fauna from the Wordian (Middle Permian) Khuff Formation in the interior

Haushi-Huqf area, Sultanate of Oman. *Palaeontology,* 56(2):303-343.

Kornicker, L.S. and Sohn, I.G. 2000. Myodocopid Ostracoda from the late Permian of Greece and a basic classification for Paleozoic and Mesozoic Myodocopida. *Smithsonian Contributions to Paleobiology,* 91:1-33.

Kottek, A. 1964. Fischreste aus dem griechischen Lias. *Annales géologiques de pays hélleniques,* 39:175 - 181+1 tab.

Kozur, H. 1975. Beiträge zur Conodontenfauna des Perm. *Geologisch-Paläontologische Mitteilungen Innsbruck,* 5(4):1-44+4pls.

Maisey, J.G. 1975. The interrelationships of phalacanthus selachians. *Neues Jahrbuch für Geologie und Paläontologie - Abhandlungen,* 9:553-565.

Maisey, J.G. 1982. The anatomy and interrelationships of Mesozoic hybodont sharks. *American Museum Novitates,* 2724:1-48.

Maisey, J.G. 1989. *Hamiltonichthys mapesi*, g. & sp. nov. (Chondrichthyes; Elasmobranchii), from the Upper Pennsylvanian of Kansas. *American Museum Novitates,* 2931:1-42.

Maisey, J.G. 2011. The braincase of the Middle Triassic shark *Acronemus tuberculatus* (Bassani, 1886). *Palaeontology,* 54(2):417-428.

Murdock, D.J.E., Dong, X.-P., Repetski, J.E., Marone, F., Stampanoni, M., and Donoghue, P.C.J. 2013. The origin of conodonts and of vertebrate mineralized skeletons. *Nature,* 502(7472):546-549.

Mutter, R.J. 1998a. Tooth variability and reconstruction of dentition in *Acrodus* sp. (Chondrichthyes, Selachii, Hybodontoidea) from the Grenzbitumenzone (Middle Triassic) of Monte San Giorgio (Ticino, Switzerland). *Geologia Insubrica,* 3(1):23-31.

Mutter, R.J. 1998b. Zur systematischen Stellung einer Bezahnungsreste von *Acrodus georgii* sp. nov. (Selachii,Hybodontoidea) aus der Grenzbitumenzone (Mittlere Trias) des Monte San Giorgio (Kanton Tessin, Schweiz). *Eclogae Geologicae Helvetiae,* 91:513-519.

Mutter, R.J., de Blanger, K., and Neuman, A.G. 2007. Elasmobranchs from the Lower Triassic Sulphur Mountain Formation near Wapiti Lake (BC, Canada). *Zoological Journal of the Linnean Society,* 149:309-337.

Mutter, R.J., Neuman, A.G., and de Blanger, K. 2008. *Homalodontus* nom. nov., a replacement name for *Wapitiodus* Mutter, de Blanger and Neuman, 2007 (Homalodontidae nom. nov., ?Hybodontoidea), preoccupied by *Wapitiodus* Orchard, 2005. *Zoological Journal of the Linnean Society,* 154:419-420.

Nestell, M.K. and Wardlaw, B.R. 1987. Upper Permian conodonts from Hydra, Greece. *Journal of Paleontology,* 61(04):758-772.

Rees, J. and Underwood, C.J. 2002. The status of the shark genus *Lissodus* Brough, 1935, and the position of nominal *Lissodus* species within the Hybodontoidea (Selachii). *Journal of Vertebrate Paleontology,* 22(3):471-479.

Reif, W.-E. 1978. Types of morphogenesis of the dermal skeleton in fossil sharks. *Paläontologische Zeitschrift,* 52(1):110-128.

Renz, C. 1910. Stratigraphische Untersuchungen im griechischen Mesozoikum und Paläozoikum. *Jahrbuch der Kaiserlich Königlichen Geologischen Reichsanstalt,* 60(3):57-87.

Rieppel, O. 1981. The hybodontiform sharks from the Middle Triassic of Mte. San Giorgio, Switzerland. *Neues Jahrbuch für Geologie und Paläontologie - Abhandlungen,* 161(3):324-353.

Rieppel, O. 1982. A new genus of shark from the Middle Triassic of Monte San Giorgio, Switzerland. *Palaeontology,* 25(2):399-412.

Rieppel, O., Kindliman, R., and Bucher, H. 1996. A new fossil fish fauna from the Middle Triassic (Anisian) of North-Western Nevada, p. 501-512. In Arratia, G. and Viohl, G. (eds.), *Mesozoic Fishes - Systematics and Paleoecology*. Dr. Friedrich Pfeil, München, Germany.

Romano, C. and Brinkmann, W. 2010. A new specimen of the hybodont shark *Palaeobates polaris* with three-dimensionally preserved Meckel's cartilage from the Smithian (Early Triassic) of Spitsbergen. *Journal of Vertebrate Paleontology,* 30(6):1673-1683.

Romano, C., Koot, M.B., Kogan, I., Brayard, A., Minikh, A.V., Brinkmann, W., Bucher, H., and Kriwet, J. 2016. Permian–Triassic Osteichthyes (bony fishes): diversity dynamics and body size evolution. *Biological Reviews,* 91(1):106-147.

Schaumberg, E. 1977. Der Richelsdorfer Kupferschiefer und seine Fossilien, III. Die tierischen Fossilien des Kupferschiefers 2. Vertebraten. *der Aufschluss,* 28:297-352.

Shen, S.-Z. and Clapham, M.E. 2009. Wuchiapingian (Lopingian, late Permian) brachiopods from the Episkopi Formation of Hydra Island, Greece. *Palaeontology,* 52(4):713-743.

Trikolas, N. 2008. *Geological study of the wider area of Aegialia and Kalavryta*, Unpublished PhD Thesis, National Technical University of Athens, Athens, Greece. (In Greek)

Turner, S., Burrow, C.J., Schultze, H.-P., Blieck, A., Reif, W.-E., Rexroad, C.B., Bultynck, P., and Nowlan, G.S. 2010. False teeth: conodont-vertebrate phylogenetic relationships revisited. *Geodiversitas,* 32(4):545-594.

Vachard, D., Martini, R., and Zaninetti, L. 1995. Le Murgabien á Fusulinoides des iles d'Hydra, Crète et Mytilène (Permien supérieur de Grèce). *Geobios,* 28(4):395-406.

Vachard, D., Rettori, R., Angiolini, L., and Checconi, A. 2008. *Glomomidiella* gen. n. (Foraminifera, Miliolata, Neodiscidae): a new genus from the late Guadalupian–Lopingian of Hydra Island. *Rivista Italiana di Paleontologia e Stratigrafia,* 114(3):349-361+2 pls.

Acknowledgments

First of all, I would like to express my gratitude towards my supervisor, Prof. Marcelo Sánchez-Villagra, for giving me the opportunity to pursue a Ph.D. in his lab. His continuous guidance and support, as well as his academically stimulating research group, helped me to not only complete my thesis, but also expand my background on a broad array of topics related to evolutionary morphology and development, and methods for studying these in vertebrates. I am deeply indebted to Prof. Matt Friedman (University of Michigan) for hosting me in his lab for a year, trusting me with the study of fossil material and use of lab equipment, and for supervising part of my thesis. I extend my sincere thanks to the other members of my Ph.D. committee: Dr. Torsten Scheyer (PIMUZ), Dr. Marcus Clauss (Vetsuisse, UZH), and Dr. Olga Otero (University of Poitiers) for particularly useful discussions and advice that helped stream-line this project.

I am grateful to my dear friends (and coauthors) Dr. Carlo Romano and Dr. Jorge D. Carrillo-Briceño, who were always available to share their experience and discuss my project, and also invited me to participate in their research projects. My work greatly benefitted from collaboration with a number of people, whom I would like to warmly acknowledge. These include: Dr. Erin E. Maxwell (Staatliches Museum für Naturkunde Stuttgart), Dr. Sam Giles (University of Oxford), Dr. Heinz Furrer (PIMUZ), Dr. Ilja Kogan (TU Bergakademie Freiberg) and Dr. Rudolf Stockar (Museo cantonale di storia naturale, Lugano). Dr. Gabriel Aguirre-Fernández (PIMUZ), Tiago Simoes-Rodrigues, Oksana Vernygora (both University of Alberta) and Kelly Matsunaga (University of Michigan) are thanked for particularly useful discussions on various methods. Dr. Eric Hilton and Dr. Sarah Huber (both Virginia institute of marine science), Dr. Paul Sindilariu (Tropenhaus Frutigen AG), Dr. Douglas Nelson (University of Michigan), Bent E. K. Lindow, Kristian M. Gregersen (both Natural History Museum of Denmark), Dr. Stephanie Pierce (Harvard University) are thanked for kindly providing access to fossil and/or recent material in their care. Heike Götzmann and Alexandra Wegmann (PIMUZ) and Cindy Stauch (University of Michigan) are thanked for administrative support.

My research stay at the University of Michigan was supported by the P1ZHP3_168253 Swiss National Science Foundation doctoral mobility grant.

This work would have not been possible without support from all my friends at the PIMUZ (including PIMUZ alumni and affiliates) and the UMMP. Finally, I would like to express my sincere gratitude to my family for believing in me, and bearing with me throughout this long thesis process.

PERSONAL INFORMATION

Last name	ARGYRIOU
First name	THODORIS
Date and place of birth	05.08.1986, Athens, Greece
Nationality	Greek

EDUCATION

04.2014 – expected 05.2018

PhD in Evolutionary Biology, University of Zurich

Research on the paleobiology and systematics of Permian-Triassic Actinopterygii, supervised by Prof. Dr. Marcelo Sánchez, Palaeontological Institute and Museum, University of Zurich

09.2011 – 02.2014

Department of Biological Sciences, University of Alberta.
M.Sc. in Systematics and Evolution. GPA 4/4.

Master thesis: “Description, paleoenvironmental and paleobiogeographical implications of Miocene fish faunas from Jabal Zaltan and Sahabi (Libya)”(supervisor: Prof. Dr. Alison Murray)

09.2004 – 07.2010

Department of Geology and Geoenvironment, National and Kapodistrian University of Athens, Greece.
B.Sc. in Geology with major in Palaeontology. Grade obtained: “Very Good” (GPA 7,23/10).

Bachelor thesis “Study of the fossilized ichthyofauna from the Upper Pliocene of Aegina Island (Greece)” (supervisor: Prof. Dr. Georgios Theodorou, grade 10/10)

06.2004

Varvakeio Experimental highschool
highschool diploma (Apolytirion), grade 17.1/20

ACADEMIC CAREER

09.2016 – 07.2017

Visiting research scholar at the Museum of Paleontology of the University of Michigan. Host: Prof. Dr. Matt Friedman.

09.2013 – 12.2013; 09.2012 – 04.2013; 01.2012 – 04.2012

Teaching assistant at the Department of Biological Sciences, University of Alberta. Lab sections taught: Comparative Anatomy of Vertebrates, Paleobiology of Lower Vertebrates.

04.2013 – 08.2013; 04.2012 – 08.2012; 09.2011 – 12.2011

Research assistant at the Department of Biological Sciences, University of Alberta.

06.2010 – 07.2010

Field assistant in paleontological excavation, processing and study of vertebrate fossils from Pikermi, Greece.

07.2006 – 08.2006

Internship at the Natural History Museum of the Petrified Forest of Sigri, Lesvos Island, Greece. Work included: tours, excavations and fossil preparation. (funded by the National and Kapodistrian University of Athens).

AWARDS AND GRANTS

11.2017	Swiss Paleontological Society travel award: 900 CHF
05.2017	Canadian Society of Vertebrate Palaeontology travel award: 500 CAD
09.2016 – 07.2017	SNF Ph.D. mobility fellowship to Thodoris Argyriou. Project title: “Ancestral anatomy of an exceptional vertebrate clade: a paleobiological approach”: 43,800 USD
2013	Teaching excellence commendation, University of Alberta
11.2013	University of Alberta, Faculty of Graduate Studies and Research travel award: 1100 CAD
11.2013	Jackson student travel grant (offered by the SVP): 500 USD
06.2013	Raymonde Rivoallan Award (offered by the EAVP): 250 EUR
10.2012	University of Alberta, Department of Biological Sciences travel award: 300 CAD
10.2012	Graduate Students Association, professional development grant: 500 CAD
09.2011 – 12.2013	Graduate differential fee supplement awarded by the University of Alberta: approx. 3590 CAD per year

FIELDWORK EXPERIENCE

05.2015	Paleontological and geological prospecting in the Paleozoic of the Tafilalt Basin, Morocco
04.2010 – 08.2010; 07.2009 – 08.2009	Palaeontological excavation in the Neogene site of Pikermi, Attiki, Greece
01.2010 – 03.2010; 02.2008 – 03.2008	Palaeontological excavation and prospecting on the Neogene Jabal Zaltan and As Sahabi, Libya
2008 – 2009	Field surveys in: Crete Island, Aegina Island, Euboea Island, Greece, for the collection of fossil fish specimens for B.Sc. thesis
09.2007 – 10.2007	Palaeontological excavation in the Quaternary fossil site of Aghia Napa, Cyprus
10.2006	Palaeontological excavation of the Neogene site near Kerassia Village, Euboea Island, Greece
07.2006 – 08.2006	Excavation and preparation of collected fossilized plant specimens at the Natural History museum of the Petrified Forest of Sigri, Lesvos Island, Greece.

COMMUNITY OUTREACH

REVIEWER	PLoS ONE, Journal of Vertebrate Paleontology, Rivista Italiana di Paleontologia e Stratigraphia
12.2015	Science Trail featuring the Paleontological Museum and infrastructure of the University of Zurich. Guided tours through the collections
06.2011	Museum Thalassa, Aghia Napa, Cyprus. Preparation and installation of the permanent exhibition of endemic mammals from Cyprus and the Aegean
09.2010	Preparation and installation of the Exhibition titled: “The last European hippopotamuses; evidence of the environmental change in Cyprus”. First housed in the Cypriot Consulate, Athens, Greece

PUBLISHED RESEARCH ARTICLES

Maxwell, E.E., **Argyriou, T.**, Stockar, R., Furrer, H., 2018, Re-evaluation of the ontogeny and reproductive biology of the Triassic fish *Saurichthys* (Actinopterygii: Saurichthyidae). Palaeontology.

Murray, A.M., **Argyriou, T.**, Coté, S., McLatchley, L., 2017. The fishes of Bukwa, Uganda, a lower Miocene (Burdigalian) locality of East Africa. Journal of Vertebrate Paleontology 37(3):e1324460.

Argyriou, T., Romano, C., Carrillo-Briceño, J.D., Brosse, M., Hoffman, R., 2017. The oldest record of gnathostome fossils from Greece: Chondrichthyes from the Lopingian of Hydra Island. Palaeontologia Electronica 20.1.8A: 1-9.

Carrillo-Briceño, J.D., **Argyriou, T.**, Zapata, V., Jaramillo, C., 2016. A new early Miocene (Aquitanian) Elasmobranchii assemblage from the Guajira Peninsula, Colombia. Ameghiniana.

Argyriou, T., Clauss, M., Maxwell, E.E., Furrer, H., Sánchez-Villagra, M.R., 2016. Exceptional preservation reveals gastrointestinal anatomy and evolution in early actinopterygian fishes. Scientific Reports 6, 18758.

Argyriou, T., Cook, T.D., Muftah, A.M., Pavlakis, P., Boaz, N.T., Murray, A.M., 2015. A fish assemblage from an early Miocene horizon from Jabal Zaltan, Libya. Journal of African Earth Sciences 102, 86–101.

Murray, A.M., **Argyriou, T.**, Cook, T.D., 2014. Palaeobiogeographic relationships and palaeoenvironmental implications of an earliest Oligocene Tethyan ichthyofauna from Egypt. Canadian Journal of Earth Sciences 51, 909-918.

Otero, O., Bearez, P., **Argyriou, T.**, 2013. Presence of the genus *Argyrosomus* (Teleostei, Sciaenidae) in Neogene African outcrops. Geodiversitas 35 (1), 49–65.

Argyriou, T., Otero, O., Pavlakis, P., Boaz, N.T., 2012. Description and paleobiogeographical implications of new *Semlikiichthys* (Teleostei, Perciformes) fish material from the Late Miocene deposits of Sahabi, Libya. Geobios 45, 429–436.

SUBMITTED RESEARCH ARTICLES

Argyriou, T., Giles, S., Friedman, M., Romano, C., Kogan, I., Sánchez-Villagra, M.R. submitted. Internal cranial anatomy of Early Triassic species of *†Saurichthys*: implications for the phylogenetic placement of †saurichthyiforms. BMC evolutionary biology.

Romano, C., **Argyriou, T.** & Krummenacker, L.J., Paris Biota Team., submitted. Chondrichthyan teeth from the Early Triassic Paris Biota (Bear Lake County, Idaho, USA). Geobios.

CONFERENCE PRESENTATIONS AND ABSTRACTS

Argyriou, T., 2017. Paleobiology and interrelationships of *Saurichthys* (Actinopterygii, Saurichthyidae), and the importance of the Swiss fossil record. 15th Swiss Geoscience Meeting, Davos, Switzerland (oral presentation).

Argyriou, T., Giles, S., Friedman, M., 2017. New insights on ancestral neopterygian morphology from computed microtomography (μCT). 15th Annual Meeting of the European Association of Vertebrate Palaeontologists. Munich, Germany. (oral presentation).

Maxwell, E.E., **Argyriou, T.**, Stockar, R., Furrer, H., 2017. Evolutionary implications of the ontogeny and reproductive biology of Saurichthyidae (Actinopterygii). 15th Annual Meeting of the European Association of Vertebrate Palaeontologists. Munich, Germany. 62.

Giles, S., **Argyriou, T.**, 2017. Reassessment of *Perleidus stoschiensis* from the Early Triassic of Greenland. 14th International Symposium on Early/Lower Vertebrates, Geopark Kielce, Poland.

Argyriou, T., 2017. Skeletal anatomy and systematic placement of the Permian actinopterygian *Brachydegma caelatum* based on new data from μCT. Canadian Society of Vertebrate Paleontology, 5th annual meeting, Dinosaur Provincial Park, Alberta, Canada (oral presentation for the Caroll Prize Session).

Argyriou, T., Friedman, M., Romano, C., Kogan, I., Sánchez-Villagra, M.R., 2016. Endocranial anatomy and interrelationships of the Permo–Triassic early actinopterygian *Saurichthys* investigated with high-resolution computer-assisted microtomography (μCT). Society of Vertebrate Paleontology, 76th annual meeting, Salt Lake City, Utah, USA (oral presentation).

Abdelgawad, M. K., **Argyriou, T.**, Carrillo Briceño, J. D., Hamdan, M., El-Barkooky, A., Miller, E., Gunnell, G. F., 2016. A diverse fossil fish assemblage from the lower Miocene Moghra Formation, Egypt. Society of Vertebrate Paleontology, 76th annual meeting, Salt Lake City, Utah, USA.

Kogan, I., Pacholak, S., **Argyriou, T.**, Romano, C., Licht, M., 2016. Living torpedoes of the Triassic: design and function of *Saurichthys*, the first elaborate fast-start predator. Paläontologische Gesellschaft, 87th Annual Conference, Dresden, Germany.

Argyriou, T., Maxwell, E.E., Furrer, H., Sánchez-Villagra, M.R., 2014. First description of the spiral intestine in *Saurichthys* fishes: The effect of axial elongation on the anatomy of the viscera, Society of Vertebrate Paleontology, 74th annual meeting, Berlin, Germany (poster presentation).

Argyriou, T., Maxwell, E., Furrer, H., Sánchez-Villagra, M.R., 2014. First description of spiral cololites from *Saurichthys* (Actinopterygii, Saurichthyidae): Body shape as a factor for determining intestinal morphology, 4th International Palaeontological conference, Mendoza, Argentina (poster presentation).

Argyriou, T., Murray, A.M., 2013, Fish diversity and paleoenvironments from the late Miocene of Sahabi, Libya, Society of Vertebrate Paleontology, 73rd annual meeting. Los Angeles, California, U.S.A. (poster presentation).

Murray,A.M., **Argyriou, T.**, Cook, T.D., 2013, Elasmobranchs of the lower Jbel Qatrani Formation, Fayum, Egypt, Society of Vertebrate Paleontology, 73rd annual meeting. Los Angeles, California, U.S.A.

Argyriou, T., Murray, A.M., Otero, O., Pinton, A., 2013, The actinopterygian fauna from the Miocene of Jabal Zaltan, Libya, European Association of Vertebrate Paleontologists 11th annual meeting. Villers-sur-Mer, France. (Poster Presentation).

Argyriou, T., Cook, T.D., Murray, A.M., 2012, New additions to the elasmobranch fauna from the Miocene of Jabal Zaltan, Libya, Society of Vertebrate Paleontology, 72nd annual meeting. Raleigh, North Carolina, U.S.A. (Poster presentation).

Argyriou, T., Theodorou, G., 2011, New findings from the Pliocene (Zanclean) ichthyofauna of Aegina island, Greece, in: van der Geer, Athanassiou (Eds), European Association of Vertebrate Paleontologists 9th annual meeting. Heraklion, 13. (Oral presentation).